NANYANG TECHNOLOGICAL UNIVERSITY

RESPONSIVE MATERIALS AS DRAW AGENTS FOR FORWARD OSMOSIS DESALINATION

CAI YUFENG

School of Materials Science and Engineering

2016

RESPONSIVE MATERIALS AS DRAW AGENTS FOR FORWARD OSMOSIS DESALINATION

School of Materials Science and Engineering

A thesis submitted to the Nanyang Technological University
in partial fulfillment of the requirement for the degree of
Doctor of Philosophy

2016

Abstract

Alternative energy-efficient desalination technology is an exciting research field. Forward osmosis (FO) as a novel desalination technology has attracted much attention in that it is driven by chemical potential with low fouling potential and high fouling reversibility. In FO, the draw agent interacts with water forming a draw solution to reduce the water chemical potential, and thus water would automatically permeate through a selective membrane from brackish water to dilute the draw solution. The draw agent should also separate from water in the regeneration process to leave fresh water behind as the final product. In this thesis, I synthesized a series of responsive materials as draw agents, including hydrogels, polymers and (poly) ionic liquids, and studied the importance of balanced FO and regeneration performances. The merit of responsive draw agent is that the regeneration process can be realized with external stimulus, e.g., temperature, instead of solely relying on traditional reverse osmosis that consumes high-grade electrical energy and faces membrane fouling. The purpose of this thesis is to reveal the potential of responsive draw agents to enable FO to desalinate seawater or even brine with energy cost competent to other technologies.

Thermally responsive hydrogels, including semi-interpenetrating network hydrogels and polyionic liquid hydrogels, are studied as responsive draw agents in FO desalination. All these hydrogels are designed with both hydrophilicity and hydrophobicity in structures to assume thermosensitivity. The hydrogels can automatically swell and absorb fresh water from brackish water through an FO membrane at temperatures below their lower critical solution temperature (LCST); at temperatures above the LCST, the hydrogels deswell to release the readily available fresh water. This is quite interesting since I realize a desalination process driven by temperature modulation between room temperature and, for example, 40℃. The thermal energy requirement is lower than that of thermal distillation methods since the enthalpy and temperature of responsive draw agent phase separation with water are much lower than those of water vaporization. Although hydrogels are unfortunately found incapable to desalinate seawater, the aim of this thesis is quite clear, which is to utilize low grade thermal energy from industrial waste heat or

solar source to completely or at least largely replace the high grade electrical energy consumption in seawater or even brine desalination.

A dual responsive polymer is synthesized and studied in order to fulfill this target. The dual responsive polymer can be reversibly switched by introducing and removal of CO_2 between a polyelectrolyte state that can generate water flux from seawater, and a thermally responsive state that facilitates regeneration at temperatures above the LCST. Again, a temperature of 50℃ is sufficient to precipitate the majority of polymers, and a nanofiltration process is then employed to polish the water quality with a low hydraulic pressure of only 1.5 bar. Our aim is partially fulfilled since the majority amount of energy input is low grade thermal energy, if regeneration of CO_2 is not considered.

A group of thermally responsive ionic liquids are found to be able to generate a water flux from 1.6 M NaCl solution, which is almost 3 times the salinity of seawater. Meanwhile, their diluted draw solutions can undergo a liquid-liquid phase separation at 50℃ to generate a sedimentation phase that can be directly reused as draw solution without regeneration, and a supernatant phase with an osmotic pressure of less than 6 bar. The theoretical energy calculation reveals that FO requires only about one fifth of RO's electrical energy consumption for seawater desalination (theoretically 1.1 kWh/m^3), and the energy cost of FO is much lower than (less than half of) RO owing to the utilization of much cheaper low grade thermal energy. Finally, a proprietary draw agent is studied to be able to concentrate feed solution into a 17 wt% NaCl solution that facilitates ensuing crystallization process for zero-liquid discharge. Combining with a typical seawater RO plant, the energy consumption for brine treatment would be only the electrical energy equal to that of seawater RO, and additional low grade thermal energy associated with temperature modulation between 20 and 50℃. Therefore, FO enabled by responsive draw agents would be a competent desalination technology to challenge RO and thermal distillation methods in seawater and brine treatment.

Acknowledgements

Upon graduation, all the days I have spent in Singapore flash back before my eyes. From the age of 23 to 27, I dedicated my precious four years in research at NTU. First of all, I gratefully express my sincere respect and gratitude to my supervisor, Professor HU Xiao, for his guidance, patience and support during my PhD study. In my pursuit of scientific research, he offered me many invaluable suggestions as well as opportunities and sweated his blood in polishing my research articles. I really cherish the time we spent in his office discussing on not only research, but the meaning and gaining in life.

Also, I would like to acknowledge my co-supervisor, Professor WANG Rong, without whom I cannot have access to Singapore Membrane Technology Centre and rub shoulders with water-related expertise and equipments. She also taught me to be positive and pragmatic when facing research obstacles. I would also like to acknowledge Professor William (Bill) Krantz for his professional guidance to oral and poster presentation, as well as his word-by-word perusal and polishing in my papers.

I would like to extend my gratitude to the assistance, encouragement and suggestions from my group members. It is also my pleasure to thank Assistant Professor CHONG Tzyy Haur, Dr. LONG Yi, Dr. YU Hui, Dr. WEI Jing, Dr. LI Xuesong, Dr. WANG Penghua and WU Weiyi for their invaluable training, materials support and discussions.

Last but not least, I would like to thank my parents and my girlfriend Miss XIONG Wei for their understanding and support.

Table of Contents

Abstract ..... **i**

Acknowledgements ..... **iii**

Table Captions ..... **xi**

Figure Captions ..... **xiii**

Abbreviations ..... **xxi**

1. Introduction **1**

1.1. Research Background 1

1.2. Objectives and Scope 2

1.3. Thesis Overview 3

1.4. Findings and Originality 4

References 5

2. Literature Review **7**

2.1. Review of desalination technologies 7

2.1.1. MSF, MED and VC 7

2.1.2. Freezing desalination 8

2.1.3. Humidification-dehumidification 9

2.1.4. Hydration 9

2.1.5. Electro-dialysis, microbial cell and other electric field related technologies 9

2.1.6. Membrane distillation 10

2.1.7. Reverse osmosis 10

2.1.8. Summary 11

2.2. The introduction of forward osmosis 11

2.2.1. The principles of forward osmosis 11

2.2.2. Osmotic pressure 14

2.2.3. Concentration polarization 15
2.3. The development of draw agents 17
2.3.1. Draw agents for indirect desalination 17
2.3.2. Draw agents for direct desalination 18
2.3.2.1. Inorganic salts 18
2.3.2.2. Polyelectrolytes 19
2.3.2.3. Organic salts 19
2.3.2.4. Nanoparticles 20
2.3.2.5. Hydrogels 20
2.3.2.6. Draw agents regenerated by metathesis precipitation 21
2.3.2.7. CO_2-NH_3 system 21
2.3.2.8. Switchable polarity solvent 22
2.3.2.9. LCST type small molecular non-electrolyte 22
2.4. Summary 23
References 24
3. Experimental Methodology 33
3.1. Synthesis of responsive draw agents 33
3.1.1. Synthesis of SI-0.2PSA semi-IPN hydrogel 33
3.1.2. Synthesis of SI-0.2PVA semi-IPN hydrogel 34
3.1.3. Synthesis of SI-0.5PVA semi-IPN hydrogel 34
3.1.4. Synthesis of tetrabutyl phosphonium p-styrenesulfonate (P4444 SS) and tributylhexyl phosphonium p-styrenesulfonate (P4446 SS) 34
3.1.5. Synthesis of poly (P4444 SS) and poly (P444-6 SS) hydrogels 35
3.1.6. Synthesis of poly[2-(dimethylamino)ethyl methacrylate] (PDMAEMA) 35
3.1.7. Synthesis of tetrabutylphosphonium 2,4-dimethylbenzenesulfonate (P4444 DMBS) and tetrabutylphosphonium mesitylenesulfonate (P4444 TMBS) 36
3.2. Characterizations 36

3.2.1. ^{1}H Nuclear Magnetic Resonance (^{1}H NMR) 36
3.2.2. Gel Permeation Chromatography (GPC) 36
3.2.3. Differential Scanning Calorimetry (DSC) 37
3.2.4. Karl Fischer titration 37
3.2.5. UV-visible absorption spectroscopy 37
3.2.6. Osmotic pressure measurement 37
3.2.7. Water flux measurement 40
3.2.8. Back diffusion and Salt rejection 41
References 41
4. TOWARDS TEMPERATURE DRIVEN FORWARD OSMOSIS DESALINATION USING SEMI-IPN HYDROGELS AS REVERSIBLE DRAW AGENTS 43
4.1. Introduction 43
4.2. Material and methods 45
4.2.1. Materials 45
4.2.2. Preparation of hydrogels 46
4.2.3. Characterization of hydrogel thermosensitivity 47
4.2.4. Hydrogel dewatering and performance in FO process 47
4.3. Results and discussion 49
4.3.1. Swelling and deswelling of semi-IPN hydrogels 49
4.3.2. Performance in FO process and reversibility 52
4.3.3. Quasi-continuous FO desalination driven by temperature 57
4.4. Conclusions 60
References 60
5. INVESTIGATION OF BRACKISH WATER DESALINATION VIA FORWARD OSMOSIS ENABLED BY THERMALLY RESPONSIVE POLY IONIC LIQUID HYDROGELS 65

5.1. Introduction 65

5.2. Experimental Section 68

5.2.1. Synthesis of ionic liquid monomers 68

5.2.2. Synthesis of hydrogels 69

5.2.3. Characterizations 69

5.3. Results and discussion 70

5.3.1. The synthesis of ionic liquid monomers and hydrogels 70

5.3.2. The FO performances of hydrogels 72

5.3.3. The influence of hydrogel particle-particle contact and membrane type on FO performance 74

5.3.4. The thermosensitivity and dewatering performance 76

5.3.5. The selection criterion of hydrogel with the best performance as draw agent 78

5.3.6. The performance enhancement from tuning hydrogel's composition, membrane structure and particle-particle contact condition 81

5.3.7. The performance enhancement from optimizing hydrogel's area density and one FO-regeneration cycle duration 83

5.4. Conclusion 87

References 88

6. DUAL RESPONSIVE POLYMERS AS DRAW AGENTS FOR FORWARD OSMOSIS DESALINATION 93

6.1. Introduction 93

6.2. Experimental section 96

6.2.1. Materials 96

6.2.2. Polymer synthesis 96

6.2.3. Water flux measurement 97

6.2.4. Draw agent back diffusion measurement 98

6.2.5. FO membrane salt rejection measurement 98
6.3. Results and discussion 99
6.3.1. The draw agent synthesis 99
6.3.2. The protonation and FO performance of draw agents 100
6.3.3. Draw agent back diffusion and membrane salt rejection 104
6.3.4. Deprotonation and regeneration of draw agent 105
6.3.5. Insight of this draw agent's significance 108
6.4. Conclusions 109
References 109
7. ENERGY-EFFICIENT DESALINATION BY FORWARD OSMOSIS USING RESPONSIVE IONIC LIQUID DRAW AGENTS 113
7.1. Introduction 113
7.2. Experimental section 116
7.2.1. Materials and equipments 116
7.2.2. Syntheses of ionic liquids 117
7.2.3. Draw agents' influence on membrane 117
7.2.4. Water flux measurement 117
7.2.5. Draw agent back diffusion 118
7.3. Results and discussion 119
7.3.1. Synthesis of draw agents 119
7.3.2. The amphiphilicity of thermally responsive ionic liquids 120
7.3.3. FO performance of thermally responsive ionic liquids 124
7.3.4. Draw agents regeneration 128
7.3.5. Energy consumption estimation 132
7.3.6. Water quality and draw agent toxicity 138

7.4. Conclusions 139

References 139

8. A NOVEL UCST-TYPE FORWARD OSMOSIS DRAW AGENT FOR BRINE TREATMENT 145

8.1. Introduction 145

8.2. Experimental section 148

8.2.1. Materials and apparatus 148

8.2.2. Draw agent solubility in water 148

8.2.3. Measurements of water flux, draw agent back diffusion and membrane salt rejection 149

8.3. Results and discussion 150

8.4. Conclusions 157

References 157

9. CONCLUSIONS AND RECOMMENDED FUTURE WORKS 161

9.1. Conclusions 161

9.2. Recommendation for future work 164

References 166

LIST OF PUBLICATIONS 168

Table Captions

Table 4.1 Summary of ingredients for hydrogels synthesis.[a] 46

Table 4.2 OPSR, EPSR and the reversible swelling ratio range of thermally responsive hydrogels.[*] 55

Table 5.1 The comparison of comprehensive FO-Regeneration performances of each hydrogel. 82

Table 5.2 The influence of area density of PP444-6 SS on the water production rate. ... 85

Table 5.3 The comprehensive performance of PP444-6 SS when one FO-regeneration cycle was fixed within 30 minutes. 87

Table 6.1 Summary of number average molecular weight (M_n), weight average molecular weight (M_w) and polymer dispersity index (PDI) of the three PDMAEMA polymers synthesized. 100

Table 7.1 The correlation between predicted osmolality and weight concentration of draw solutions. The conversion from weight concentration to molality was according to the equation mentioned above, and the correlation between molality and osmolality was based on the fittings in Figure 7.5. 123

Figure Captions

Figure 2.1 Schematic illustrations of (a) MSF, (b) MED, (c) VC and (d) ED. (a) and (b) are adapted from Ref.4. (d) is adapted from Ref.5. 8

Figure 2.2 Schematic illustrations of RO, PRO and FO with the correlation between hydraulic pressure, osmotic pressure and water flux direction. ΔP and $\Delta\pi$ are the hydraulic pressure and osmotic pressure difference, respectively, between draw solution and feed solution. 13

Figure 2.3 The concentration polarizations of (a) when selective layer faces draw solution and (b) when porous supportive layer faces draw solution. This figure is adapted from Ref.19 16

Figure 2.4 Illustration of FO for direct desalination application. 18

Figure 2.5 Schematic illustration of using hydrogels as draw agents for FO desalination.[69] 21

Figure 3.1 Temperature profiles of pure water and solution during osmolality measurements. This figure is adapted from Ref.4. 39

Figure 3.2 The illustration of water flux measuring apparatus for hydrogels as draw agent. 39

Figure 3.3 Illustration of cross-flow setup for water flux measurement. 40

Figure 4.1 (a) Schematic and (b) photo of the home-made apparatus for water flux measurement. The covering plastic film is to isolate hydrogels from atmosphere. (c) The hydrogel disc fabricated from dry hydrogel particles. (d) The photo showing the robustness and shape integrity of the hydrogel disc. 48

Figure 4.2 (a) Equilibrium swelling ratio at room temperature, swelling ratio after complete deswelling at 40℃ in water and water recovery after 10 minutes at 40℃ of the bulk hydrogels. (b) Deswelling profile of hydrogel discs from a swelling ratio of approximately 2 g/g. All the hydrogels had a diameter of 24 mm and thickness of 3 mm. 49

Figure 4.3 The illustrations of (a) evenly distributed charges and (b) localized charges on the formation of hydrophobic aggregate in copolymer hydrogel and semi-IPN hydrogel, respectively. 51

Figure 4.4 The LCSTs of the hydrogels studied in this chapter. Co-0.2PSA does not show any thermal effect within the temperature range studied. Downward is endothermic.52
Figure 4.5 The hourly average water flux generated by thermally responsive hydrogels (column) and the corresponding swelling ratio (dot) in the 5 hour FO test. For instance, the first column of each hydrogel represents the average water flux in the first hour, and the first two dots are the swelling ratios before and after the first hour swelling. The dots at 0 hour are the OPSRs. 53
Figure 4.6 (a) The correlation curves for the water flux versus swelling ratio for hydrogels in a 5 hour FO process. (b) Schematic illustration for reversible hydrogel performance optimization. A better hydrogel should have a lower OPSR and a higher EPSR simultaneously to expand the reversible swelling ratio range. The red solid line indicates the reversible range of swelling ratio between OPSR and EPSR. 54
Figure 4.7 The reversibility of hydrogels for three FO-dewatering cycles. The five dots in each cycle represent the average water flux for the corresponding one hour. The dewatering process duration is 10 minutes and represented by dashed lines. The dewatering process is not to scale relative to the FO process duration. 56
Figure 4.8 The influence of contact area between hydrogel and membrane on the FO performance of SI-0.2PSA. The weight of dried hydrogel is 400 mg and 2000 ppm NaCl brackish water is used as feed solution. 58
Figure 4.9 Quasi-continuous FO desalination using a semi-IPN hydrogel as the draw agent. Besides inevitable electrical energy for pumping, the periodic temperature modulation within 15 ℃ is essentially the only required energy input for desalination in this conceptual design. This temperature difference can be readily obtained using warm air/water generated from industrial waste heat. 59
Figure 5.1 The ^{1}H NMR spectrum of tetrabutylphosphonium *p*-styrene sulfonate (P4444 SS). 70
Figure 5.2 The ^{1}H NMR spectrum of tributylhexylphosphonium *p*-styrenesulfonate (P4446 SS). 71
Figure 5.3 Optical images of (a) PP4444 SS, (b) PP444-6 SS, (c) neat PNIPAm and (d) PNIPAm-PVA semi-IPN hydrogel powder. The scale bar is 200 μm. 71

Figure 5.4 The water flux and swelling ratio profile of each hydrogel from dry state. The hydrogels were in powder form contacting a HTI cellulose triacetate membrane with a area density of 0.6 g/4.5 cm^2. Feed solution was 2000 ppm NaCl solution. 72
Figure 5.5 The swelling ratio and the corresponding generated water flux correlation of each hydrogel. Feed solution was 2000 ppm NaCl solution. Inlet was the equilibrium swelling ratio of each hydrogel immersing in DI water at room temperature. 73
Figure 5.6 The improved water flux in FO of PP4444 SS and PP444-6 SS due to much reduced interstitial volume between particles in disc form and a thinner FO membrane. 75
Figure 5.7 FESEM images of cellulose triacetate membrane from HTI (left) and thin film composite (TFC) membrane (right). The thickness of selective layer of each membrane was roughly indicated. 75
Figure 5.8 The DSC measurements of each hydrogel with a swelling ratio of 3 g/g. The peak of LCST and the enthalpy of phase transition were marked. 76
Figure 5.9 Deswelling profile of each hydrogel at 60 ℃ 77
Figure 5.10 Fraction of liquid water released during deswelling process. 78
Figure 5.11 Schematic illustration of the criterion for a hydrogel's comprehensive performance in reversible FO-Regeneration cycles. T_{FO} and $T_{des.}$ are the duration of FO process and regeneration process, respectively. SR_0 is swelling ratio obtainable after regeneration, which can be found in Figure 5.9 for each hydrogel. A is the active membrane area, which is 4.5 cm^2 throughout this paper. ΔSR is the swelling ratio increment during the FO process and m_{gel} is the weight of dry hydrogel. M_{water} is the amount of water absorbed that can also be fully released during regeneration process in one cycle. Therefore, the apparent water flux ($J_{app.}$) calculated in this criterion is the water production rate. 79
Figure 5.12 The fittings of swelling ratio versus FO time for different hydrogel in powder form with HTI membrane and in disc form with TFC membrane. 80
Figure 5.13 Comparison of comprehensive performance of each hydrogel in one reversible FO-regeneration cycle within one hour. T_{FO} and $T_{des.}$ were allotted that SR_0 can be obtained after regeneration to make the cycle reversible. Hydrogel's area densitiy was fixed at 0.6 g/4.5 cm^2. 2000 ppm NaCl was used as feed solution. 82

Figure 5.14 The influence of area density on the hydrogel FO performance. The hydrogel was P444-6 SS in disc form and TFC membrane was used as the FO membrane. Feed solution was 2000 ppm NaCl solution. 83
Figure 5.15 The fittings of the correlation between swelling ratio and FO time for PP444-6 SS with different area density. The hydrogel was in disc form using TFC membrane. 2000 ppm NaCl solution was used as feed solution. 84
Figure 5.16 The influence of hydrogel area density on the hydrogel's comprehensive performance in terms of water production rate. The hydrogel was PP444-6 SS in disc form on TFC membrane. 2000 ppm NaCl solution was used as feed solution. 85
Figure 5.17 The comprehensive performance of PP444-6 SS when one FO-regeneration cycle was fixed within 30 minutes. PP444-6 SS was used in disc form on TFC membrane. 2000 ppm NaCl solution was used as feed solution. 86
Figure 6.1 Schematic illustration of the CO_2 and thermally dual responsive draw agent for forward osmosis desalination. 95
Figure 6.2 The water flux measurement by a home-made apparatus. The right chamber contains the draw solution with an initial concentration of 0.4 g/g and the left chamber contains the brackish solution with an initial concentration of 0.15 M NaCl. The magnetic stirring rate is 600 rpm. 97
Figure 6.3 The calibration curve for NaCl solution conductivity versus concentration. 99
Figure 6.4 The osmolality profiles of deprotonated and protonated draw agents. The horizontal lines depict the osmolalities of 0.15 M, 0.4 M and 0.6 M NaCl solutions, respectively. 101
Figure 6.5 The profiles of protonated draw solution with various concentrations. 102
Figure 6.6 The water flux profile of various protonated draw solution concentrations against different feed solution salinities. The FO membrane was in PRO mode. 103
Figure 6.7 (a) Draw agent back diffusion flux as a function of molecular weight and concentration. (b) The ratio of draw agent back diffusion flux to the water flux as a function of molecular weight and concentration. 104
Figure 6.8 Conductivity monitoring during the protonation-deprotonation cycle of P4000 and P9000. The CO_2 was purged at 25℃ and Ar was purged at 60℃. Gas flow rate was 300 ml/min. 105

Figure 6.9 Protonation-deprotonation reversibility shown by osmolality (a,b) and pH (c,d) measurements. The protonation was done by purging CO_2 at 25℃ and deprotonation was done by purging Ar at 60 ℃. The gas flow was 300 ml/min..... 106

Figure 6.10 The measurements of UV-vis transmittance (700 nm) for P4000 (left) and P9000 (right) in the as-synthesized (initial), protonated and deprotonated states. 106

Figure 6.11 The deprotonated draw solutions undergo a solid-liquid phase separation at temperatures higher than the LCST. The upper row is the P9000 and the bottom row is the P4000. 107

Figure 7.1 Setup for water flux measurement in FO..... 118

Figure 7.2 DSC measurements of the three pure ionic liquids. 119

Figure 7.3 The schematic illustration of FO desalination using thermally responsive ionic liquids as draw agents. The molecular structures of these three draw agents are also demonstrated. 120

Figure 7.4 The nonlinear correlations between molality and osmolality of these three draw agents indicate the effect of ion-pairing besides dissociation..... 121

Figure 7.5 The fittings for osmolality-molality correlations at osmolality-measurable concentrations. 122

Figure 7.6 The panoramic correlation between osmolality and weight concentration. . 124

Figure 7.7 Water flux profile of $P_{4448}Br$ with different concentrations. Feed solution is 2000 ppm NaCl and the temperature is 14±1 ℃. 124

Figure 7.8 Water flux profiles of $P_{4444}DMBS$ and $P_{4444}TMBS$ draw solutions with various concentrations against feed solutions of various salinities at different temperatures. 125

Figure 7.9 Water fluxes of 70 wt% $P_{4444}DMBS$ draw solution generated from feed solutions with salinities higher than seawater. The FO test was conducted at 14±1 ℃. 126

Figure 7.10 The correlation between draw agent back diffusion flux to water flux ratio and draw solution concentration. This ratio indicates the mass (mg) of draw agents back diffused as per litre of water permeated through membrane. DI water was the feed solution..... 127

Figure 7.11 Comparison of salt rejection of as-received membranes and those immersed for 7 days in 70 wt% $P_{4444}DMBS$ or $P_{4444}TMBS$ draw solution. 128

Figure 7.12 The LCSTs of the draw solutions at different concentrations. 128
Figure 7.13 Phase separation of 40 wt% P_{4444}DMBS as a function of time at 50℃. The white plastic cap under vial was used for avoiding direct contact with the hot plate. 129
Figure 7.14 Draw agent concentrations in the water-rich supernatant phase and draw agent-rich sedimentation phase after phase separation at different temperatures. The initial draw solution concentration was 30 wt%. 130
Figure 7.15 Draw agent concentrations in the water-rich supernatant phase and draw agent-rich sedimentation phase at 16℃ above the corresponding LCST of different initial draw solution concentrations. 131
Figure 7.16 The entire FO desalination processes in phase diagram. C_{sedi}, C_{dilu} and C_{super} represent the concentration of draw agent-rich sedimentation phase, diluted draw solution after FO process and water-rich supernatant phase, respectively. 132
Figure 7.17 The osmotic pressure profiles of feed solution and draw solution in co-current and counter-current module. Π_d and Π_f are osmotic pressure of draw solution and feed solution, respectively. 134
Figure 7.18 (a) Water fluxes during water recovery via low pressure nanofiltration with various hydraulic pressures. (b) Schematic depiction of further phase separation during the low and constant pressure NF process as water is recovered. 135
Figure 7.19 The DSC of 50 wt% draw solution phase separation. 136
Figure 7.20 The scheme of FO-regeneration process using thermally responsive ionic liquids as draw agents. The capacity is fixed at 1000 kg per hour that is irrelevant with the capital energy calculation. The concentration and liquid flow rate at each step were marked. The water recovery of the entire seawater desalination process (counter-current pattern) is assumed to be 50% since 50 wt% draw solution can generate water flux from seawater, and 70 wt% draw solution can generate water flux from 1.2 M NaCl. 137
Figure 8.1 The draw agent's solubility (in solid line) as function of temperature. Four typical "smart" ionic species with solubility dependence on temperature were also shown in comparison. The solubility concentration is presented in mole of draw agent per kilogram of water. 151
Figure 8.2 Water flux generated by draw solutions of different concentrations against feed solutions with salinities equal to or higher than seawater in (a) PRO mode and (b)

FO mode. Draw solution and feed solution were maintained at 50±1 ℃ and 46±2 ℃, respectively. 152

Figure 8.3 (a) back diffusion of draw agent in FO process. 2 wt% NaCl was used as the feed solution. (b) salt rejection of FO membrane in FO process with 2 wt% and 3.5 wt% NaCl as feed solutions. The draw solution and feed solution were maintained at 50±1 ℃ and 46±2 ℃, respectively. FO mode was used throughout the back diffusion and salt rejection measurements..... 153

Figure 8.4 Schematic illustration of phase diagram of this UCST-type draw agent circulation in FO-regeneration processes modulated by temperature..... 155

Figure 8.5 Schematic illustration of brine treatment via FO using our draw agent that concentrate the brine to 17 wt% NaCl solution that is difficult to treat directly using an RO process. Diluted draw solution after FO process is first cooled to 20℃ at which a majority of the draw agent is regenerated by phase separation. The sedimentation phase can be used directly as draw solution again, while the supernatant can be regenerated by an isobaric RO or NF process. 156

Figure 9.1 The structure of a PNIPAm-graft-Polyacrlyic acid polymer (left) and its interestingly constant LCST in solution irrespective of acrylic acid content (right). This figure is adapted from Reference 4. 165

Abbreviations

APS	Ammonium Persulfate
ATRP	Atom Transfer Radical Polymerization
CMC	Critical Micellar Concentration
CP	Concentration Polarization
DMAEMA	2-(Dimethylamino) ethyl methacrylate
ED	Electro-Dialysis
EPSR	End Point Swelling Ratio
FO	Forward Osmosis
HDH	Humidification-Dehumidification
HMTETA	1,1,4,7,10,10-Hexamethyltriethylenetetramine
LCST	Lower Critical Solution Temperature
LMH	Litre per square Meter per Hour
MBA	*N,N*'-methylenebisacrylamide
MD	Membrane Distillation
MED	Multi-Effect Distillation
MSF	Multi-Stage Flash
NIPAm	*N*-Isopropylacrylamide
OPSR	Onset Point Swelling Ratio
P4444 DMBS	Tetrabutyl phosphonium 2,4-dimethylbenzenesulfonate
P4444 TMBS	Tetrabutyl phosphonium mesitylenesulfonate
P4444 SS	Tetrabutyl phosphonium p-styrenesulfonate
P4446 SS	Tributyl-hexyl Phosphonium p-styrenesulfonate
P4448 Br	Tributyl-octyl phosphonium bromide
PNIPAm	Poly N-isopropylacrylamide
PSA	Poly Sodium Acrylate
PSS	Poly sodium 4-styrenesulfonate
PVA	Poly Vinyl Alcohol
TEMED	*N,N,N',N'*-Tetramethylethylenediamine
THF	Tetrahydrofuran

TRIL	Thermally Responsive Ionic Liquid
UCST	Upper Critical Solution Temperature
VC	Vapor Compression

1. Introduction

In this chapter, the background, objective and novelty of this thesis have been briefly introduced and summarized. In addition, the structure of this thesis and the main content of each chapter are summarized.

1.1. Research Background

Water scarcity has become not only an environmental issue but a political issue nowadays to the human society sustainable development. This crisis stems from limited amount of fresh water and its uneven distribution. Although there is 1.4 billion cubic kilometer of water on Earth, 97.5% of the reserves are seawater as well as brackish water and only 2.5% is potable fresh water. Unfortunately, out of the 2.5% fresh water reserves, only one eighth is in liquid form available for consumption.[1] In addition, the water scarcity problem has been intensified by fast growing water demand due to overpopulation and water pollution by industrialization and urbanization.

Desalination technologies are one of the critical solutions to mitigate the crisis. Desalination can purify salty water and extend our fresh water reservoir to seawater and brackish water. Traditionally, mature desalination technologies include thermally based multi-stage flash (MSF) and multi-effect distillation (MD), membrane based reverse osmosis (RO) and nano-filtration (NF) and electrically based electro-dialysis (ED). Nevertheless, MSF and MED need a huge amount of thermal energy from fossil fuels to vaporize seawater; ED consumes electrical energy but are not capable of handling seawater; RO also needs to consume electrical energy for high hydraulic pressure generation to force water to permeate through non-porous membrane.[2] In a world that is also haunted by energy-related problems, we need a more energy-efficient desalination technology to ameliorate water scarcity.

Forward osmosis (FO) technology has emerged as a promising energy-efficient technology to address the problems of desalination and wastewater treatment.[3-5] FO is an automatic process driven by water chemical potential gradient across the membrane and

no external energy is required. However, the development of this technology has been hampered by lack of suitable draw agents. A suitable draw agent should meet several criteria that will be discussed in Chapter 2. Non-functional draw agents including NaCl, $MgCl_2$ and sugars, *etc*., would not help realize the promised advantages of FO for desalination since their regeneration is still an energy-intensive process solely depending on RO, NF or other thermal processes. Thus, it would be of great interest to explore the opportunity of using responsive materials as smart draw agents for FO desalination to realize its promised advantages.

1.2. Objectives and Scope

For forward osmosis desalination in which the fresh water is the final product, the draw agent regeneration is as equally important as its performances in FO process. This is because although sole FO is an automatic process, the ensuing draw agent regeneration process consumes energy to separate water from draw agent. Therefore, in order to make FO desalination an energy-efficient process, the draw agent's facile regeneration is paramount and imperative to determine whether FO can fulfill its promises. Unfortunately, there is always a compromise between FO and regeneration performances. This is because in the FO process, draw agent is required to interact strongly with water to generate high osmotic pressure, while this very interaction prohibits facile regeneration. There are many research papers on draw agents that are indulged in generating high water flux in FO process and ignoring the role of regeneration in the comprehensive performances of draw agent, especially in terms of energy consumption and cost compared with other desalination technologies.[3,4] In addition, few research papers on draw agents ever systematically study the potential of using responsive draw agents for FO desalination. My ultimate goal in this thesis is to synthesize a series of responsive draw agents with balanced FO and regeneration performances, and to study their potentials to enable FO towards the goal of desalinating seawater or even brine with energy cost competent to other technologies. Therefore, the objectives of this thesis were:

1. Synthesize responsive draw agents that can generate a high water flux in FO process as well as be easily regenerated by external stimulus.

2. Study the importance of a balanced FO-regeneration performance on the draw agent's comprehensive ability.
3. Improve the draw agent's capability from treating brackish water to seawater or even brine without sacrificing the easy draw agent regeneration at stimulus.
4. Provide an initial energy cost analysis of FO desalination enabled by the responsive draw agents, and point out the application outlook of FO desalination.

1.3. Thesis Overview

This thesis is about exploring and investigating the role of responsive draw agents with balanced drawing and regeneration abilities in enabling energy-efficient forward osmosis desalination. Chapter 1 provides the background to this project. Given the increasing global demand for fresh water, it is crucial and urgent to explore alternative energy-efficient desalination methods. Forward osmosis is quite promising since it is driven by water chemical potential gradient. Chapter 2 briefly summarizes the developed and developing desalination technologies with their drawbacks, and an obvious technology gap is revealed for seawater and brine desalination. Forward osmosis is a promising technology to fill in the gap, albeit it is hindered by limited choice of ideal draw agent that can not only generate a high water flux, but be energy-efficiently regenerated. Besides, other criteria including low back diffusion into feed solution, low toxicity and being benign to membrane should be met to be an ideal draw agent. Chapter 3 provides the details of synthesizing responsive draw agents and the experimental procedures. The first work of using thermally responsive semi-IPN hydrogels as draw agents was studied in Chapter 4. The linear hydrophilic polymer of poly vinyl alcohol or poly sodium acrylate was entrapped into the crosslinked poly(N-isopropylacrylamide) (PNIPAm) network. The water flux generated by these semi-IPN hydrogels increased compared with neat PNIPAm hydrogel, and the thermosensitivity of PNIPAm was preserved to release water under mild heating. The reasons of superior overall performance to copolymer hydrogels were analyzed, and the concept of temperature modulated desalination was for the first time proposed. However, the water flux was found to be relatively low. In chapter 5, the subtle balance between hydrophilicity and hydrophobicity was achieved in the design of hydrogel monomer structure. The synthesized thermally responsive

polyionic liquid hydrogels improved the water flux to six times that of semi-IPN hydrogel. More importantly, a universal judging criterion for hydrogel's comprehensive performance as draw agent for FO desalination was for the first time proposed. Nevertheless, these hydrogels still cannot desalinate seawater probably due to severe concentration polarization originated from slow water diffusion. In chapter 6, dual responsive polymers were investigated. The polyelectrolyte state in FO and thermally responsive state in regeneration was reversibly switched by addition and removal of CO_2. These polymers show potential for seawater desalination and their energy consumption majorly came from low-grade heat. It pointed out a possible solution for an energy-efficient desalination, which is to replace the expensive electrical energy with cheaper low-grade thermal energy. However, since the CO_2 also needs regeneration, I did not quantify the energy consumption of FO enabled by these polymers. This thermal-replacing-electrical concept is further discussed in chapter 7, where thermally responsive ionic liquids were investigated as draw agents. These draw agents were able to generate water flux from 1.6 M NaCl solution, and under mild heating to 50-60℃, the diluted draw solution underwent a phase separation resulting in a sedimentation phase that can be directly reused as draw solution, as well as a supernatant phase that could be treated via low pressure nanofiltration. I calculated the theoretical energy consumption of FO enabled by these draw agents, and found that it was higher than the theoretical value for RO. However, the electrical energy consumption was much lower, and the much cheaper thermal energy used helped reduce the energy cost lower than that of RO. In chapter 8, I introduced a proprietary draw agent that can concentrate the feed solution to 17 wt% NaCl, and simultaneously the regeneration can be done at any seawater RO plant. The FO-RO hybrid probably would be competent to challenge thermal distillation technologies in brine treatment. In chapter 9, I made conclusions of this project and recommendations for the future work.

1.4. Findings and Originality

This work involves s systematic study of the responsive materials including hydrogels, polymers and ionic liquids as draw agents for forward osmosis desalination. The main contributions of this work include:

1. I clarified the importance of balanced FO-regeneration performances of draw agents in FO desalination.
2. The thermally responsive polyionic liquid hydrogels, dual responsive polymers and thermally responsive ionic liquids were for the first time investigated as draw agents for FO desalination.
3. The theoretical energy consumption of FO is calculated. It was found that FO may consume more energy than RO, however FO enables the consumption other source of energy than electricity, e.g., low grade waste heat, and the energy cost of FO can be lower than RO for seawater desalination.

References

1. Gleick, P. H., Water resources. *Encyclopedia of climate and weather* **1996,** *2*, 817-823.
2. Ghalavand, Y.; Hatamipour, M. S.; Rahimi, A., A review on energy consumption of desalination processes. *Desalination and Water Treatment* **2014**, 1-16.
3. Hoover, L. A.; Phillip, W. A.; Tiraferri, A.; Yip, N. Y.; Elimelech, M., Forward with osmosis: emerging applications for greater sustainability. *Environmental science & technology* **2011,** *45*, (23), 9824-9830.
4. Klaysom, C.; Cath, T. Y.; Depuydt, T.; Vankelecom, I. F., Forward and pressure retarded osmosis: potential solutions for global challenges in energy and water supply. *Chem Soc Rev* **2013,** *42*, (16), 6959-6989.
5. Cath, T.; Childress, A.; Elimelech, M., Forward osmosis: Principles, applications, and recent developments. *Journal of Membrane Science* **2006,** *281*, (1-2), 70-87.

2. Literature Review

In this chapter, desalination technologies that have been utilized in industry or are still in laboratory bench-scale are introduced. Their mechanisms and drawbacks are summarized and the gap for an efficient technology for seawater and brine treatment is revealed. Forward osmosis, as a promising low-energy process to fill in the gap, is thoroughly introduced in section 2.2. Section 2.3 summarizes all the developed draw agents trying to realize FO's advantages and the importance of developing new responsive draw agents is addressed at the end of this chapter.

2.1. Review of desalination technologies

In this section, I categorize the desalination technologies as thermal methods, membrane methods and other technologies. Forward osmosis, although it is a membrane based technology, will be discussed in the Section 2.2.

2.1.1. MSF, MED and VC

Distillation is possibly the oldest desalination technology which has been utilized for several thousand years. Water evaporates into vapor and leaves the salt behind in the retentate liquid to achieve the goal. In industry, distillation methods are always coupled with heat recovery devices to reuse the latent heat of vapor condensation in order to make distillation more economic. Multi-stage flash (MSF) is probably the most widely used distillation technology.[1] In MSF, as shown in Figure 2.1a, incoming seawater is preheated by heat-exchanger and further heated by external high temperature steam to reach the process temperature of 80 to 90 ℃, and then is introduced to the first vacuum chamber so that a portion of the seawater flashes into fresh water vapor. The vapor is condensed by the incoming seawater and the remaining brine is introduced to next chamber with higher vacuum degree to harvest more fresh water. Multi-effect distillation (MED) is quite similar to MSF. In MED, as shown in Figure 2.1b, the produced vapor from the seawater

is transferred into the next column where the vapor is condensed into liquid fresh water, and latent heat released is used to evaporate the slightly concentrated seawater. Finally, fresh water is obtained from numerous columns while remaining brines are discarded. In industry, advanced MED plants always have effects as many as possible, typically more than ten, to increase the internal energy recovery.[2, 3] Vapor compression (VC) is another widely used distillation technology. As shown in Figure 2.1c, centrifugal compressors are used in VC, which can both produce a vacuum in the distillation device to facilitate vaporization and increase the dew point to higher than the seawater boiling point. Therefore, vapor condensation accompanies vapor production from seawater to exploit the latent heat. In summary, MSF, MED and VC are basically all simple distillation methods but with condensation latent heat reuse to maximize the amount of water produced with a fixed amount of vapor and (thermal) energy input.

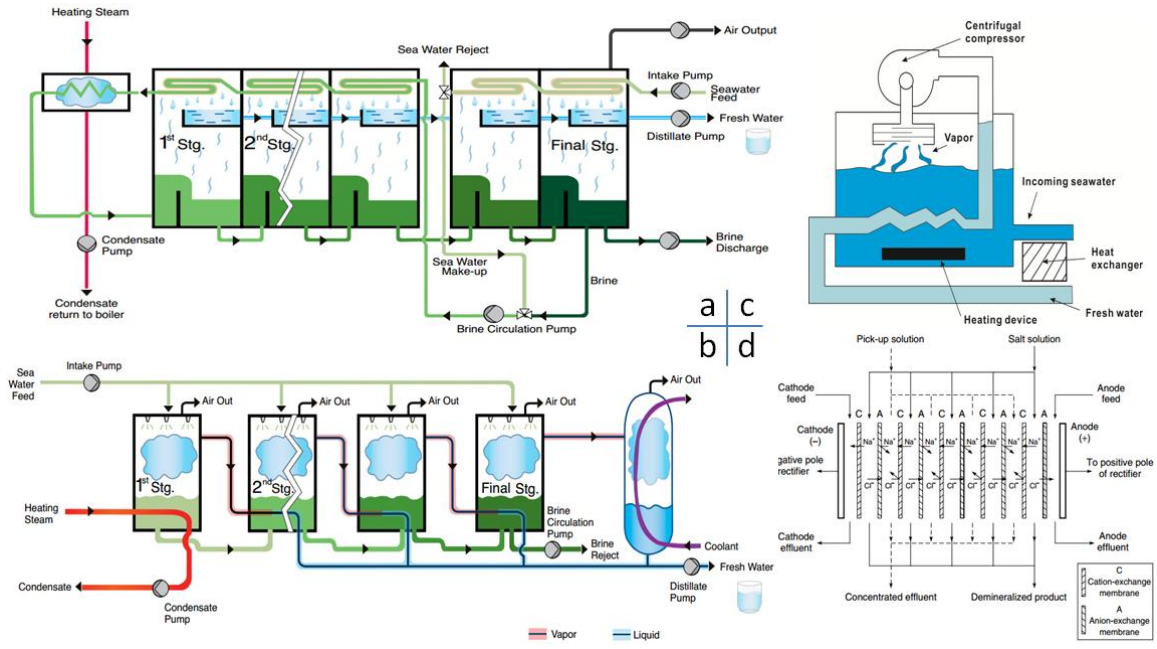

Figure 2.1 Schematic illustrations of (a) MSF, (b) MED, (c) VC and (d) ED. (a) and (b) are adapted from Ref.4. (d) is adapted from Ref.5.

2.1.2. Freezing desalination

Instead of boiling the seawater to produce vapor for desalination, decreasing the temperature below the melting point would also achieve desalination in that the salt is excluded during the ice crystal formation. Usually the seawater is cooled by the

evaporation of liquid hydrocarbon that can be reused by compression, and ice crystals are separated and washed, then melted to produce fresh water.[6] However, this technology has not been commercially developed.

2.1.3. Humidification-dehumidification

Humidification-dehumidification desalination technology is based on the saturated vapor pressure dependence on temperature. Air can contain tremendously more vapor at high temperatures (~80 ℃) than at room temperature. When hot seawater is exposed to air, distilled vapor is extracted by air and fresh water can be obtained by exposing the humid air to cool surface to condensate a portion of the vapor in the air.

2.1.4. Hydration

At proper temperatures and pressures, some small molecules (usually gases and hydrocarbon), either polar or non-polar, can form a clathrate crystal structure with water. In this ice-resembling crystal, the molecules are entrapped within a cage formed by water molecules. In the crystallization process, salt again, like in the freezing or evaporation desalination, is excluded. Water can be obtained by temperature or pressure modulation to sabotage the crystal and gases can be reused by compression. This technology is still under development albeit some researchers claim that this technology probably has higher comprehensive cost than that of MSF or RO.[7]

2.1.5. Electro-dialysis, microbial cell and other electric field related technologies

In an electro-dialysis (ED), the cation and anion exchange membranes are arranged in an alternating pattern between anode and cathode, as shown in Figure 2.1d. Cation exchange membrane allows the passage of cations while rejects the anions; anion exchange membrane allows the passage of anions while rejects the cations. When an electric potential is imposed between anode and cathode, cations in the brackish solution tends to migrate towards cathode while anions to anode. Due to the charge-selectivity of membranes, there will be alternating cells with depleted and enriched ions. Microbial cell is another unique desalination technology that derivates from ED. The difference is that in microbial cell, the electric current as driven force, is generated by bacterial on anode.

With the help of ion exchange membranes, salt-depletion zone can be produced. More information can be obtained elsewhere.[8] Capacitive desalination[9, 10] is an alternative electrically controlled method by utilizing the high specific surface area of electrodes. When the electrode is charged, ions would be adsorbed in the electrical double layer region to achieve desalination. Recently, a new electrically mediated desalination method was proposed.[11] Electric field gradient was used to redirect ions in the seawater to brine channel. Desalinated water bifurcates with brine at the depletion zone. However, only 25% of desalination can be achieved by this method although an incredibly low energy consumption of 25 Wh/m^3 was claimed.

2.1.6. Membrane distillation

Membrane distillation (MD) is a novel desalination method that uses distillation. However, unlike MSF and MED, the brackish water is only heated to 40-90 ℃ and a hydrophobic membrane is used to separate the hot brackish water from cold fresh water, sweep gas or even vacuum. The driving force is the imbalance of water vapor pressure across the membrane. The vapor can penetrate the hydrophobic membrane while liquid cannot, and vapor was transferred and condensed on the other side. More information about MD can be found in a published thorough review.[12]

2.1.7. Reverse osmosis

Reverse osmosis (RO) is currently the only technology that has been widely utilized in industry besides thermal distillation counterparts (MSF, MED, VC) in seawater desalination. In RO, external hydraulic pressure that was higher than osmotic pressure was imposed on seawater pushing fresh water to permeate through the RO membrane. Compared with thermal distillation technologies, the advantage of RO is the absence of water phase change and lower energy consumption. For example, the energy consumption of thermal distillation methods varies from 6~16 kWh/m^3 (thermal and electrical combined);[13] while for the state-of-the-art RO plant, the electrical energy consumption is 2-5 kWh/m^3.[14] This is very close to the theoretical minimum of 1.1 kWh/m^3 determined by thermodynamics. In fact, currently there is limited space for further reduction of energy consumption in the permeation process owing to the advent of

energy recovery devices,[15] and more focus is put on the energy minimization in pretreatment and post-treatment.[13] Admittedly, RO is now a very mature and advanced technology for seawater desalination, there are still some inevitable and inherent drawbacks. The first one is inevitable dependence on thorough pretreatment to alleviate fouling of membrane and prolong membrane longevity. This really complicates the entire desalination process and increases overall cost.[16] The second one is that RO is not suitable for treatment of brine with a higher salinity than seawater. This is because external hydraulic pressure requirement is proportional to osmotic pressure. Excessively high hydraulic pressure would challenge the robustness of membrane, valve and joint to increase operation cost as well as energy cost, and consequently make it impractical and less competitive to distillation methods.

2.1.8. Summary

Basically, almost all the proposed or developed desalination technologies can be categorized into either thermal, electrical or membrane methods. Others that do not fall into these categories including supercritical desalination,[17] hydration and solvent extraction[18] are still far from practicality. For the treatment of brackish water with low salinity, *e.g.*, lower than 2,000 ppm, the most suitable methods are the ED and microbial cell. For the treatment of more concentrated brackish water (*e.g.*, salinity between 2,000 ppm and 20,000 ppm), RO is the most suitable technology. For the seawater desalination, RO and thermal methods (MSF, MED and VC) share the market. RO has relatively lower energy consumption; while MSF and MED have lower requirement for pretreatment and no membrane replacement cost. However, currently only thermal distillation methods can treat brines that have a higher salinity than seawater, and obviously there is a technology gap in seawater and brine desalination.

2.2. The introduction of forward osmosis

2.2.1. The principles of forward osmosis

The development of forward osmosis (FO), or direct osmosis, is originated from the phenomenon of osmosis. Osmosis is a prevalent process that has been realized and utilized for a long time. For instance, the reason that only physiological saline rather than

fresh water is allowed to be injected into human body is because water osmosis into cells should be curbed to protect cells from bursting. Since the early days of human civilization, osmosis has been exploited to desiccate food for long term preservation.[19] From physical chemistry perspective, if solute is dissolved into pure water, the water chemical potential in solution is

$$\mu_A\,(T,p) = \mu_A^{\Theta}\,(T,p) + RT\ln(\gamma_A X_A) \qquad \text{(Equation 2.1)}$$

where $\mu_A{}^{\Theta}\,(T,p)$ is the chemical potential of pure water, R is the gas constant, T is the absolute temperature, γ_A is activity coefficient of water and X_A is the mole fraction of water. $\gamma_A X_A$ is also known as water activity α_w. Apparently, the water chemical potential in solution is lower than that of pure water since α_w is less than 1. Therefore, if the aqueous solution and pure water are separated by a semi-permeable membrane that rejects solute but allows the passage of water, water will automatically permeate from the fresh water side to the aqueous solution side driven by water chemical potential gradient. The water permeation stops when a proper hydraulic pressure is imposed on the side with lower water chemical potential, namely

$$\mu_A^{\Theta}(p, X_A = 1) = \mu_A(p + \Pi, X_A < 1) \qquad \text{(Equation 2.2)}$$

The imposed pressure, Π, is called osmotic pressure. For the rest part of this thesis, I define the side with higher water chemical potential (lower osmotic pressure) as feed solution, while the other side with lower water chemical potential (higher osmotic pressure) as draw solution.

Based on the presence of hydraulic pressure on the low chemical potential side and the water flux direction, the osmosis processes can be characterized into three categories, as shown in Figure 2.2. The FO process operates at absence of, or insignificant, external hydraulic pressure. When the hydraulic pressure is lower than that of osmotic pressure, water will still permeate from feed solution to draw solution despite the hydraulic pressure, and this process is called pressure retarded osmosis (PRO). PRO is mostly used for osmotic energy harvesting and more relevant information can be found elsewhere.[20-22] When the hydraulic pressure exceeds osmotic pressure, then water will be forced to

permeate against chemical potential gradient and this is the reverse osmosis (RO). Compared with RO, FO has many inherent advantages. The first one is that FO operates at no or low hydraulic pressure since FO is an osmotically driven process. Practically only a few bars of hydraulic pressure is needed to conquer the liquid flow resistance. Therefore, not only can FO essentially reduce the energy consumption as it operates under the osmotic driving force which is the intrinsic energy source among molecules without any external aid, such as heat or hydraulic pressure, but should have a much lower fouling propensity and the membrane in FO should be easier to clean. In addition, FO is more suitable than RO in handling solutions from pharmaceutical and food industries due to FO's lower fouling propensity and the feed solutes' probable sensitivity to pressure. Furthermore, due to the absence of hydraulic pressure, the requirement in robustness of membranes and other equipments is reduced to save cost.

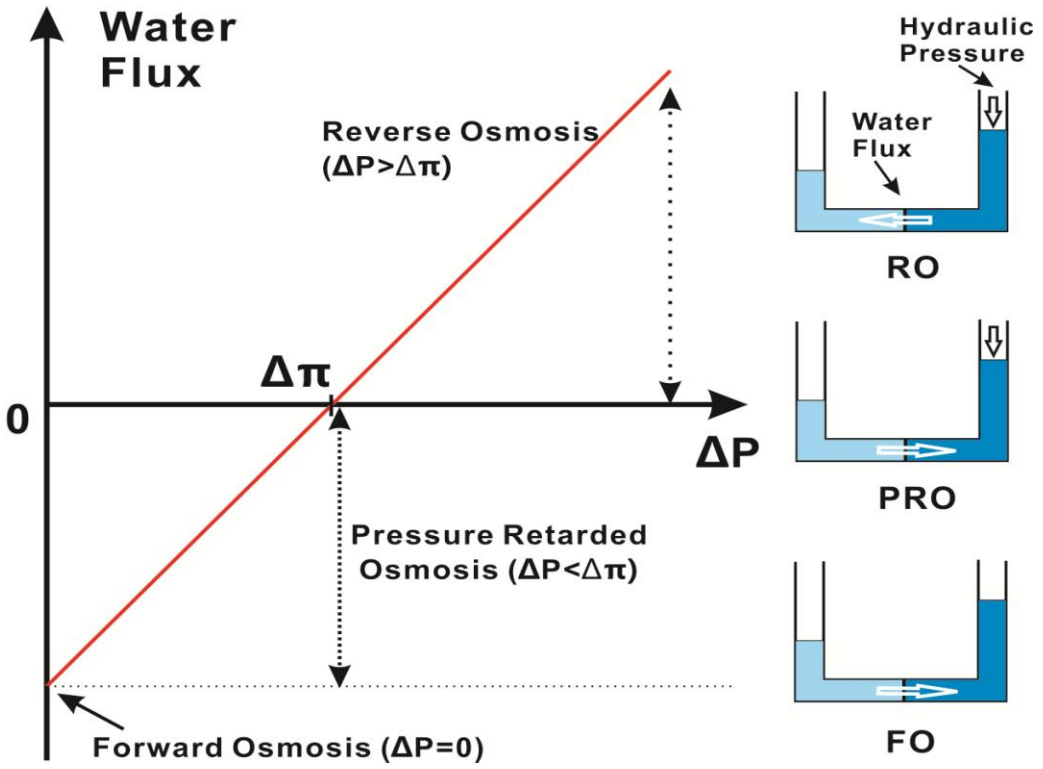

Figure 2.2 Schematic illustrations of RO, PRO and FO with the correlation between hydraulic pressure, osmotic pressure and water flux direction. ΔP and Δπ are the hydraulic pressure and osmotic pressure difference, respectively, between draw solution and feed solution.

2.2.2. Osmotic pressure

Forward osmosis is a water chemical potential gradient driven process, and an external hydraulic pressure equal to osmotic pressure exerted against water flux direction can stop the water permeation. Therefore, there must be a close correlation between water chemical potential and osmotic pressure. In practice, osmotic pressure is more widely used than water chemical potential in forward osmosis as pressure is always more tangible and easier to measure. As can be seen in equation 2.1 and 2.2, when the temperature is constant, water chemical potential is a function of pressure and water activity.

$$\mu_A = f(P, \alpha_w) \qquad \text{(Equation 2.3)}$$

When the osmotic pressure is exerted on the lower water chemical potential side, equilibrium is achieved and $d\mu_A=0$, namely

$$d\mu_A = \left(\frac{\partial \mu_A}{\partial P}\right) dP + \left(\frac{\partial \mu_A}{\partial \alpha_w}\right) d\alpha_w = 0 \qquad \text{(Equation 2.4)}$$

because $\left(\frac{\partial \mu_A}{\partial P}\right) = V_A$, $\left(\frac{\partial \mu_A}{\partial \alpha_w}\right) = \left(\frac{RT}{\alpha_w}\right)$, where V_A is the molar volume of water, therefore

$$V_A dp + \frac{RT}{\alpha_w} d\alpha_w = 0 \qquad \text{(Equation 2.5)}$$

If one integrates for α_w (from 1 to α_w) and P (from P to P+Π), then

$$-RT \int_1^{\alpha_w} d\ln(\alpha_w) = \int_P^{P+\pi} V_A \, dP \qquad \text{(Equation 2.6)}$$

If one takes molar volume of water as not a function of pressure (water is incompressible), and combined this with Equation 2.1, one obtains

$$\Pi V_A = -RT\ln\alpha_w = \mu_A^{\theta}(T, P) - \mu_A(T, P) \qquad \text{(Equation 2.7)}$$

Equation 2.7 incisively shows the correlation between water chemical potential reduction and osmotic pressure. For diluted solution of small molecular solute, $-\ln\alpha_w \approx N_B/N_A$, therefore from Equation 2.7, $N_BRT = N_AV_A\Pi \approx V\Pi$, we have

$$\Pi = \frac{N_BRT}{V} = C_BRT \qquad \text{(Equation 2.8)}$$

where C_B is the molar concentration of impermeable solute (mol/m^3). It is important to note that the osmotic pressure is a colligative property and it depends on the solute's concentration while has nothing to do with the specific nature of the solute. Equation 2.8 is only valid for diluted solutions with small molecular weight solutes. Thus, for the exact osmotic pressure measurement of draw solution that is always concentrated, other colligative properties like freezing point depression should be utilized.

2.2.3. Concentration polarization

According to the introduction above, FO is an osmotically driven process and the water flux in FO should be easily predicted to be

$$J_W = A\,(\Delta\Pi - \Delta P) \qquad \text{(Equation 2.9)}$$

where J_w is the water flux, A the FO membrane's water permeability, $\Delta\Pi$ the osmotic pressure difference (driving force) and ΔP the hydraulic pressure (resistant force) difference. However, in any membrane separation process including FO, water and solute permeate through membrane at tremendously different rates, concentration gradients form in the solutions on both sides of the membrane. This is known as concentration polarization (CP). Therefore, the predicted water flux determined by Equation 2.9 is always an overestimation because the actual osmotic pressure difference is lower than that between bulk draw solution and bulk feed solution.[23-25] Currently, all the FO membranes are asymmetric structure with a porous supportive layer and a thin dense selective layer on top. Thus, the membrane orientation in FO process would influence the osmotic pressure (or rather water chemical potential) gradient across the membrane. As shown in Figure 2.3a, when the porous layer is facing feed solution and selective layer is facing draw solution, which is called PRO mode, there are concentrative external CP and

dilutive external CP at the vicinities of membrane in the feed solution and draw solution side, respectively. Apart from that, concentration gradient will be also built in the porous supportive layer, which is called concentrative internal CP. Similarly, when the selective layer is facing feed solution, which is FO mode as shown in Figure 2.3b, there is dilutive

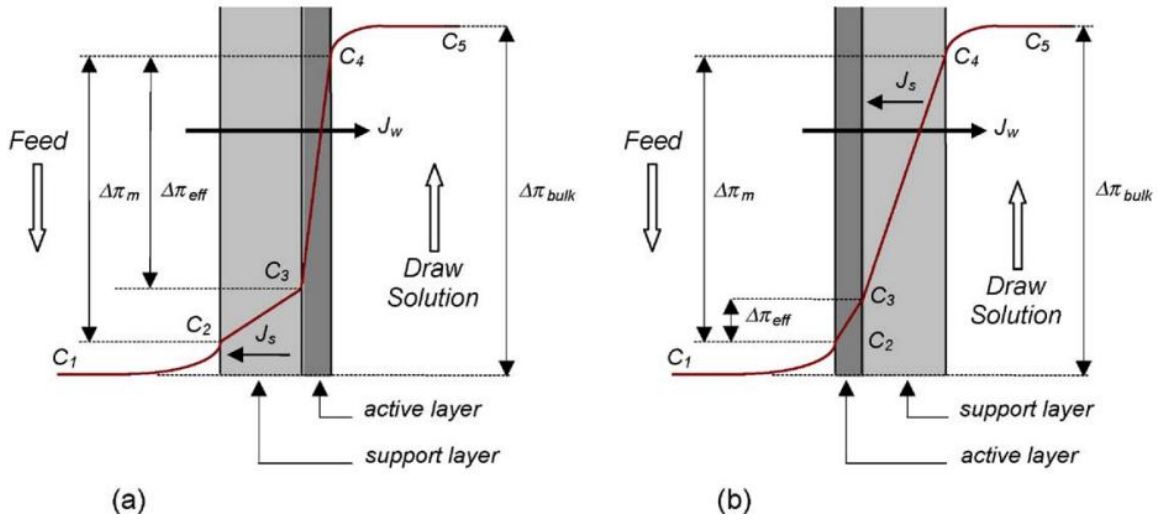

Figure 2.3 The concentration polarizations of (a) when selective layer faces draw solution and (b) when porous supportive layer faces draw solution. This figure is adapted from Ref.19

internal CP besides concentrative and dilutive external CPs in feed solution side and draw solution side, respectively. Both internal and external CP reduce the effective osmotic pressure difference and consequently reduce water flux. The external CP can be mitigated by increasing flow velocity and introducing turbulence on membrane surface, and external CP plays a minor role in FO and is not the main cause for the lower-than-expected water flux.[19] On the contrary, internal CP cannot be mitigated by turbulence and is the prim culprit for lower-than-expected water flux. Membranes with lower tortuosity and higher porosity would be preferred for internal CP mitigation. Apart from that, solute that has a high diffusion coefficient would be beneficial for mitigating CP. This can also help explain why the effective osmotic pressure difference and water flux in PRO mode is always higher than those in FO mode. NaCl is among the simplest salts and has a relatively higher diffusion coefficient, while draw solute, which always has much higher molecular weight, would assume a lower diffusion coefficient. Therefore, the concentrative internal CP in PRO mode is not as severe as dilutive internal CP in FO mode, which results a higher water flux in PRO mode.

2.3. The development of draw agents

As an indispensable part of FO technology, efficient draw agents that help decrease the draw solution's chemical potential to assist it absorb water from the feed solution are imperative. Depending on the application of the FO process, the draw agents can be categorized into two subgroups: for indirect desalination and for direct desalination.

2.3.1. Draw agents for indirect desalination

In the case of indirect desalination, either the diluted draw solution or the concentrated feed solution, or the water permeation process itself is the most important part. In this case, the draw agent recovery, namely the separation of draw agent from water, is not the key issue. NaCl is one of the draw agents that have been widely utilized for indirect desalination. Seawater can serve as the draw solution to concentrate impaired water (e.g., brackish water and municipal wastewater) and the consequent diluted seawater can be sent to RO plant as low energy seawater desalination.[26-29] Alternatively, RO brine can also serve as draw solution to dilute itself before discharge to conserve the marine environment.[30] Other indirect desalination applications of FO include using sugars for hydration bags;[19] using fertilizers for irrigation[31, 32] and using lignin sulfonate for desert restoration.[33] However, one of the inherent problems of directly exploiting diluted draw solution is that the concentration is too high and usage without dilution would not be practical.[32, 34] Recently, FO was also applied to replenish make-up water for a cooling tower.[35, 36] Water permeated from seawater or brackish water to dilute draw solution, and then the draw solution was re-concentrated by water evaporation in the cooling tower.

In summary, if FO is used for indirect desalination applications, the most important part is the direct application of diluted draw solution, concentrated feed solution or the FO process itself. The FO indirect desalination has limitations in application, albeit it imposes less strict requirements on draw agents.

2.3.2. Draw agents for direct desalination

If FO is used for direct desalination, as shown in Figure 2.4, the draw agent regeneration after FO process is inevitable and fresh water should be the product. This thesis focuses on the research of draw agents of FO for direct desalination.

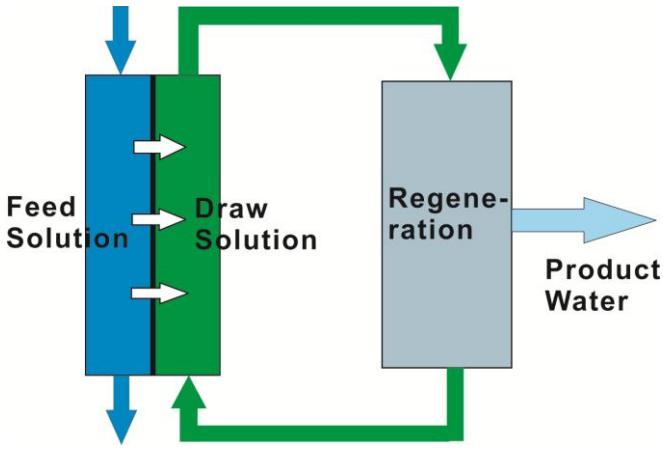

Figure 2.4 Illustration of FO for direct desalination application.

2.3.2.1. Inorganic salts

Inexpensive and easily commercially available inorganic salts including NaCl, $MgCl_2$, Na_2SO_4, $CaCl_2$, $(NH_4)_2SO_4$, $Ca(NO_3)_2$ and $KHCO_3$, *etc.*, have been studied as draw agents for direct desalination purpose.[37] FO desalination using these draw agents is more like a pretreatment step in a RO plant. Concentrated draw solution absorbs water from seawater, and separating water from draw agent relies only on RO, NF or membrane distillation. From process simplicity perspective, FO using these draw solutes is gaining no advantages over traditional seawater RO. However, the FO process rejects the foulants in seawater and draw agent regeneration needs no pretreatment and fears no fouling, at least in theory. In addition, it was claimed that if divalent salts were used as draw agents, less dense NF membrane instead of RO membrane can be used in regeneration. In fact, nowadays FO-NF or FO-RO hybrid system for seawater desalination attracts interests and more information can be found elsewhere.[38-40]

2.3.2.2. Polyelectrolytes

Linear poly (sodium acrylate) (PSA) has been tested as a draw agent for seawater desalination.[41] Initial water flux of ~5 LMH was achieved against seawater and NF was used for draw agent regeneration. Compared with conventional inorganic salts with small molecular weights, the polyelectrolyte's back diffusion into feed solution was much lower due to higher molecular weight. However, the viscosity of polyelectrolyte solution would cause problems of severe CP in FO and low efficiency in NF, and these adverse effects are more detrimental for polyelectrolytes with higher molecular weights.[42] Methods of copolymerization with thermally responsive polymer like PNIPAm would facilitate regeneration via MD or NF.[43, 44] However, non-polyelectrolyte polymers always generate insufficient osmotic pressure due to absence of couterions,[45-47] and copolymerization with non-polyelectrolyte would decrease the charge density in polyelectrolyte and result in a lower osmotic pressure.[48] Alternatively, dendrimer polyelectrolytes with similar osmotic pressure but lower viscosity compared with linear polyelectrolyte were possibly another group of candidates to improve performances.[49]

2.3.2.3. Organic salts

Organic salts can be deemed as electrolytes with molecular weights between those of typical inorganic salts and polyelectrolytes, roughly between 100 to 1000 g/mol. Draw agents of hexavalent phosphazene salts,[50] ethylenediamine tetrapropionic salts,[51] ethylenediamine tetraacetic salts,[52] zwitterions,[53] hydroacid complexes[54, 55] and ionic liquids[56] have been tested. Similar to polyelectrolyte, there regeneration depends on NF or MD and their role is to replace monovalent inorganic salts like NaCl as draw agent owing to lower back diffusion and comparable water flux. However, among the few researches on economics of these draw agents replacing NaCl, even the commercially available zwitterions were found to have higher replenishment cost than NaCl despite lower back diffusion,[53] and probably the replenishment cost would be even higher for those elaborately synthesized. Another important group of organic salts is surfactants. The relatively constant, though not very high, osmotic pressure at concentrations above the CMC is desirable in obtaining stable water flux, and a micellar solution has been applied in FO based membrane bioreactor.[57, 58]

2.3.2.4. Nanoparticles

Nanoparticles are particles with dimension between 1 nm to 100 nm. Draw agents of nanoparticles dispersing in water would theoretically produce no back diffusion since their dimension is larger than the voids between polymer chains in the nonporous FO membrane. Ionic species are always coated on the surface of nanoparticles to increase the osmotic pressure. For instance, Na^+ coated carbon quantum dots were found to be able to generate a water flux from seawater and MD was used in regeneration.[59] However, more research focus of using nanoparticles as draw agents has been put on paramagnetic nanoparticles. Hydrophilic polymers as well as polyelectrolytes were coated on Fe_3O_4 nanoparticle surface and interestingly magnetic field was applied in the draw agent regeneration.[60-65] Nanoparticle agglomeration in regeneration facilitates further water polishing process while it is a problem in FO process due to lower osmotic pressure. Small nanoparticles result in insufficient separation even under strong magnetic field while big nanoparticles result in irreversible agglomeration.[66] Apart from being regenerated by MD and magnetic fields, use of electric fields has also been studied as an option.[67]

2.3.2.5. Hydrogels

Hydrogels are crosslinked hydrophilic polymers with water entrapped within the networks. Li *et al.* for the first time applied hydrogels to serve as a novel group of draw agents. As shown in Figure 2.5, the draw solution side is no longer aqueous solution but semi-solution swollen hydrogels. In regeneration process, the water released is theoretically pure that exempts any further polishing steps since the crosslinked polymer networks do not dissolve in water. In addition, hydrogels as draw agents do not suffer from back diffusion problem. Although osmotic pressure does not apply to hydrogels, the hydrogel's swelling is still driven by water chemical potential gradient. Doubtlessly, hydrogel made of polyelectrolyte (*e.g.,* PSA) would generate a higher water flux than those made of non-polyelectrolytes (*e.g.,* PNIPAm), because the stronger interaction between polyelectrolyte network and water molecules would help decrease water chemical potential to a lower extent.[68] Nevertheless, this very interaction hinders water release for PSA hydrogels in regeneration process, while thermally responsive PNIPAm

hydrogels showed the best regeneration performance.[69] Copolymerization of NIPAm and sodium acrylate improved the water flux compared with neat PNIPAm hydrogel, but failed to preserve the thermosensitivity. Efforts for improving the hydrogels' regeneration performance included incorporation of dye, carbon particles, graphene and magnetic Fe_3O_4 nanoparticles into PNIPAm-PSA hydrogels and PNIPAm/PSA two layers structure,[70-74] but a great portion of the released water is still in vapor form and balanced reversible FO-regeneration cycles were never achieved.

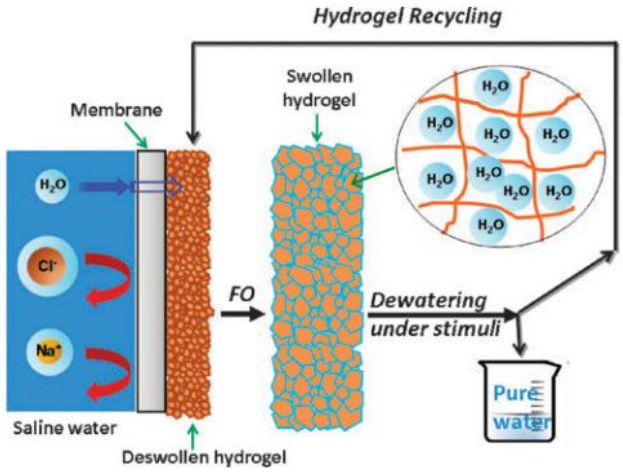

Figure 2.5 Schematic illustration of using hydrogels as draw agents for FO desalination.[69]

2.3.2.6. Draw agents regenerated by metathesis precipitation

Some inorganic salts including $CuSO_4$,[75] $MgSO_4$[76] and $Al_2(SO_4)_3$[77] have been tested as draw agents not being regenerated by NF but by metathesis precipitation. Barium hydroxide or calcium oxide was dosed into diluted draw solution to precipitate the draw agents. After filtration of solid, sulfuric acid was introduced to recover the draw agent. Basically high water quality can be obtained, but the large amount of alkaline and acid needed makes these draw agents infeasible and uneconomic.

2.3.2.7. CO_2-NH_3 system

CO_2-NH_3 system is probably the most widely studied draw agent for FO desalination due to its simplicity and desirable performance. Carbon dioxide and ammonia can form a series of thermolytic salts that generate a high osmotic pressure, which can also be easily

regenerated by heating into gases.[78, 79] Due to the low solubility of ammonium bicarbonate, the molar ratio of ammonia to carbon dioxide is always higher than 1 to form more soluble salts like ammonium carbonate and ammonium carbamate conferring an alkaline pH on the draw solution.[80] There are still some formidable problems haunting this draw agent. Apart from the high pH that may result in a membrane endurance issue and scaling problem, the complete removal of ammonia residue from product water is a critical issue since trace amount of ammonia in water may preclude the water from meeting stringent drinking standards. Recently, a volatile amine has replaced ammonia in this system to reduce the draw agent back diffusion, while its advantages and drawbacks are still similar with that of the CO_2-NH_3 system.[81]

2.3.2.8. Switchable polarity solvent

Switchable polarity solvent is a novel class of draw agent that is mainly tertiary amine with a small molecular weight.[82-84] The most evident advantage of these draw agents is that the compromise between the ability to generate high osmotic pressure (hydrophilicity) and ease of regeneration (hydrophobicity) does not need to be achieved in the molecular structure design. The original (deprotonated) draw agent is basically hydrophobic with a limited solubility in water (*e.g.*, 20 g/L). Upon reaction with CO_2, the tertiary amine is protonated and becomes a hydrophilic salt that can generate a high osmotic pressure. The regeneration is achieved by removal of CO_2 by inert gas sweeping at high temperature (*e.g.*, 60℃). Switchable polarity solvent is a quite promising draw agent albeit some of its problems, including corroding and swelling the membrane as well as CO_2 recyclable use (efficient separation from inert sweeping gas), need to be conquered.

2.3.2.9. LCST type small molecular non-electrolyte

Contrary to the switchable polarity solvent introduced in previous section, the LCST type small molecular non-electrolyte[85-88] is an apotheosis in achieving the subtle balance between hydrophilicity and hydrophobicity. Superior to LCST type polymers like PNIPAm, these draw agents can achieve a higher osmotic pressure owing to their lower molecular weights. In regeneration, the draw solution would undergo a phase separation at a temperature above the lower critical solution temperature (LCST) to facilitate draw

agent reuse and water polishing. However, due to the nature of non-electrolyte and absence of counterions, their drawing ability is still too low for seawater desalination.

2.4. Summary

Improving desalination technology is a vital part of alleviating water scarcity, which is a severe threat to human society sustainable development. Among all the mature desalination technologies, there is an obvious gap for energy-efficient seawater and brine treatment. Forward osmosis is a promising technology to fill in the gap because it is an automatic process driven by water chemical potential gradient with no external energy input. The development of a suitable draw agent holds the key to fulfill the promised mission of FO.

For direct desalination applications where fresh water is the final product, a suitable draw agent is even more imperative in that energy needs to be consumed in the regeneration process. A suitable draw agent should (1) generate high enough osmotic pressure and (2) be easily regenerated. In addition, other criteria including (3) being benign to FO membrane, (4) having low or no back diffusion, (5) being no toxic to human being and environment and (6) being inexpensive should be met. Developing a suitable draw agent is a challenging task. Currently no draw agent is perfect but some may be successful in a specific situation. Overall, non-responsive draw agents (e.g., polyelectrolyte, NaCl, $MgCl_2$, small organic salts, *etc.*) might not be hopeful in realizing the promised advantages of FO for direct desalination since their osmotic pressure after FO is higher than that of feed solution and their regeneration solely depends on NF, RO or MD, which imparts them no process simplicity or reduced energy cost over directly treating feed solution with RO and MD. Responsive draw agents, on the other hand, can respond to external stimuli and reduce their concentrations in draw solution after the FO process. Methods of RO, NF or MD in regeneration are mainly for water quality polishing instead of draw agent recovery. Draw agents of responsive hydrogel can even exempt the regeneration step since the water released under external stimuli is theoretically pure. Therefore, FO direct desalination enabled by responsive draw agents probably can be a promising technology to treat seawater or brine with a low energy cost.

References

1. El-Dessouky, H. T.; Ettouney, H. M.; Al-Roumi, Y., Multi-stage flash desalination: present and future outlook. Chemical Engineering Journal 1999, 73, (2), 173-190.

2. Khawaji, A. D.; Kutubkhanah, I. K.; Wie, J.-M., Advances in seawater desalination technologies. Desalination 2008, 221, (1), 47-69.

3. He, T. X.; Yan, L. J., Application of alternative energy integration technology in seawater desalination. Desalination 2009, 249, (1), 104-108.

4. Ruhrpumpen brochure, Desalination: Reverse Osmosis, Mult-stage Flash and Multi-Effect Distillation; Ruhrpumpen Corporation: 2011.

5. Baker, R. W., Membrane Technology and Applications,Second Edition. Wiley Online Library: 2004.

6. Rich, A.; Mandri, Y.; Bendaoud, N.; Mangin, D.; Abderafi, S.; Bebon, C.; Semlali, N.; Klein, J.-P.; Bounahmidi, T.; Bouhaouss, A., Freezing desalination of sea water in a static layer crystallizer. Desalination and Water Treatment 2010, 13, (1-3), 120-127.

7. Javanmardi, J.; Moshfeghian, M., Energy consumption and economic evaluation of water desalination by hydrate phenomenon. Applied thermal engineering 2003, 23, (7), 845-857.

8. Cao, X.; Huang, X.; Liang, P.; Xiao, K.; Zhou, Y.; Zhang, X.; Logan, B. E., A new method for water desalination using microbial desalination cells. Environmental science & technology 2009, 43, (18), 7148-7152.

9. Welgemoed, T.; Schutte, C., Capacitive deionization technology™: an alternative desalination solution. Desalination 2005, 183, (1), 327-340.

10. Oren, Y., Capacitive deionization (CDI) for desalination and water treatment—past, present and future (a review). Desalination 2008, 228, (1), 10-29.

11. Knust, K. N.; Hlushkou, D.; Anand, R. K.; Tallarek, U.; Crooks, R. M., Electrochemically mediated seawater desalination. Angewandte Chemie International Edition 2013, 52, (31), 8107-8110.

12. Alkhudhiri, A.; Darwish, N.; Hilal, N., Membrane distillation: A comprehensive review. Desalination 2012, 287, 2-18.

13. Liyanaarachchi, S.; Shu, L.; Muthukumaran, S.; Jegatheesan, V.; Baskaran, K., Problems in seawater industrial desalination processes and potential sustainable solutions: a review. Reviews in Environmental Science and Bio/Technology 2013, 13, (2), 203-214.

14. Ghalavand, Y.; Hatamipour, M. S.; Rahimi, A., A review on energy consumption of desalination processes. Desalination and Water Treatment 2014, 1-16.

15. Elimelech, M.; Phillip, W. A., The future of seawater desalination: energy, technology, and the environment. Science 2011, 333, (6043), 712-717.

16. Kim, Y. M.; Kim, S. J.; Kim, Y. S.; Lee, S.; Kim, I. S.; Kim, J. H., Overview of systems engineering approaches for a large-scale seawater desalination plant with a reverse osmosis network. Desalination 2009, 238, (1), 312-332.

17. Leusbrock, I. Removal of inorganic compounds via supercritical water: fundamentals and applications, University of groningen, 2011.

18. Bajpayee, A.; Luo, T.; Muto, A.; Chen, G., Very low temperature membrane-free desalination by directional solvent extraction. Energy Environ. Sci. 2011, 4, (5), 1672-1675.

19. Cath, T.; Childress, A.; Elimelech, M., Forward osmosis: Principles, applications, and recent developments. Journal of Membrane Science 2006, 281, (1-2), 70-87.

20. Achilli, A.; Childress, A. E., Pressure retarded osmosis: From the vision of Sidney Loeb to the first prototype installation—Review. Desalination 2010, 261, (3), 205-211.

21. Yip, N. Y.; Elimelech, M., Thermodynamic and energy efficiency analysis of power generation from natural salinity gradients by pressure retarded osmosis. Environmental science & technology 2012, 46, (9), 5230-5239.

22. Helfer, F.; Lemckert, C.; Anissimov, Y. G., Osmotic power with Pressure Retarded Osmosis: Theory, performance and trends–A review. Journal of Membrane Science 2014, 453, 337-358.

23. Mehta, G. D.; Loeb, S., Internal polarization in the porous substructure of a semipermeable membrane under pressure-retarded osmosis. Journal of Membrane Science 1979, 4, 261-265.

24. Loeb, S.; Titelman, L.; Korngold, E.; Freiman, J., Effect of porous support fabric on osmosis through a Loeb-Sourirajan type asymmetric membrane. Journal of Membrane Science 1997, 129, (2), 243-249.

25. Seppälä, A.; Lampinen, M. J., On the non-linearity of osmotic flow. Experimental thermal and fluid science 2004, 28, (4), 283-296.

26. Cath, T. Y.; Hancock, N. T.; Lundin, C. D.; Hoppe-Jones, C.; Drewes, J. E., A multi-barrier osmotic dilution process for simultaneous desalination and purification of impaired water. Journal of Membrane Science 2010, 362, (1), 417-426.

27. Klaysom, C.; Cath, T. Y.; Depuydt, T.; Vankelecom, I. F., Forward and pressure retarded osmosis: potential solutions for global challenges in energy and water supply. Chem Soc Rev 2013, 42, (16), 6959-6989.

28. Bamaga, O.; Yokochi, A.; Beaudry, E., Application of forward osmosis in pretreatment of seawater for small reverse osmosis desalination units. Desalination and Water Treatment 2009, 5, (1-3), 183-191.

29. Xue, W.; Tobino, T.; Nakajima, F.; Yamamoto, K., Seawater-driven forward osmosis for enriching nitrogen and phosphorous in treated municipal wastewater: effect of membrane properties and feed solution chemistry. Water Res 2015, 69, 120-130.

30. Hoover, L. A.; Phillip, W. A.; Tiraferri, A.; Yip, N. Y.; Elimelech, M., Forward with osmosis: emerging applications for greater sustainability. Environ Sci Technol 2011, 45, (23), 9824-9830.

31. Majeed, T.; Sahebi, S.; Lotfi, F.; Kim, J. E.; Phuntsho, S.; Tijing, L. D.; Shon, H. K., Fertilizer-drawn forward osmosis for irrigation of tomatoes. Desalination and Water Treatment 2014, 53, (10), 2746-2759.

32. Phuntsho, S.; Shon, H. K.; Hong, S.; Lee, S.; Vigneswaran, S.; Kandasamy, J., Fertiliser drawn forward osmosis desalination: the concept, performance and limitations for fertigation. Reviews in Environmental Science and Bio/Technology 2011, 11, (2), 147-168.

33. Duan, J.; Litwiller, E.; Choi, S.-H.; Pinnau, I., Evaluation of sodium lignin sulfonate as draw solute in forward osmosis for desert restoration. Journal of Membrane Science 2014, 453, 463-470.

34. Liu, P.; Gao, B.; Shon, H. K.; Ma, D.; Rong, H.; Zhao, P.; Zhao, S.; Yue, Q.; Li, Q., Water flux behavior of blended solutions of ammonium bicarbonate mixed with eight salts respectively as draw solutions in forward osmosis. Desalination 2014, 353, 39-47.

35. Nicoll, P. G.; Thompson, N. A.; Bedford, M. R. In Manipulated Osmosis Applied To Evaporative Cooling Make-Up Water–Revolutionary Technology, Proceedings IDA World Congress, Perth, Western Australia, 2011; 2011.

36. Wang, W.; Zhang, Y.; Esparra-Alvarado, M.; Wang, X.; Yang, H.; Xie, Y., Effects of pH and temperature on forward osmosis membrane flux using rainwater as the makeup for cooling water dilution. Desalination 2014, 351, 70-76.

37. Achilli, A.; Cath, T. Y.; Childress, A. E., Selection of inorganic-based draw solutions for forward osmosis applications. Journal of Membrane Science 2010, 364, (1-2), 233-241.

38. Bamaga, O.; Yokochi, A.; Zabara, B.; Babaqi, A., Hybrid FO/RO desalination system: Preliminary assessment of osmotic energy recovery and designs of new FO membrane module configurations. Desalination 2011, 268, (1), 163-169.

39. Zhao, S.; Zou, L.; Mulcahy, D., Brackish water desalination by a hybrid forward osmosis–nanofiltration system using divalent draw solute. Desalination 2012, 284, 175-181.

40. Tan, C.; Ng, H., A novel hybrid forward osmosis-nanofiltration (FO-NF) process for seawater desalination: draw solution selection and system configuration. Desalination and Water Treatment 2010, 13, (1-3), 356-361.

41. Ge, Q.; Su, J.; Amy, G. L.; Chung, T. S., Exploration of polyelectrolytes as draw solutes in forward osmosis processes. Water Res 2012, 46, (4), 1318-1326.

42. Tian, E.; Hu, C.; Qin, Y.; Ren, Y.; Wang, X.; Wang, X.; Xiao, P.; Yang, X., A study of poly (sodium 4-styrenesulfonate) as draw solute in forward osmosis. Desalination 2015, 360, 130-137.

43. Ou, R.; Wang, Y.; Wang, H.; Xu, T., Thermo-sensitive polyelectrolytes as draw solutions in forward osmosis process. Desalination 2013, 318, 48-55.

44. Zhao, D.; Wang, P.; Zhao, Q.; Chen, N.; Lu, X., Thermoresponsive copolymer-based draw solution for seawater desalination in a combined process of forward osmosis and membrane distillation. Desalination 2014, 348, 26-32.

45. Sarp, S.; Lee, S.; Park, K.; Park, M.; Kim, J. H.; Cho, J., Using macromolecules as osmotically active compounds in osmosis followed by filtration (OF) system. Desalination and Water Treatment 2012, 43, (1-3), 131-137.

46. Jun, B.-M.; Nguyen, T. P. N.; Ahn, S.-H.; Kim, I.-C.; Kwon, Y.-N., The application of polyethyleneimine draw solution in a combined forward osmosis/nanofiltration system. Journal of Applied Polymer Science 2015, 132, (27), n/a-n/a.

47. Zhao, P.; Gao, B.; Yue, Q.; Kong, J.; Shon, H. K.; Liu, P.; Gao, Y., Explore the forward osmosis performance using hydrolyzed polyacrylamide as draw solute for dye wastewater reclamation in the long-term process. Chemical Engineering Journal 2015, 273, 316-324.

48. Kim, J.-j.; Chung, J.-S.; Kang, H.; Yu, Y. A.; Choi, W. J.; Kim, H. J.; Lee, J.-C., Thermo-responsive copolymers with ionic group as novel draw solutes for forward osmosis processes. Macromolecular Research 2014, 22, (9), 963-970.

49. Zhao, D.; Chen, S.; Wang, P.; Zhao, Q.; Lu, X., A Dendrimer-Based Forward Osmosis Draw Solute for Seawater Desalination. Industrial & Engineering Chemistry Research 2014, 53, (42), 16170-16175.

50. Stone, M. L.; Wilson, A. D.; Harrup, M. K.; Stewart, F. F., An initial study of hexavalent phosphazene salts as draw solutes in forward osmosis. Desalination 2013, 312, 130-136.

51. Long, Q.; Qi, G.; Wang, Y., Synthesis and application of ethylenediamine tetrapropionic salt as a novel draw solute for forward osmosis application. AIChE Journal 2015, 61, (4), 1309-1321.

52. Hau, N. T.; Chen, S.-S.; Nguyen, N. C.; Huang, K. Z.; Ngo, H. H.; Guo, W., Exploration of EDTA sodium salt as novel draw solution in forward osmosis process for dewatering of high nutrient sludge. Journal of Membrane Science 2014, 455, 305-311.

53. Lutchmiah, K.; Lauber, L.; Roest, K.; Harmsen, D. J. H.; Post, J. W.; Rietveld, L. C.; van Lier, J. B.; Cornelissen, E. R., Zwitterions as alternative draw solutions in forward osmosis for application in wastewater reclamation. Journal of Membrane Science 2014, 460, 82-90.

54. Ge, Q.; Chung, T. S., Hydroacid complexes: a new class of draw solutes to promote forward osmosis (FO) processes. Chem Commun (Camb) 2013, 49, (76), 8471-8473.

55. Ge, Q.; Chung, T.-S., Oxalic acid complexes: promising draw solutes for forward osmosis (FO) in protein enrichment. Chem Commun (Camb) 2015, 51, (23), 4854-4857.

56. Yen, S. K.; Mehnas Haja N, F.; Su, M.; Wang, K. Y.; Chung, T.-S., Study of draw solutes using 2-methylimidazole-based compounds in forward osmosis. Journal of Membrane Science 2010, 364, (1-2), 242-252.

57. Roach, J. D.; Al-Abdulmalek, A.; Al-Naama, A.; Haji, M., Use of Micellar Solutions as Draw Agents in Forward Osmosis. Journal of Surfactants and Detergents 2014, 17, (6), 1241-1248.

58. Gadelha, G.; Nawaz, M. S.; Hankins, N. P.; Khan, S. J.; Wang, R.; Tang, C. Y., Assessment of micellar solutions as draw solutions for forward osmosis. Desalination 2014, 354, 97-106.

59. Guo, C. X.; Zhao, D.; Zhao, Q.; Wang, P.; Lu, X., Na(+)-functionalized carbon quantum dots: a new draw solute in forward osmosis for seawater desalination. Chem Commun (Camb) 2014, 50, (55), 7318-7321.

60. Ling, M. M.; Chung, T. S.; Lu, X., Facile synthesis of thermosensitive magnetic nanoparticles as "smart" draw solutes in forward osmosis. Chem Commun (Camb) 2011, 47, (38), 10788-10790.

61. Ling, M. M.; Chung, T.-S., Desalination process using super hydrophilic nanoparticles via forward osmosis integrated with ultrafiltration regeneration. Desalination 2011, 278, (1-3), 194-202.

62. Ling, M. M.; Wang, K. Y.; Chung, T.-S., Highly water-soluble magnetic nanoparticles as novel draw solutes in forward osmosis for water reuse. Industrial & Engineering Chemistry Research 2010, 49, (12), 5869-5876.

63. Bai, H.; Liu, Z.; Sun, D. D., Highly water soluble and recovered dextran coated Fe3O4 magnetic nanoparticles for brackish water desalination. Separation and Purification Technology 2011, 81, (3), 392-399.

64. Ge, Q.; Su, J.; Chung, T.-S.; Amy, G., Hydrophilic superparamagnetic nanoparticles: synthesis, characterization, and performance in forward osmosis processes. Industrial & Engineering Chemistry Research 2010, 50, (1), 382-388.

65. Zhao, Q.; Chen, N.; Zhao, D.; Lu, X., Thermoresponsive magnetic nanoparticles for seawater desalination. ACS Appl Mater Interfaces 2013, 5, (21), 11453-11461.

66. Kim, Y. C.; Han, S.; Hong, S., A feasibility study of magnetic separation of magnetic nanoparticle for forward osmosis. Water Science & Technology 2011, 64, (2), 469.

67. Ling, M. M.; Chung, T.-S., Surface-dissociated nanoparticle draw solutions in forward osmosis and the regeneration in an integrated electric field and nanofiltration system. Industrial & Engineering Chemistry Research 2012, 51, (47), 15463-15471.

68. Luo, H.; Wang, Q.; Tao, T.; Zhang, T. C.; Zhou, A., Performance of Strong Ionic Hydrogels Based on 2-Acrylamido-2-Methylpropane Sulfonate as Draw Agents for Forward Osmosis. Journal of Environmental Engineering 2014, 140, (12), 04014044.

69. Li, D.; Zhang, X.; Yao, J.; Simon, G. P.; Wang, H., Stimuli-responsive polymer hydrogels as a new class of draw agent for forward osmosis desalination. Chem Commun (Camb) 2011, 47, (6), 1710-1712.

70. Li, D.; Zhang, X.; Yao, J.; Zeng, Y.; Simon, G. P.; Wang, H., Composite polymer hydrogels as draw agents in forward osmosis and solar dewatering. Soft Matter 2011, 7, (21), 10048-10056.

71. Zeng, Y.; Qiu, L.; Wang, K.; Yao, J.; Li, D.; Simon, G. P.; Wang, R.; Wang, H., Significantly enhanced water flux in forward osmosis desalination with polymer-graphene composite hydrogels as a draw agent. RSC Adv. 2013, 3, (3), 887-894.

72. Razmjou, A.; Barati, M. R.; Simon, G. P.; Suzuki, K.; Wang, H., Fast deswelling of nanocomposite polymer hydrogels via magnetic field-induced heating for emerging FO desalination. Environ Sci Technol 2013, 47, (12), 6297-6305.

73. Razmjou, A.; Liu, Q.; Simon, G. P.; Wang, H., Bifunctional polymer hydrogel layers as forward osmosis draw agents for continuous production of fresh water using solar energy. Environ Sci Technol 2013, 47, (22), 13160-13166.

74. Ao, X.; Li, D.; Simon, G.; Wang, H., Dye-incorporated polymer hydrogels as draw agents in forward osmosis desalination. In CHEMECA, Wellington, New Zealand, 2012.

75. Alnaizy, R.; Aidan, A.; Qasim, M., Copper sulfate as draw solute in forward osmosis desalination. Journal of Environmental Chemical Engineering 2013, 1, (3), 424-430.

76. Alnaizy, R.; Aidan, A.; Qasim, M., Draw solute recovery by metathesis precipitation in forward osmosis desalination. Desalination and Water Treatment 2013, 51, (28-30), 5516-5525.

77. Liu, Z.; Bai, H.; Lee, J.; Sun, D. D., A low-energy forward osmosis process to produce drinking water. Energy & Environmental Science 2011, 4, (7), 2582-2585.

78. McCutcheon, J. R.; McGinnis, R. L.; Elimelech, M., A novel ammonia—carbon dioxide forward (direct) osmosis desalination process. Desalination 2005, 174, (1), 1-11.

79. McCutcheon, J. R.; McGinnis, R. L.; Elimelech, M., Desalination by ammonia–carbon dioxide forward osmosis: influence of draw and feed solution concentrations on process performance. Journal of Membrane Science 2006, 278, (1), 114-123.

80. McGinnis, R. L.; Hancock, N. T.; Nowosielski-Slepowron, M. S.; McGurgan, G. D., Pilot demonstration of the NH3/CO2 forward osmosis desalination process on high salinity brines. Desalination 2013, 312, 67-74.

81. Boo, C.; Khalil, Y. F.; Elimelech, M., Performance evaluation of trimethylamine–carbon dioxide thermolytic draw solution for engineered osmosis. Journal of Membrane Science 2015, 473, 302-309.

82. Stone, M. L.; Rae, C.; Stewart, F. F.; Wilson, A. D., Switchable polarity solvents as draw solutes for forward osmosis. Desalination 2013, 312, 124-129.

83. Wilson, A. D.; Orme, C. J., Concentration dependent speciation and mass transport properties of switchable polarity solvents. RSC Advances 2015, 5, (10), 7740-7751.

84. Wilson, A. D.; Stewart, F. F., Structure–function study of tertiary amines as switchable polarity solvents. RSC Advances 2014, 4, (22), 11039-11049.

85. Mok, Y.; Nakayama, D.; Noh, M.; Jang, S.; Kim, T.; Lee, Y., Circulatory osmotic desalination driven by a mild temperature gradient based on lower critical solution temperature (LCST) phase transition materials. Phys Chem Chem Phys 2013, 15, (44), 19510-19517.

86. Noh, M.; Mok, Y.; Lee, S.; Kim, H.; Lee, S. H.; Jin, G. W.; Seo, J. H.; Koo, H.; Park, T. H.; Lee, Y., Novel lower critical solution temperature phase transition materials effectively control osmosis by mild temperature changes. Chem Commun (Camb) 2012, 48, (32), 3845-3847.

87. Nakayama, D.; Mok, Y.; Noh, M.; Park, J.; Kang, S.; Lee, Y., Lower critical solution temperature (LCST) phase separation of glycol ethers for forward osmotic control. Phys Chem Chem Phys 2014, 16, (11), 5319-5325.

88. Jorgensen, M. K. Investigation of Polypropylene Glycol 425 as Possible Draw Solution for Forward Osmosis. Aalborg University, Aalborg, 2009.

3. Experimental Methodology

In this chapter, the materials syntheses and characterizations are described in details. In addition, the measurements of water flux, draw agent back diffusion and salt rejection in the FO process are thoroughly introduced and the mechanism of using cryoscopic method in measuring osmolality is discussed.

3.1. Synthesis of responsive draw agents

Four types of responsive draw agents, including semi-interpenetrating network (semi-IPN) hydrogels, polyionic liquid hydrogels, dual responsive polymers and thermally responsive ionic liquids were synthesized in this thesis. Semi-IPN hydrogels were synthesized by polymerization and crosslinking of NIPAm in the presence of polyvinyl alcohol (PVA) or PSA. The sum of monomer concentration and PSA or PVA repeating unit concentration is 1M. The amount of initiator, crosslinker and accelerator is 1 mol%, 2 mol% and 1 mol%, respectively, with respect to the amount of monomer. The polyionic liquid hydrogels were synthesized by bulk polymerization of the ionic liquid monomer(s). The amount of initiator and crosslinker were 1 mol% and 2 mol% to that of monomer(s), respectively. The dual responsive poly [2-(dimethylamino)ethyl methacrylate] (PDMAEMA) with narrow molecular weight distribution was synthesized by atom transfer radical polymerization (ATRP) to better study the influence of molecular weight on the performance.

3.1.1. Synthesis of SI-0.2PSA semi-IPN hydrogel

0.376 g dried prepared poly sodium acrylate (PSA) and 1.808 g of N-isopropylacrylamide (NIPAm) were dissolved into deionized (DI) water to make a 20 ml homogeneous solution under stirring. 49.3 mg of N,N'-methylenebisacrylamide (MBA) and 18.6 mg of *N*,*N*,*N*',*N*'-tetramethylethylenediamine (TEMED) were then added into the solution and nitrogen was bubbled for 15 minutes to remove the oxygen before 36.5 mg of ammonium persulfate (APS) was added to initiate the polymerization. The polymerization was

conducted at room temperature in sealed vials for 24 hours. After that, hydrogel was thoroughly washed with DI water, dried and pulverized.

3.1.2. Synthesis of SI-0.2PVA semi-IPN hydrogel

0.176 g poly vinyl alcohol (PVA) and 1.808 g NIPAm were dissolved into DI water to make a 20 ml homogeneous solution under stirring at 70 ℃. After cooling to room temperature, 49.3 mg of MBA and 18.6 mg of TEMED were then added into the solution and nitrogen was bubbled for 15 minutes to remove the oxygen before 36.5 mg of APS was added to initiate the polymerization. The polymerization was conducted at room temperature in sealed vials for 24 hours. After that, the hydrogel was thoroughly washed with DI water, dried and pulverized.

3.1.3. Synthesis of SI-0.5PVA semi-IPN hydrogel

0.440 g PVA and 1.130 g NIPAm were dissolved into DI water to make a 20 ml homogeneous solution under stirring at 70 ℃. After cooling to room temperature, 30.8 mg of MBA and 11.6 mg of TEMED were then added into the solution and nitrogen was bubbled for 15 minutes to remove the oxygen before 22.8 mg of APS was added to initiate the polymerization. The polymerization was conducted at room temperature in sealed vials for 24 hours. After that, the hydrogel was thoroughly washed with DI water, dried and pulverized.

3.1.4. Synthesis of tetrabutyl phosphonium p-styrenesulfonate (P4444 SS) and tributylhexyl phosphonium p-styrenesulfonate (P4446 SS)

P4444 SS was synthesized by ion exchange. 20 g of tetrabutylphophonium bromide and 17.7 g of sodium *p*-styrenesulfonate were dissolved in 30 ml DI water and the homogeneous solution was stirred for 24 hours before 80 ml of dichloromethane was added to extract the ionic liquid. The dichloromethane phase was washed with 20 ml DI water for three times. The synthesis of P4446 SS was conducted in a similar method. 20 g of tributyl-hexyl phosphonium bromide and 16.3 g of sodium *p*-styrenesulfonate were dissolved into 30 ml water. The solution turned into opaque suspension since P4446 SS is

hydrophobic. After 24 hours stirring, the ionic liquid was extracted by 80 ml dichloromethane and washed with 20 ml DI water for three times. The majority of dichloromethane was evaporated by rotary evaporator and the rest trace amount was removed in high vacuum (<0.1 mbar) at room temperature for 72 hours.

3.1.5. Synthesis of poly (P4444 SS) and poly (P444-6 SS) hydrogels

For the synthesis of polyionic liquid hydrogel poly(P4444 SS), 44.8 mg of polyethylene glycol dimethacrylate and 20.6 mg of benzophenone were dissolved in 5 g P4444 SS. The homogeneous solution was purged with N_2 for 15 minutes and the polymerization was conducted under UV (365 nm, 54 mW/cm^2) for 2 hours. For the synthesis of polyionic liquid hydrogel poly(P444-6 SS), 1.05 g of P4446 SS, 44.2 mg of polyethylene glycol dimethacrylate and 20.3 mg of benzophenone were dissolved into 3.95 g P4444 SS. The homogeneous solution was purged with N_2 for 15 minutes and the polymerization was conducted under UV (365 nm, 54 mW/cm^2) for 2 hours. Both hydrogels were thoroughly washed with DI water, dried and pulverized.

3.1.6. Synthesis of poly[2-(dimethylamino)ethyl methacrylate] (PDMAEMA)

Atom transfer radical polymerization of DMAEMA was carried out in the solvent of tetrahydrofuran (THF) using 1,1,4,7,10,10-hexamethyltriethylenetetramine (HMTETA) as the ligand, CuBr as the catalyst and ethyl α-bromoisobytrate as the initiator. The molecular weight can be tuned by the molar ratio of monomer to initiator. In a typical synthesis, 5 ml THF was purged with pure nitrogen for 15 minutes before 85 mg CuBr, 323 μl HMTETA and 5 ml DMAEMA were charged. 87 μl α-bromoisobytrate was injected into the system at 50 ℃ to initiate the polymerization. The polymerization was terminated by immersing into liquid nitrogen. The ligand-catalyst complex was removed by passing the diluted polymer solution through a neutral aluminum oxide column. The polymer was precipitated in hexane and dried in a vacuum oven at 60 ℃ after the supernatant was decanted.

3.1.7. Synthesis of tetrabutylphosphonium 2,4-dimethylbenzenesulfonate (P4444 DMBS) and tetrabutylphosphonium mesitylenesulfonate (P4444 TMBS)

Both ionic liquids were synthesized by ion exchange. For the synthesis of P4444 DMBS, 10 g of tetrabutyl phosphonium bromide and 7.5 g of sodium 2,4-dimethylbenzenesulfonate were dissolved into 30 g of DI water. This aqueous solution was stirred for 24 hours and the ionic liquid inside was extracted by dichloromethane and washed with DI water for several times. The dichloromethane was then evaporated in rotary evaporator and completely removed in vacuum oven (1 mbar) at 100 ℃ until constant weight was reached. For synthesis of P4444 TMBS, 10 g of tetrabutyl phosphonium bromide and 8 g of sodium mesitylenesulfonate were dissolved into 30 g of DI water. The rest processes of ionic liquid extraction and purification are similar with those of P4444 DMBS.

3.2. Characterizations

3.2.1. ^{1}H Nuclear Magnetic Resonance (^{1}H NMR)

The ^{1}H NMR spectra of the synthesized ionic liquids were characterized by a Bruker DRX 300 instrument, with $CDCl_3$ as solvent at 25 ℃. The chemical compositions of the ionic liquids synthesized were determined by the characteristic peak shape and shift from ^{1}H NMR spectra in $CDCl_3$.

3.2.2. Gel Permeation Chromatography (GPC)

GPC was done using an Agilent 1100 series GPC system with a LC pump, PLgel 5 MIXED-C column and RI detector. GPC determined the PDMAEMA molecular weights and molecular weight distribution. The GPC column was calibrated using Agilent EasiCal polystyrene standards having a narrow molecular weight distribution. Chloroform (HPLC grade) was used as the mobile phase with 0.5 % triethylamine. The flow rate was 1.0 ml/min and temperature was 35 ℃.

3.2.3. Differential Scanning Calorimetry (DSC)

The melting points of ionic liquids and the LCSTs of all the thermally responsive draw solutions were tested by a Q10 series DSC from TA Instruments. Despite the temperature range difference for different materials, the heating/cooling rates are the same to be 3 ℃/min. Dry nitrogen was used for purging at a flow rate of 50 ml/min. For hydrogels, the tests were done with a fixed swelling ratio of 3 g/g in aluminum hermetic pan.

3.2.4. Karl Fischer titration

Karl Fischer titration (CA-200 Moisturemeter, Mitsubishi Chemical Analytech) was used to determine the water content in ionic liquid-water mixture. The titration cell consists of anode solution and cathode solution that are separated by an ion-permeable membrane. Anode solution contains alcohol, imidazole, SO_2 and I^- ions. A platinum anode is suspended in the anode solution but connects to the circuit. The sample with water is injected into anode solution. When the titration starts, the current provided oxidize I^- to I_2 around platinum plate, I_2 then oxidizes SO_2 and reacts with water in the anode solution. The amount of iodine and water consumed can be easily calculated from the quantity of electricity.

3.2.5. UV-visible absorption spectroscopy

UV-visible absorption spectra were characterized by a Shimadzu UV-visible Spectrophotometer (UV-2501PC). UV-Vis was only used for the turbid-point temperature determination of PDMAEMA solution. The wavelength was set at 700 nm.

3.2.6. Osmotic pressure measurement

As mentioned in Chapter 2, Equation 2.8 for osmotic pressure calculation is only valid for diluted solution of low molecular weight solutes. For the real either polymer solution or electrolyte solution with osmotic pressures sufficiently high for forward osmosis application, using freeze point depression method is more accurate.

The relationship between water activity (α_w) and freezing point depression is

$$-\ln\alpha_w = \frac{\Delta H_f}{RT_f^2}\Delta T \qquad \text{(Equation 3.1)}^{1,2}$$

where ΔH_f is the molar fusion heat of water (6020 J/mol), R is the ideal gas constant (8.314 $J \cdot mol^{-1} \cdot K^{-1}$), T_f is the freezing temperature of pure water (273 K) and ΔT is the freezing point depression (K). Combined with Equation 2.7, we have

$$\pi = \frac{\Delta H_f \cdot T}{T_f^2 \cdot V_w}\Delta T \qquad \text{(Equation 3.2)}$$

T is room temperature (298K). It is clear that the osmotic pressure is linear to freezing point depression. In fact, osmotic pressure expressed in osmolality (osmol/kg) is more recommended and convenient,[3] and osmolality is mainly used to evaluate feed solution and draw solution in this thesis. The osmolality can be expressed as

$$C_{osm} = \frac{\Delta T}{K} \qquad \text{(Equation 3.3)}$$

where C_{osm} is the osmolality (osmol/kg), ΔT is the freezing point depression (℃) and K is the freezing point constant (1.858 ℃·kg/osmol). Since osmol/kg = *i*·mol/kg, if molality (mol/kg) is plotted against osmolality (osmol/kg), the slope of the fitted line should be the average van't Hoff index (*i*) and the linearity of the line provides additional insight of the interaction between solute and solvent.[3]

The osmolality of solution was measured by a cryoscopic osmometer (OSMOMAT 030, Gonotec) with a resolution of 0.001 osmol/kg. The mechanism is described in Figure 3.1. The solution to be measured is firstly supercooled to several degrees below zero Celsius degree and crystallization is automatically initiated by injecting the solution with a stainless steel needle whose tip contains small ice crystals formed from the moisture in the air. When crystallization begins, the heat that was removed during super-cooling is released again and the temperature rises to the freezing point. As shown in Figure 3.1, if the sample is pure water, then the temperature would remain constant because heat removed will result in more formation of ice. The temperature falls again when the ice-water equilibrium is broken. If the solution contains draw agents, then the draw agents in

the solution will be located outside of ice crystal and in the rest of the solution. Therefore, when the freezing point temperature is measured, the concentration of the solution is higher than in the original solution. Therefore, the temperature begins to fall immediately after an osmolality reading is taken.

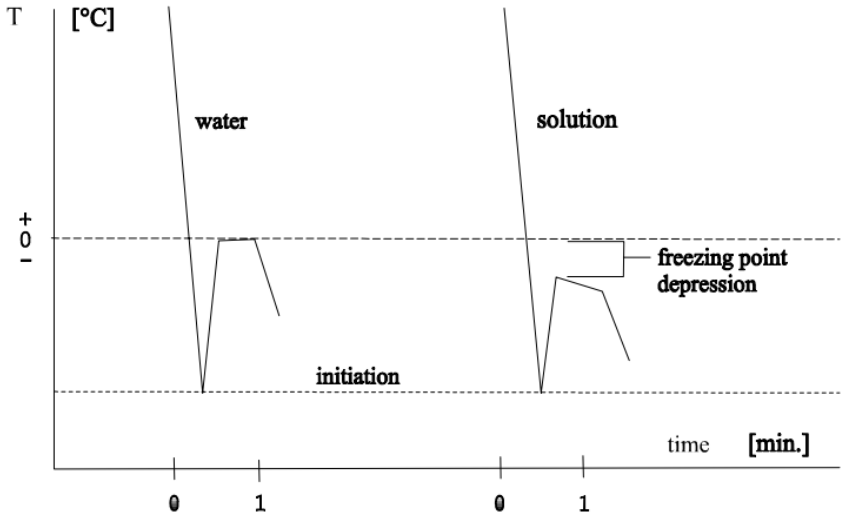

Figure 3.1 Temperature profiles of pure water and solution during osmolality measurements. This figure is adapted from Ref.4.

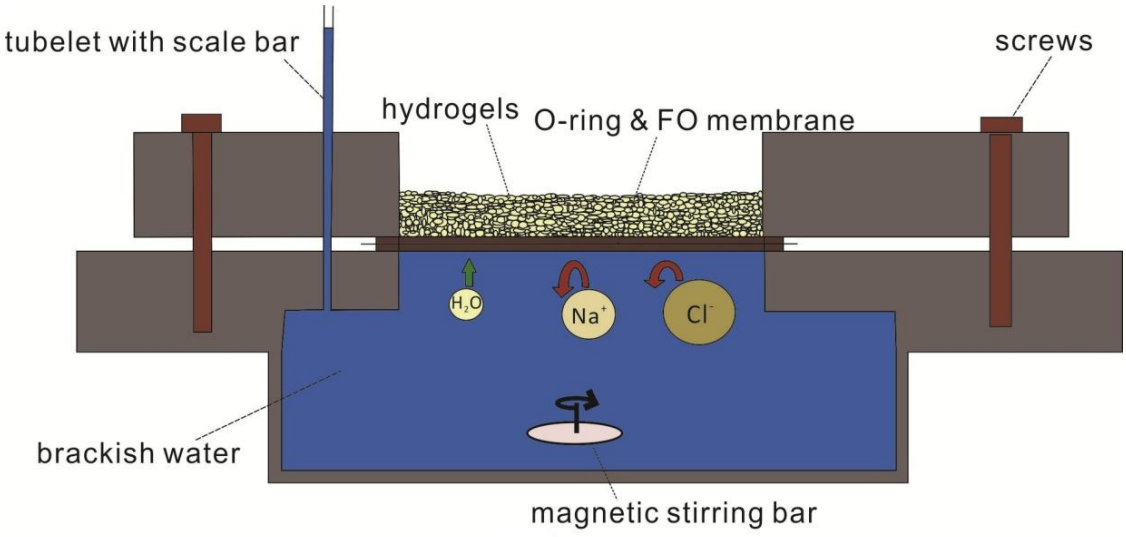

Figure 3.2 The illustration of water flux measuring apparatus for hydrogels as draw agent.

3.2.7. Water flux measurement

Water flux is a key parameter in the FO performances. The water fluxes in this thesis are determined gravimetrically by monitoring either feed solution weight decrease or draw solution weight increase with fixed area of membrane. For the measurement of water flux generated by hydrogels, the feed solution concentration is constant while hydrogel's swelling ratio increases. For the measurement of water flux generated by other draw agents dissolved in draw solution, the concentrations of both feed solution and draw solution are constant. I assume that the water permeating through the membrane has a density of 1 kg/l, thus the unit of water flux is litre per square meter per hour (LMH). Figure 3.2 shows the home-made apparatus of water flux measurement for hydrogels.

For the water flux measurement of draw agents dissolving in draw solution (except PDMAEMA), a set of cross-flow apparatus in Figure 3.3 was used. In the case when PDMAEMA was used as draw agent, a special and similar apparatus that requires much smaller amount of draw solution was used, and will be shown in Chapter 6.

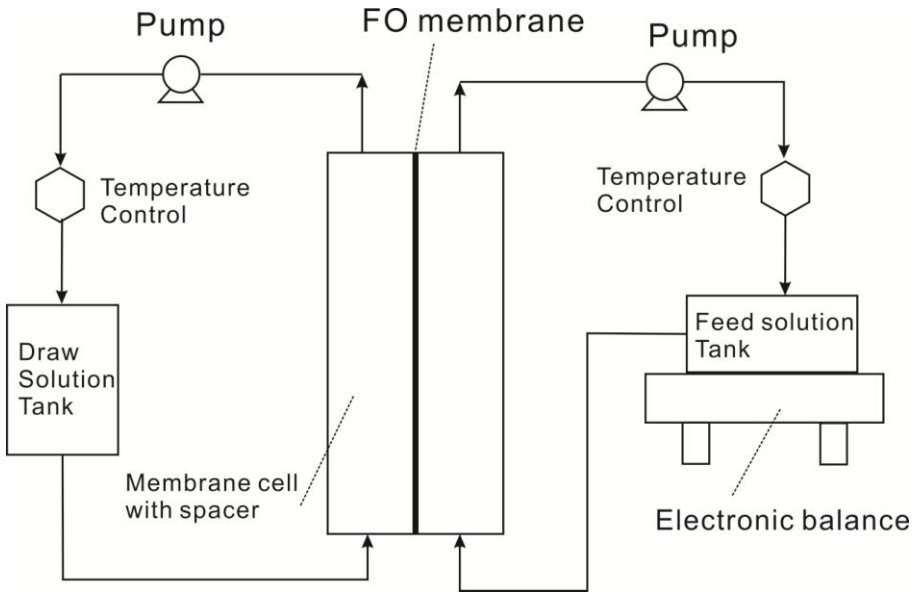

Figure 3.3 Illustration of cross-flow setup for water flux measurement.

3.2.8. Back diffusion and Salt rejection

The draw agent back diffusion and salt rejection of the FO process are another two important parameters besides water flux. The amount of draw agent permeating from draw solution to feed solution was determined by total organic carbon (TOC) or ion-chromatography (IC) while the salt rejection was calculated by conductivity measurements or ion-chromatography.

References

1. Boyd, R. H.; Phillips, P. J., *The science of polymer molecules*. Cambridge University Press New York, NY:: 1996.

2. Bergethon, P. R., *The physical basis of biochemistry: the foundations of molecular biophysics*. Springer Science & Business Media: 1998.

3. Wilson, A. D.; Stewart, F. F., Deriving osmotic pressures of draw solutes used in osmotically driven membrane processes. *Journal of Membrane Science* 2013, *431*, 205-211.

4. OSMOMAT 030 User Guide, http://memphys.dk/sites/default/files/files/basic_page/%3Cem%3EEdit%20Basic%20page%3C/em%3E%20Small%20equipment/Osmomat%20030.pdf

4. TOWARDS TEMPERATURE DRIVEN FORWARD OSMOSIS DESALINATION USING SEMI-IPN HYDROGELS AS REVERSIBLE DRAW AGENTS

In this chapter, PNIPAm-based semi-IPN hydrogels are studied as draw agents for FO. The presence of entangled hydrophilic polymer chains preserves the thermosensitivity of PNIPAm network and improves the hydrogels' water flux performances. The concept of desalination achieved by temperature modulation is proposed for the first time.

4.1. Introduction

Forward osmosis (FO) is a novel membrane-based separation technology that has attracted intensive research attention recently. FO is an automatic process driven by osmotic pressure gradient and has many advantages over reverse osmosis including low energy consumption, higher water recovery and less fouling problems.[1, 2] One of the formidable challenges in FO desalination is lack of ideal draw agents. As mentioned in Chapter 2, an ideal draw agent should at least generate a high osmotic pressure and be readily regenerated with low energy consumption.[2] Besides, other criteria such as low back diffusion, minimal membrane degradation and low toxicity should also be considered. Glucose[3, 4] and ammonia-carbon dioxide[5, 6] have been tested as draw agents to desalinate seawater through the FO process. Nevertheless, the application of sugar as a draw agent is limited to point-of-use emergency life saving cases like hydration bag, but not large-scale desalination for fresh water production since its separation from water is energy-intensive. Ammonia-carbon dioxide system suffers from problems such as severe reverse salt diffusion and potential health issues due to the high solubility of the gases in water. Hydrophilic polymer and polyelectrolyte surface-modified paramagnetic nanoparticles[7-9] were thought to have potential in that they might be regenerated by a magnetic field and provide a reasonable osmotic pressure due to their nano-scale dimensions and surface decoration. However, the irreversible nanoparticles agglomeration under a strong magnetic field and the concomitant decline in osmotic

pressures in ensuing FO process have not been properly addressed. A broad range of other draw agent candidates including polypropylene glycol,[10] polyelectrolytes,[11] inorganic salt-magnetic nanoparticles complex[12] and ionic liquids[13] have also been studied in the pursuit for the "ideal" draw agent.

A hydrogel is a crosslinked polymer with water entrapped within its network. The first attempt to apply hydrogels in desalination was done by Johannes Hopfner *et al.*[14] poly sodium acrylate hydrogels were allowed to swell in seawater and the hydrogel was recovered under an enormous hydraulic pressure of 80 bar. The desalination mechanism is believed to be Donnan effect that ions could not evenly distribute within and outside of the charged hydrogel, but salt rejection is too low for practical desalination. Recently, hydrogels have been proposed as a novel type of FO draw agent.[15] When a hydrogel serves as draw agent, it absorbs water through a FO membrane that can achieve a far higher salt rejection than Donnan effect. Thus, desalination is achieved by a membrane, and the FO process is automatic. The insoluble crosslinked network of a hydrogel enables dewatering under various external stimuli including temperature and mechanical pressure, and further water quality polishing steps for water released from hydrogel are exempted. The crosslinked poly sodium acrylate (PSA) hydrogel produced the highest water flux among all the hydrogels tested, but only less than 5% of the water in hydrogel can be released at harsh conditions of 50 ℃and 3 MPa. Although the thermally responsive poly N-isopropylacrylamide (PNIPAm) hydrogel can release more than 70% of the water within hydrogel, the water flux generated by PNIPAm was too low compared with PSA. Surprisingly, attempts to copolymerize NIPAm and sodium acrylate did not achieve the desired and anticipated synergy of high water flux as well as high water recovery.[15] The water flux of the copolymer hydrogel did increase compared with that of the neat PNIPAm hydrogel owing to the introduction of ionic SA, but the expected thermally responsive dewatering behavior was not observed. In ensuing researches, fillers including graphene oxide and carbon particles were incorporated into the NIPAm-SA copolymer hydrogel to help improve dewatering. The thermal dewatering of these composite hydrogels was conducted indirectly via exposure to simulated sunlight, and the incorporated fillers served as solar absorbents that can emit heat under light to increase

the hydrogel temperature to about 60 ℃. The composite hydrogel's water release performance was improved albeit the dewatering time was still long. Another important issue worth mentioning is that most of the water was released in vapor form. This hints that the composite hydrogels' dewatering processes were in nature desiccation processes by heat, rather than dewatering processes via phase separation as desired for thermally responsive hydrogels. In addition, the dependence on light irradiation my put extra challenges for these hydrogels' convenient packing into a desalination module. Thus, although hydrogels could be potentially very attractive draw agents due to the absence of back diffusion and water quality polishing processes, the challenge of improving water flux without sacrificing thermosensitivity needs to be solved.

In this chapter, I studied the syntheses of PINPAm-PVA and PNIPAm-PSA semi-interpenetrating network (semi-IPN) hydrogels and the underlying mechanisms with which the temperature driven FO desalination can be achieved by these semi-IPN hydrogels. Although the preparation of semi-IPN hydrogels has been widely reported[16, 17] and is not novel, there is no discussion relative to the desalination application. The current work proves that balanced performances in FO process and dewatering process, or rather a balanced hydrophilicity and hydrophobicity in hydrogel, is crucial for a temperature driven FO desalination.

4.2. Material and methods

4.2.1. Materials

N,*N*'-methylenebis(acrlyamide) (MBA, ≥99%, crosslinker), polyvinyl alcohol (PVA, M_w=61,000 g/mol), sodium acrlyate (97%) and *N*,*N*,*N'*,*N'*-tetramethylethylenediamine (TEMED, 99%, accelerator) were purchased from Sigma-Aldrich. *N*-isopropylacrylamide (NIPAm, ≥98%) was purchased from Wako Pure Chemical Industries. Ammonium peroxydisulfate (APS, 98%, initiator) was purchased from Alfa Aesar. The linear PSA was synthesized by free readical polymerization via standard methods.[18, 19] FO membranes used in this chapter were made from cellulose triacetate by Hydration Technologies Inc. (HTI). All chemicals were used as received and deionized water was used in all experiments.

4.2.2. Preparation of hydrogels

Two types of hydrogels, semi-IPN hydrogels and copolymers, were synthesized in this chapter. The PNIPAm-PVA and PNIPAm-PSA semi-IPN hydrogels were prepared by polymerizing and crosslinking NIPAm in the presence of linear PVA or PSA polymer, respectively. However, poly(NIPAm-SA) copolymer hydrogel was prepared by random copolymerization of SA and NIPAm. The ingredients and their concentrations are summarized in Table 4.1.

Table 4.1 Summary of ingredients for hydrogels synthesis.[a]

Sample	Code	NIPAm (M)	SA (M)	PVA (M)	MBA (mM)	APS (mM)	TEMED (mM)
PNIPAm	**PNIPAm**	1	-	-	20	10	10
PNIPAm-IPN-PVA(0.8M:0.2M)	**SI-0.2 PVA**	0.8	-	0.2	16	8	8
PNIPAm-IPN-PVA(0.5M:0.5M)	**SI-0.5 PVA**	0.5	-	0.5	10	5	5
PNIPAm-IPN-PSA(0.8M:0.2M)	**SI-0.2 PSA**	0.8	0.2[b]	-	16	8	8
PNIPAm-co-PSA(0.8M:0.2M)	**co-0.2 PSA**	0.8	0.2	-	20	10	10

a. The amount of crosslinker, initiator and accelerator are 2 mol%, 1 mol% and 1 mol% with respect to polymerizable monomer, respectively. Monomer is NIPAm for all semi-IPN hydrogels; while for copolymers, monomers include NIPAm and SA. b. Refers to the concentration of PSA repeating unit.

For the hydrogel synthesis in this chapter, the concentration of polymers' total repeating units was 1 M. For instance, the NIPAm and PVA repeating unit concentration were both 0.5 M in the synthesis of SI-0.5PVA semi-IPN hydrogel; while the NIPAm and SA monomer concentration were 0.8 M and 0.2 M, respectively for the synthesis of copolymer hydrogel co-0.2PSA. In actual hydrogels synthesis, predetermined amount of NIPAm and MBA, as well as SA, PSA or PVA depending on the hydrogel type to

synthesize, were first dissolved in DI water at 70 ℃ under constant stirring until a homogeneous solution was made. This solution was then cooled to room temperature and purged with pure N_2 for 15 minutes before accelerator TEMED and initiator APS were introduced. The polymerization was carried out for 24 hours, and the hydrogels were washed with large quantities of DI water to leach out the unreacted molecules.

4.2.3. Characterization of hydrogel thermosensitivity

The washed hydrogels were allowed to freely swell in DI water to reach the equilibrium swollen state. The fully swollen hydrogels were cut into disk shapes with dimensions of 24 mm in diameter and approximately 3 mm in thickness, and their dewatering profiles were measured in 40 ℃water for 10 minutes. The hydrogels were subjected to a gentle vacuum suction for 2 seconds before each weighing to remove the excess free water on the hydrogel surface. The hydrogel disks after the deswelling measurements at 40 ℃ were dried in a vacuum oven until a constant weight (W_d) was reached, with which the swelling ratios and water retentions during the dewatering or deswelling process could be calculated. The swelling ratio is defined throughout this thesis as $(W_t-W_d)/W_d$, where W_t is the weight of hydrogel at a specific time during the deswelling, W_d is the completely dry hydrogel weight.

Differential scanning calorimeter was used to determine the LCST, if existed, of each hydrogel. Approximately 20 mg of swollen hydrogel was placed within a sealed aluminum pan, and the temperature tested was between 20 and 50 ℃ with a heating rate of 3 ℃/min. Dry nitrogen was used for purging at a flow rate of 50 ml/min.

4.2.4. Hydrogel dewatering and performance in FO process

For the hydrogel performance in FO swelling process as well as regeneration dewatering process, a 24 mm diameter, disk-shaped hydrogel aggregate fabricated by 400 mg dry hydrogel particles with dimensions less than 200 μm was used. The disk was allowed to swell to a roughly 2 g/g swelling ratio to form an integral aggregate with a thickness of approximately 3 mm, as shown in Figure 4.1c. The swollen disk then shrunk in 40 ℃ water and the deswelling profile was available by measuring the weight decrease with

time. The hydrogel discs could maintain the shape integrity during cyclic swelling and deswelling processes. The shrunk hydrogel disc after dewatering in 40℃water was then put on the FO membrane to measure its FO performance. The water flux in FO process is defined as $\Delta m/(A \cdot \Delta t)$, where Δm is the hydrogel weight increase (kg) within allotted time Δt (h) and the membrane area is A (m^2). In this chapter, FO process was conducted for 5 hours using a home-made apparatus as shown in Figure 4.1a and 4.1b. Feed solution of 2000 ppm NaCl was filled within the chamber that was sealed by a FO membrane with rubber O-rings. A small tube canalized the feed solution chamber to ambit air and the

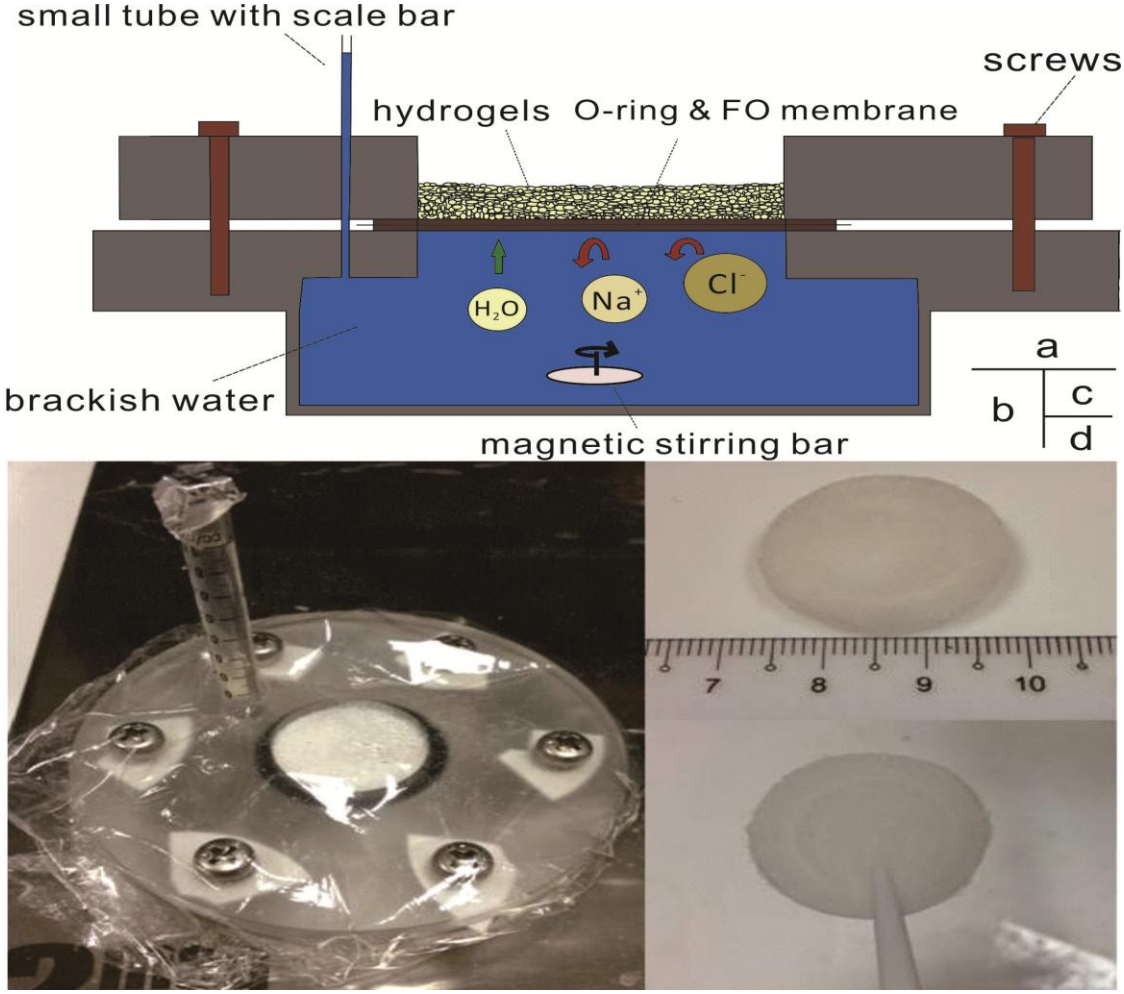

Figure 4.1 (a) Schematic and (b) photo of the home-made apparatus for water flux measurement. The covering plastic film is to isolate hydrogels from atmosphere. (c) The hydrogel disc fabricated from dry hydrogel particles. (d) The photo showing the robustness and shape integrity of the hydrogel disc.

water level in it was always maintained higher than the FO membrane to ensure the feed solution contacts with the entire FO membrane. The hydrogel disc finishing the FO process was regenerated again in 40℃ water to squeeze out the absorbed water. This FO-dewatering cycle was repeated for three times to investigate these hydrogels' reversibility as draw agents.

4.3. Results and discussion

4.3.1. Swelling and deswelling of semi-IPN hydrogels

The incorporation of linear polyelectrolyte PSA and hydrophilic PVA into the thermally responsive PNIPAm network, as shown in Figure 4.2a, has tremendously increased the equilibrium swelling ratio compared with that of neat PNIPAm hydrogel. In addition, all the semi-IPN hydrogels show excellent dewatering performances at 40℃, which are even superior to that of neat PNIPAm hydrogel in terms of water recovery. This can be ascribed to the presence of linear polymer chains (PVA or PSA) fabricating a kind of water release channel that facilitates the thermally induced water release from core to surface, albeit the semi-IPN hydrogels are essentially more hydrophilic than neat PNIPAm hydrogel.[20] Having the same chemical composition as the semi-IPN (SI-0.2PSA)

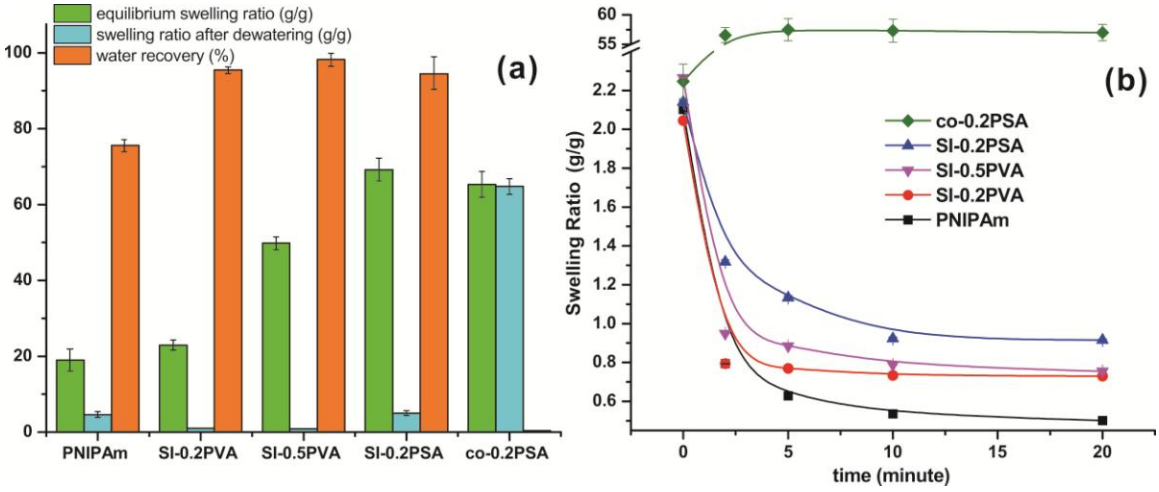

Figure 4.2 (a) Equilibrium swelling ratio at room temperature, swelling ratio after complete deswelling at 40℃ in water and water recovery after 10 minutes at 40 ℃ of the bulk hydrogels. (b) Deswelling profile of hydrogel discs from a swelling ratio of approximately 2 g/g. All the hydrogels had a diameter of 24 mm and thickness of 3 mm.

hydrogel, the NIPAm-SA copolymer hydrogel (co-0.2PSA) also shows an increased equilibrium swelling ratio compared with neat PNIPAm hydrogel. However, co-0.2PSA shows virtually no water recovery at the same dewatering conditions. I believe that, although investigating the hydrogels' dewatering behavior from their equilibrium swelling ratios would give an insight on the presence of thermosensitivity as shown in Figure 4.2a, a study focused on these hydrogels' dewatering behaviors from a lower initial swelling ratio of about 2 g/g would be more useful to their application as draw agents in FO desalination in that the water flux generally diminishes when the swelling ratio exceeds 2 g/g according to our study. As shown in Figure 4.2b, the neat PNIPAm hydrogel and all the semi-IPN hydrogel particle aggregate discs can rapidly deswell from the swelling ratio of approximately 2 g/g at 40 ℃. All the thermally responsive hydrogels can reach the corresponding minimum swelling ratio within 10 minutes during dewatering, while the NIPAm-SA copolymer hydrogel swells in 40℃ water and no water is released. The efficient and fast thermally induced water release from a low swelling ratio of the semi-IPN hydrogels is an advantageous attribute as FO draw agent and this will be discussed later. For a better comparison, the minimum plateau swelling ratio in dewatering at 40 ℃ was defined as the onset point swelling ratio (OPSR), from which the hydrogels commence to draw water and swell in the FO process. The OPSRs for SI-0.2PSA, SI-0.5PVA, SI-0.2PVA and neat PNIPAm are 0.92 ± 0.01, 0.75 ± 0.01, 0.73 ± 0.01 and 0.50 ± 0.01, respectively from Figure 4.2b. The increase of OPSRs of semi-IPN hydrogels, especially SI-0.2PSA, was due to the enhanced water affinity by the incorporation of PVA or PSA compared with neat PNIPAm. However, the semi-IPN hydrogels' thermosensitivities were preserved that enabled an effective water release under thermal stimulus.

Another interesting issue that needs elaborating is the deswelling performance distinction between co-0.2PSA and SI-0.2PSA despite their similar equilibrium swelling ratios at room temperature (Figure 4.2a). Ionic SA copolymerizing with NIPAm in the molar ratio of 1:4 (co-0.2PSA) increases the copolymer hydrogel's LCST to above 80℃,[21] while the semi-IPN hydrogel with the identical SA-NIPAm molar ratio preserved PNIPAm's thermosensitivity. This distinction in performance can be ascribed to the charge

distribution within hydrogel as shown in Figure 4.3. Evenly distributed charges from random copolymerization jeopardize the hydrophobic aggregates formation owing to the strong electrostatic repulsion as well as the hydration of immobilized carboxylate and sodium ions.[22] On the contrary, the localized charges from semi-IPN hydrogels and the mobility of linear polymers minimize the adverse influences of the formation of hydrophobic aggregates.

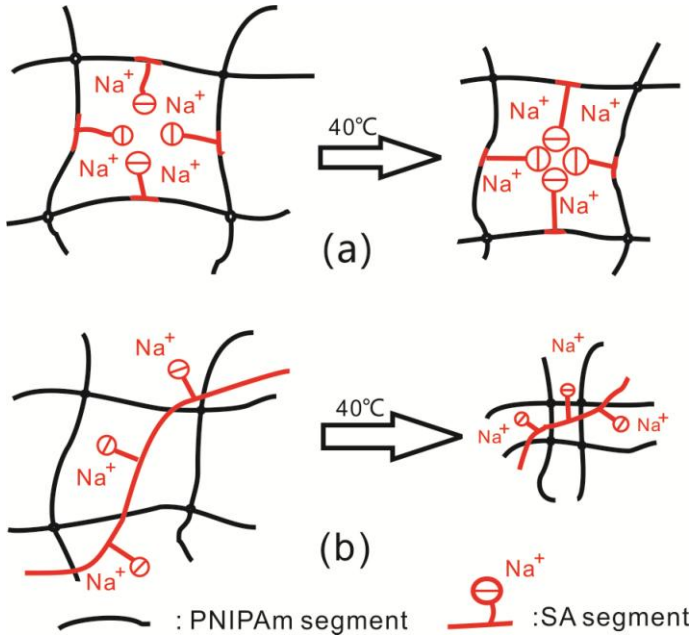

Figure 4.3 The illustrations of (a) evenly distributed charges and (b) localized charges on the formation of hydrophobic aggregate in copolymer hydrogel and semi-IPN hydrogel, respectively.

Figure 4.4 demonstrates that all the semi-IPN hydrogels are thermally responsive with LCSTs in the range of 33 ℃ to 35 ℃. Interestingly, the introduction of charges to the semi-IPN hydrogels counter-intuitively reduces the LCSTs to lower than that of neat PNIPAm. This abnormal phenomenon may be ascribed to hydrogen bonding between PNIPAm and PVA for PNIPAm-PVA semi-IPN hydrogels.[23] However, the reduction of the LCST for PNIPAm-PSA semi-IPN hydrogels with possibly more complex mechanisms has not been reported. It is believed that, besides the possible weak hydrogen bonding between PNIPAm and PSA, the polyelectrolyte PSA may impose an effect analogous to inorganic electrolyte such as $NaNO_3$ and NaCl, which have been

proven to reduce the LCST of PNIPAm.[24] The presence of the LCST in the semi-IPN hydrogels containing hydrophilic polymer or polyelectrolyte is the foundation for these hydrogels to assume a higher drawing ability than the neat PNIPAm while preserving a desirable dewatering performance under elevated temperatures.

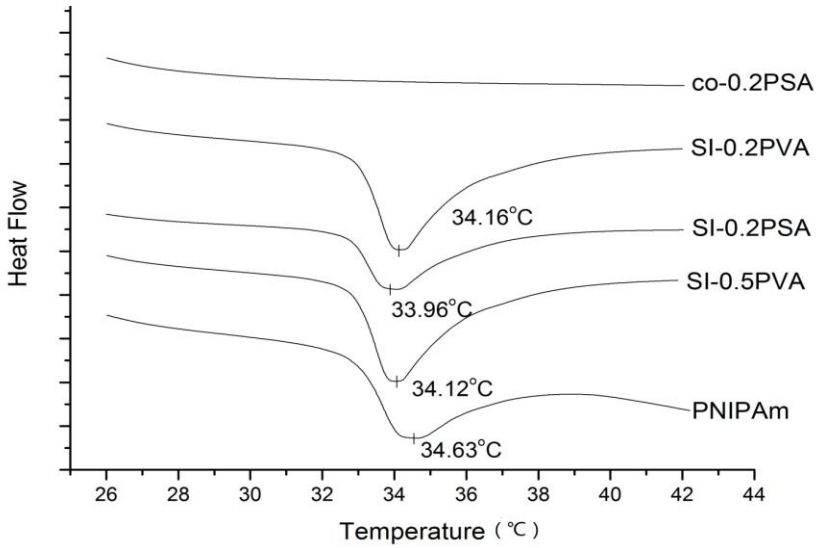

Figure 4.4 The LCSTs of the hydrogels studied in this chapter. Co-0.2PSA does not show any thermal effect within the temperature range studied. Downward is endothermic.

4.3.2. Performance in FO process and reversibility

A remarkable difference of this study is that in prior work using hydrogels as draw agents, the one-time FO process started with completely dry hydrogels;[15] while the FO process in this chapter started with swollen hydrogels with swelling ratios equal to the corresponding OPSRs. This is because in hydrogel's FO-dewatering cyclic perspective, hydrogels after dewatering process cannot be completely dry but have swelling ratios equal to the OPSRs. This is the very state in which the hydrogel commences the ensuing FO process. Figure 4.5 demonstrates profiles the water flux and corresponding hydrogel's swelling ratio in the FO process. The incorporation of PVA or PSA imparts two contrasting effects on water flux. On the one hand, the presence of hydrophilic polymer and polyelectrolyte dramatically increase the water flux generated by hydrogels. Figure 4.5 clearly shows that all the semi-IPN hydrogels generate a higher water flux than that of the neat PNIPAm hydrogel, and SI-0.2PSA generates a higher water flux than SI-0.2PVA

probably due to stronger hydrophilicity of PSA. A more fair and meaningful method to compare the hydrogel's hydrophilicity is to compare the generated water flux at the same swelling ratio. The plots of water flux as a function of swelling ratio for each hydrogel, as shown in Figure 4.6a, clearly demonstrate the trend of decreasing water flux with increasing swelling ratio. Each of the three semi-IPN hydrogels, as expected, generates a higher water flux than that of neat PNIPAm hydrogel at each swelling ratio. For instance, at the swelling ratio of 1 g/g, the water fluxes generated are assumed to be 0.12, 0.18 and

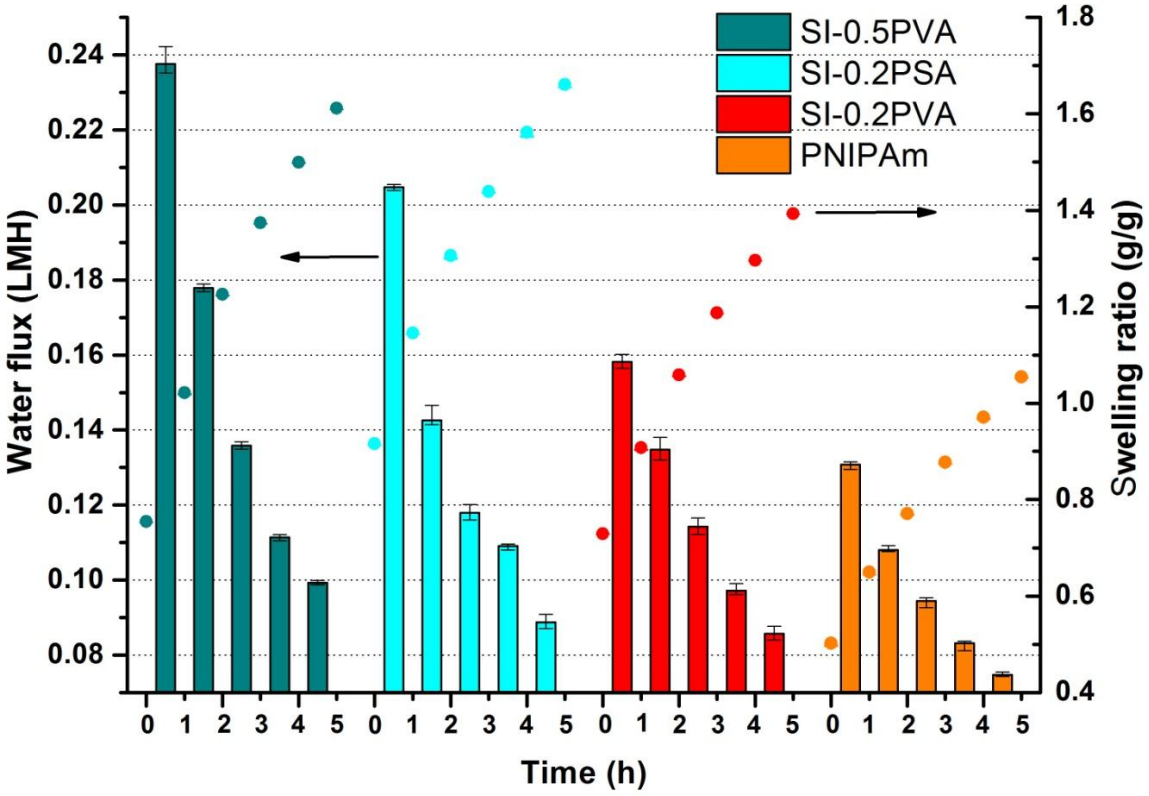

Figure 4.5 The hourly average water flux generated by thermally responsive hydrogels (column) and the corresponding swelling ratio (dot) in the 5 hour FO test. For instance, the first column of each hydrogel represents the average water flux in the first hour, and the first two dots are the swelling ratios before and after the first hour swelling. The dots at 0 hour are the OPSRs.

0.18 LMH for SI-0.2PVA, SI-0.5PVA and SI-0.2PSA, which are 1.7, 2.6 and 2.6 times the 0.07 LMH generated by neat PNIPAm hydrogel. On the other hand, as mentioned earlier in Figure 4.2b, the introduction of PSA or PVA increases the OPSRs with which the hydrogels commence the FO process. Thus, the semi-IPN hydrogels operate with

higher swelling ratios than that of NIPAm in the FO-dewatering cycle, which imposes adverse effect on water flux. Fortunately, the positive drawing ability enhancement outweighs the negative effect of increasing the OPSR by introducing PVA or PSA as shown in Figure 4.5. The average water flux for the first hour in FO generated by SI-0.2PSA and SI-0.5PVA is still 58% and 85%, respectively, higher than that of the neat PNIPAm hydrogel.

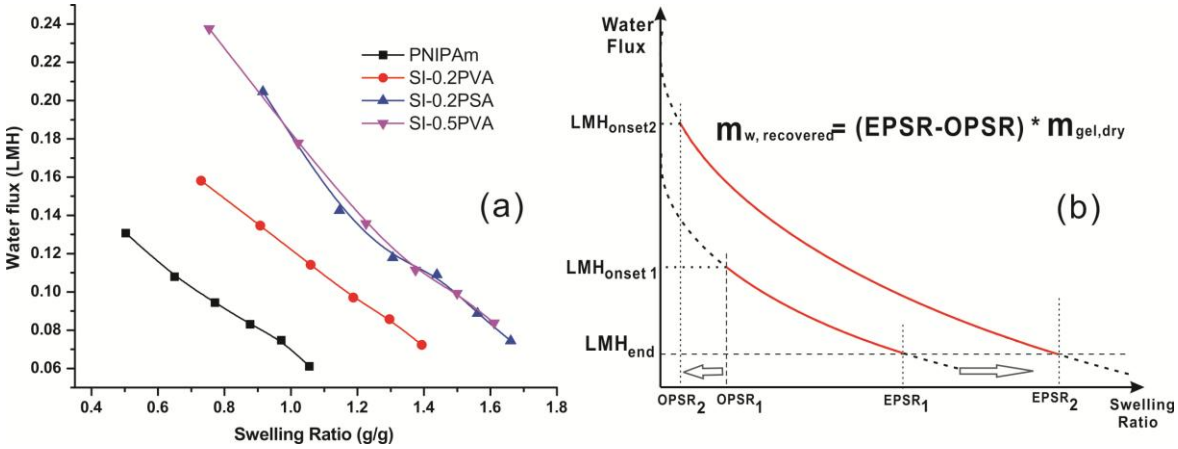

Figure 4.6 (a) The correlation curves for the water flux versus swelling ratio for hydrogels in a 5 hour FO process. (b) Schematic illustration for reversible hydrogel performance optimization. A better hydrogel should have a lower OPSR and a higher EPSR simultaneously to expand the reversible swelling ratio range. The red solid line indicates the reversible range of swelling ratio between OPSR and EPSR.

These two conflicting effects in these three semi-IPN hydrogel candidates also compete to affect their comprehensive performance in the FO process. As demonstrated in Figure 4.6a, at the same swelling ratios of 1 g/g, the water flux generated by SI-0.2PSA (0.183 LMH) is virtually the same as that for SI-0.5PVA (0.177 LMH). This indicates that SI-SI-0.5PVA and 0.2PSA should have virtually identical drawing ability as draw agents. However, compared with SI-0.2PSA, SI-0.5PVA has a lower OPSR and therefore a wider reversible swelling ratio range between the shrunk state at 40℃ and swollen state at room temperature. In fact for hydrogels serving as draw agents, the reversible swelling ratio span is also a critical parameter to consider besides the water flux value. For instance, Figure 4.6a demonstrates that the swelling ratio increased from OPSR by 0.54 g/g, 0.66

g/g, 0.74 g/g and 0.87 g/g for neat PNIPAm, SI-0.2PVA, SI-0.2PSA and SI-0.5PVA, respectively in the FO process. This indicates that while SI-0.2PSA generates 37% more available water than neat PNIPAm, the SI-0.5PVA generates 61% more available water than neat PNIPAm, albeit these two semi-IPN hydrogels have quite similar drawing abilities since the plots for SI-0.5PVA and SI-0.2PSA overlap each other as shown in Figure 4.6a.

In order to further understand the importance of balanced performance of hydrogels in FO and dewatering process, it is helpful to introduce a new parameter, the difference between the EPSR (end point swelling ratio) and OPSR, or rather reversible swelling ratio span. The EPSR is the hydrogel's swelling ratio at the end of FO process as well as prior to the dewatering process. Figure 4.6b schematically demonstrates the decline of water flux with swelling ratio increased from OPSR to EPSR in FO process. Thanks to the thermosensitivity of hydrogels, the swollen hydrogel will undergo shrinking to the OPSR upon heating at 40 ℃. This enables the next FO process and stable cyclic performances. The amount of water ($m_{w,\ recovered}$) that is absorbed by hydrogel in FO process and consequently released in dewatering process is the very amount of water available for use, and it is proportional to the reversible swelling ratio range as shown in Figure 4.6b. For ease of hydrogel performance comparison, I define the EPSR to be the

Table 4.2 OPSR, EPSR and the reversible swelling ratio range of thermally responsive hydrogels.*

Hydrogel Code	OPSR	EPSR	EPSR-OPSR
PNIPAm	0.50	0.72	0.22
SI-0.2PVA	0.73	1.18	0.45
SI-0.2PSA	0.92	1.50	0.58
SI-0.5PVA	0.75	1.50	0.75

*The EPSR is defined as the corresponding swelling ratio when water flux is declined to 0.1 LMH

swelling ratio when the water flux reduced to 0.1 LMH, and the corresponding EPSRs of the hydrogels can be determined in Figure 4.6a. Table 2 tabulates the values of OPSR, EPSR and the (EPSR-OPSR) of these hydrogels. All the semi-IPN hydrogels have a higher EPSR than neat PNIPAm hydrogel due to increased hydrophilicity. The reversible swelling ratio spans (EPSR-OPSR) of these semi-IPN hydrogels are also wider than that of neat PNIPAm hydrogel despite their higher OPSRs. For instance, the reversible

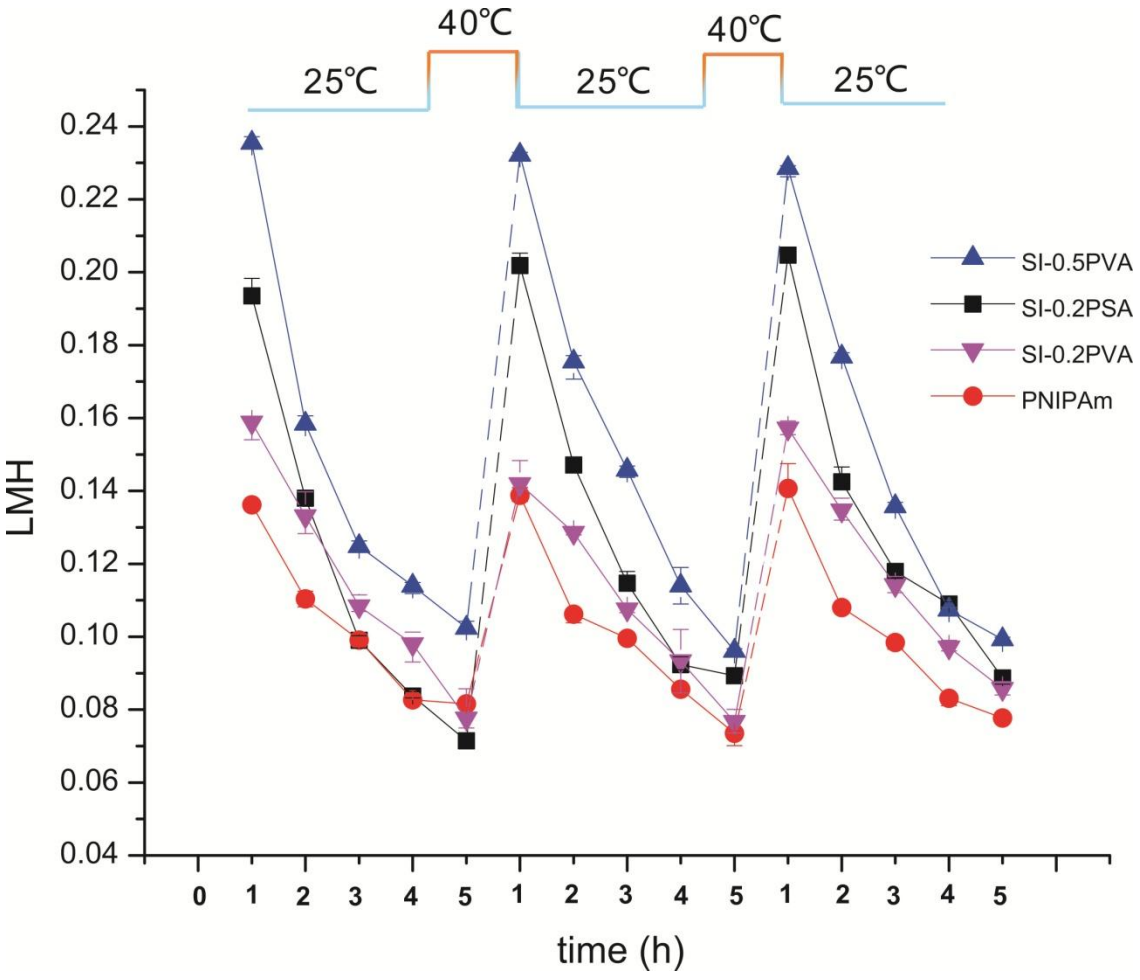

Figure 4.7 The reversibility of hydrogels for three FO-dewatering cycles. The five dots in each cycle represent the average water flux for the corresponding one hour. The dewatering process duration is 10 minutes and represented by dashed lines. The dewatering process is not to scale relative to the FO process duration.

swelling range for SI-0.5PVA is 0.75 g/g and 240% higher than that of neat PNIPAm hydrogel. For hydrogels with various SA to NIPAm ratio, the neat PSA hydrogel should

have the highest equilibrium swelling ratio and drawing ability, and therefore the highest EPSR. Nevertheless, neat PSA's OPSR is also very high and theoretically should be the same as EPSR since PSA hydrogel is not expected to deswell at 40 ℃. Therefore, the $m_{w,recovered}$ is virtually zero during the temperature cycles between room temperature and 40 ℃. This explanation also goes for the non-thermally responsive poly(NIPAm-SA) random copolymer hydrogel. On the contrary, although neat PNIPAm hydrogel has a low OPSR owing to thermosensitivity, its EPSR is also low due to absence of charges and counterions. Hence, the amount of recovered water is small in either case. For the semi-IPN hydrogels, the entangled hydrophilic PVA or polyelectrolyte PSA chains not only increase the water flux and EPSR, but preserve the desirable thermosensitivity. Admittedly, their OPSR values are higher than that of neat PNIPAm hydrogel, large amounts of available water still are generated by semi-IPN hydrogels during the FO-dewatering cycle. Therefore, balanced performances in FO and dewatering processes are the essential characteristics to make these semi-IPN hydrogels more suitable FO draw agents.

Figure 4.7 shows the water flux profiles for three consecutive cycles of the neat PNIPAm and semi-IPN hydrogels. High reversibility was observed for each candidate in the FO-dewatering cycle. The reversibility of these hydrogels was ascribed to the PNIPAm network's thermo-sensitivity, while the presence of linear PVA or PSA entitles the semi-IPN hydrogels to absorb and subsequently release more water within one cycle than neat PNIPAm hydrogel.

4.3.3. Quasi-continuous FO desalination driven by temperature

Admittedly, the water flux generated by semi-IPN hydrogels are still low compared to those generated by ammonia-carbon dioxide system, yet they are still quite interesting because hydrogels exempt the need of further treatment of the released water. In addition, the water fluxes reported above do not always accurately reveal the actual FO performance for hydrogel draw agents since water flux is significantly affected by contact area between FO membrane and hydrogel. It is evidently demonstrated in Figure 4.8 that a larger contact area and the same hydrogel weight led to tremendously faster water

absorption and hydrogel swelling. The possible underlying reason is that the water diffusion path and particle-particle boundary are decreased due to reduction in hydrogel layer thickness. These results indicate that better water flux performance would be achieved and the duration of FO process can be further reduced by optimizing the hydrogel layer thickness. One potential embodiment of the semi-IPN hydrogels as draw agents is to integrate them into a FO hollow fiber membrane module. Figure 4.9 shows a conceptual design of a quasi-continuous desalination module driven by temperature

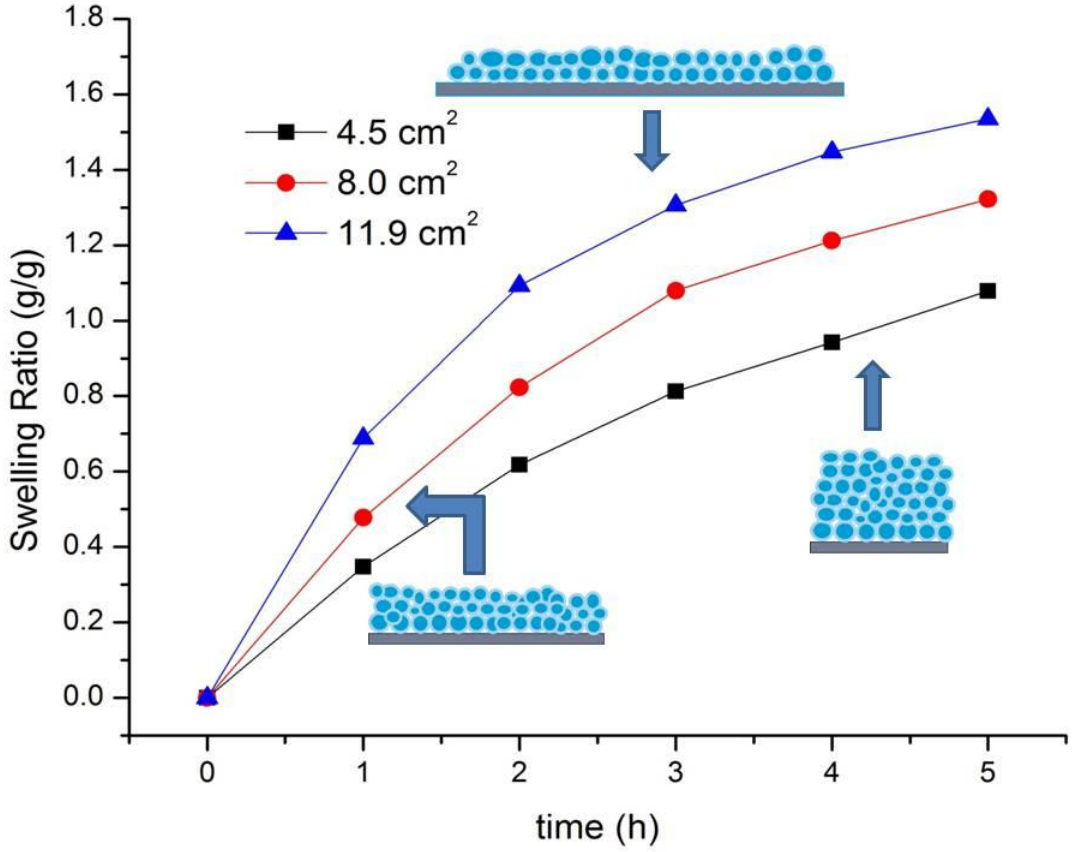

Figure 4.8 The influence of contact area between hydrogel and membrane on the FO performance of SI-0.2PSA. The weight of dried hydrogel is 400 mg and 2000 ppm NaCl brackish water is used as feed solution.

modulation, which is enabled by semi-IPN hydrogels being coated onto the outside surface of the FO hollow fiber membranes. The feed solution flows through the hollow fiber lumen and water permeates through the membrane automatically to swell the semi-IPN hydrogel in the FO process at room temperature. Subsequently, the dewatering

process is conducted at 40 ℃ in which the swollen hydrogel releases the entrapped water. The cooling and heating cycles, as demonstrated in Figure 4.9, allow an essentially temperature-driven FO desalination. The design is deemed a quasi-continuous process since the desalinated water can only be collected during each heating induced dewatering stage at 40 ℃. A temperature modulation of about 15 ℃ is sufficient to drive the desalination process, and the dewatering condition of 40 ℃ is desirable in that it not only consumes less energy, but precludes membrane degradation since 43 ℃ is the upper limit

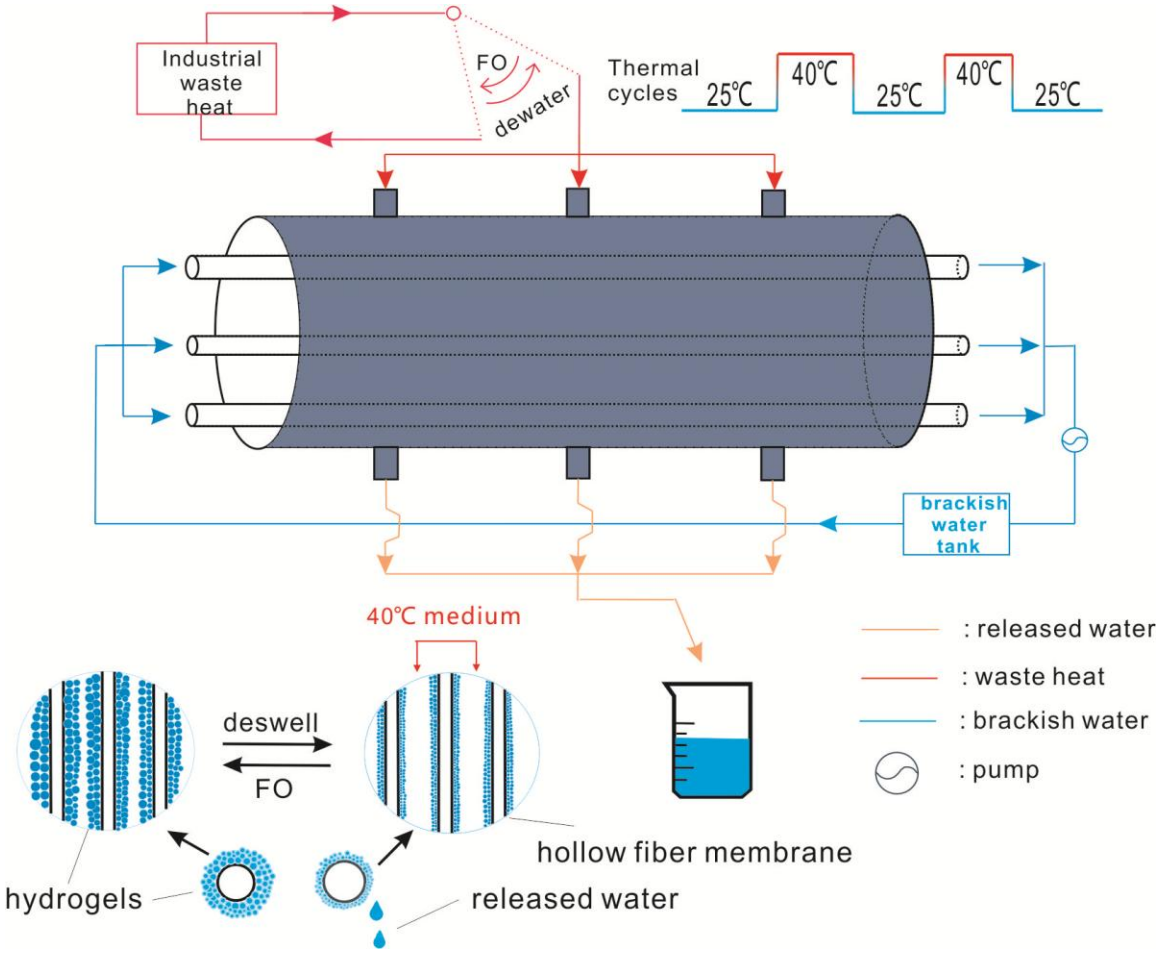

Figure 4.9 Quasi-continuous FO desalination using a semi-IPN hydrogel as the draw agent. Besides inevitable electrical energy for pumping, the periodic temperature modulation within 15 ℃ is essentially the only required energy input for desalination in this conceptual design. This temperature difference can be readily obtained using warm air/water generated from industrial waste heat.

for long term housing of the cellulose triacetate membrane. Apart from the electrical energy necessary to pump the saline water through the hollow fiber membrane lumen, the periodic temperature modulation is the virtually the only driving force and this thermal energy input can be easily achieved with industrial low-grade waste heat. It is also possible to improve the balanced FO-dewatering performance or further reduce the temperature difference in the cooling and heating cycles by optimizing the molecular structure of the hydrogels.

4.4. Conclusions

In this chapter, a series of draw agents based on PNIPAm-PVA and PNIPAm-PSA semi-IPN hydrogels with superior and more balanced performances have been successfully synthesized. The entangled linear PVA or PSA polymers within the PNIPAm network not only enhance the hydrophilicity and consequently water flux compared with neat PNIPAm hydrogel, but preserve the thermosensitivity to facilitate liquid water release at elevated temperatures above their LCSTs, while their copolymer counterparts with the same monomer composition did not assume such potential. A conceptual design of a quasi-continuous FO-dewatering cyclic desalination process is proposed, which employs a membrane module containing hollow fibers with a layer of thermally responsive hydrogel coated on the outer surface. This process is theoretically driven by temperature modulation within a 15 ℃ range. The low energy consumption and process-simplicity make responsive hydrogels attractive as draw agents for FO. Furthermore, key parameters like the reversible swelling ratio range (EPSR-OPSR) was defined to provide a qualitative performance gauge for hydrogels as draw agents. The results of this study are significant and enlighten the future of using responsive hydrogels as the draw agents for FO, albeit parameter optimization is still necessary to enhance comprehensive performance.

References

1. Cath, T.; Childress, A.; Elimelech, M., Forward osmosis: Principles, applications, and recent developments. *Journal of Membrane Science* **2006,** *281*, (1-2), 70-87.

2. Chekli, L.; Phuntsho, S.; Shon, H. K.; Vigneswaran, S.; Kandasamy, J.; Chanan, A., A review of draw solutes in forward osmosis process and their use in modern applications. *Desalination and Water Treatment* **2012,** *43*, (1-3), 167-184.

3. Kessler, J.; Moody, C., Drinking water from sea water by forward osmosis. *Desalination* **1976,** *18*, (3), 297-306.

4. Kravath, R. E.; Davis, J. A., Desalination of sea water by direct osmosis. *Desalination* **1975,** *16*, (2), 151-155.

5. McCutcheon, J. R.; McGinnis, R. L.; Elimelech, M., A novel ammonia—carbon dioxide forward (direct) osmosis desalination process. *Desalination* **2005,** *174*, (1), 1-11.

6. McCutcheon, J. R.; McGinnis, R. L.; Elimelech, M., Desalination by ammonia–carbon dioxide forward osmosis: influence of draw and feed solution concentrations on process performance. *Journal of Membrane Science* **2006,** *278*, (1), 114-123.

7. Bai, H.; Liu, Z.; Sun, D. D., Highly water soluble and recovered dextran coated Fe3O4 magnetic nanoparticles for brackish water desalination. *Separation and Purification Technology* **2011,** *81*, (3), 392-399.

8. Ge, Q.; Su, J.; Chung, T.-S.; Amy, G., Hydrophilic superparamagnetic nanoparticles: synthesis, characterization, and performance in forward osmosis processes. *Industrial & Engineering Chemistry Research* **2010,** *50*, (1), 382-388.

9. Ling, M. M.; Chung, T. S.; Lu, X., Facile synthesis of thermosensitive magnetic nanoparticles as "smart" draw solutes in forward osmosis. *Chem Commun (Camb)* **2011,** *47*, (38), 10788-10790.

10. Jorgensen, M. K. Investigation of Polypropylene Glycol 425 as Possible Draw Solution for Forward Osmosis. Aalborg University, Aalborg, 2009.

11. Ge, Q.; Su, J.; Amy, G. L.; Chung, T. S., Exploration of polyelectrolytes as draw solutes in forward osmosis processes. *Water Res* **2012,** *46*, (4), 1318-1326.

12. Liu, Z.; Bai, H.; Lee, J.; Sun, D. D., A low-energy forward osmosis process to produce drinking water. *Energy & Environmental Science* **2011,** *4*, (7), 2582.

13. Yen, S. K.; Mehnas Haja N, F.; Su, M.; Wang, K. Y.; Chung, T.-S., Study of draw solutes using 2-methylimidazole-based compounds in forward osmosis. *Journal of Membrane Science* **2010,** *364*, (1-2), 242-252.

14. Höpfner, J.; Klein, C.; Wilhelm, M., A novel approach for the desalination of seawater by means of reusable poly (acrylic acid) hydrogels and mechanical force. *Macromolecular rapid communications* **2010,** *31*, (15), 1337-1342.

15. Li, D.; Zhang, X.; Yao, J.; Simon, G. P.; Wang, H., Stimuli-responsive polymer hydrogels as a new class of draw agent for forward osmosis desalination. *Chem Commun (Camb)* **2011,** *47*, (6), 1710-1712.

16. Dhara, D.; Nisha, C.; Chatterji, P. R., Interpenetrating Networks of Poly (N-isopropyl-acrylamide) with Anionic and Cationic Polymers. *Macromolecular chemistry and physics* **2001,** *202*, (18), 3617-3623.

17. Harmon, M. E.; Schrof, W.; Frank, C. W., Fast-responsive semi-interpenetrating hydrogel networks imaged with confocal fluorescence microscopy. *Polymer* **2003,** *44*, (22), 6927-6936.

18. Li, Y.; Li, X.; Zhou, L.; Zhu, X.; Li, B., Study on the synthesis and application of salt-resisting polymeric hydrogels. *Polymers for Advanced Technologies* **2004,** *15*, (1-2), 34-38.

19. Yamashita, K.; Nishimura, T.; Nango, M., Preparation of IPN-type stimuli-Responsive heavy-Metal-Ion adsorbent gel. *Polymers for Advanced Technologies* **2003,** *14*, (3-5), 189-194.

20. Zhang, J.-T.; Cheng, S.-X.; Zhuo, R.-X., Poly (vinyl alcohol)/poly (N-isopropylacrylamide) semi-interpenetrating polymer network hydrogels with rapid response to temperature changes. *Colloid and Polymer Science* **2003,** *281*, (6), 580-583.

21. Hirose, Y.; Amiya, T.; Hirokawa, Y.; Tanaka, T., Phase transition of submicron gel beads. *Macromolecules* **1987,** *20*, (6), 1342-1344.

22. Kokufuta, E.; Wang, B.; Yoshida, R.; Khokhlov, A. R.; Hirata, M., Volume phase transition of polyelectrolyte gels with different charge distributions. *Macromolecules* **1998,** *31*, (20), 6878-6884.

23. Shin, B. C.; Jhon, M. S.; Lee, H. B.; Yuk, S. H., Temperature-induced phase transition of semi-interpenetrating polymer networks composed of poly (N-isopropyl acrylamide) and hydrophilic polymers. *European Polymer Journal-Paper Edition* **1998,** *34*, (2), 171-174.

24. Zhang, Y.; Cremer, P. S., Interactions between macromolecules and ions: the Hofmeister series. *Current opinion in chemical biology* **2006,** *10*, (6), 658-663.

5. INVESTIGATION OF BRACKISH WATER DESALINATION VIA FORWARD OSMOSIS ENABLED BY THERMALLY RESPONSIVE POLY IONIC LIQUID HYDROGELS

In this chapter, thermally responsive poly ionic liquid hydrogels with a subtle balance of hydrophilicity and hydrophobicity in monomer structures are proved to achieve a much higher water flux compared with the PNIPAm-based hydrogels. Many other factors influencing the water flux, including membrane structure, hydrogel area density, contact condition between hydrogel particles and the duration of one FO-regeneration cycle, are also investigated. In addition, a criterion to judge a hydrogel's comprehensive performance as draw agent is proposed.

5.1. Introduction

Forward osmosis (FO) is an automatic process driven by water chemical potential gradient across a semi-permeable membrane that rejects the solute but allows the water passage.[1] Compared with reverse osmosis (RO), FO has many advantages such as operating at low or no hydraulic pressure and consequent lower membrane fouling propensity.[2] However, unlike RO whose product is fresh water, FO process alone only results in diluted draw solution. Therefore, except for special cases where the diluted draw solution can be utilized directly,[3, 4] the draw agent regeneration cum water recovery process is necessary after FO process to obtain purified water and reuse draw agents. Among all the draw agents developed to date,[1, 5, 6] majority of them are dissolved[7-12] or dispersed[13-15] in water to make aqueous draw solution. Therefore, in order to obtain high quality water and minimum draw agent loss, additional membrane processes including nanofiltration (NF), ultrafiltration (UF), RO or membrane distillation are indispensable as the final step regardless of any possible previous separation by external stimulus[9, 11, 14] in

the draw solution regeneration process. Undoubtedly, these would bring in additional equipment and energy costs for FO desalination.

Hydrogels are crosslinked hydrophilic polymers or polyelectrolytes with water entrapped within the network. This novel material was firstly explored for desalination purpose by swelling neutralized poly acrylic acid in brackish water and deswelling the hydrogel under hydraulic pressure.[16, 17] However, the Donnan effect did not effectively expel salts from entering the hydrogel network, and the water released under a high pressure of 80 bar still maintained 65% salinity of original brackish water. Later, Li *et al*[18] introduced hydrogels as the draw agents for FO desalination. The FO membrane separated hydrogels from brackish water (feed solution) and undertook the function of rejecting salt from feed solution. The water flux from feed solution to hydrogel is generated by the difference of water chemical potential across the membrane.[19,20] The advantages of using hydrogels as draw agents include no draw agent loss or back diffusion, and most importantly, hydrogels can easily release theoretically pure water by shrinking network under external stimulus, *e.g.*, temperature change, therefore exempting any further tedious membrane based water polishing processes.

Obviously, a good hydrogel draw agent should achieve a balanced performance in FO and regeneration processes. An attempt to combine high water flux and thermosensitivity by random copolymerization of NIPAm and SA was unsuccessful in that the randomly distributed charges from SA jeopardize the aggregation of PNIPAm segments and deprive the hydrogel of its thermosensitivity,[21] albeit the generated water flux indeed increased compared with pure PNIPAm. Organic and inorganic fillers including black carbon particles, graphene and Fe_3O_4 were incorporated into the NIPAm-SA copolymer hydrogels to enhance deswelling performance.[22-24] However, the NIPAm-SA copolymer hydrogel was still not thermally responsive. Majority of the water released was in vapor state due to evaporation under heat, albeit the heat was smartly and indirectly generated from solar energy or magnetic induction. In addition, in all the papers mentioned above using hydrogels as draw agents, the FO performance and deswelling performance were studied separately and never evaluated in a comprehensive FO-regeneration cyclic

continuous process perspective. What is more, the absence of comparison criterion of hydrogels' overall performances in entire FO-regeneration cyclic processes hinders the progress of exploring better hydrogels as draw agents.

Semi-IPN hydrogels as reversible draw agents for FO desalination were studied in the previous Chapter 4. PNIPAm network's thermosensitivity was maintained with the presence of linear nonionic hydrophilic polymers or even polyelectrolyte entangled within the network, which assisted in water flux augment from pure PNIPAm hydrogel. The balanced swelling and deswelling performances of semi-IPN enabled the realization of continuous FO desalination by temperature modulation, and I for the first time proposed the criterion judging hydrogel's comprehensive performance in FO-regeneration cycles. However, in that criterion, the factor of time was not considered and the flux of product water of ~0.2 LMH generated by semi-IPN still left room for improvement.

In this chapter, I determined the criterion to judge a hydrogel's performance as draw agent in FO desalination by comparing the production rate of available water in reversible FO-dewatering cycle. In addition, in order to improve the hydrogel's performance, in this chapter I shelve the PNIPAm based semi-IPN hydrogel system and managed to incorporate the characteristics of SA (ionic) and NIPAm (thermosensitivity) into a single monomer which is a thermally responsive ionic liquid (TRIL). As shown in Figure 5.1 and Figure 5.2, the TRILs are composed of a hydrophilic sulfonate anion and a relatively hydrophobic phosphonium cation. The subtle balance between hydrophilicity and hydrophobicity guarantees thermosensitivity and below the LCST the dissociation of ionic liquid assists in decreasing water chemical potential to achieve a higher water flux. Although TRIL was discovered decades ago,[25] its potential in desalination application has not been studied. In this chapter, I scrutinize the influences of many factors, including the poly ionic liquid hydrogel's composition, the hydrogel-hydrogel powder contact condition, FO membrane structure, area density of hydrogel and one FO-regeneration cycle duration, on the available water production rate. After optimization of each factor, an unprecedented product water flux of 1.22 LMH is reported.

5.2. Experimental Section

N-isopropylacrylamide (NIPAm, ≥98%) was purchased from Wako Pure Chemical Industrials Ltd. (Japan). *N,N'*-methylenebis(acrylamide) (≥99%), polyvinyl alcohol (PVA, M_w=61,000 Da), *N,N,N',N'*-tetramethylethylenediamine (TEMED, 99%), benzophenone (≥99%) and dichloromethane (≥99%) were purchased from Sigma-Aldrich. Ammonium peroxydisulfate (98%) and polyethylene glycol methacrylate (M_w=198 Da) were purchased from Alfa Aesar. Tetrabutylphosphonium bromide (>99%) and sodium p-styrenesulfonate (>98%) were purchased from Tokyo Chemical Industry Ltd. Tributyl-hexyl phosphonium bromide was purchased from Sino Rarechem Labs. All chemicals were used directly without any purification. Two kinds of FO membranes were received from Hydration Technology Innovations (HTI) and synthesized according to literature,[26] respectively.

5.2.1. Synthesis of ionic liquid monomers

Tetrabutylphosphonium *p*-styrenesulfonate (P4444 SS) was synthesized by ion exchange. For example, 20 g of tetrabutylphosphonium bromide and 17.7 g of sodium *p*-styrenesulfonate were dissolved in 30 ml of deionized (DI) water and the homogeneous solution was stirred for 48 hours before 80 ml of dichloromethane was added to extract the ionic liquid. The dichloromethane phase was washed with 20 ml DI water for three times. The dichloromethane was evaporated by high vacuum (<0.1 mbar) at room temperature for 72 hours. The synthesis of tributyl-hexyl phosphonium *p*-styrenesulfonate (P4446 SS) was conducted in a similar method. 20 g of tributyl-hexyl phosphonium bromide and 16.3 g of sodium p-styrenesulfonate were dissolved into 30 ml water. The solution turned into an opaque suspension since the target ionic liquid P4446 SS is hydrophobic. After 48 hours stirring, the ionic liquid was extracted by 80 ml dichloromethane and washed with 20 ml DI water for three times. The ionic liquid was purified at room temperature under a high vacuum for 72 hours. Both P4444 SS and P4446 SS are stored at -22℃ to avoid polymerization.

5.2.2. Synthesis of hydrogels

The neat PNIPAm and PNIPAm-PVA semi-IPN hydrogels were synthesized in accordance with the methods described in Chapter 4. For the synthesis of polyionic liquid hydrogel poly(tetrabutylphosphonium *p*-styrenesulfonate) (PP4444 SS), 44.8 mg (0.226 mmol) of crosslinker polyethylene glycol dimethacrylate (M_w=198 Da) and 20.6 mg (0.113 mmol) of photo-initiator benzophenone were dissolved in 5 g (11.3 mmol) P4444 SS. The homogenous solution was purged with N_2 for 15 minutes and the polymerization was conducted under UV (365 nm, 54 mW/cm^2) for 2 hours. The copolymer hydrogel of PP444-6 SS with 80 mol% P4444 SS and 20 mol% of P4446 SS were synthesized in a similar method. The crosslinker and photo-initiator used were still 2 mol% and 1 mol%, respectively with respect to monomers. 1.05 g (2.23 mmol) of P4446 SS, 44.2 mg (0.223 mmol) of polyethylene glycol dimethacrylate and 20.3 mg (0.111 mmol) of benzophenone were dissolved into 3.95 g (8.93 mmol) P4444 SS. The homogeneous solution was purged with N_2 for 15 minutes and the polymerization was conducted under UV (365 nm, 54 mW/cm^2) for 2 hours. All the hydrogels were allowed to swell to equilibrium swelling ratio in DI water to leach unreacted molecules and dried until constant weight before being ball-milled into powders ready for use.

5.2.3. Characterizations

The morphologies of dried hydrogel powder and FO membranes were characterized by optical microscopy (Olympus BX51) and FESEM (JEOL, 6340F), respectively. The LCST of each hydrogel was determined by a differential scanning calorimeter (TA Q10 Modulated DSC, TA Instruments). The hydrogels were swollen to a swelling ratio of about 3 g/g before the DSC measurement. For each DSC measurement, approximately 20 mg of swollen hydrogel was placed into a hermetically sealed aluminum pan. The temperature range was from 10 to 75 ℃ at a heating rate of 3 ℃/min. Dry nitrogen was used for purging at a flow rate of 50 ml/min. The 1H NMR spectra of the synthesized ionic liquid monomers were characterized by a Bruker DRX 300 instrument, with $CDCl_3$ as solvent and tetramethylsilane (TMS) as calibrator at 25 ℃.

The swelling ratio, water flux and deswelling performances of hydrogels were studied by utilizing gravimetric method. Hydrogel's swelling ratio was defined as $SR=m_{water}/m_{dry}$, where m_{water} is the weight of absorbed water within hydrogel while m_{dry} is weight of dry hydrogel. For water flux measurement in FO process, dry hydrogel powders or discs were put onto the FO membrane with selective layer facing the hydrogel (PRO mode) during the FO process. The water flux during FO process was determined by the hydrogel weight increment with given time and FO membrane area:

$$Flux = V/(A * t)$$

Where V is the volume of water (dm^3) permeating through the membrane, assuming water density is 1 kg/dm^3, it can be replaced by weigh increment (kg) of hydrogel during measurement. A is the membrane area (m^2), t is the FO time (h). Thus, the unit of water flux is LMH. Hydrogel's deswelling was conducted by putting 2 g swollen hydrogel (SR~3.8 g/g) on the surface of 60 ℃ hotplate and monitoring hydrogel's weight change with deswelling time. The hydrogel was covered by wiper (kimwipes) to absorb the released liquid water. The wiper was weighed to determine the amount of liquid water released and it was replaced whenever the hydrogel's weight was measured.

5.3. Results and discussion

5.3.1. The synthesis of ionic liquid monomers and hydrogels

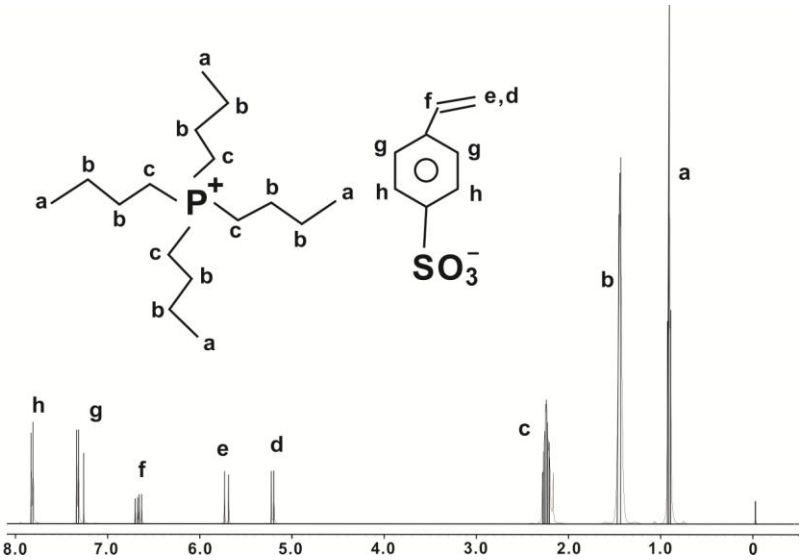

Figure 5.1 The ^1H NMR spectrum of tetrabutylphosphonium *p*-styrene sulfonate (P4444 SS).

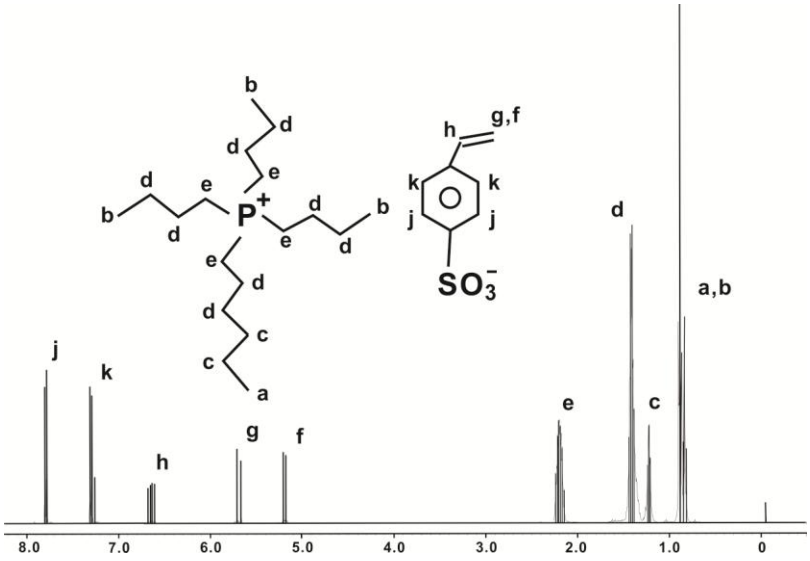

Figure 5.2 The ^{1}H NMR spectrum of tributylhexylphosphonium *p*-styrenesulfonate (P4446 SS).

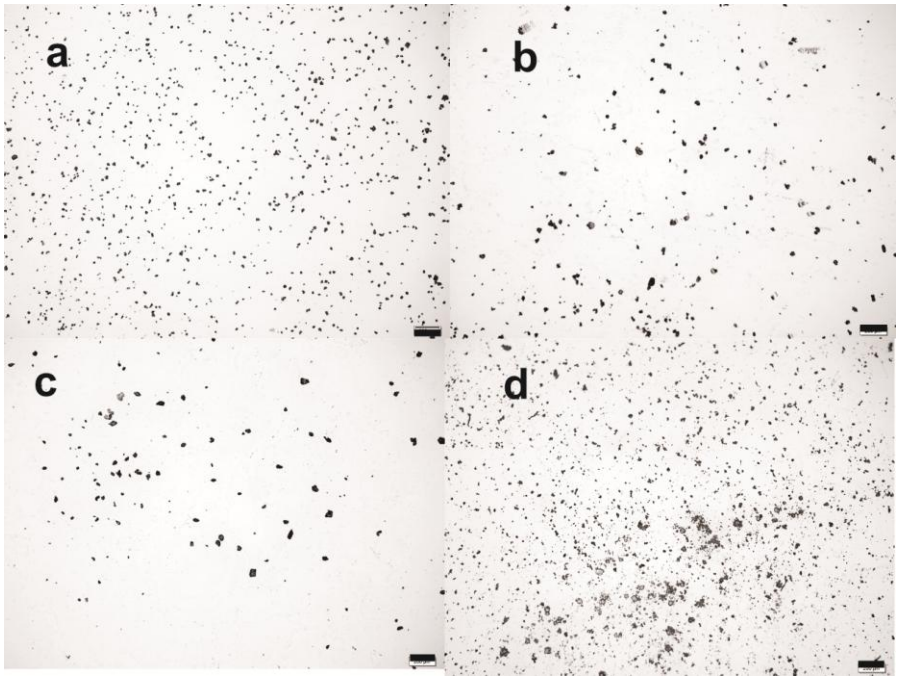

Figure 5.3 Optical images of (a) PP4444 SS, (b) PP444-6 SS, (c) neat PNIPAm and (d) PNIPAm-PVA semi-IPN hydrogel powder. The scale bar is 200 μm.

The ionic liquid monomers were successfully synthesized, which is proven by ^{1}H NMR spectrum shown in Figure 5.1 and 5.2. **P4444 SS**: 1H NMR, δ_H (400 MHz, $CDCl_3$): 0.89-0.93 (t, 12H, CH_3), 1.43-1.45 (m, 16H, CH_2), 2.23-2.25 (m, 8H, CH_2), 5.19-5.22 (d, 1H,

CH), 5.69-5.73 (d, 1H, CH), 6.63-6.68 (q, 1H, CH), 7.26-7.34 (d, 2H, CH), 7.81-7.83 (d, 2H, CH) ppm. **P4446 SS**: 1H NMR, δ_H (400 MHz, $CDCl_3$): 0.83-0.85 (t, 3H, CH_3), 0.88-0.90 (t, 9H, CH_3), 1.19-1.22 (m, 4H, CH_2), 1.39-1.43 (m, 16H, CH_2), 2.18-2.21(m, 8H, CH_2), 5.18-5.20 (d, 1H, CH), 5.67-5.71 (d, 1H, CH), 6.63-6.68 (q, 1H, CH), 7.26-7.34 (d, 2H, CH), 7.81-7.83 (d, 2H, CH) ppm.

Figure 5.3 shows all the hydrogels were successfully polymerized and fine hydrogel particles with dimensions of tens of micrometers were prepared.

5.3.2. The FO performances of hydrogels

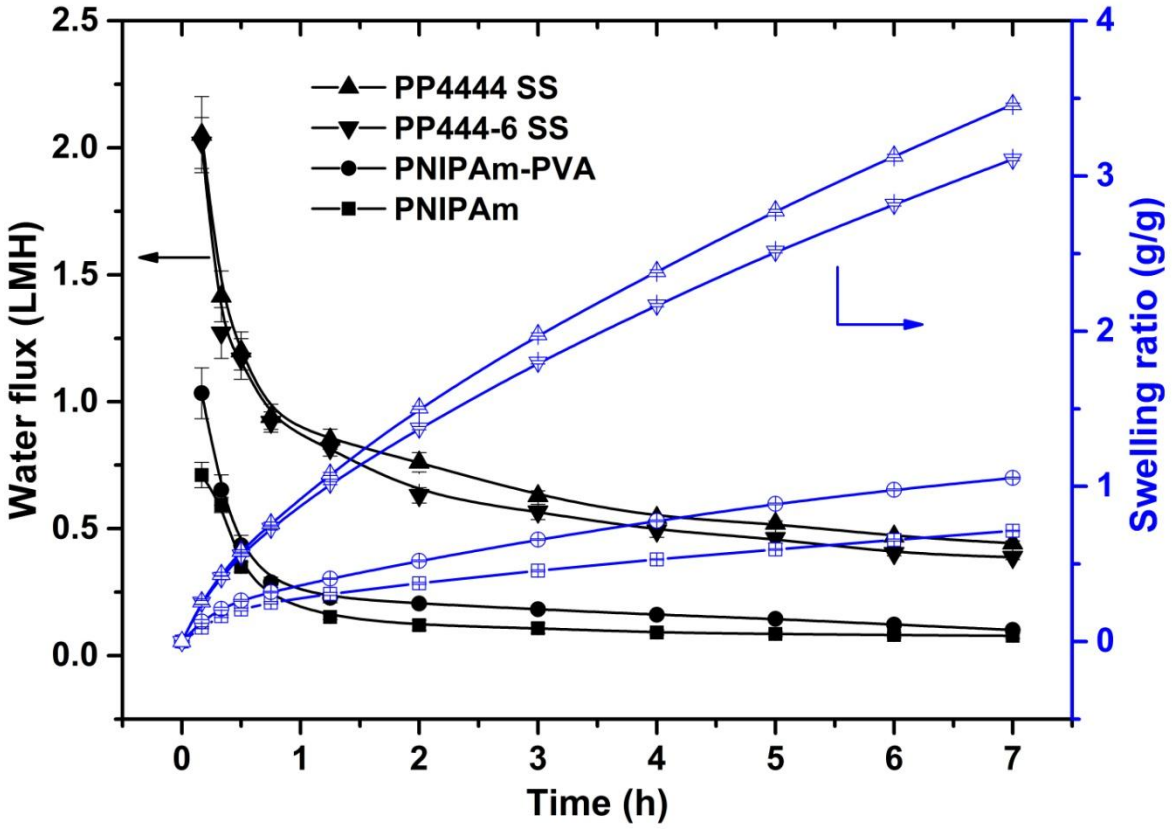

Figure 5.4 The water flux and swelling ratio profile of each hydrogel from dry state. The hydrogels were in powder form contacting a HTI cellulose triacetate membrane with a area density of 0.6 g/4.5 cm^2. Feed solution was 2000 ppm NaCl solution.

Figure 5.4 demonstrated the water flux and swelling ratio profiles as a function of FO process duration of each hydrogel in powder form with a HTI membrane. For each

hydrogel as draw agent, the water flux decayed and swelling ratio ascended as time elapsed in FO process. The PNIPAm hydrogel, doubtlessly, showed the weakest drawing ability that the initial water flux generated from dry state was only below 0.8 LMH and the plateau water flux after one hour FO was reduced to below 0.1 LMH. The incorporation of linear hydrophilic PVA into PNIPAm network, which is the strategy adopted in Chapter 4, slightly improved the water flux albeit the swelling ratio of the semi-IPN hydrogel was still only about 1 g/g (50 wt% water) after seven hours. This is because any hydrophilic modifications, *e.g.*, incorporating linear PVA or PSA into the PNIPAm network, cannot overwhelm the dominance of PNIPAm presence in order to preserve the thermosensitivity and thus the water flux improvement is limited. In order to further increase thermally responsive hydrogels' performance in FO process, a new route other than copolymerization or semi-IPN to blending hydrophobicity and hydrophilicity

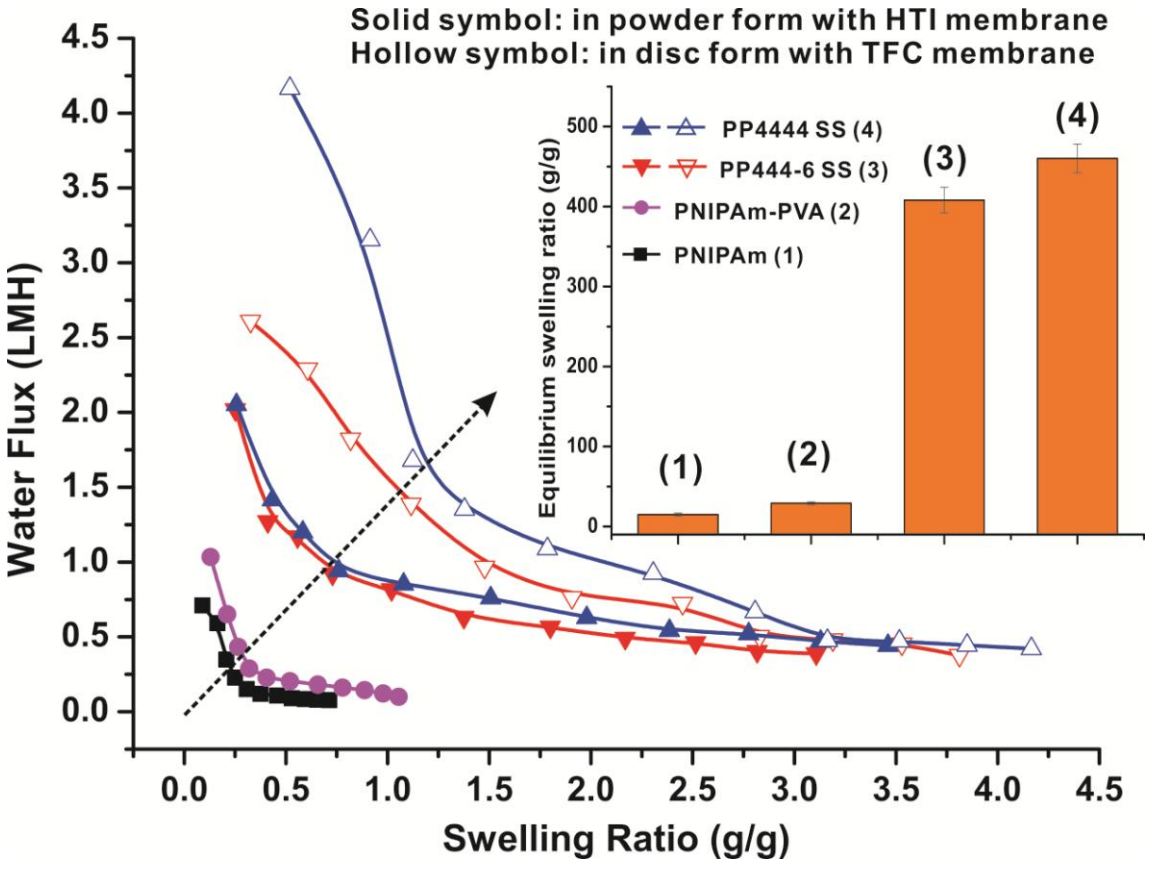

Figure 5.5 The swelling ratio and the corresponding generated water flux correlation of each hydrogel. Feed solution was 2000 ppm NaCl solution. Inlet was the equilibrium swelling ratio of each hydrogel immersing in DI water at room temperature.

in a hydrogel is needed. Replacing the cationic sodium of electrolyte sodium *p*-styrenesulfonate with a more hydrophobic phosphonium cation, the synthesized thermally responsive ionic liquid P4444 SS has achieved hydrophobicity and hydrophilicity coalition in monomer level, and its homopolymer hydrogel demonstrated significantly improved performance in FO process. As shown in Figure 5.4, the initially generated water flux was higher than 2 LMH and after 7 hours the decayed plateau flux maintained at about 0.5 LMH. Similar with the PNIPAm, this thermally responsive poly ionic liquid hydrogel with much better FO performance can also be copolymerized with other species to finely tune the properties. As can be seen in Figure 5.4, after copolymerizing with 20 mol% of more hydrophobic P4446 SS, the swelling ratio as well as water flux of PP444-6 SS decreased due to declined hydrophilicity.

A hydrogel's performance in FO process can also be qualitatively characterized by plotting water flux generated at various swelling ratios, as shown in Figure 5.5. Obviously, hydrogel with desirable FO performance should generate a very high water flux from dry state and the water flux declines insignificantly as swelling ratio increases. The PNIPAm-based hydrogels could only generate initial water flux of ~1 LMH, which quickly fell below 0.1 LMH when hydrogel was swollen to a swelling ratio of only about 1 g/g. The poly ionic liquid hydrogel, PP4444 SS, however, not only generated a higher initial water flux of more than 2 LMH, but maintained an acceptable water flux of ~0.5 LMH even at a swelling ratio of 4 g/g. The improved FO performance of polyionic liquid hydrogels may be ascribed to ~20 times higher equilibrium swelling ratios than those of PNIPAm-based hydrogels, as shown in Figure 5.5 inlet. Higher equilibrium swelling ratio indicates more clearance for water chemical potential reduction, therefore, imparts hydrogel the ability to generate a higher water flux at the same swelling ratio.

5.3.3. The influence of hydrogel particle-particle contact and membrane type on FO performance

In order to fully reveal the polyionic liquid hydrogels' potential capacity in FO process, other aspects influencing water diffusion such as hydrogel particle-particle contact conditions and FO membrane have also be scrutinized. As shown in Figure 5.6, PP4444

SS and PP444-6 SS demonstrated improved FO performances when the hydrogel powders were compressed into disc form. This is because the compressed interstitial

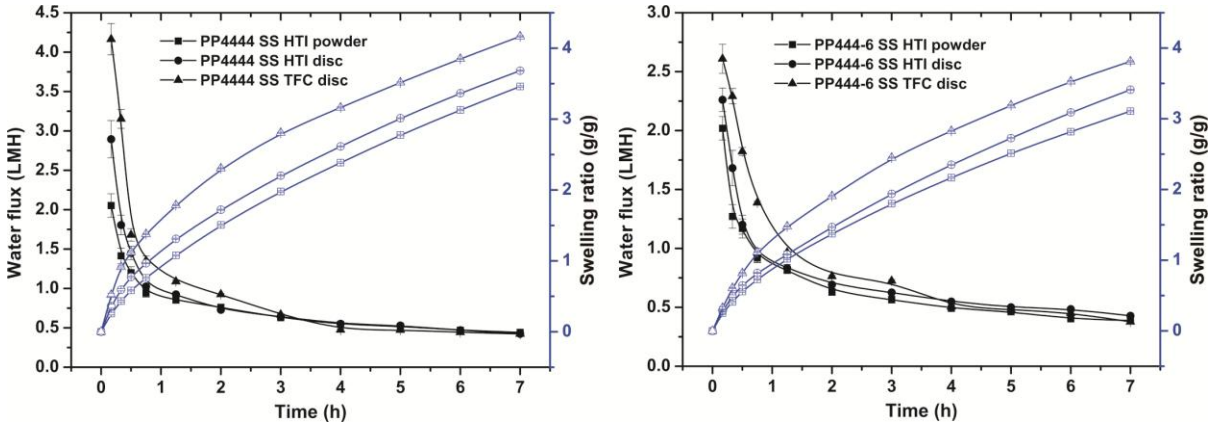

Figure 5.6 The improved water flux in FO of PP4444 SS and PP444-6 SS due to much reduced interstitial volume between particles in disc form and a thinner FO membrane.

volume between particles in the disc form improves the inter-particle contact condition and facilitates water diffusion across hydrogel particle boundaries.[27] Similarly, the improved water diffusion through a much thinner FO membrane synthesized in our lab

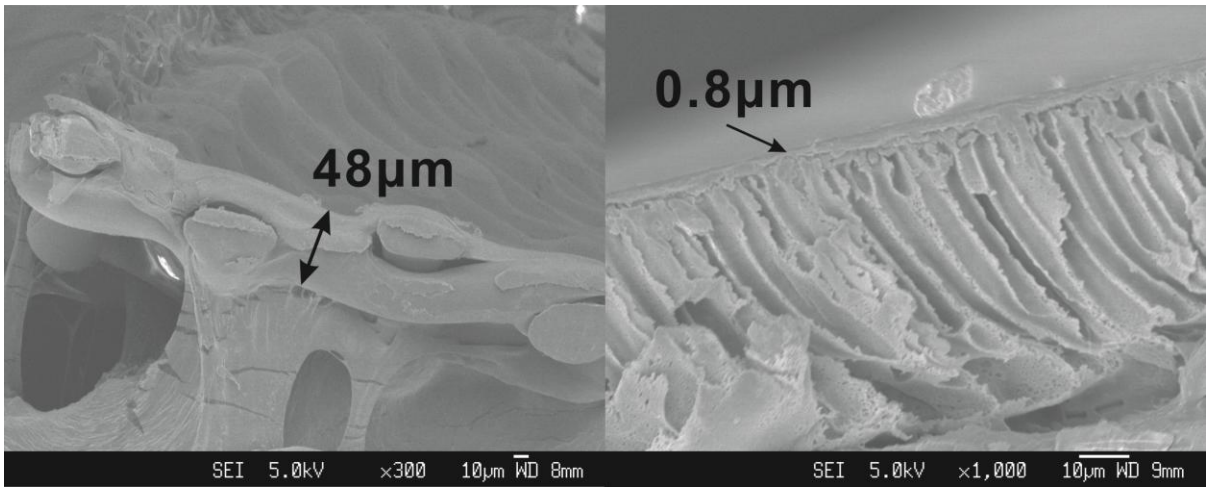

Figure 5.7 FESEM images of cellulose triacetate membrane from HTI (left) and thin film composite (TFC) membrane (right). The thickness of selective layer of each membrane was roughly indicated.

(see Figure 5.7) would also upgrade the hydrogel's FO performance. As shown in Figure 5.5, after optimization in water diffusion conditions, PP4444 SS could generate an initial

water flux of higher than 4 LMH and maintain it at roughly 2.5 LMH at the swelling ratio of 1 g/g, while PNIPAm-PVA semi-IPN hydrogel in powder form can only generate ~0.1 LMH at the same swelling ratio on a HTI membrane.

5.3.4. The thermosensitivity and dewatering performance

An ideal hydrogel as draw agent should not only generate a high water flux, but easily and swiftly release the absorbed water to make the desalinated water available. The hydrogels' LCSTs as well as swelling ratio profiles at 60 ℃ as function of dewatering time are shown in Figure 5.8 and Figure 5.9, respectively. The subtle balance between

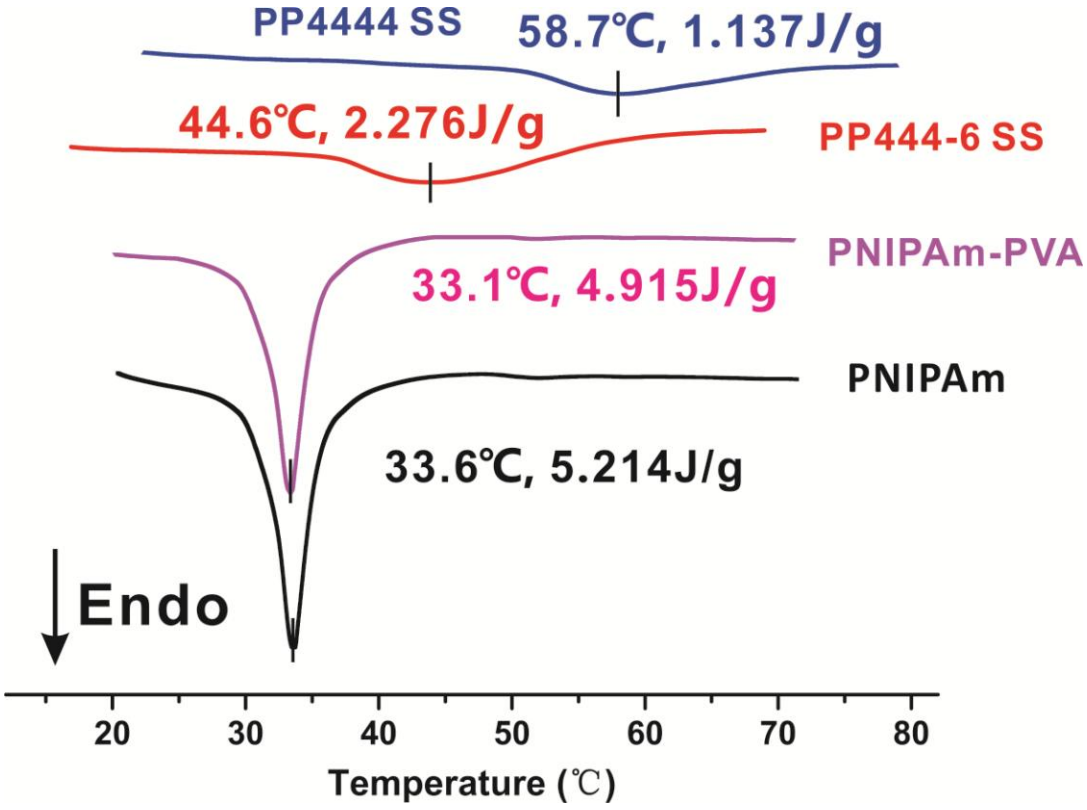

Figure 5.8 The DSC measurements of each hydrogel with a swelling ratio of 3 g/g. The peak of LCST and the enthalpy of phase transition were marked.

hydrophobicity and hydrophilicity imparts thermosensitivity to the PP4444 SS with a LCST of 58.7 ℃. Thus, the swelling ratio of PP4444 SS can reduce from 3.8 g/g to 1.7 g/g after 15 minutes at 60 ℃. It is worth noting that the LCST peaks of polyionic liquid hydrogels are quite broad.[28] The deswelling temperature of 60 ℃ falls within the peak

region of PP4444 SS and might not be high enough to guarantee a complete phase transition. Instead of increasing deswelling temperature to achieve faster hydrogel regeneration, declining the hydrogels' LCSTs would be a more feasible and attractive method. After copolymerizing with 20 mol% more hydrophobic P4446 SS, the poly ionic liquid hydrogel PP444-6 SS has an acceptable LCST of ~44 ℃ and the deswelling temperature of 60 ℃ locates above the entire phase separation range. Therefore, PP444-6 SS has better deswelling performance than PP4444 SS that it can reach a swelling ratio of 0.85 g/g after 15 minute deswelling. Actually besides the LCST, the deswelling process of hydrogels can also be depicted by the phase transition heat as shown in Figure 5.8. This energy input is an indication of the extent or severity of the thermally responsive hydrogels' structural change including bound water to free water transition and

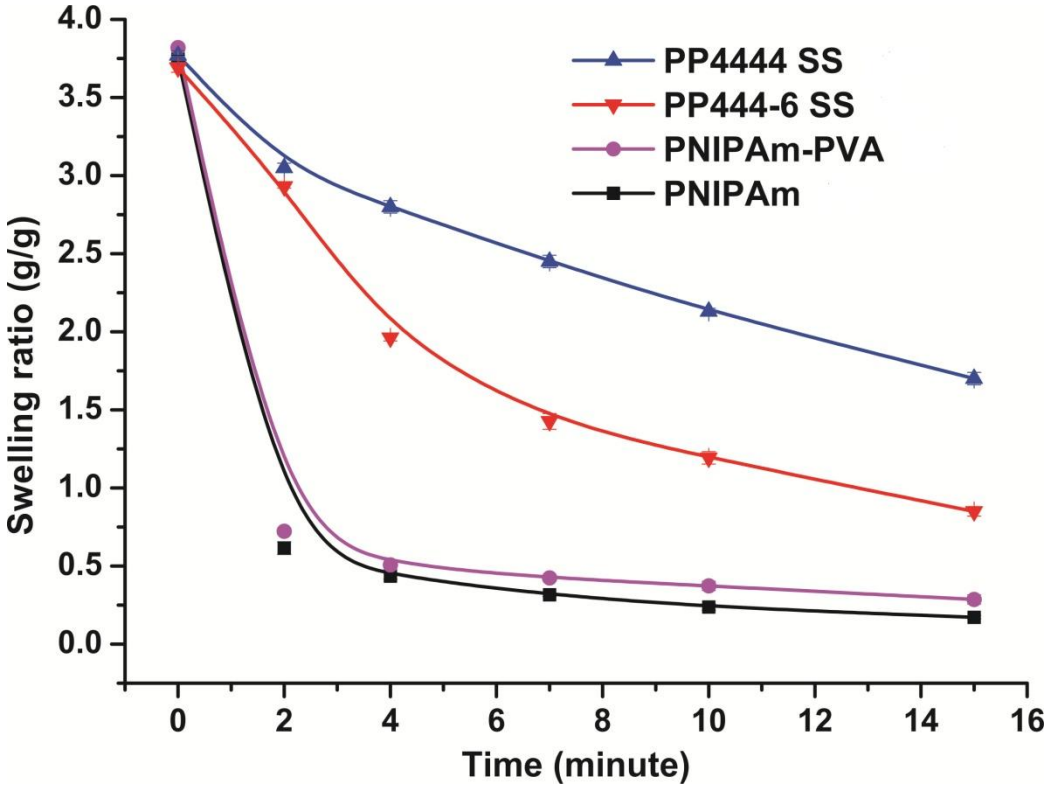

Figure 5.9 Deswelling profile of each hydrogel at 60 ℃.

hydrophobic association, *etc*.[29] Therefore, hydrogels like PSA and its copolymer with NIPAm have no phase transition making the majority of water released at high temperature in vapor form; while typical thermally responsive PNIPAm and PNIPAm-

PVA hydrogels have very high transition heat inputs indicating a very strong phase transition at LCST, resulting in a quite high liquid water recovery (>80%) since the water was majorly squeezed out, as shown in Figure 5.10. Although the poly ionic liquid hydrogels may have a unique phase transition mechanism,[30] the rule also applies that incorporating more hydrophobic segments into backbone reduces LCST. The PP444-6 SS demonstrated not only reduced LCST but increased transition heat compared with PP4444 SS hydrogel. Therefore, the liquid water recovery of PP444-6 SS was increased to ~50% albeit still lower than those of PNIPAm-based hydrogels.

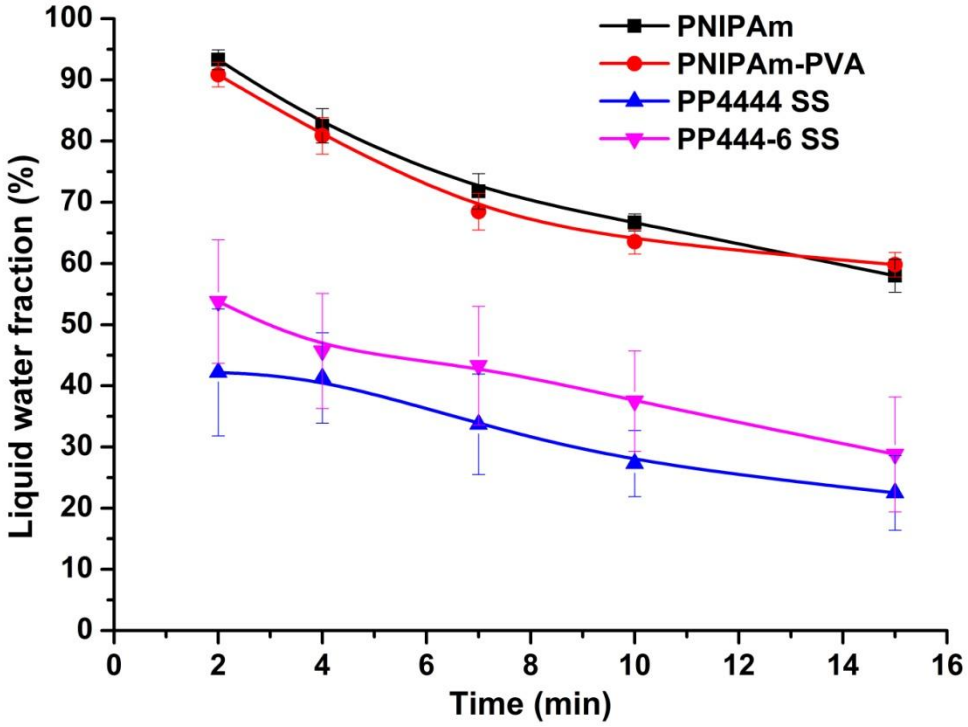

Figure 5.10 Fraction of liquid water released during deswelling process.

5.3.5. The selection criterion of hydrogel with the best performance as draw agent

The required abilities of hydrogels as draw agents to generate a high water flux in FO process and easily release absorbed water in regeneration process are always contradictory. Increasing the drawing ability in FO process inevitably jeopardizes the deswelling properties in regeneration process. As can be seen in Figure 5.5 and Figure 5.9 that the FO performance ascends in the order of PNIPAm< PNIPAm-PVA<PP444-6

SS<PP4444 SS, while the performance in regeneration process descends in the order of PNIPAm>PNIPAm-PVA>PP444-6 SS>PP4444 SS. This compromise also appeared in all the previously published papers about hydrogels as draw agents,[18, 22-24, 31] where the FO and dewatering performances were discussed separately and never considered together to evaluate the comprehensive performance in a cyclic manner. In the previous Chapter 4, I managed to set up a criterion to compare hydrogels' overall performance by calculating the amount of water absorbed by a hydrogel from a swollen state with the swelling ratio after deswelling until an arbitrary water flux (e.g., 0.1 LMH) was reached. However, the factor of time consuming was still not considered. In this chapter, I will

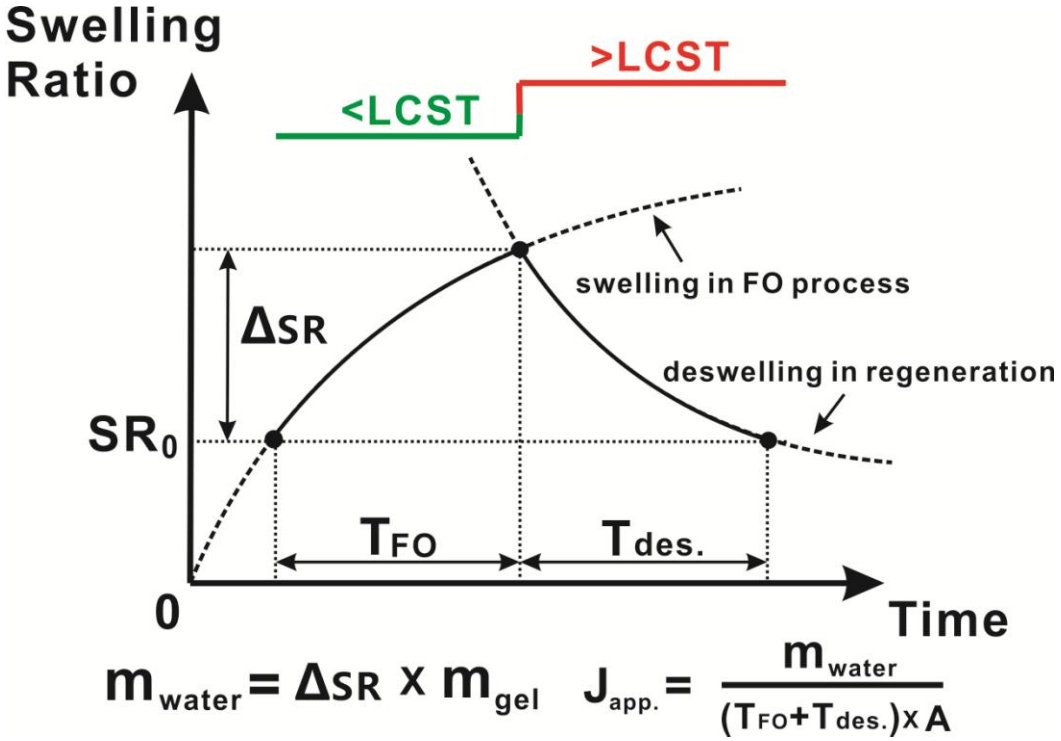

Figure 5.11 Schematic illustration of the criterion for a hydrogel's comprehensive performance in reversible FO-Regeneration cycles. T_{FO} and $T_{des.}$ are the duration of FO process and regeneration process, respectively. SR_0 is swelling ratio obtainable after regeneration, which can be found in Figure 5.9 for each hydrogel. A is the active membrane area, which is 4.5 cm^2 throughout this chapter. ΔSR is the swelling ratio increment during the FO process and m_{gel} is the weight of dry hydrogel. M_{water} is the amount of water absorbed that can also be fully released during regeneration process in one cycle. Therefore, the apparent water flux ($J_{app.}$) calculated in this criterion is the water production rate.

judge the hydrogels' comprehensive performance by comparing how fast they can produce (absorb and release) water in a cyclic manner.

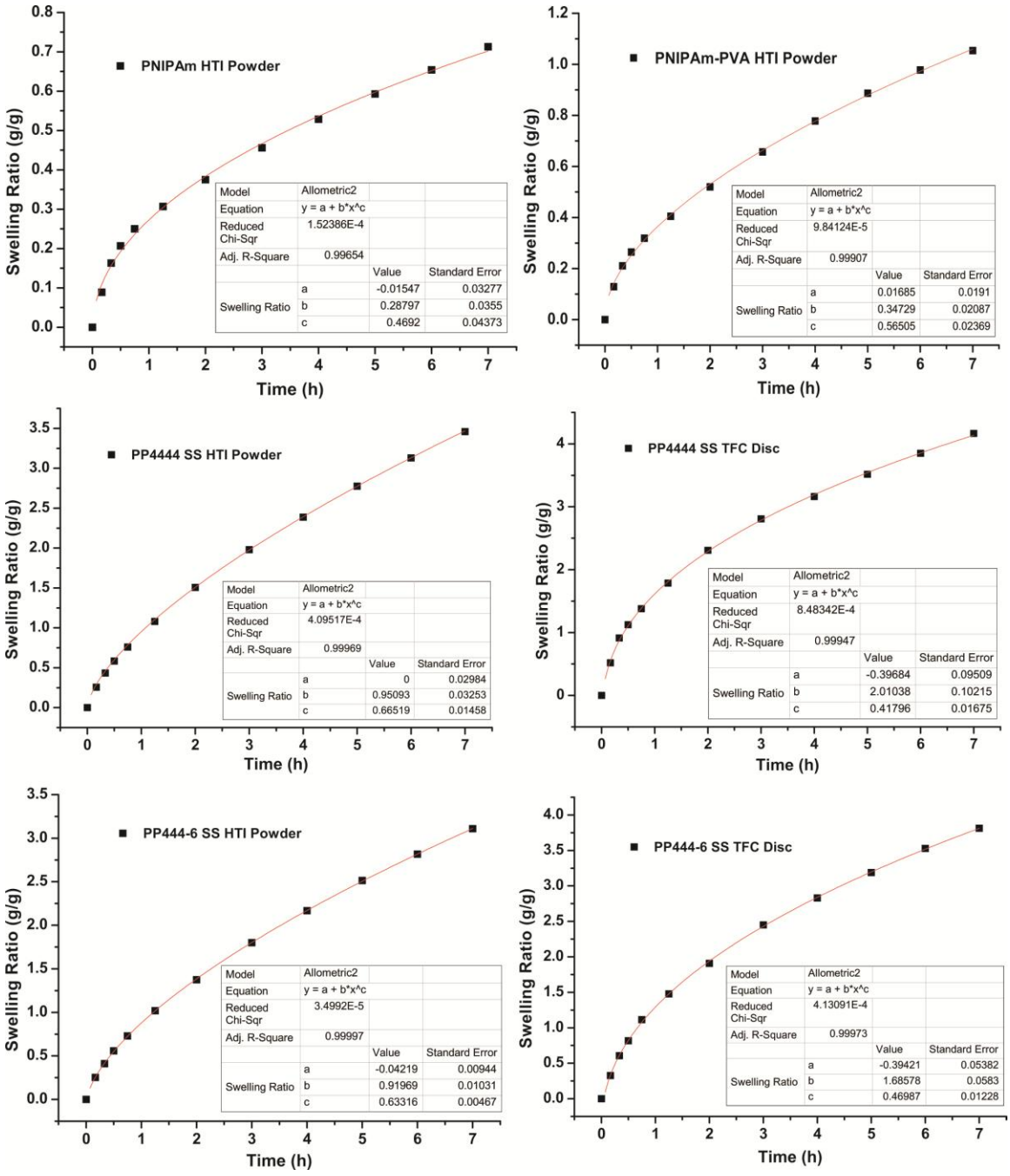

Figure 5.12 The fittings of swelling ratio versus FO time for different hydrogel in powder form with HTI membrane and in disc form with TFC membrane.

Figure 5.11 is the schematic of the universal criterion of hydrogel's comprehensive performance as a draw agent in FO desalination. Since all the thermally responsive hydrogels cannot retain their completely dry state after deswelling process, the hydrogel would start the next FO process with a swelling ratio of SR_0 obtained after the deswelling in regeneration process. All the water absorbed in the FO process with hydrogel starting from swollen state (SR_0) could be released in regeneration process to make the FO-regeneration cycle reversible, and the water flux calculated in this criterion depicts the desalinated water production rate rather than the water absorbing rate in sole FO process. For example, after knowing the fitting function of the correlation between swelling ratio and FO time of each hydrogel as shown in Figure 5.12, one can easily calculate the increment of swelling ratio (ΔSR) from SR_0 in FO process whose duration is T_{FO}. The duration of regeneration process ($T_{des.}$) should be long enough to restore SR_0. Then the desalinated water production rate can be calculated given the dry hydrogel weight and total duration of one FO-regeneration cycle.

5.3.6. The performance enhancement from tuning hydrogel's composition, membrane structure and particle-particle contact condition

After setting up the criterion, I use it to compare the comprehensive performance of hydrogels as draw agents for the rest of this chapter. If I fix one FO-regeneration cycle within one hour, the swelling ratio profiles of each thermally responsive hydrogel within one FO-regeneration cycle are shown in Figure 5.13 and the key parameters of the criterion were summarized in Table 5.1. The PNIPAm's inherently poor drawing ability makes the lowest desalinated water production rate of ~0.18 LMH though the hydrogel's swelling in FO process starts from a almost dry state (SR_0=0.17 g/g). The incorporation of hydrophilic linear PVA only slightly improves the comprehensive performance with a water flux of 0.22 LMH. The PP4444 SS can generate the highest water flux from dry state as mentioned above; however, its relatively poor deswelling performance resulted in the highest swelling ratio after deswelling (SR_0=1.70 g/g), which in turn paralyzed its FO performance in cyclic perspective. More balanced FO and regeneration performances achieved by PP444-6 SS make it the best draw agent for FO desalination that can achieve a desalinated water production rate of 0.61 LMH. In addition, as mentioned, the water

diffusion from brackish water into hydrogels also hinges on the barriers generated from membrane structure, membrane-hydrogel and hydrogel particle-particle contact

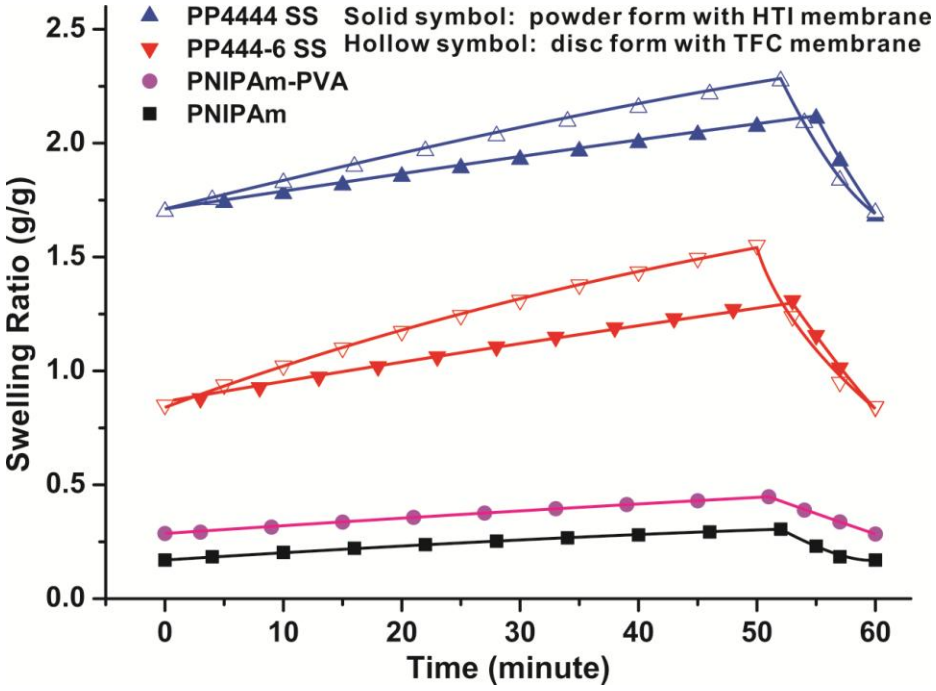

Figure 5.13 Comparison of comprehensive performance of each hydrogel in one reversible FO-regeneration cycle within one hour. T_{FO} and $T_{des.}$ were allotted that SR_0 can be obtained after regeneration to make the cycle reversible. Hydrogel's area densitiy was fixed at 0.6 g/4.5 cm^2. 2000 ppm NaCl was used as feed solution.

Table 5.1 The comparison of comprehensive FO-Regeneration performances of each hydrogel.

	PNIPAm	PNIPAm-PVA	PP4444 SS	PP4444 SS*	PP444-6 SS	PP444-6 SS*
T_{FO} (min)	52	51	55	52	53	50
$T_{des.}$ (min)	8	9	5	8	7	10
SR_0 (g/g)	0.17	0.28	1.70	1.70	0.85	0.85
ΔSR (g/g)	0.134	0.161	0.409	0.574	0.459	0.702
M_{water} (mg)	80.4	96.6	245.4	344.4	275.4	421.2
$J_{app.}$ (LMH)	0.18	0.22	0.55	0.77	0.61	0.94

Note: The entire one FO-regeneration process was one hour. Hydrogels without asteroid mark were using HTI membrane in powder form, while the ones with an asteroid mark were using TFC membrane in disc form. Dry hydrogel weight was 0.6 g and membrane area was 4.5 cm^2. The SR_0 was obtained from Figure 5.9.

condition. After using a thinner membrane and improving the hydrogel contact condition by compressing it into disc form, the water production rate of PP444-6 SS can be further enhanced to 0.94 LMH.

5.3.7. The performance enhancement from optimizing hydrogel's area density and one FO-regeneration cycle duration

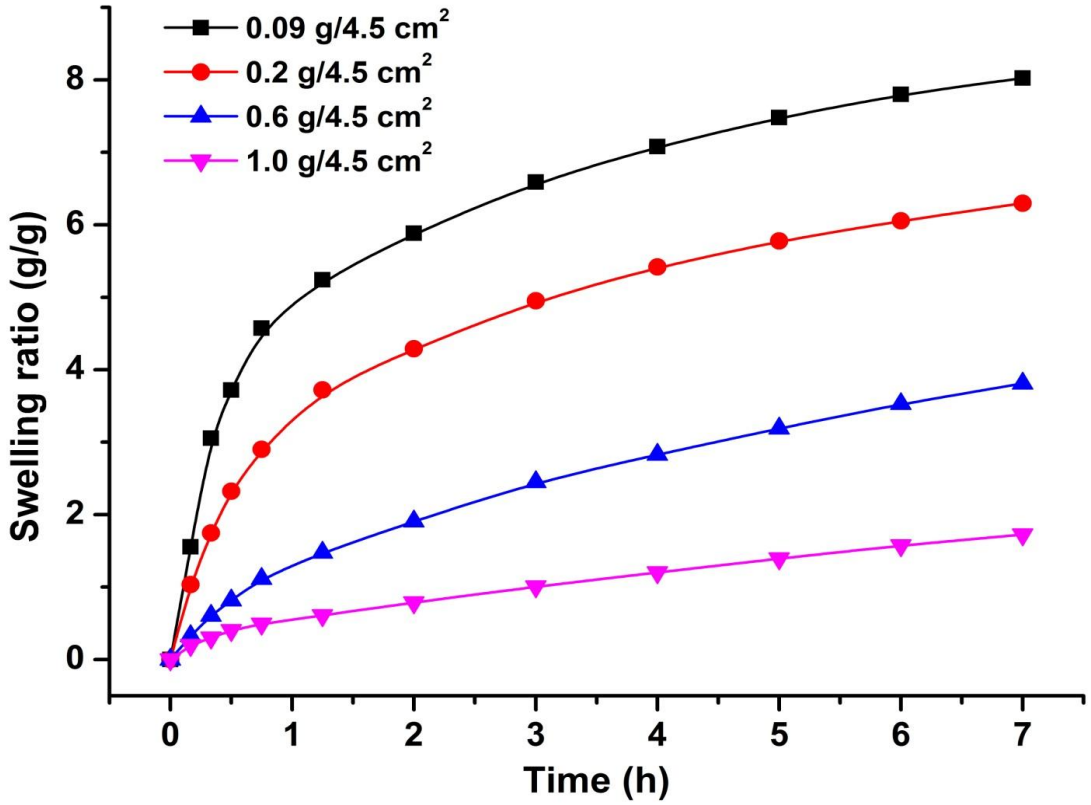

Figure 5.14 The influence of area density on the hydrogel FO performance. The hydrogel was P444-6 SS in disc form and TFC membrane was used as the FO membrane. Feed solution was 2000 ppm NaCl solution.

The hydrogel PP444-6 SS with the best comprehensive performance among all the thermally responsive hydrogels was selected to achieve higher desalinated water production rate by tuning the area density (weight of hydrogel/area of membrane) of hydrogel. Figure 5.14 shows that the swelling ratio of a hydrogel with a smaller area density increases faster than that of a hydrogel with a larger one. This was also reported in Chapter 4 and was probably due to the influence of water diffusion path length through

the hydrogels. On a fixed membrane area and within fixed FO time, less amount of hydrogel would lead to a larger swelling ratio increment, while the amount of water is calculated by the swelling ratio increment multiplying the weight of dry hydrogel. Therefore, there should be a best hydrogel area density that can maximize the amount of water produced. Again, I simulated the correlation between swelling ratio and FO time of PP444-6 SS with different area densities as shown in Figure 5.15 and fixed one FO-regeneration cycle in one hour to compare the desalinated water production rate.

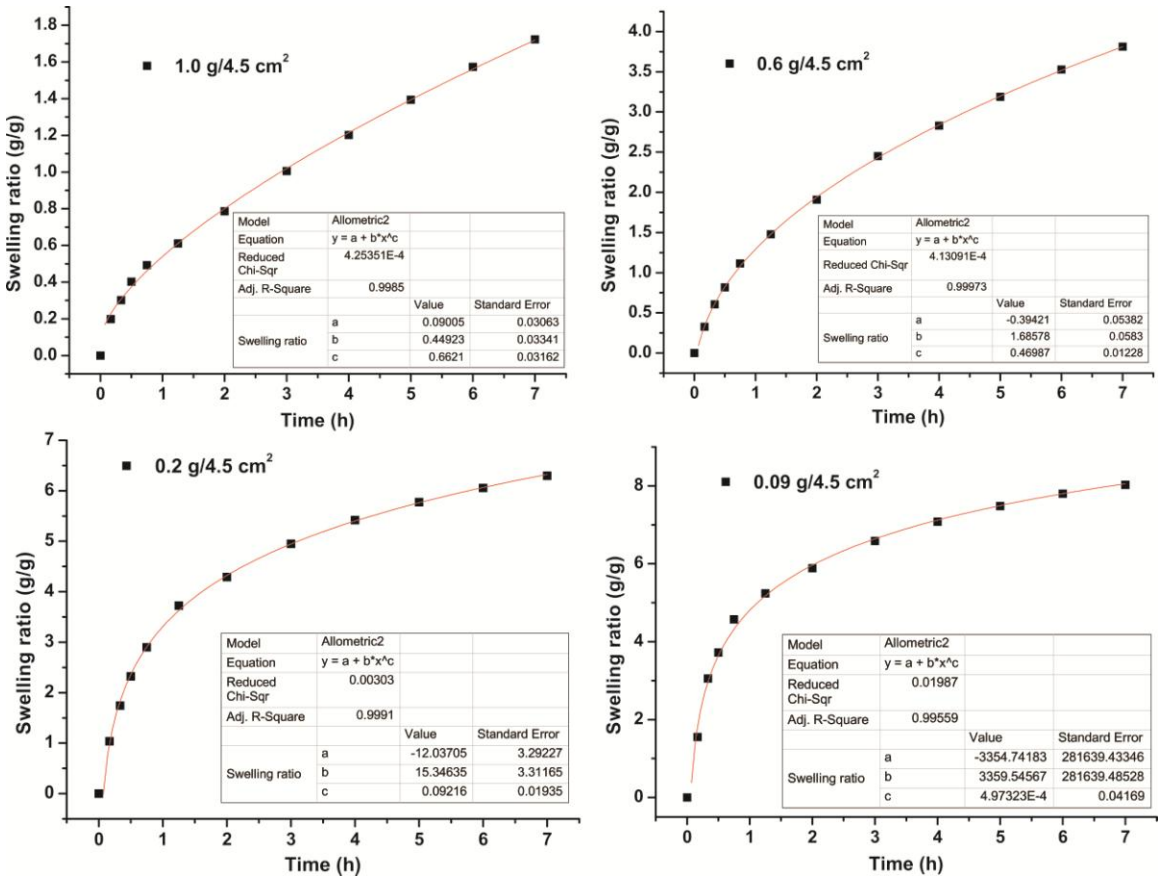

Figure 5.15 The fittings of the correlation between swelling ratio and FO time for PP444-6 SS with different area density. The hydrogel was in disc form using TFC membrane. 2000 ppm NaCl solution was used as feed solution.

The swelling ratio profiles within one FO-regeneration cycle is shown in Figure 5.16 and the key parameters in the criterion were summarized in Table 5.2. It can be observed that although the area density of 0.09 g/4.5 cm^2 can generate the highest swelling ratio

increment due to the lowest disc thickness and water diffusion path length, the area density of 0.2 g/4.5 cm^2 produces the largest amount of water during one FO-regeneration cycle and the highest desalinated water production rate of ~1.04 LMH.

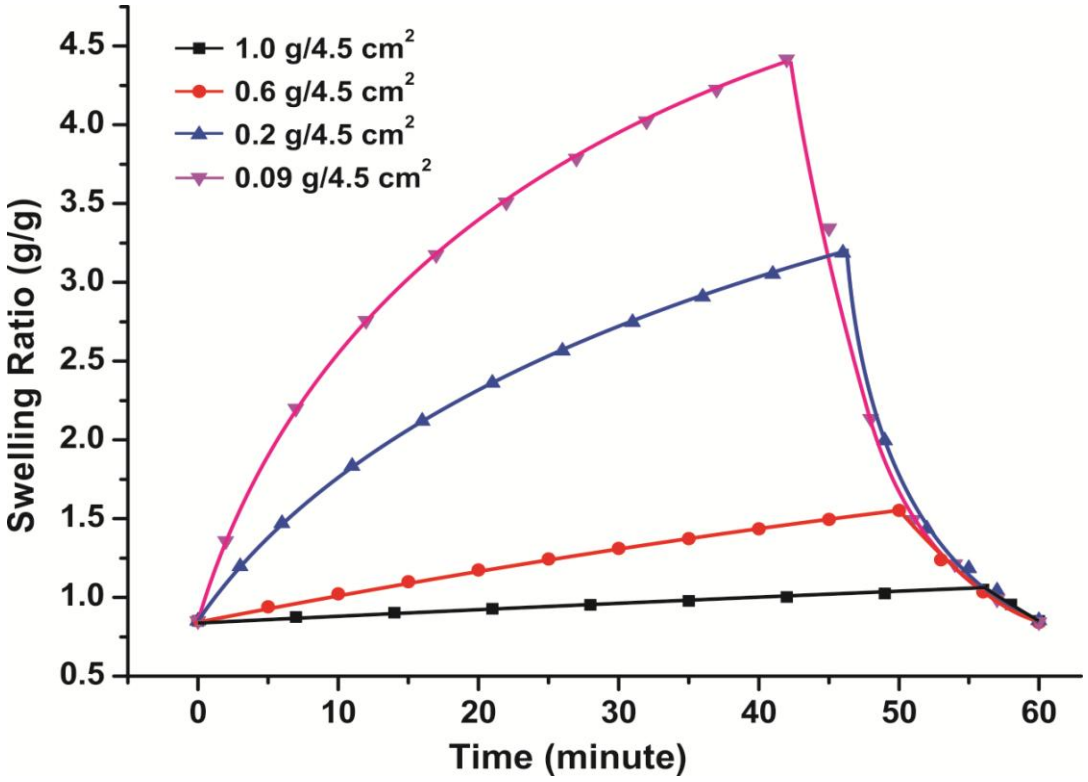

Figure 5.16 The influence of hydrogel area density on the hydrogel's comprehensive performance in terms of water production rate. The hydrogel was PP444-6 SS in disc form on TFC membrane. 2000 ppm NaCl solution was used as feed solution.

Table 5.2 The influence of area density of PP444-6 SS on the water production rate.

	1.0 g/4.5 cm^2	**0.6 g/4.5 cm^2**	**0.2 g/4.5 cm^2**	**0.09 g/4.5 cm^2**
T_{FO} (min)	**56**	**50**	**46**	**42**
$T_{des.}$ (min)	**4**	**10**	**14**	**18**
SR_0 (g/g)	**0.85**	**0.85**	**0.85**	**0.85**
ΔSR (g/g)	**0.199**	**0.702**	**2.337**	**3.568**
m_{water} (mg)	**199.0**	**421.2**	**467.4**	**321.1**
$J_{app.}$ (LMH)	**0.44**	**0.94**	**1.04**	**0.71**

Note: The hydrogel was in disc form on TFC membrane, with 2000 ppm NaCl as feed solution.

The reduction of area density from 0.6 g/4.5 cm^2 to 0.2 g/4.5 cm^2 not only increases the desalinated water production rate, but reduces the amount of hydrogel required on the membrane surface and is a decline in hydrogel synthesis cost for possible future scale-up.

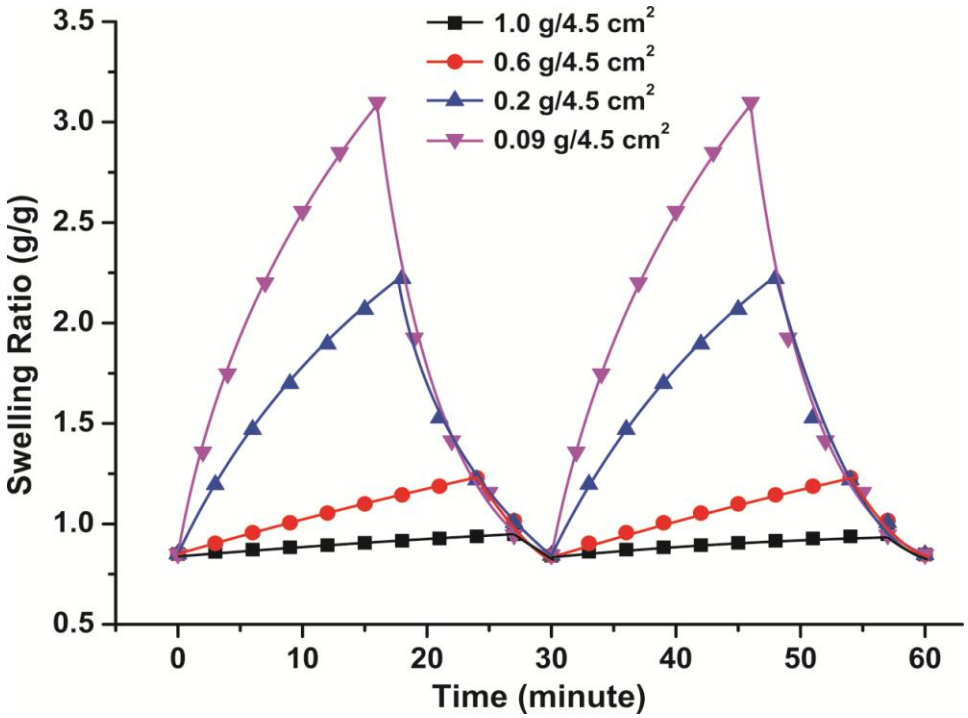

Figure 5.17 The comprehensive performance of PP444-6 SS when one FO-regeneration cycle was fixed within 30 minutes. PP444-6 SS was used in disc form on TFC membrane. 2000 ppm NaCl solution was used as feed solution.

After the optimization of parameters including hydrogel structure, water diffusion conditions and area density, one FO-regeneration cycle duration is another important parameter for study to achieve the highest possible water production rate. As shown in Figure 5.17, I reduced the duration of one FO-regeneration cycle from one hour to 30 minutes trying to make more use of the steep section in swelling ratio-FO time curve to increase water flux. Similarly as seen from the key parameters summarized in Table 5.3, the area density of 0.2 g/4.5 cm^2 still generates the highest water flux of 1.22 LMH. The distribution of 18 minutes in FO process and 12 minutes in regeneration process in a 30-mintue cycle is also a macroscopic indication of a well balanced performance achieved by the PP444-6 SS hydrogel. This water production rate of 1.22 LMH was quite

promising in that if one coated the hydrogel on the surface of hollow fiber membranes to make a module as envisaged in Chapter 4, due to the large surface to volume ratio characteristics of hollow fiber membrane, the amount of water produced from a moderate volume module would be attractive. For example, if one coats the PP444-6 SS hydrogel on 100 m^2 hollow fiber membrane using an area density of 0.2 g/4.5 cm^2, only less than 45 kg of dry hydrogel would be needed and replenishment of hydrogel was theoretically not necessary. The amount of water that can be achieved is 122 liters per hour, or roughly 3 tons per day consuming thermal energy from solar source or industrial waste heat.

Table 5.3 The comprehensive performance of PP444-6 SS when one FO-regeneration cycle was fixed within 30 minutes.

	1.0 g/4.5 cm^2	**0.6 g/4.5 cm^2**	**0.2 g/4.5 cm^2**	**0.09 g/4.5 cm^2**
T_{FO} (min)	**27**	**24**	**18**	**16**
$T_{des.}$ (min)	**3**	**6**	**12**	**14**
SR_0 (g/g)	**0.85**	**0.85**	**0.85**	**0.85**
ΔSR (g/g)	**0.099**	**0.380**	**1.371**	**2.249**
M_{water} (mg)	**99.0**	**228.0**	**274.2**	**202.4**
$J_{app.}$ (LMH)	**0.44**	**1.01**	**1.22**	**0.90**

Note: The hydrogel was in disc form on TFC membrane. Feed solution was 2000 ppm NaCl solution.

5.4. Conclusion

The thermally responsive polyionic liquid hydrogels were for the first time scrutinized as draw agents in forward osmosis desalination. They can absorb water from brackish solution at room temperature and squeeze absorbed water out at temperatures above their LCSTs. The thermally responsive ionic liquid can copolymerize with other species to subtly tune the balance of performances in FO and regeneration processes. In addition, other aspects that can influence the FO performance including the contact condition between hydrogel particles and FO membrane structure were also studied. I for the first time come up with a criterion to judge a hydrogel's comprehensive performance as draw agent in FO desalination, which is by comparing the desalinated water production rate in

reversible FO-regeneration cycles. With this criterion, I picked the best hydrogel and improved desalinated water production rate to about 1.22 LMH after optimizing the area density of hydrogel on membrane and the duration of one FO-regeneration cycle. This is an exciting value in that less than 45 kg of replenishment-free hydrogel coated on 100 m^2 hollow fiber membrane would produce about 3 tons of purified water per day only at the cost of thermal energy from solar source or industrial waste heat.

References

1. Cath, T.; Childress, A.; Elimelech, M., Forward osmosis: Principles, applications, and recent developments. *Journal of Membrane Science* **2006,** *281*, (1-2), 70-87.

2. Mi, B.; Elimelech, M., Organic fouling of forward osmosis membranes: fouling reversibility and cleaning without chemical reagents. *Journal of Membrane Science* **2010,** *348*, (1), 337-345.

3. Hoover, L. A.; Phillip, W. A.; Tiraferri, A.; Yip, N. Y.; Elimelech, M., Forward with osmosis: emerging applications for greater sustainability. *Environmental science & technology* **2011,** *45*, (23), 9824-9830.

4. Duan, J.; Litwiller, E.; Choi, S.-H.; Pinnau, I., Evaluation of sodium lignin sulfonate as draw solute in forward osmosis for desert restoration. *Journal of Membrane Science* **2014,** *453*, 463-470.

5. Chekli, L.; Phuntsho, S.; Shon, H. K.; Vigneswaran, S.; Kandasamy, J.; Chanan, A., A review of draw solutes in forward osmosis process and their use in modern applications. *Desalination and Water Treatment* **2012,** *43*, (1-3), 167-184.

6. Klaysom, C.; Cath, T. Y.; Depuydt, T.; Vankelecom, I. F., Forward and pressure retarded osmosis: potential solutions for global challenges in energy and water supply. *Chem Soc Rev* **2013,** *42*, (16), 6959-6989.

7. Lutchmiah, K.; Lauber, L.; Roest, K.; Harmsen, D. J. H.; Post, J. W.; Rietveld, L. C.; van Lier, J. B.; Cornelissen, E. R., Zwitterions as alternative draw solutions in forward osmosis for application in wastewater reclamation. *Journal of Membrane Science* **2014,** *460*, 82-90.

8. McCutcheon, J. R.; McGinnis, R. L.; Elimelech, M., A novel ammonia—carbon dioxide forward (direct) osmosis desalination process. *Desalination* **2005,** *174*, (1), 1-11.

9. Stone, M. L.; Rae, C.; Stewart, F. F.; Wilson, A. D., Switchable polarity solvents as draw solutes for forward osmosis. *Desalination* **2013,** *312*, 124-129.

10. Stone, M. L.; Wilson, A. D.; Harrup, M. K.; Stewart, F. F., An initial study of hexavalent phosphazene salts as draw solutes in forward osmosis. *Desalination* **2013,** *312*, 130-136.

11. Mok, Y.; Nakayama, D.; Noh, M.; Jang, S.; Kim, T.; Lee, Y., Circulatory osmotic desalination driven by a mild temperature gradient based on lower critical solution temperature (LCST) phase transition materials. *Phys Chem Chem Phys* **2013,** *15*, (44), 19510-19517.

12. Alnaizy, R.; Aidan, A.; Qasim, M., Copper sulfate as draw solute in forward osmosis desalination. *Journal of Environmental Chemical Engineering* **2013,** *1*, (3), 424-430.

13. Ling, M. M.; Chung, T. S.; Lu, X., Facile synthesis of thermosensitive magnetic nanoparticles as "smart" draw solutes in forward osmosis. *Chem Commun (Camb)* **2011,** *47*, (38), 10788-10790.

14. Liu, Z.; Bai, H.; Lee, J.; Sun, D. D., A low-energy forward osmosis process to produce drinking water. *Energy & Environmental Science* **2011,** *4*, (7), 2582.

15. Zhao, Q.; Chen, N.; Zhao, D.; Lu, X., Thermoresponsive magnetic nanoparticles for seawater desalination. *ACS Appl Mater Interfaces* **2013,** *5*, (21), 11453-11461.

16. Höpfner, J.; Klein, C.; Wilhelm, M., A novel approach for the desalination of seawater by means of reusable poly (acrylic acid) hydrogels and mechanical force. *Macromolecular rapid communications* **2010,** *31*, (15), 1337-1342.

17. Höpfner, J.; Richter, T.; Košovan, P.; Holm, C.; Wilhelm, M., Seawater desalination via hydrogels: Practical realisation and first coarse grained simulations. In *Intelligent Hydrogels*, Springer: 2013; pp 247-263.

18. Li, D.; Zhang, X.; Yao, J.; Simon, G. P.; Wang, H., Stimuli-responsive polymer hydrogels as a new class of draw agent for forward osmosis desalination. *Chem Commun (Camb)* **2011,** *47*, (6), 1710-1712.

19. Zhao, S., Osmotic pressure versus swelling pressure: comment on "bifunctional polymer hydrogel layers as forward osmosis draw agents for continuous production of

fresh water using solar energy". *Environmental science & technology* **2014,** *48*, (7), 4212-4213.

20. Wang, H.; Wei, J.; Simon, G. P., Response to osmotic pressure versus swelling pressure: comment on "bifunctional polymer hydrogel layers as forward osmosis draw agents for continuous production of fresh water using solar energy". *Environmental science & technology* **2014,** *48*, (7), 4214-4215.

21. Kokufuta, E.; Wang, B.; Yoshida, R.; Khokhlov, A. R.; Hirata, M., Volume phase transition of polyelectrolyte gels with different charge distributions. *Macromolecules* **1998,** *31*, (20), 6878-6884.

22. Razmjou, A.; Barati, M. R.; Simon, G. P.; Suzuki, K.; Wang, H., Fast deswelling of nanocomposite polymer hydrogels via magnetic field-induced heating for emerging FO desalination. *Environmental science & technology* **2013,** *47*, (12), 6297-6305.

23. Zeng, Y.; Qiu, L.; Wang, K.; Yao, J.; Li, D.; Simon, G. P.; Wang, R.; Wang, H., Significantly enhanced water flux in forward osmosis desalination with polymer-graphene composite hydrogels as a draw agent. *RSC Adv.* **2013,** *3*, (3), 887-894.

24. Li, D.; Zhang, X.; Yao, J.; Zeng, Y.; Simon, G. P.; Wang, H., Composite polymer hydrogels as draw agents in forward osmosis and solar dewatering. *Soft Matter* **2011,** *7*, (21), 10048.

25. Kleemeier, M.; Schröer, W.; Weingärtner, H., Critical behavior of the ionic system n-Propyl-tri-n-butylammonium iodide+ water near its upper and lower consolute points. *Journal of molecular liquids* **1997,** *73*, 501-511.

26. Wei, J.; Qiu, C.; Tang, C. Y.; Wang, R.; Fane, A. G., Synthesis and characterization of flat-sheet thin film composite forward osmosis membranes. *Journal of Membrane Science* **2011,** *372*, (1), 292-302.

27. Razmjou, A.; Simon, G. P.; Wang, H., Effect of particle size on the performance of forward osmosis desalination by stimuli-responsive polymer hydrogels as a draw agent. *Chemical Engineering Journal* **2013,** *215*, 913-920.

28. Ziółkowski, B.; Diamond, D., Thermoresponsive poly (ionic liquid) hydrogels. *Chem Commun (Camb)* **2013,** *49*, (87), 10308-10310.

29. Cho, E. C.; Lee, J.; Cho, K., Role of bound water and hydrophobic interaction in phase transition of poly (N-isopropylacrylamide) aqueous solution. *Macromolecules* **2003,** *36*, (26), 9929-9934.

30. Li, W.; Wu, P., Unusual thermal phase transition behavior of an ionic liquid and poly (ionic liquid) in water with significantly different LCST and dynamic mechanism. *Polymer Chemistry* **2014,** *5*, (19), 5578-5590.

31. Razmjou, A.; Liu, Q.; Simon, G. P.; Wang, H., Bifunctional polymer hydrogel layers as forward osmosis draw agents for continuous production of fresh water using solar energy. *Environmental science & technology* **2013,** *47*, (22), 13160-13166.

6. DUAL RESPONSIVE POLYMERS AS DRAW AGENTS FOR FORWARD OSMOSIS DESALINATION

In this chapter, a novel CO_2 and temperature dual responsive polymer dissolves in water to make a draw solution. This draw agent can be reversibly switched between a polyelectrolyte state desirable in the FO process and a thermally responsive state facilitating draw agent precipitation in regeneration process by addition and removal of CO_2, respectively.

6.1. Introduction

Compared with pressure-driven membrane separation processes, forward osmosis (FO) desalination has the advantages of less membrane fouling and low energy consumption.[1] One of the obstacles to the FO technology development is the lack of suitable draw agents. As summarized in Chapter 2, a suitable draw agent should (1) be able to generate a high osmotic pressure and (2) be easily regenerated. Apart from that, other criteria including (3) having low toxicity to environment and human health, (4) imposing no damage to membrane and (5) low back diffusion of draw agent should be met. Ammonia-carbon dioxide is currently the most widely used draw agent that can generate a very high osmotic pressure dissolving in water and be relatively easily recovered by heating in vacuum.[2] However, the severe draw agent back diffusion and the complete separation of draw agent from water in regeneration are still formidable issues. The presence of ammonia-dioxide draw agent in environment due to back diffusion and in product water due to incomplete regeneration would impose adverse effects on ecosystem and human being health. Other developed non-functional draw agents including glucose[3], inorganic[4] or organic salts[5] and polyelectrolytes[6] always encounter the compromise between easy regeneration and producing high osmotic pressures. Thus, they either are incorporated into the final product for applications other than water production,[7, 8] or have to realize regeneration solely via certain pressure-driven membrane separation process, consequently resulting in membrane fouling or clogging as well as low water recovery.[9]

Hydrogels are another promising group of draw agent. The crosslinked polymer network does not dissolve in water, thus there are no problems of draw agent back diffusion and incomplete recovery. In addition, hydrogels as draw agent exempt any need for further water quality polishing steps. In Chapter 4 and Chapter 5, I thoroughly discussed the thermally responsive hydrogels' potential as draw agents for FO desalination. After optimization of a series of parameters including hydrogel structure, membrane structure, area density and FO-regeneration duration, a 1.2 LMH water production rate generated by thermally responsive polyionic liquid hydrogel was reported, which is almost 6 times that of semi-IPN hydrogels reported in Chapter 4. Further increasing the hydrogel's water production rate should be extremely difficult, albeit not impossible. This is because for a balanced comprehensive performance, enhanced drawing ability (hydrophilicity) should always be counterbalanced by enhanced hydrophobicity to facilitate water release. Furthermore and more importantly, severe concentration polarization brought by hydrogels is inherently difficult to mitigate. As mentioned in Chapter 2, concentration polarization (CP) is the prim culprit for water flux reduction. For the case of hydrogel as draw agent, CP at feed solution side is negligible since the feed solution salinity is low and the water flux is also relatively low. However, there is severe dilutive CP at the draw agent side since the water transportation mechanism within hydrogel is diffusion, which is believed to be several orders of magnitude lower than that of the small molecular draw agent in water. In addition, the dilutive CP can be mitigated by turbulence for small molecules draw agent due to convection, while this is impossible for hydrogels and water diffusion is even decelerated by hydrogel-hydrogel boundary. Therefore, FO water flux may not increase dramatically if hydrogel is still used as draw agent.

A natural way to solve this problem is to disengage the crosslinker of hydrogel and use responsive polymers dissolving in water as the draw solution. The dilutive CP at draw solution side should be largely mitigated since the contact condition between draw solution and membrane as well as the molecule diffusion conditions can be improved. However, the guidelines for hydrogel structure design also go for polymers. On the one hand, polyelectrolyte is preferred for generating a high water flux; on the other hand, responsive polymer such as thermally responsive PNIPAm is preferred for an easy

regeneration. Random copolymers of thermally responsive species and electrolyte have been tested as draw agents for FO desalination.[10-12] It is anticipated and conceivable to see that none of these copolymers as draw agents can generate water flux from seawater in a FO desalination. This is because the trade-offs between high drawing ability and easy regeneration will prevent either property from excelling. Some non-electrolyte thermally responsive oligmers were also tested as draw agents.[13, 14] Their drawing ability should be higher than non-polyelectrolyte polymers due to lower molecular weight. However, being thermally responsive indicates the existence of hydrophobic segment in the molecule that reduces the interaction between draw agent and water and consequently the drawing ability. Therefore, these non-electrolyte oligmers can generate essentially no water flux from seawater.

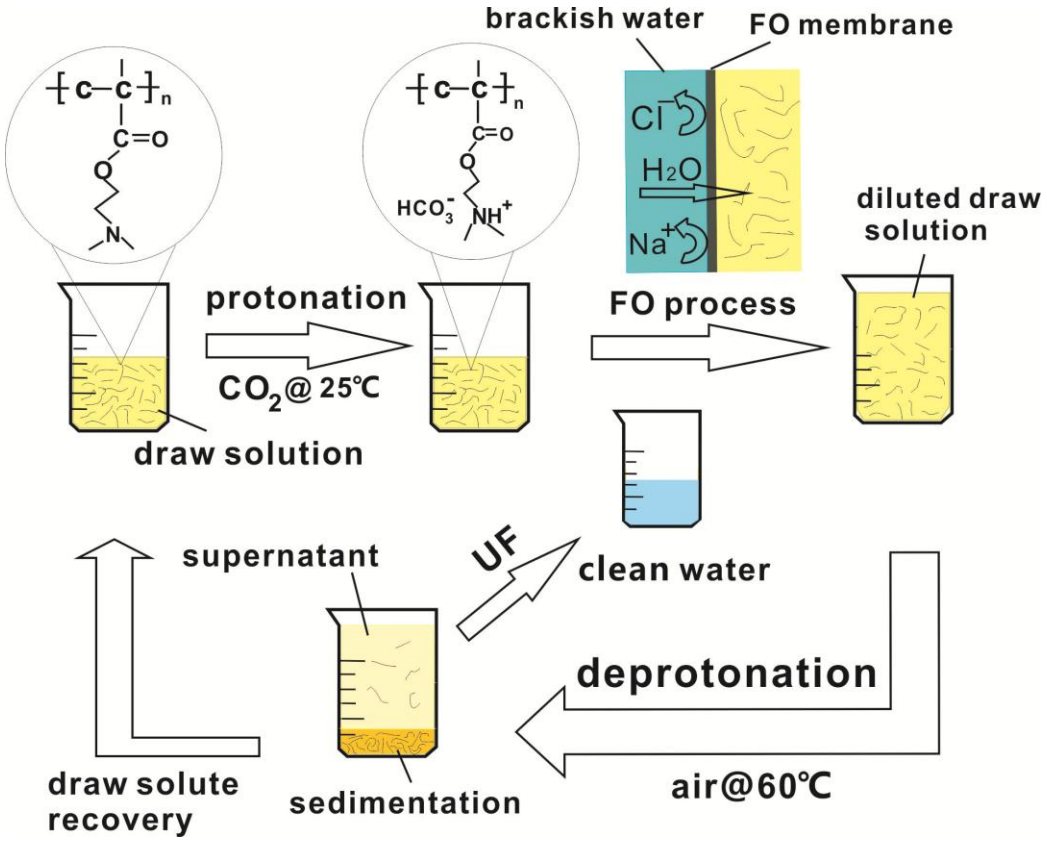

Figure 6.1 Schematic illustration of the CO_2 and thermally dual responsive draw agent for forward osmosis desalination.

In this chapter, a novel dual responsive polymer, poly [2-(dimethylamino) ethyl methacrylate] (PDMAEMA), was synthesized and tested as draw agent for FO desalination. The novelty of this draw agent is that it breaks the trade-off between hydrophilicity and hydrophobicity in molecular design with the help of CO_2. As shown in Figure 6.1, the draw agent after protonation is able to generate a sufficiently high osmotic pressure for seawater desalination; while the deprotonated draw agent is thermally responsive and precipitates from draw solution at temperatures above its LCST at around 40℃ facilitating the draw agent regeneration. These two states can be reversibly switched by introduction and removal of CO_2. The distinct advantage of this dual responsive draw agent is the reversible switching between a highly ionized state ideal for FO process and the thermally responsive state ready for regeneration. Compared with polarity switchable solvent,[15] the dual responsive polymer has a much lower back diffusion and is benign to membrane. I believe that this is one of the most successful designs that possess the combination of all the five desirable characteristics for an ideal draw agent as earlier mentioned.

6.2. Experimental section

6.2.1. Materials

2-(dimethylamino) ethyl methacrylate (DMAEMA), ethyl α-bromoisobutyrate (EBiB), 1,1,4,7,10,10-hexamethyltriethylenetetramine (HMTETA), CuBr, neutral aluminum oxide, and the solvent THF as well as hexane were all purchased from Aldrich and used as received. The FO membrane was cellulose triacetate from HTI.

6.2.2. Polymer synthesis

In order to study the polymer molecular weight's influence on the performance, the author used atom transfer radical polymerization (ATRP) to synthesize polymer with a narrow molecular weight distribution. The expected molecular weight is tuned by the molar ratio of monomer to initiator. In a typical synthesis, 5 mL THF was purged with pure nitrogen for 15 minutes before 85 mg (0.59 mmol) CuBr, 323 μL (1.18 mmol) HMTETA and 5 mL (29.6 mmol) DMAEMA were charged. 87 μL (0.59 mmol) EBib

was injected into the system at 50 ℃ to initiate the polymerization. The polymerization was terminated by liquid nitrogen. The ligand-catalyst complex was removed by passing the diluted polymer solution through a neutral aluminum oxide column. The polymer was precipitated in hexane and dried in a vacuum oven at 60 ℃ after the supernatant was decanted. The polymers used for the back diffusion measurements, membrane salt rejection and produced water quality analyses were further precipitated once from aqueous solution and then freeze-dried to remove trace amounts of the ligand.

6.2.3. Water flux measurement

The water flux in FO process was measured by a home-made apparatus shown in Figure 6.2. Two chambers were separated by a cellulose triacetate FO membrane from Hydration Technologies Inc. (HTI) with the orientation of the active layer towards the draw solution (PRO mode). Magnetic stirring was used to reduce external concentration

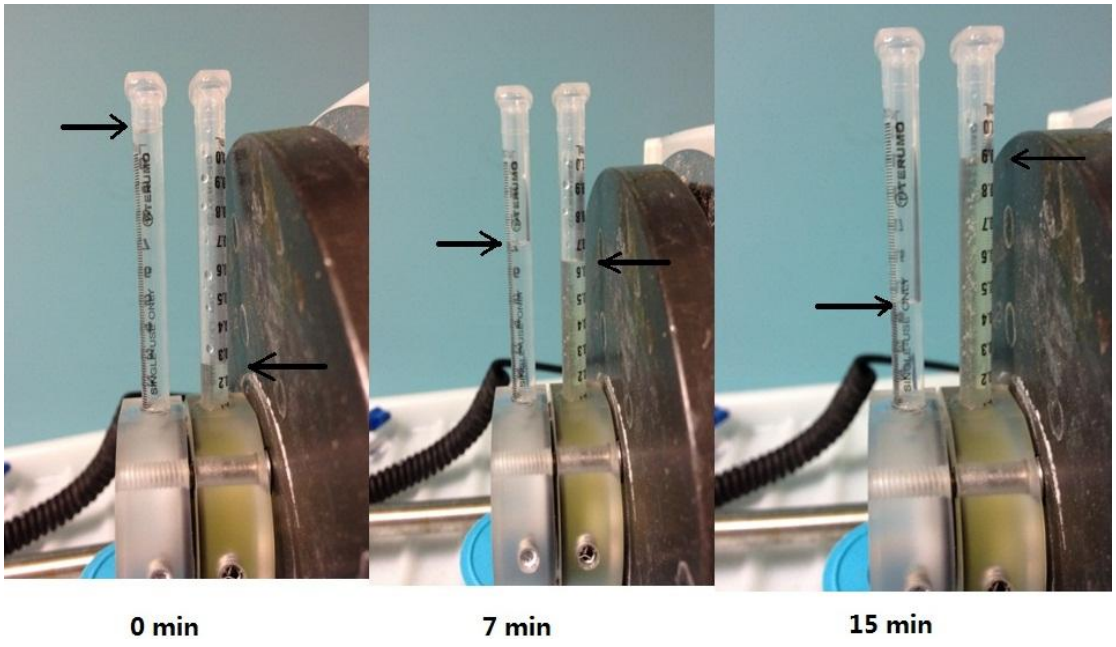

Figure 6.2 The water flux measurement by a home-made apparatus. The right chamber contains the draw solution with an initial concentration of 0.4 g/g and the left chamber contains the brackish solution with an initial concentration of 0.15 M NaCl. The magnetic stirring rate is 600 rpm.

polarization. The water flux was calculated as $\Delta m/(A \cdot t)$, where Δm is the weight increase of draw solution (kg), A is the membrane area (m^2) and t is the FO duration (h). In this chapter I set the FO duration at 15 minutes according to the FO membrane area, feed solution and draw solution volumes as well as water flux. Although a shorter FO duration would be better for practical operation, yet the associated small incremental mass collected during the FO is problematic to measure accurately. However, an excessively long FO duration time dilutes the draw solution so that the value would be largely underestimated given that the chamber volume is about 7 ml. The draw solution was injected and taken out by a syringe and needle to ensure that no draw solution was lost before and during weight measurement. When the concentration of the polymer rises over 0.6 g/g, the solution viscosity is too high for the draw solution to pass through the needle with the pressure that can be applied via the syringe; however, this would not be a problem if a pump were used in a larger scale cross-flow FO process.

6.2.4. Draw agent back diffusion measurement

Protonated polymer (molecular weight 4000 g/mol and 9000 g/mol) aqueous solutions at concentrations of 0.2 g/g and 0.3 g/g, respectively, were used as the draw solution and DI water was used as the feed solution. The amount of draw agent diffusing into the feed solution was determined from the concentration of draw agent in the feed solution and the volume of feed solution after the FO process. The draw agent concentration was determined from total organic carbon (TOC) measurement. Traditional measuring method by conductivity is not accurate here, because the contribution of permeated CO_2 and draw agent to conductivity is unknown.

6.2.5. FO membrane salt rejection measurement

The draw and feed solution concentrations were 0.3 g/g (molecular weight 9000 g/mol) and 0.1 M NaCl, respectively. After 1 g of water permeated to draw solution, the FO process was stopped and the draw solution was purged with argon at 60 ℃ to deprotonate and precipitate the draw agent. The supernatant was filtrated isothermally with a syringe filter (450nm) before passing through an ultrafiltration (UF) membrane with a molecular weight cutoff (MWCO) of 3000 Da. Theoretically all the draw agent should be removed

from the draw solution since only NaCl and water can pass through the UF membrane (actually conductivity contribution from trace amount of draw agent is negligible). By knowing the solution volume and the NaCl concentration from conductivity measurement (Figure 6.3 as the calibration curve), we can know the NaCl concentration in the permeating stream (C_p). The membrane salt rejection was calculated from $R= [1-(C_p/C_f)]*100\%$, where C_p is the NaCl concentration in the stream permeating the membrane, and C_f is the NaCl concentration in the feed solution.

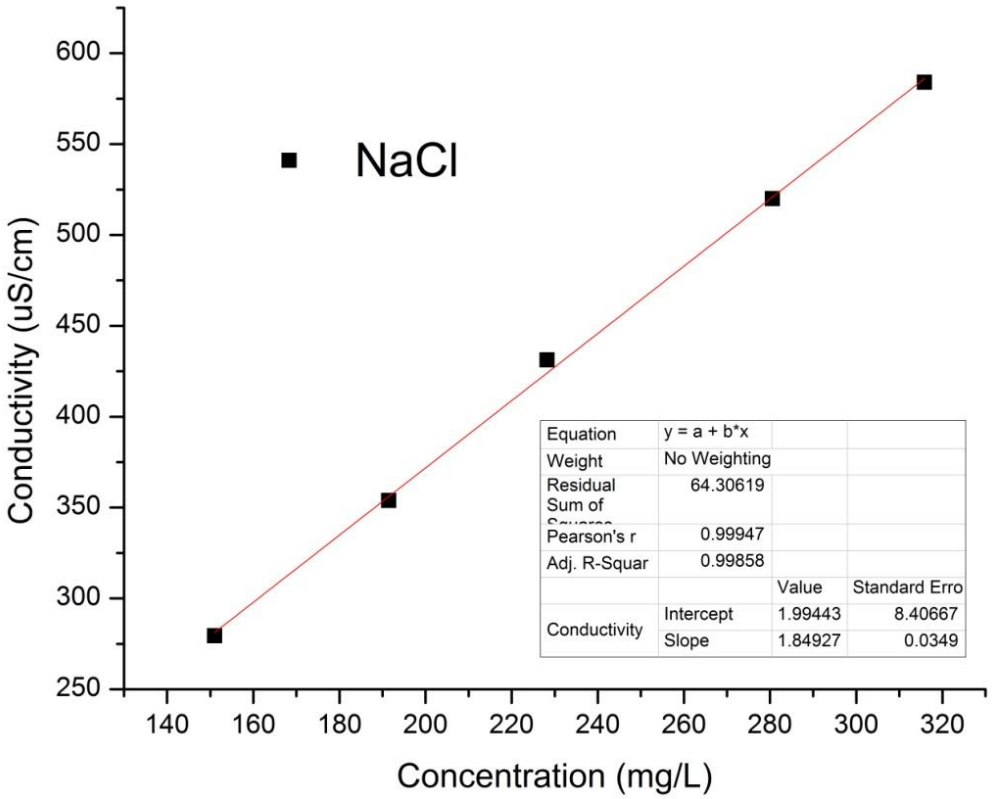

Figure 6.3 The calibration curve for NaCl solution conductivity versus concentration.

6.3. Results and discussion

6.3.1. The draw agent synthesis

The average molecular weight (M_n and M_w), and polymer dispersity index (PDI) of the three PDMAEMA polymers synthesized in this chapter are summarized in Table 6.1. The draw agents were synthesized successfully with a narrow molecular weight distribution.

Table 6.1 Summary of number average molecular weight (M_n), weight average molecular weight (M_w) and polymer dispersity index (PDI) of the three PDMAEMA polymers synthesized.

Code	M_n (g/mol)	M_w (g/mol)	PDI
P4000	**3921**	**5254**	**1.34**
P9000	**8876**	**11620**	**1.31**
P13000	**12946**	**16426**	**1.27**

Note: The molecular weights were determined by size exclusion chromatography (SEC) relative to polystyrene calibration in chloroform with 0.5% triethylamine at 35 ℃.

6.3.2. The protonation and FO performance of draw agents

The osmolality of draw solution as a function of draw agent molality is shown in Figure 6.4. As anticipated, the osmolality of the draw solution increased with concentration (molality) but decreased with draw agent molecular weight. In addition, the osmolality increased tremendously when the draw agents were switched to the protonated state by purging CO_2. For example, the osmolality of deprotonated P4000 at the concentration of 0.3 g/g (gram of polymer/gram of water) is 0.331 osmol/kg, which is almost equivalent to that of physiological saline; while after protonation, its osmolality increased to 1.208 osmol/kg which is even higher than that of seawater (1.11 osmol/kg). It is worth mentioning that the osmolality measurement throughout this thesis is conducted by cryoscopic method that has been thoroughly introduced in Chapter 2. The measured osmolalities of deprotonated draw agents were actually overestimated since the thermally responsive deprotonated draw agent would become more hydrophilic at sub-zero degree than at room temperature. However, for non-thermally responsive protonated draw agents, which are essentially polyelectrolytes, temperature has negligible influence on the osmolality and the measured osmolalities for protonated state were relatively accurate. The osmolality overestimation for deprotonated draw agents further emphasizes the enhancement of osmolality by protonation. The CO_2 induced protonation and ionization should take the responsibility for the tremendous increase in osmolality, because the saturated CO_2 aqueous solution only has an osmolality of 0.007 osmol/kg.

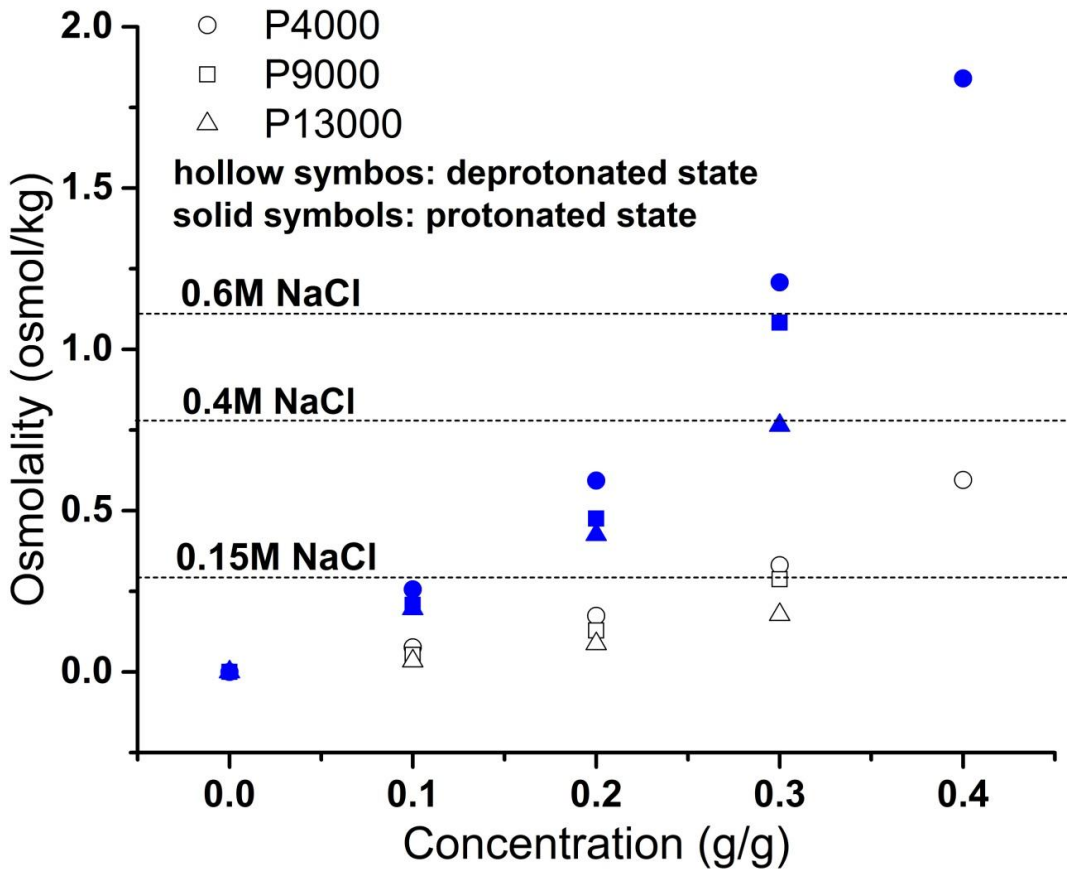

Figure 6.4 The osmolality profiles of deprotonated and protonated draw agents. The horizontal lines depict the osmolalities of 0.15 M, 0.4 M and 0.6 M NaCl solutions, respectively.

Figure 6.4 also shows that for 0.4 g/g protonated P4000, its osmolality is much higher than that of seawater. Actually, when the concentration of P4000 is 0.5 g/g or higher, the osmolality values are beyond the osmometer's detection limit. If I compare the FO performance of protonated polymer with the hydrogels, we can clearly see that disengaging the crosslinker in hydrogels definitely helps improve the performance. For the protonated polymer (polyelectrolyte) at concentration of 0.3 g/g, it is able to draw water from seawater due to higher osmolality; while neat PSA hydrogel with the same concentration (swelling ratio of 3.3 g/g) cannot generate any water flux from seawater.[16] Another interesting point worth mentioning is that the osmolality of protonated draw solution does not increase with molality linearly, but shows a positive deviation from linearity indicating a strong effect of "water hydration" due to the hydrophilic polyelectrolyte nature of the protonated draw agent.

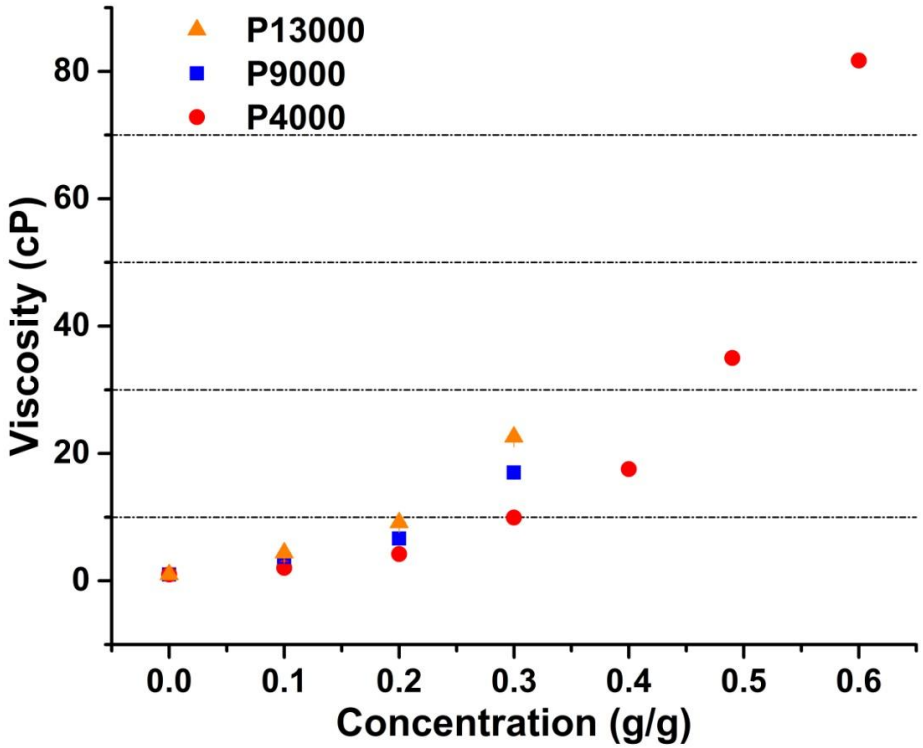

Figure 6.5 The profiles of protonated draw solution with various concentrations.

For polymer aqueous solution, viscosity is a very important issue especially for the application of draw solution because the viscosity has impact on the concentration polarization. As shown in Figure 6.5, at the same polymer weight concentration, solution of a polymer with a higher molecular weight has a higher viscosity. Although I cannot quantify the influence of viscosity on the concentration polarization as well as water flux in this thesis, it is conceivable that high solution viscosity indicates a low solute diffusivity and a low water flux. Combined with the result from Figure 6.4 that P13000 generates lower osmolality than P4000 and P9000, only the latter two candidates with lower molecular weight (P4000, P9000) would be further studied for their properties in FO and regeneration. It is worth mentioning that the viscosities of the draw solutions are relatively low and will not impose any pumping difficulties in a cross-flow setup. For the convenience of a more direct perception, milk has a viscosity of about 30 cP while olive oil has a viscosity of about 80 cP which is close to that of 0.6 g/g P4000 solution.

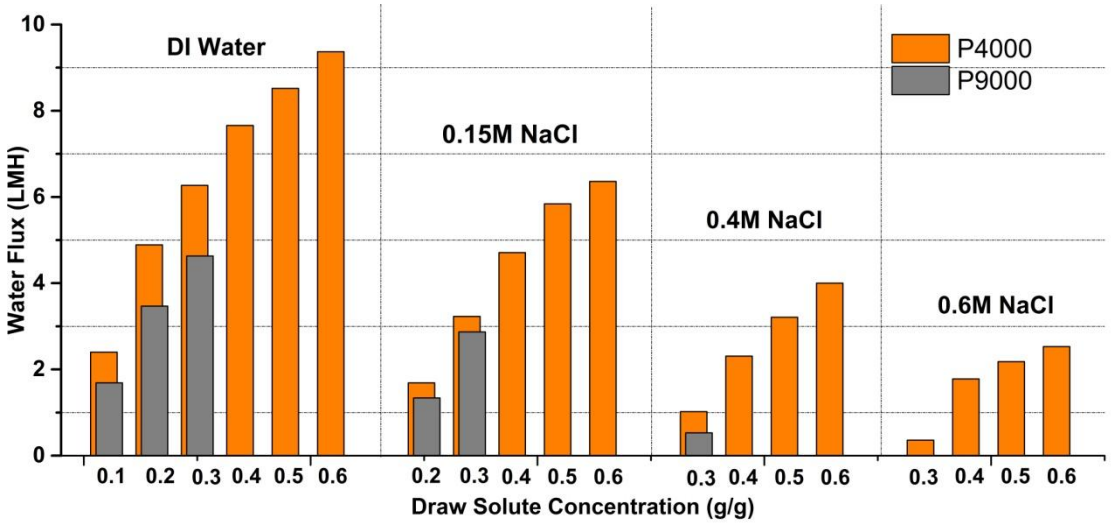

Figure 6.6 The water flux profile of various protonated draw solution concentrations against different feed solution salinities. The FO membrane was in PRO mode.

Figure 6.6 demonstrates the FO water flux as a function of draw solution concentration against four feed solutions with different salinities for P4000 and P9000, respectively. Since water flux is positively correlated to the osmotic pressure difference across the membrane, it is conceivable that a combination of a concentrated draw solution and a diluted feed solution would result in a higher water flux. As expected, the P4000 generates a higher water flux than the P9000 against the same feed solution, which corroborate well the Figure 6.4 that P4000 has a higher osmolality than P9000 at the same weight concentration. P9000 at the concentration of 0.3 g/g can generate water flux from 0.4 M NaCl but is not able to generate water flux from artificial seawater of 0.6 M NaCl since its osmolality is lower than that of 0.6 M NaCl as shown in Figure 6.4. P9000 with a higher concentration may be capable for seawater desalination, albeit I don't prepare that draw solution due to limited solubility. It is encouraging to see that P4000 can generate a reasonable water flux of >2 LMH against artificial seawater (0.6 M NaCl). The premature leveling off of the water flux at higher draw solution concentrations against seawater, as well as the relatively insignificant water flux dependence on feed solution salinity, indicate that there is relatively severe concentration polarization phenomenon in our home-made apparatus. Water fluxes are expected to be higher if severe turbulence can be introduced in a cross-flow setup.

6.3.3. Draw agent back diffusion and membrane salt rejection

A suitable draw agent also should assume a low back diffusion into feed solution to minimize its loss during the FO process. As shown in Figure 6.7a, it is clearly that the draw agent leakage aggravates with increased draw solution concentration and decreased molecular weight. This is because the draw agent flux is driven by concentration gradient

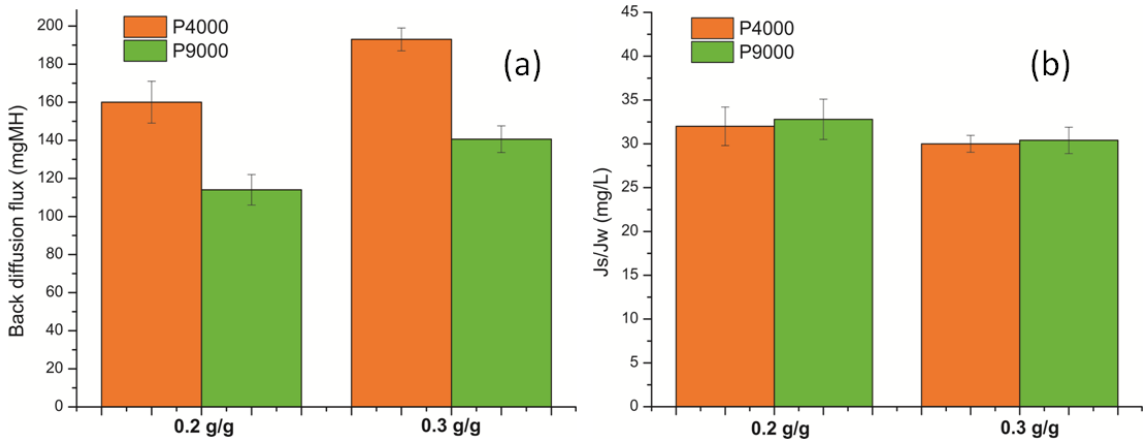

Figure 6.7 (a) Draw agent back diffusion flux as a function of molecular weight and concentration. (b) The ratio of draw agent back diffusion flux to the water flux as a function of molecular weight and concentration.

across the membrane, and smaller molecules are more prone to leak. However, the ratio of the draw agent flux to the water flux, J_s/J_w, is around 30 mg/L irrespective of the molecular weight and draw solution concentration, as demonstrated in Figure 6.7b. This indicates that only 30 mg draw agent would back-diffuse into the feed solution for every one litre of fresh water permeated. This value is one or two orders of magnitudes lower than that of small inorganic salts and even lower than the value of 80 mg/l reported for poly sodium acrylate.[4, 6] The relatively large pendent group and the presence of bicarbonate anions in the draw agent may contribute to the extraordinarily low back diffusion. This draw agent back diffusion may have potential to be further reduced if a membrane with higher water-salt selectivity than the cellulose triacetate membrane can be used.[17, 18]

An ideal draw agent should also be benign to the FO membrane to maintain the high salt rejection. In this chapter, draw solution's influence on the FO membrane was assessed by

comparing the salt rejections of an as-received membrane and the one immersed in 0.6 g/g protonated draw solution for 24 hours. The salt concentrations of the streams permeated through membranes were 243.8 mg/l and 242.1 mg/l for new and old membranes, respectively, from conductivity measurement described in section 6.2. The salt rejections for both cases were calculated to be about 96%. Although the deprotonated draw solution was alkaline with a pH up to 9.4, it reduced to 7.5 even for the concentrated 0.6 g/g protonated P4000. Since the FO membrane only contacts the protonated draw solution as shown in Figure 6.1; therefore, the membrane would not be hydrolyzed because the membrane is known to be stable at pH between 3 and 8.

6.3.4. Deprotonation and regeneration of draw agent

In order to produce fresh water from the diluted draw solution after the FO process, inert gas was purged into draw solution that was heated to temperatures above the LCST. The draw agent was then deprotonated by the removal of CO_2 and consequently regaining its

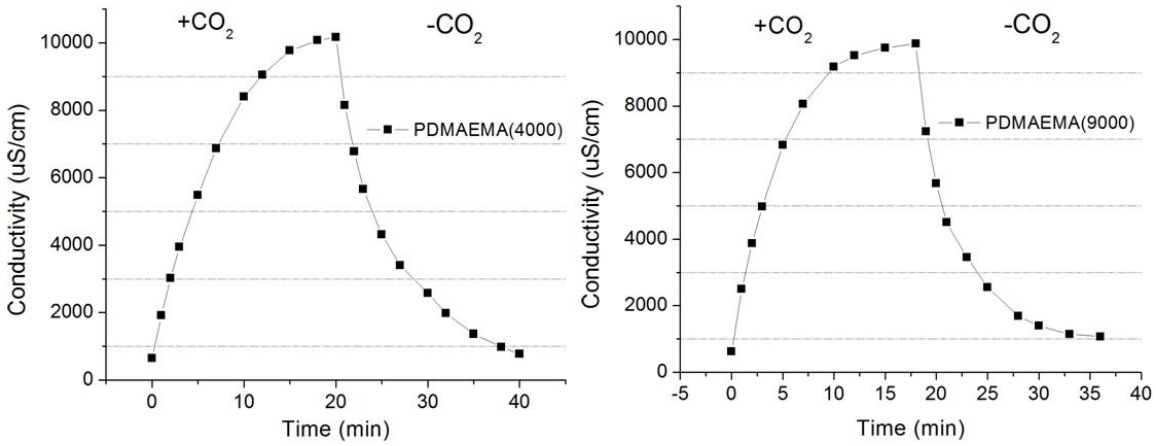

Figure 6.8 Conductivity monitoring during the protonation-deprotonation cycle of P4000 and P9000. The CO_2 was purged at 25℃ and Ar was purged at 60℃. Gas flow rate was 300 ml/min.

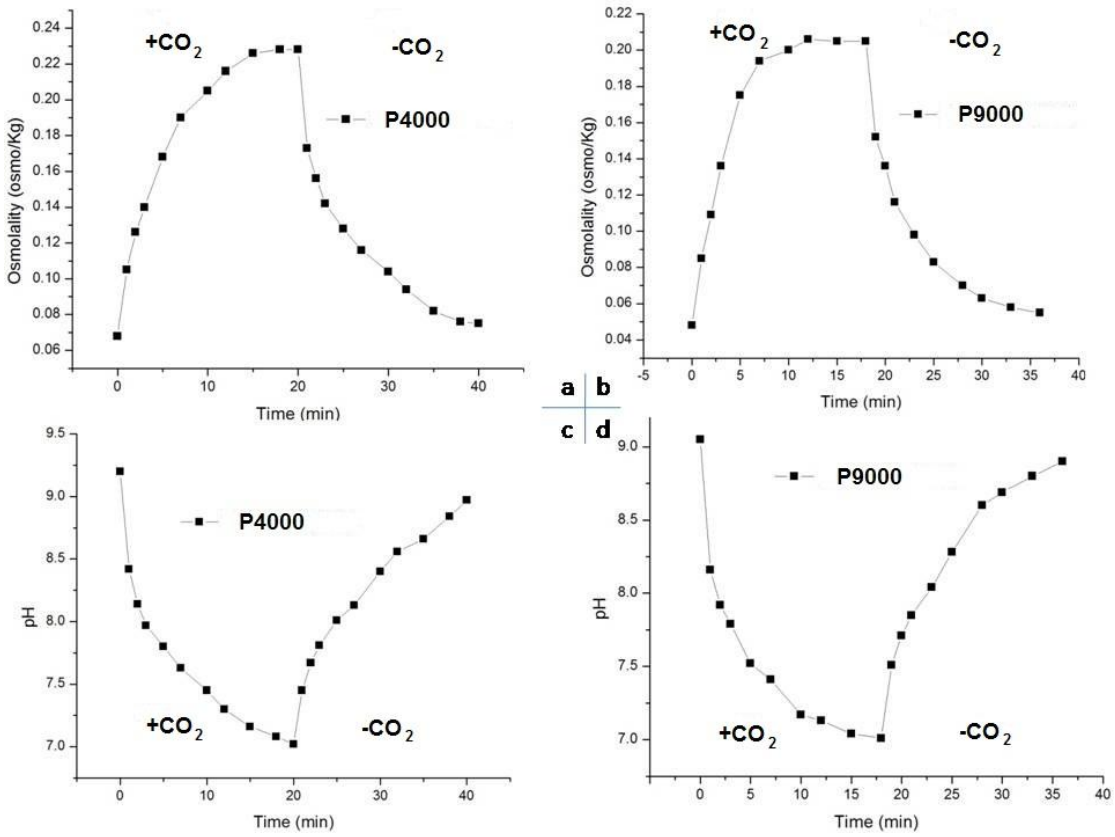

Figure 6.9 Protonation-deprotonation reversibility shown by osmolality (a,b) and pH (c,d) measurements. The protonation was done by purging CO_2 at 25℃ and deprotonation was done by purging Ar at 60 ℃. The gas flow was 300 ml/min.

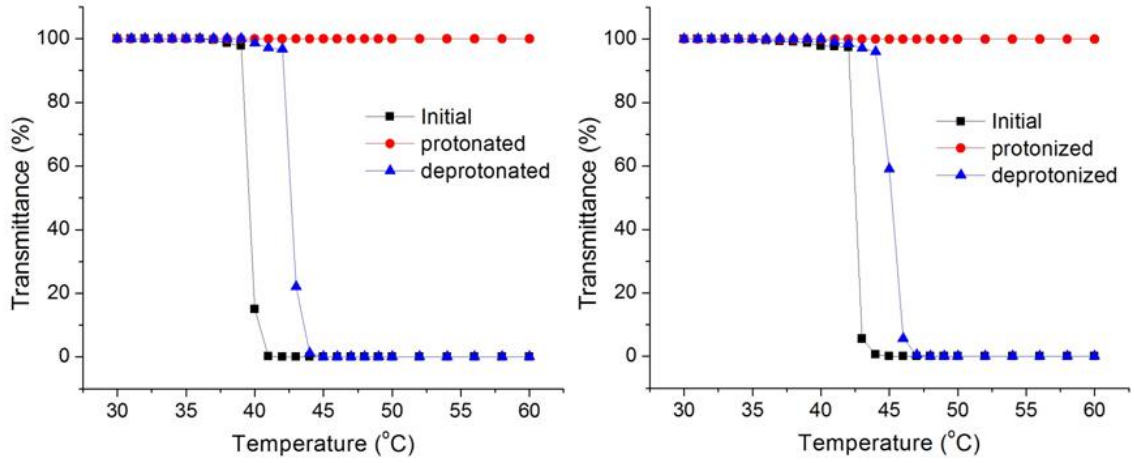

Figure 6.10 The measurements of UV-vis transmittance (700 nm) for P4000 (left) and P9000 (right) in the as-synthesized (initial), protonated and deprotonated states.

thermosensitivity. In this chapter, the draw agent deprotonation was realized by purging argon and a simultaneous heating up to 60 ℃. The concurrent heating not only precipitates the draw agents, but accelerates the CO_2 detachment and deprotonation process. In fact, other cheaper gases including nitrogen and even air can replace argon to achieve a similar effect.[19-21] The protonation-deprotonation cycle between CO_2 purging at 25℃ and argon purging at 60℃ was monitored by solution conductivity (Figure 6.8), osmolality and pH (Figure 6.9). It is clearly seen that the removal of CO_2 and the switch of draw agent to its deprotonated state are effective. In addition, light transmittance study (Figure 6.10) shows that there were only a few degrees increase of deprotonated polymer's LCST compared with as-synthesized polymer. These results also confirmed that the draw agents' deprotonation was almost complete since there was only a ~3 ℃ LCST increase from the as-synthesized state.

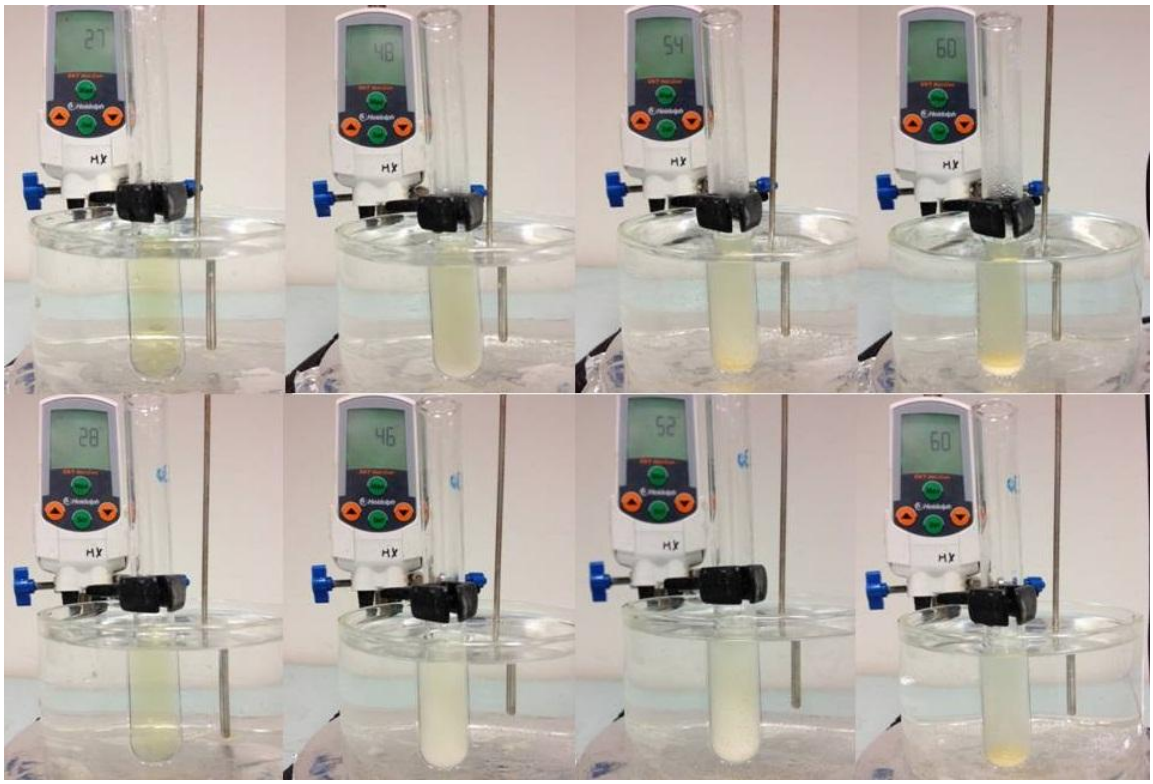

Figure 6.11 The deprotonated draw solutions undergo a solid-liquid phase separation at temperatures higher than the LCST. The upper row is the P9000 and the bottom row is the P4000.

For the deprotonated draw solution at a temperature higher than the LCST, a phase separation occured and the draw agents precipitated as shown in Figure 6.11. In order to quantify the efficiency of regeneration by precipitation, I allow the deprotonated 0.1 g/g draw solution to stabilize at 60 ℃ for 20 minutes. The water-rich supernatant phase was then isothermally filtered through a syringe filter with pore size of 450 nm to remove the unprecipitated-but-agglomerated polymer clusters. The draw agent concentration in the syringe filter permeate was determined to be 3.4 and 2.8 g/l for P9000 and P4000, respectively, by conductivity measurements. This means that about 97% of draw agent was precipitated under mild heating. The permeate was further polished via one-pass of ultrafiltration membrane with a molecular weight cutoff of 3000 Da, and the total organic carbon was measured to be 153.1 ppm and 54.6 ppm for P4000 and P9000, respectively. PDMAEMA has a relatively low toxicity (LD_{50}>1.5 g/kg for DMAEMA) and has been widely investigated in the application of drug delivery.[22] The quality of the final product water may not be good enough for long term consumption; however, I believe the TOC can be further reduced by one-pass nanofiltration of RO to meet the potable water standard. The water recovery in water polishing step, *e.g.*, UF in this case, is up to 95% with a very low pressure of 1.5 bar due to the low polymer concentration and osmolality in the supernatant after precipitation. Therefore, though the dual responsive polymers as draw agents necessitated a water polishing step as a part of the regeneration, the majority of draw agents were recovered by precipitation and the very low concentration in the supernatant would not impose too much difficulties, such as membrane clogging and low water recovery, to ensuing membrane process to produce high quality water.

6.3.5. Insight of this draw agent's significance

According to the discussions above, dual responsive polymers can be regarded as an upgraded version of hydrogel as smart draw agents for FO desalination. Both thermally responsive hydrogels and dual responsive polymers utilize low grade thermal energy to accomplish the draw agent regeneration instead of electricity needed in the regeneration of non-responsive draw agents. The hydrogel's merits include no back-diffusion or water polishing step, while dual responsive polymers generate higher water flux due to amelioration of concentration polarization. In addition, the promise of FO being a low

energy desalination method may be realized by these responsive draw agents since thermal energy from waste heat provides a large portion of energy needed (all for hydrogel) for regeneration. However, from the economic point of view, the cost for evading the trade-off between hydrophilicity and hydrophobicity in draw agent design is the introduction of CO_2. Energy consumption estimation of FO desalination is not possible and meaningless if the energy consumption of CO_2 regeneration from the mixture with inert gas used in deprotonation is overlooked. Fortunately, for some cases where the CO_2 regeneration is not necessary, for example using the flue gas that is emitted anyway, FO desalination realized by this dual responsive draw agent is quite promising not only economically, but environmental friendly. The participation of waster heat and waste gas in desalination lowers the energy cost as well as the carbon footprint.

6.4. Conclusions

In this chapter, a new concept of using dual responsive low molecular weight polymers as draw agents for FO desalination was proposed. When the draw agent is protonated via reaction with CO_2, the draw agent becomes polyelectrolyte that generates sufficiently high osmotic pressure for seawater desalination. Upon deprotonation where CO_2 is removed, draw agents regain their thermosensitivity and precipitate at temperatures above the LCSTs to facilitate draw agent regeneration. The ensuing membrane based polishing steps are used to improve water product quality with low hydraulic pressure. Furthermore, these draw agents have other merits including much lower back diffusion compared with inorganic salts, no degradation to membranes and low toxicity. These dual responsive draw agents are potentially ideal for FO desalination to realize its promise of low energy consumption.

References

1. Chekli, L.; Phuntsho, S.; Shon, H. K.; Vigneswaran, S.; Kandasamy, J.; Chanan, A., A review of draw solutes in forward osmosis process and their use in modern applications. *Desalination and Water Treatment* **2012,** *43*, (1-3), 167-184.

2. McCutcheon, J. R.; McGinnis, R. L.; Elimelech, M., A novel ammonia—carbon dioxide forward (direct) osmosis desalination process. *Desalination* **2005,** *174*, (1), 1-11.

3. Kravath, R. E.; Davis, J. A., Desalination of sea water by direct osmosis. *Desalination* **1975,** *16*, (2), 151-155.

4. Achilli, A.; Cath, T. Y.; Childress, A. E., Selection of inorganic-based draw solutions for forward osmosis applications. *Journal of Membrane Science* **2010,** *364*, (1-2), 233-241.

5. Stone, M. L.; Wilson, A. D.; Harrup, M. K.; Stewart, F. F., An initial study of hexavalent phosphazene salts as draw solutes in forward osmosis. *Desalination* **2013,** *312*, 130-136.

6. Ge, Q.; Su, J.; Amy, G. L.; Chung, T. S., Exploration of polyelectrolytes as draw solutes in forward osmosis processes. *Water Res* **2012,** *46*, (4), 1318-1326.

7. Duan, J.; Litwiller, E.; Choi, S.-H.; Pinnau, I., Evaluation of sodium lignin sulfonate as draw solute in forward osmosis for desert restoration. *Journal of Membrane Science* **2014,** *453*, 463-470.

8. Hoover, L. A.; Phillip, W. A.; Tiraferri, A.; Yip, N. Y.; Elimelech, M., Forward with osmosis: emerging applications for greater sustainability. *Environmental science & technology* **2011,** *45*, (23), 9824-9830.

9. Li, D.; Simon, G. P.; Wang, H., Assessment of polyelectrolytedraw agents in forward osmosis desalination. In *CHEMECA 2011: Engineering a Better World* Sydney Hilton Hotel, Australia, 2011.

10. Kim, J.-j.; Chung, J.-S.; Kang, H.; Yu, Y. A.; Choi, W. J.; Kim, H. J.; Lee, J.-C., Thermo-responsive copolymers with ionic group as novel draw solutes for forward osmosis processes. *Macromolecular Research* **2014,** *22*, (9), 963-970.

11. Zhao, D.; Wang, P.; Zhao, Q.; Chen, N.; Lu, X., Thermoresponsive copolymer-based draw solution for seawater desalination in a combined process of forward osmosis and membrane distillation. *Desalination* **2014,** *348*, 26-32.

12. Ou, R.; Wang, Y.; Wang, H.; Xu, T., Thermo-sensitive polyelectrolytes as draw solutions in forward osmosis process. *Desalination* **2013,** *318*, 48-55.

13. Mok, Y.; Nakayama, D.; Noh, M.; Jang, S.; Kim, T.; Lee, Y., Circulatory osmotic desalination driven by a mild temperature gradient based on lower critical solution temperature (LCST) phase transition materials. *Phys Chem Chem Phys* **2013,** *15*, (44), 19510-19517.

14. Noh, M.; Mok, Y.; Lee, S.; Kim, H.; Lee, S. H.; Jin, G. W.; Seo, J. H.; Koo, H.; Park, T. H.; Lee, Y., Novel lower critical solution temperature phase transition materials effectively control osmosis by mild temperature changes. *Chem Commun (Camb)* **2012,** *48*, (32), 3845-3847.

15. Stone, M. L.; Rae, C.; Stewart, F. F.; Wilson, A. D., Switchable polarity solvents as draw solutes for forward osmosis. *Desalination* **2013,** *312*, 124-129.

16. Zeng, Y.; Qiu, L.; Wang, K.; Yao, J.; Li, D.; Simon, G. P.; Wang, R.; Wang, H., Significantly enhanced water flux in forward osmosis desalination with polymer-graphene composite hydrogels as a draw agent. *RSC Adv.* **2013,** *3*, (3), 887-894.

17. Setiawan, L.; Wang, R.; Li, K.; Fane, A. G., Fabrication of novel poly (amide–imide) forward osmosis hollow fiber membranes with a positively charged nanofiltration-like selective layer. *Journal of Membrane Science* **2011,** *369*, (1), 196-205.

18. Wang, R.; Shi, L.; Tang, C. Y.; Chou, S.; Qiu, C.; Fane, A. G., Characterization of novel forward osmosis hollow fiber membranes. *Journal of Membrane Science* **2010,** *355*, (1), 158-167.

19. Liu, Y.; Jessop, P. G.; Cunningham, M.; Eckert, C. A.; Liotta, C. L., Switchable surfactants. *Science* **2006,** *313*, (5789), 958-960.

20. Jessop, P. G.; Kozycz, L.; Rahami, Z. G.; Schoenmakers, D.; Boyd, A. R.; Wechsler, D.; Holland, A. M., Tertiary amine solvents having switchable hydrophilicity. *Green Chemistry* **2011,** *13*, (3), 619-623.

21. Han, D.; Tong, X.; Boissière, O.; Zhao, Y., General strategy for making CO2-switchable polymers. *ACS Macro Letters* **2011,** *1*, (1), 57-61.

22. Bajpai, A.; Shukla, S. K.; Bhanu, S.; Kankane, S., Responsive polymers in controlled drug delivery. *Progress in Polymer Science* **2008,** *33*, (11), 1088-1118.

7. ENERGY-EFFICIENT DESALINATION BY FORWARD OSMOSIS USING RESPONSIVE IONIC LIQUID DRAW AGENTS

In this chapter, thermally responsive ionic liquids are dissolved in water to make draw solutions. In FO process, unlike the polyionic liquid hydrogels in Chapter 5, these ionic liquid draw solutions are capable of generating water flux from seawater due to alleviated concentration polarization; while in regeneration process, draw solutions undergo a liquid-liquid phase separation at temperatures above the LCSTs. The draw agent-rich sedimentation phase can be reused as draw solution again without any treatment; while the water-rich supernatant can be polished by a low pressure NF process. The theoretical electrical energy consumption of FO enabled by these ionic liquids is less than 20% that of RO, and the theoretical energy consumption of FO is found to be much lower than RO.

7.1. Introduction

Fresh water scarcity has been recognized as a global environmental crisis to human society's sustainable development.[1] Wastewater treatment partially ameliorates the fresh water scarcity. However, only desalination technologies are able to expand our fresh water supply to saline water and ocean that hold the majority of water reservoir on Earth. One of the mature and prevalent seawater desalination technologies is distillation based MSF or MED. The product water quality is high albeit large amount of high-grade thermal energy is required for water evaporation. Reverse osmosis (RO) is another developed technology whose energy consumption is lower than MSF or MED due to absence of phase change, and has been greatly reduced after decades' development on membrane and energy recovery device.[2] However, the state-of-the-art RO still needs more than 2 kWh/m^3 of electrical energy at 50% water recovery that is about double the theoretical minimum. What is more, the high hydraulic pressures needed in RO and the

concomitant severe membrane fouling issues are still inherent drawbacks of reverse osmosis.

Among all the developing desalination technologies, forward osmosis (FO) has been considered potentially as an energy efficient process.[3] Unlike the other membrane based RO technology that is driven by excessive hydraulic pressure, the water permeation in FO is driven by osmotic pressure gradient across the membrane that is virtually an energy-input-free process. In addition, membrane fouling problem is hopefully much less severe than in RO owing to the absence or tremendously lower hydraulic pressure. Despite the progresses in manufacturing new FO membranes,[4] the practical FO application to date are limited to a few cases in which the diluted draw solution can be exploited directly without regeneration.[5-7] One typical example is that fertilizers can serve as draw agent for FO desalination, and the diluted draw solution can be used for irrigation.[8] However, for direction desalination application where the fresh water should be the final product, the lack of suitable draw agents has become the obstacle undermining the FO desalination's future by not fulfilling its promised advantages. Among the criteria to be a suitable draw agent, the basic requirement of subtle balance between ease regeneration and generating a high osmotic pressure is quite obvious but extremely challenging to achieve. There are still limited draw agents to choose from. Many non-responsive draw agents including inorganic[9] and organic salts,[10-12] glucose,[13] hydroacid complexes,[14] and polyelectrolytes[15] can generate sufficiently high osmotic pressure for seawater desalination. However, their regenerations from the diluted draw solution solely rely on electricity-consuming membrane based technologies including ultrafiltration, nanofiltration and reverse osmosis. Actually, although FO process is an automatic process with no energy input, the regeneration process of these non-responsive draw agents theoretically consumes more energy. This is because the hydraulic pressure involved in regeneration needs to be higher than the diluted draw solution's osmotic pressure, which by default, is higher than the feed solution's osmotic pressure. Therefore, the electrical energy consumption of FO desalination using these non-responsive draw agents is very unlikely to be lower than that of directly using RO to treat the feed solution.

I believe that one effective method to substantially slash the electrical energy consumption in regeneration process is to use responsive draw agent that would undergo certain change to enable the draw agent separation with water under external stimuli. Therefore, draw agent concentration in diluted draw solution is much reduced and any subsequent process, if necessary, is to purify the water from a much diluted solution with an osmolality substantially lower than that of the initial feed solution. Hence, I believe the use of a suitable responsive draw agent may fulfill the promise of FO with low electrical energy consumption and potentially challenge or complement the RO process for the treatment of seawater or even brine. Previously in Chapter 4 and Chapter 5, I studied the thermally responsive hydrogels as draw agents for FO desalination. The merits of hydrogels are no draw agent back diffusion and exemption of any further water polishing steps for the water squeezed. Modulation of temperature within a narrow range is the only driving force for FO and regeneration. However, due to the severe concentration polarization (CP), these thermally responsive hydrogels are only able to treat brackish water. In order to ameliorate the CP and reveal the real drawing ability of responsive draw agents, dissolving or dispersing in water would be a better way since the CP can be much reduced by convection from cross-flow turbulence that does not apply for hydrogels. In Chapter 6, I tested dual responsive polymers dissolving in water as draw agents. Protonated state that can generate a high osmotic pressure for seawater desalination, and a deprotonated state that can be easily precipitated under heating can be reversibly switched by introduction and removal of CO_2. Thermal energy is mainly used in regeneration and the electrical energy used in polishing steps is presumably low due to the low hydraulic pressure of 1.5 bar used. However, the theoretical energy consumption estimation was not done for the dual responsive polymer since the CO_2 regeneration from inert gas used for deprotonation also consumes energy.

In this chapter, I will study a group of novel thermally responsive ionic liquids as the draw agents for FO desalination. These thermally responsive ionic liquids are the apotheosis in achieving the hydrophilicity-hydrophobicity balance. While traditional NIPAm-based copolymer[16] and other non-ionic thermally responsive oligmers[17, 18] can sparingly generate water flux from seawater, these thermally responsive ionic liquids are

able to generate water flux from brine with salinity up to 1.6 M NaCl, which is almost 3 times that of seawater. When the temperature is increased above the LCSTs between 32℃ to 49℃, the diluted draw solution immediately undergoes a liquid-liquid phase separation. The sedimentation phase abounds in draw agent and can be reused directly as the draw solution in FO process again without further treatment. The supernatant is a water-rich phase having an osmotic pressure of less than 6 bar. Therefore, a much lower hydraulic pressure and consequently much lower electrical energy than seawater RO is needed in the regeneration of draw agents with nanofiltration membrane.

7.2. Experimental section

7.2.1. Materials and equipments

Tributyloctyl phosphonium bromide was purchased from Wako Pure Chemical Industries. tetrabutylphosphonium bromide, Sodium 2,4-dimethylbenzenesulfonate and sodium mesitylenesulfonate were purchased from Tokyo Chemical Industry. Sodium chloride (>99.5%) and anhydrous dichloromethane (>99.8%) were purchased from Sigma-Aldrich. All chemicals were used as received without further purification. The FO membrane used in this chapter was a thin film composite membrane prepared according to a reported method.[19] Nanofiltration membranes with molecular weight cut-off of 270 Da and 90 Da were purchased from Dow FilmTec. The osmolality of draw solution was measured by a cryoscopic method using OSMOMAT 030, Gonotech. The FO water flux in FO process was measured by monitoring feed solution's weight decrease with time in a cross-flow cell with a flow rate of 4 ml/s for both feed and draw solutions. The effective membrane area was 15 mm × 30 mm and membrane was oriented in PRO mode. The correlation between hydraulic pressure and water flux in NF was tested in a dead-end filtration setup at room temperature with stirring. Viscosity was obtained by a Physica MCR 101 rheometer, Anton Paar. The water content in ionic liquid solution was measured by Karl Fischer titration (CA-200 Moisturemeter, Mitsubishi Chemical Analytech). Back diffusion of draw agent was measured by monitoring the total organic carbon (TOC) of feed solution. The latent heat of draw solution phase transition and melting of pure ionic liquids were determined by DSC (Q10, TA instruments).

7.2.2. Syntheses of ionic liquids

Three thermally responsive ionic liquid draw agents were investigated in this chapter. Tetrabutylphosphonium 2,4-dimethylbenzenesulfonate (P_{4444} DMBS) was synthesized through simple ion exchange reactions. Tetrabutylphophonium bromide and slightly excess equal molar of sodium 2,4-dimethylbenzenesulfonate were mixed and dissolved in DI water to form a 40 wt% solution and stirred at room temperature for 24 hours. The ionic liquid P_{4444} DMBS inside was extracted by dichloromethane and the organic phase was washed with DI water several times. The organic phase's volume was reduced by rotary evaporator, and the concentrated solution was then put in vacuum oven (~1 mbar) at 100 ℃ to remove the organic solvent until constant weight was reached. Tetrabutylphosphonium mesitylenesulfonate (P4444 TMBS) was prepared using a similar method from sodium mesitylenesulfonate and tetrabutylphophonium bromide. The third ionic liquid tributyloctylphosphonium bromide (P4448 Br) was used as received. The structures of P_{4444} DMBS and P_{4444} TMBS were identified by ^{1}H NMR.

7.2.3. Draw agents' influence on membrane

The influence of draw agents' presence on the membrane's performance was determined by measuring and comparing the salt rejection of a membrane before and after immersing in 70% P_{4444} DMBS or 70% P_{4444} TMBS solution for 7 days at room temperature. The measurement of membrane's salt rejection was conducted in a standard RO method. The feed solution had a salinity of 10 mM NaCl (C_f) and the hydraulic pressure was 5 bar. By measuring the permeate salinity C_p, the salt rejection can be calculated as $(1-C_p/C_f)*100\%$. Triplicate salinity measurements were conducted at an interval of 30 minutes after stabilization was achieved.

7.2.4. Water flux measurement

FO was carried out using a continuous cross-flow configuration with an effective membrane area of 4.5 cm^2, as shown in Figure 7.1. Both the feed solution and draw solution were pumped at a rate of 240 ml/min in a co-current pattern in order to minimize the strain on membrane. Plastic spacers were used at both feed and draw solution sides to

mitigate external concentration polarization. The water flux was calculated by measuring the feed solution weight reduction as function of time using the equation

$$Flux = \Delta m/(A \cdot t)$$

where Δm is the weight decrease (kg), t is the FO test time (h) and A is the membrane area (m^2).

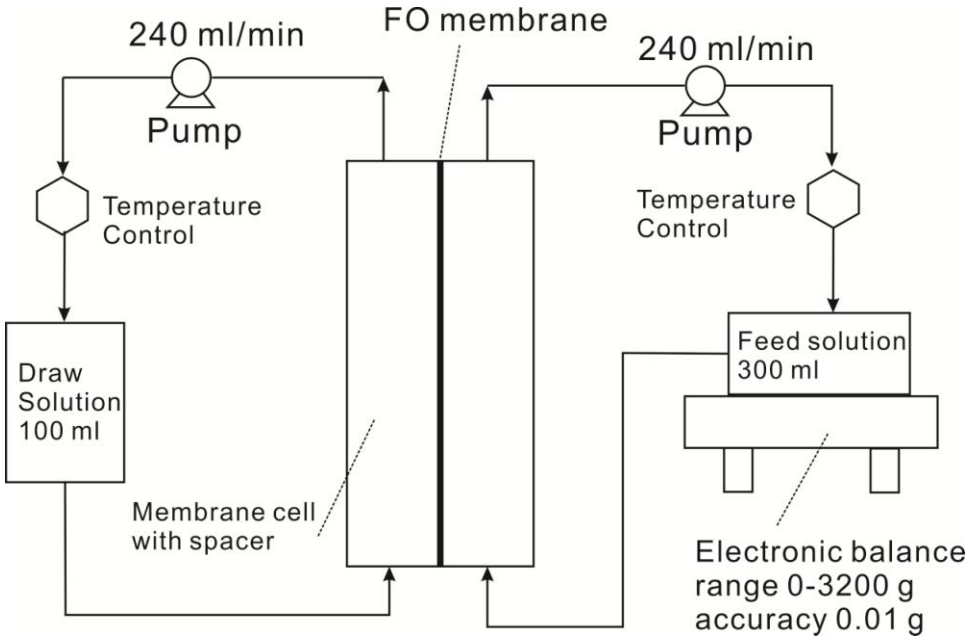

Figure 7.1 Setup for water flux measurement in FO.

7.2.5. Draw agent back diffusion

The draw agent back diffusion (J_s) was monitored by the increase of total organic carbon (ΔTOC) of feed solution,

$$J_s = \Delta TOC * V_{feed} /(A*T*C)$$

Where V_{feed} is the feed solution volume before sampling for the TOC measurement, T is the FO testing time and A is the membrane area. C is the weight concentration of carbon atoms in draw agent molecules, which is 65.50 % for P_{4444} TMBS and 64.86% for P_{4444} DMBS.

7.3. Results and discussion

7.3.1. Synthesis of draw agents

The ^{1}H NMR test in $CDCl_3$ is shown as follows. **P_{4444}TMBS** (1H, 400 MHz, $CDCl_3$, δ/ppm relative to TMS): 0.89-0.92(t,12H,CH_3), 1.42-1.47(m,16H,CH_2), 2.17(s,3H,CH_3), 2.24-2.31(m,8H,CH_2), 2.66(s,6H,CH_3), 6.75(s,2H,Ar-H). **P_{4444}DMBS** (1H, 400 MHz, $CDCl_3$, δ/ppm relative to TMS): 0.72-0.76(t,12H, CH_3), 1.23-1.27(m,16H,CH_2), 2.00-2.07(m,8H,CH_2), 2.11(s,3H,CH_3), 2.50 (s, 3H, CH_3), 6.72-6.74(d, 1H, Ar-H), 6.78 (s,1H, Ar-H), 7.66-7.68 (d, 1H, Ar-H).

At room temperature, P_{4444}DMBS is colorless viscous liquid; P_{4444}TMBS and P_{4448}Br are in opaque wax state. Their DSC results are shown in Figure 7.2. The P_{4444}DMBS is liquid in a wide temperature range from -50 ℃ to 150℃. The P_{4444}TMBS and P_{4448}Br waxes have melting points of 80 ℃ and 25℃, respectively. The exothermic peak on P_{4448}Br at around -3℃ is probably corresponding to cold crystallization, which is commonly observed in ionic liquids.[20, 21]

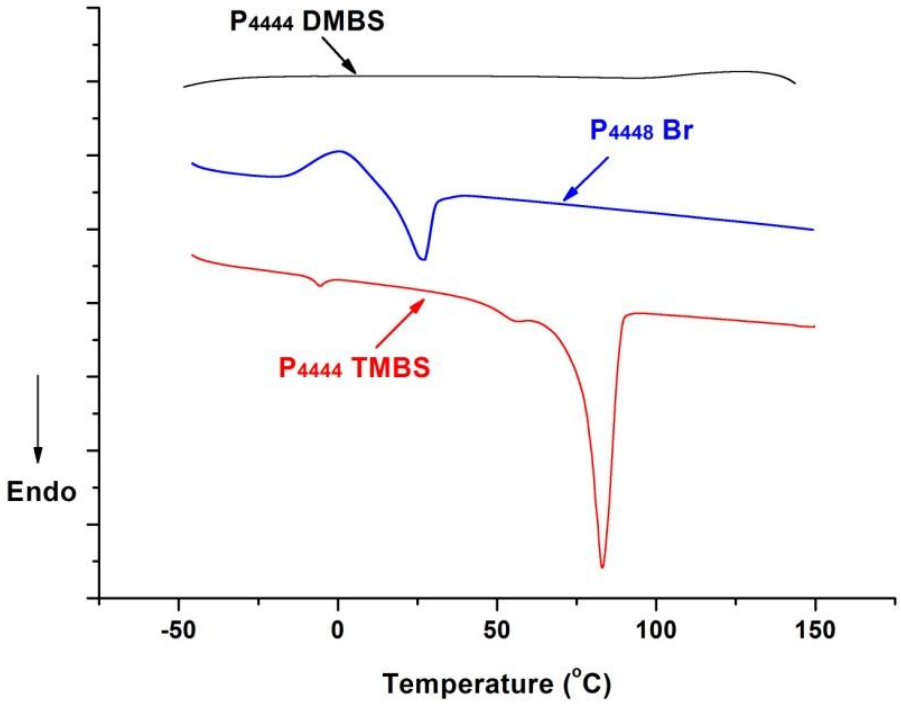

Figure 7.2 DSC measurements of the three pure ionic liquids.

7.3.2. The amphiphilicity of thermally responsive ionic liquids

Figure 7.3 shows the entire FO desalination processes enabled by a concentrated, *e.g.*, 70 wt%, aqueous solution of the thermally responsive ionic liquid as the draw solution. In FO process, the desalinated water automatically permeates through the FO membrane from the feed solution to dilute the draw solution. In regeneration process, the diluted, *e.g.*, 50 wt%, draw solution after FO undergoes a liquid-liquid phase separation with thermal energy input to increase the temperature above the LCST. The draw solution concentration in the water-rich supernatant is much reduced to less than 10 wt%. High quality water is available via a highly energy efficient low pressure NF polishing step. The sedimentation after phase separation and the retentate in NF can be pumped back for draw solution reuse in FO for a closed loop without any further treatment. In such a desalination method, energy cost reduction is envisioned since a great portion of electrical energy consumption can be replaced by low grade thermal energy for phase separation, leaving much diluted supernatant for low pressure NF process consuming less electrical energy.

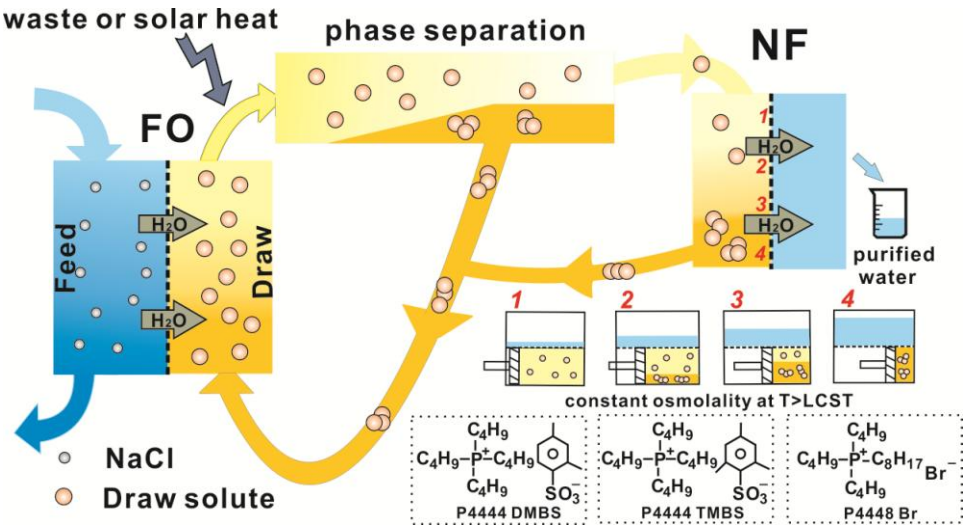

Figure 7.3 The schematic illustration of FO desalination using thermally responsive ionic liquids as draw agents. The molecular structures of these three draw agents are also demonstrated.

The molecular design of these draw agents, as shown in Figure 7.3, complies with the required balance of ease of regeneration and generating a high osmotic pressure.

Different from conventional ionic liquids that either are miscible with water showing hydrophilicity, or repel water showing hydrophobicity, these thermally responsive ionic liquids are amphiphilic. The LCSTs of these ionic liquid aqueous solutions were originated from the combination of the hydrophobicity from the alkyl groups in cations and the hydrophilicity from suitable anions. It is worth mentioning that the balance

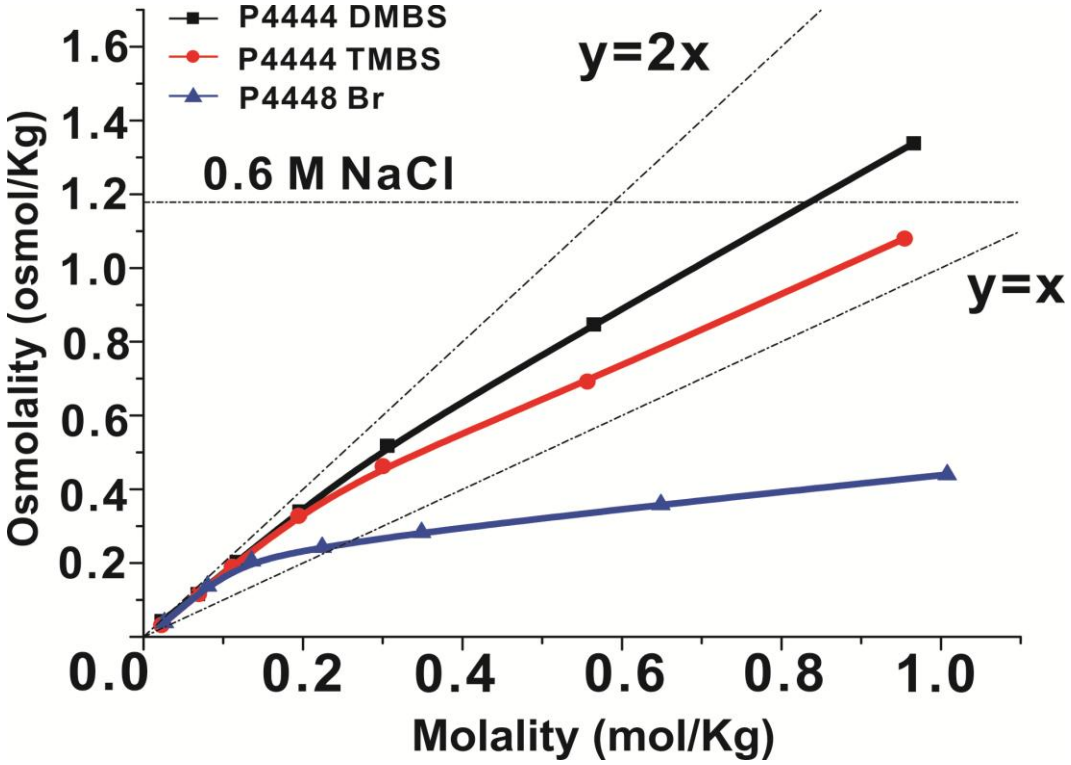

Figure 7.4 The nonlinear correlations between molality and osmolality of these three draw agents indicate the effect of ion-pairing besides dissociation.

between hydrophobicity and hydrophilicity is so subtle that any tiny molecular structure modification would eliminate the LCST. For instance, tributylhexylphosphonium 2,4-dimethylbenzene sulfonate (P_{4446}DMBS) is virtually insoluble, while tetrabutyl-phosphonium benzenesulfonate (P_{4444}BS) is highly soluble in water. The unique characteristics of these ionic liquids as draw agents can also be seen in Figure 7.4. The osmolality of these ionic liquids draw solutions increases monotonically, but showing negative deviation from linearity with molality. This is different from a conventional electrolyte showing linearity[22] and a polyelectrolyte showing positive deviation from linearity as can be seen in Chapter 6. At low concentrations (*e.g.*, <0.1 mol/kg or <5

wt%), all the three ionic liquids fully dissociate into relatively 'free' anions and cations so that the osmolality is approximately twice that of the molality anticipated for monovalent electrolyte in ideal solution. As their concentrations increase, the osmolality versus molality plots negatively deviate from the linearity. This is believed to be originated from a hydrophobic association, or ion-pairing effect, of these ionic liquid molecules.[23] Figure 7.4 also indicates that $P_{4448}Br$ has the strongest hydrophobic interaction between molecules resulting in the most severe negative deviation from the ideal osmolality-molality linearity. $P_{4444}TMBS$ and $P_{4444}DMBS$ are more hydrophilic than $P_{4448}Br$ and their 30 wt% (~0.95 mol/kg) solutions assume osmolalities of 1.08 osmol/kg and 1.34 osmol/kg, respectively, which are approaching or higher than that of seawater (1.13 osmol/kg).

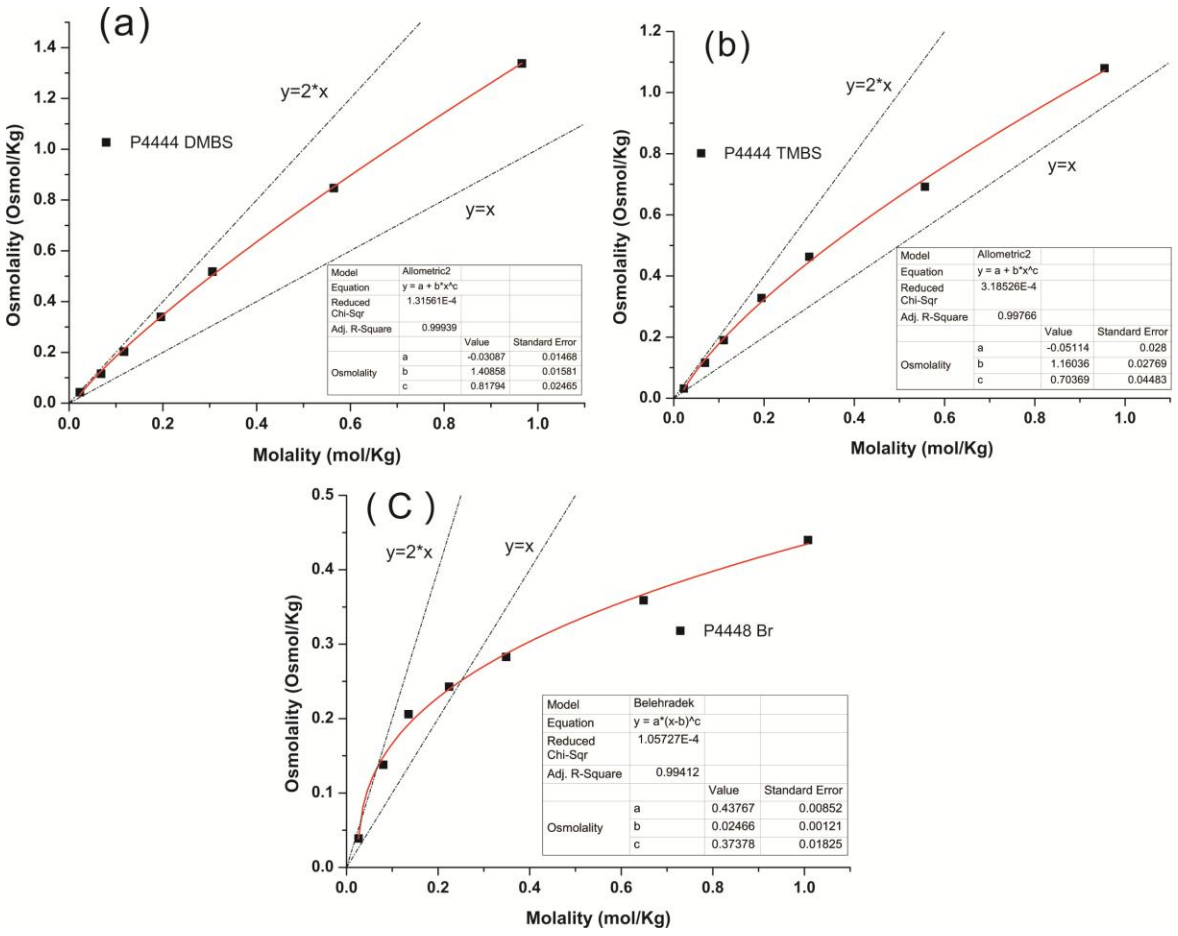

Figure 7.5 The fittings for osmolality-molality correlations at osmolality-measurable concentrations.

The osmolalities of ionic liquid draw solutions with a concentration above 30 wt% cannot be measured although the measuring limit of the apparatus has not been exceeded. This is probably due to the increased viscosity of draw solution as concentration increases. Thus, in order to have a panoramic correlation between osmolality and weight concentration, I applied the fittings of osmolality-molality correlations of the three draw agents at low concentrations, as seen in Figure 7.5, to predict the osmolality-weight concentration correlations for higher concentrations. The conversion equation between molality and weight concentration is:

$$\text{Weight concentration} = \text{molality} \times M_w / [(\text{molality} \times M_w) + 1000]$$

where M_w is the draw agent molecular weight (g/mol). The conversion from weight concentration to molality had been summarized in Table 7.1, and the correlation between osmolality and molality at high concentrations utilized the fittings in Figure 7.5.

Table 7.1 The correlation between predicted osmolality and weight concentration of draw solutions. The conversion from weight concentration to molality was according to the equation mentioned above, and the correlation between molality and osmolality was based on the fittings in Figure 7.5.

		40 wt%	50 wt%	60 wt%	70 wt%	80 wt%
P_{4444} DMBS	**Molality (mol/kg)**	1.5015	2.2523	3.3784	5.2553	9.0090
	Osmolality(osmol/kg)	1.9333	2.7057	3.7818	5.4416	8.4737
P_{4444} TMBS	**Molality (mol/kg)**	1.4556	2.1834	3.2751	5.0946	8.7336
	Osmolality(osmol/kg)	1.4647	1.9653	2.6311	3.6092	5.2975
P_{4448} Br	**Molality (mol/kg)**	1.6835	2.5253	3.7975	N.A.	N.A.
	Osmolality(osmol/kg)	0.5293	0.6171	0.7189	N.A.	N.A.

Figure 7.6 shows the measured osmolalities at low concentrations and predicted osmolalities at higher concentrations with methods mentioned above. P_{4444}TMBS and P_{4444}DMBS seem to be able to generate very high osmotic pressures. For example, 70 wt% P_{4444}TMBS and P_{4444}DMBS solution has an osmolality of 3.6 osmol/kg and 5.4 osmol/kg,

respectively, which is 3 and 4.5 times the osmolality of seawater. Such high osmolalities may be attributed to the ionic nature of these ionic liquids.

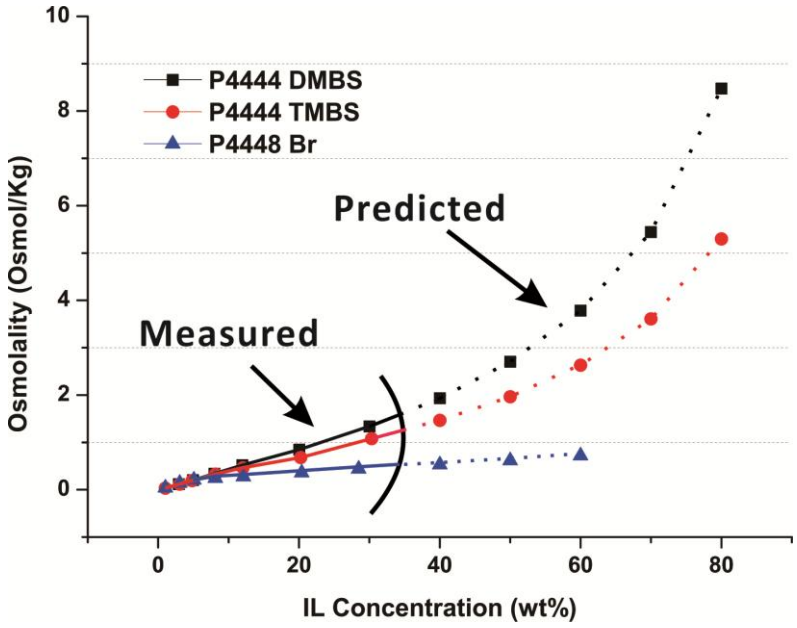

Figure 7.6 The panoramic correlation between osmolality and weight concentration.

7.3.3. FO performance of thermally responsive ionic liquids

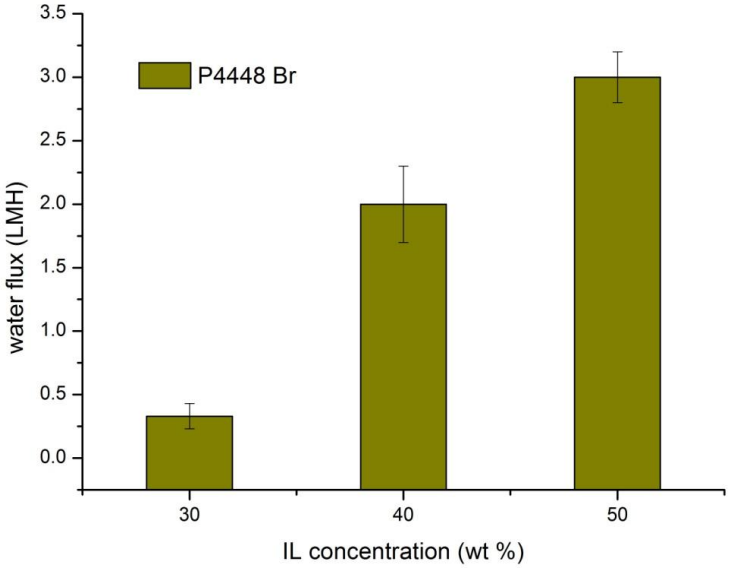

Figure 7.7 Water flux profile of $P_{4448}Br$ with different concentrations. Feed solution is 2000 ppm NaCl and the temperature is 14±1 ℃.

In order to further investigate the draw agents' osmolality influence on the FO performance, water flux measurement as a function of draw solution concentrations and feed solution salinities was conducted for P_{4444}TMBS and P_{4444}DMBS. Water flux measurement was not systematically conducted using P_{4448}Br as draw agent due to its low osmolality. As shown in Figure 7.7, the most hydrophobic P_{4448}Br can only generate a water flux from a low salinity feed solution and the water flux value is comparable with that from the polyionic liquid hydrogels studied in Chapter 5. Figure 7.8 demonstrates that P_{4444}DMBS generates a higher water flux than that from P_{4444}TMBS with the same feed solution salinity since P_{4444}DMBS is more hydrophilic than P_{4444}TMBS. Both P_{4444}DMBS and P_{4444}TMBS can generate a reasonable water flux from seawater, and these water fluxes corroborate well the trend predicted using osmolality values shown in Figure 7.6. It is worth reminding that the osmolalities were measured by cryoscopic method at subzero Celsius degree, therefore the actual osmolality values of such LCST-

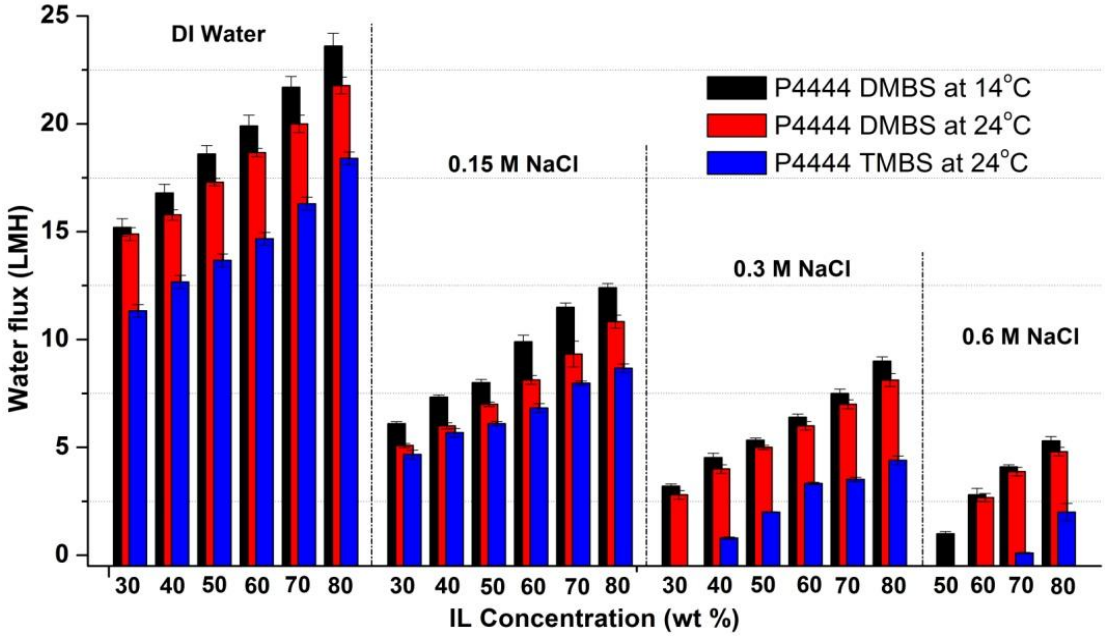

Figure 7.8 Water flux profiles of P_{4444}DMBS and P_{4444}TMBS draw solutions with various concentrations against feed solutions of various salinities at different temperatures.

type draw solutions at room temperature would be overestimated owing to stronger interactions between draw agent molecules at higher temperatures.[18] This can be seen in Figure 7.8 that, at 24 ℃ P_{4444}DMBS with concentrations at or below 50 wt% is unable to generate a measurable FO flux from seawater feed solution albeit a 30 wt% (~0.95 mol/kg) P_{4444}DMBS draw solution is measured to have a higher osmolality than that of seawater as shown in Figure 7.4. Therefore, I expect that such LCST-type draw agents would produce higher FO drawing ability at lower temperatures. Indeed the water fluxes generated by P_{4444}DMBS at 14±1 ℃ are higher than the corresponding ones measured at 24±1 ℃ as shown in Figure 7.8. Furthermore, Figure 7.9 shows that a 70 wt% P_{4444}DMBS draw solution can generate a water flux of 1.5 LMH from a 1.2 M NaCl feed solution at 14±1 ℃. Actually, it can even generate a measureable water flux from a 1.6 M NaCl solution that has 2.7 times salinity of seawater. The results indicate that this new group of draw agents may have potential to be utilized in the treatment of difficult streams such as RO brine and produced water from mining and oil and shale gas industries.

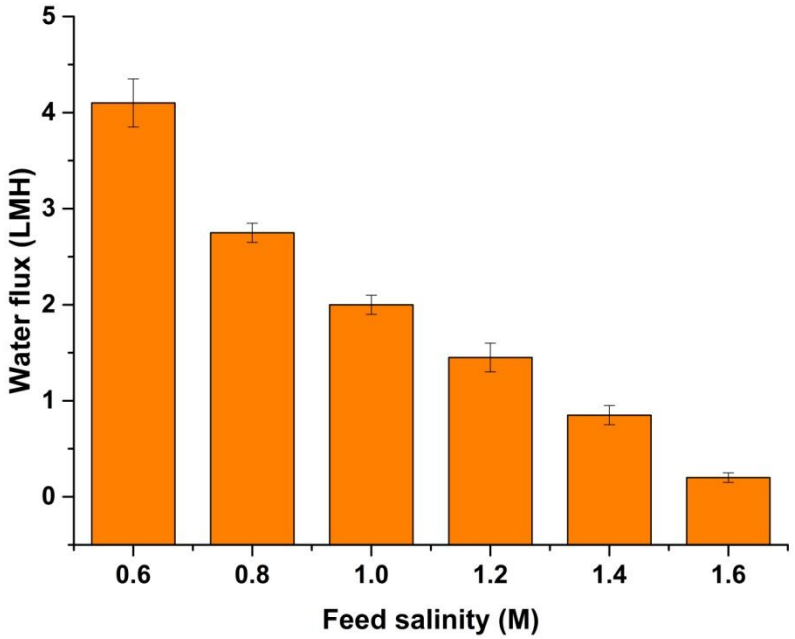

Figure 7.9 Water fluxes of 70 wt% P_{4444}DMBS draw solution generated from feed solutions with salinities higher than seawater. The FO test was conducted at 14±1 ℃.

The draw agent back diffusion during the FO process was also conducted by monitoring the total organic carbon (TOC) increase in the feed solution. Figure 7.10 summarizes the ratios of draw agent back diffusion flux to water flux (J_s/J_w) of draw solutions with different concentrations. Both P_{4444}DMBS and P_{4444}TMBS show very low back diffusion, and the ratio is around 30 mg/l owing to their relatively high molecular weights compared to traditional inorganic salt. In addition, the relatively large size of either cation or anion may also contribute to minimizing the back diffusion. It is worth mentioning that the back diffusion of these draw agents is orders of magnitude lower than that of NaCl (750 mg/l) or NH_4HCO_3 (>2000 mg/l).[9]

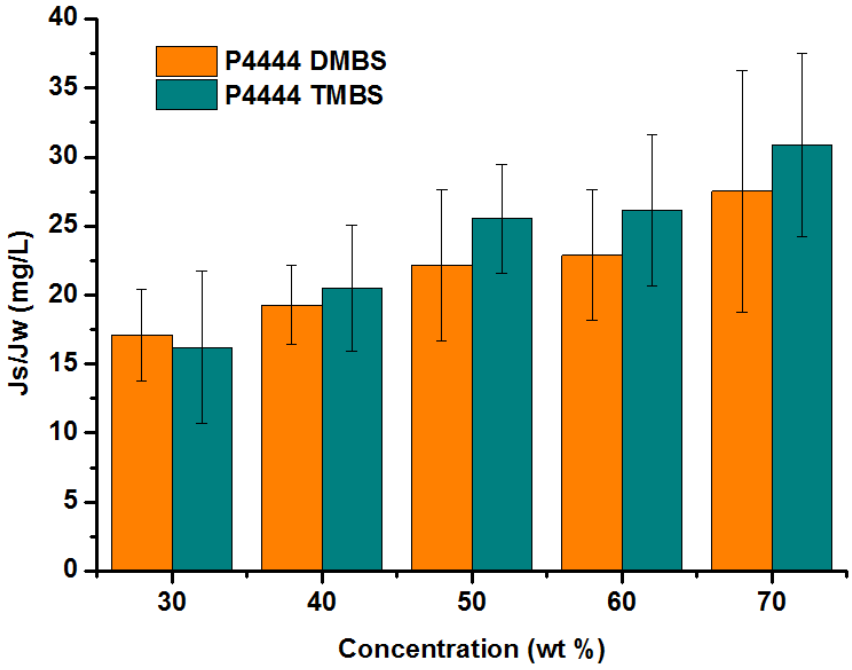

Figure 7.10 The correlation between draw agent back diffusion flux to water flux ratio and draw solution concentration. This ratio indicates the mass (mg) of draw agents back diffused as per litre of water permeated through membrane. DI water was the feed solution.

The salt rejection during the FO process was not measured in this chapter. However, I believe that the salt rejection largely depends on the membrane's intrinsic property and has little to do with the draw solution. Instead, I tested the FO membrane's intrinsic salt rejections before and after soaking into a 70 wt% draw solution for 7 days. The results shown in Figure 7.11 indicate that there is insignificant salt rejection decline after

soaking in a 70 wt% ionic liquid solution. One can assume that even the concentrated draw solution has negligible effect on the membrane. Membrane swelling in ionic liquid solution should be a manageable issue for long term operation.

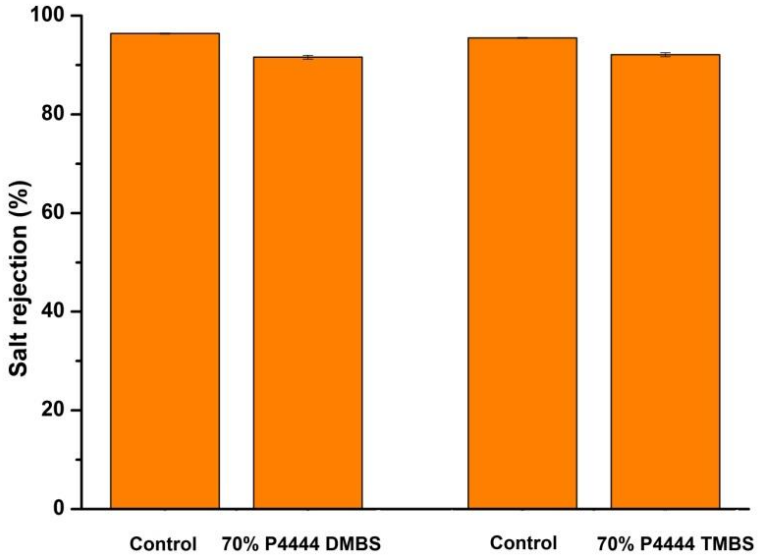

Figure 7.11 Comparison of salt rejection of as-received membranes and those immersed for 7 days in 70 wt% P_{4444}DMBS or P_{4444}TMBS draw solution.

7.3.4. Draw agents regeneration

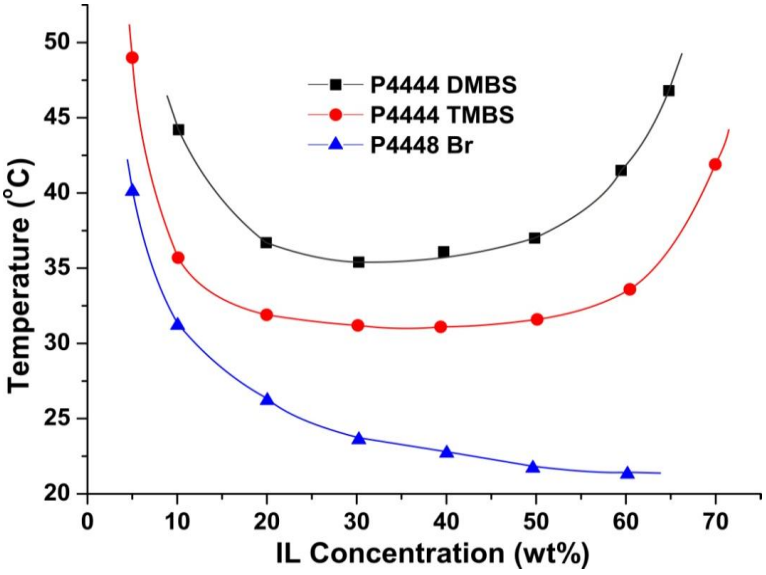

Figure 7.12 The LCSTs of the draw solutions at different concentrations.

After the FO process, the diluted draw solution goes through a regeneration process where the draw agent separation from water is achieved. The phase diagrams of these three ionic liquid solutions in Figure 7.12 show a U-shaped LCST dependence on the concentrations. The absence of an LCST rise for $P_{4448}Br$ at higher concentrations might be ascribed to its low miscibility with water. The mechanism of the LCST phenomenon in solution has been intensively studied to be driven by unfavorable entropy in mixing, and the presence of the LCST in an aqueous solution hinges on a subtle balance between

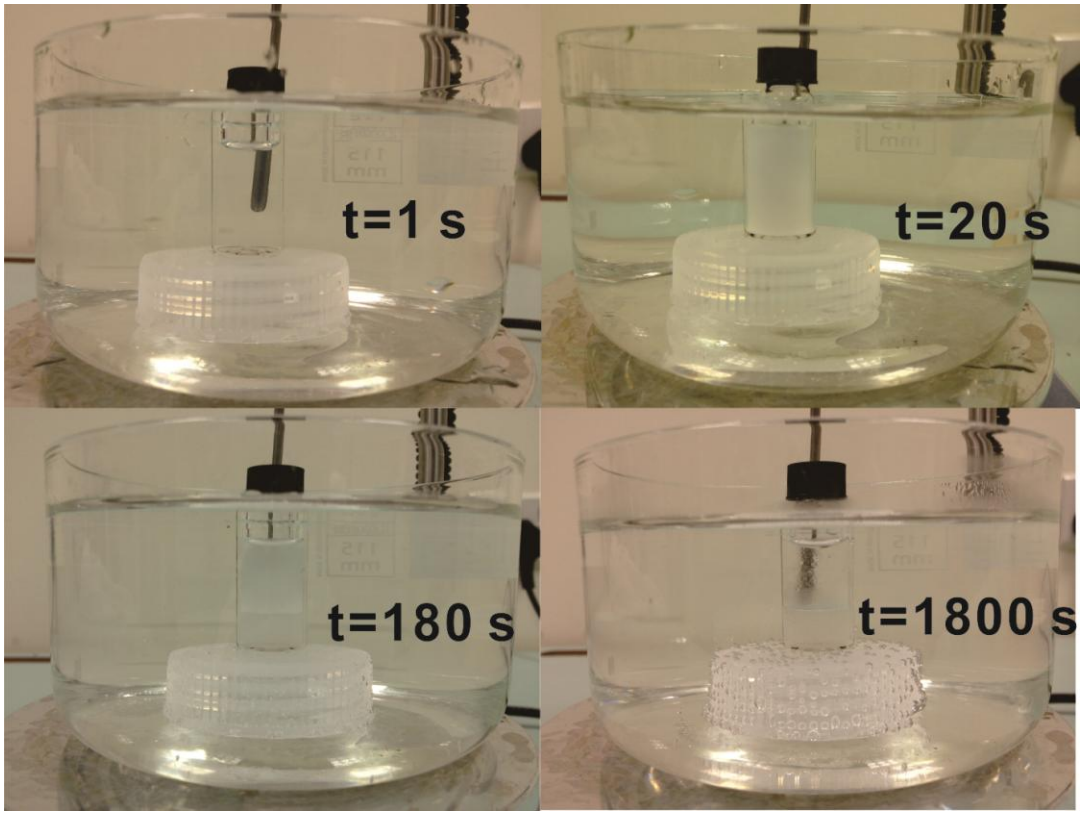

Figure 7.13 Phase separation of 40 wt% $P_{4444}DMBS$ as a function of time at 50℃. The white plastic cap under vial was used for avoiding direct contact with the hot plate.

hydrophobicity and hydrophilicity of the solute. Non-ionic Pluronics, PNIPAm and cellulose derivatives are the typical representatives for this case.[24-26] Although ionic species are rarely reported to assume the LCST in aqueous solution, the phase separation in the ionic liquid draw solutions is believed to comply with similar driving force. The observed LCSTs between 30 to 50 ℃ for $P_{4444}DMBS$ or $P_{4444}TMBS$ are not too high above room temperature and desirable for phase separation induced by solar energy or

waste heat. Moreover, the LCST decreases monotonically in FO process when a 70 wt% P_{4444}TMBS or P_{4444}DMBS draw solution is diluted to 30 wt%, which means that the thermal energy threshold for phase separation in regeneration process is even reduced. Figure 7.13 shows that when the draw solution is heated above the LCST, a clear liquid-liquid phase separation occurs resulting in a draw agent rich sedimentation phase and a

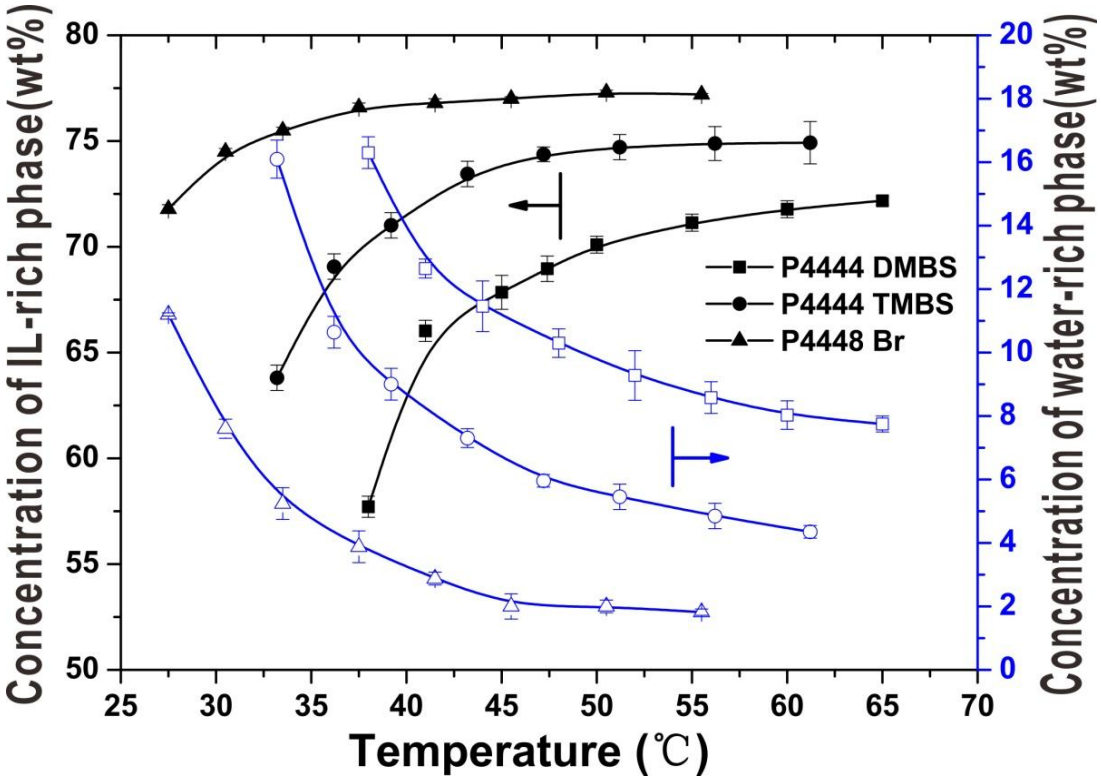

Figure 7.14 Draw agent concentrations in the water-rich supernatant phase and draw agent-rich sedimentation phase after phase separation at different temperatures. The initial draw solution concentration was 30 wt%.

water-rich supernatant phase. The most desirable and also intriguing point is that in the diluted draw solution phase separation for each of these three candidates (*e.g.*, 30 wt% as shown in Figure 7.14), draw agent concentration in the draw agent-rich bottom phase ascends to a plateau while that of the water-rich supernatant phase descends to a plateau, when the phase separation is towards completion at higher temperatures, *e.g.*, at about 16 ℃ above its corresponding LCST. Since the thermally induced phase separations of these ionic liquids have never been thoroughly studied, I also investigated the draw solutions' phase separation behaviors at various concentrations. Figure 7.15 demonstrates

that at 16 ℃ above the corresponding LCST, the draw agent concentrations are basically constants in both the draw agent-rich sedimentation and water-rich supernatant despite the different initial concentrations of these three draw solutions. This is quite important since water recovery as well as feed solution salinity would affect the diluted draw

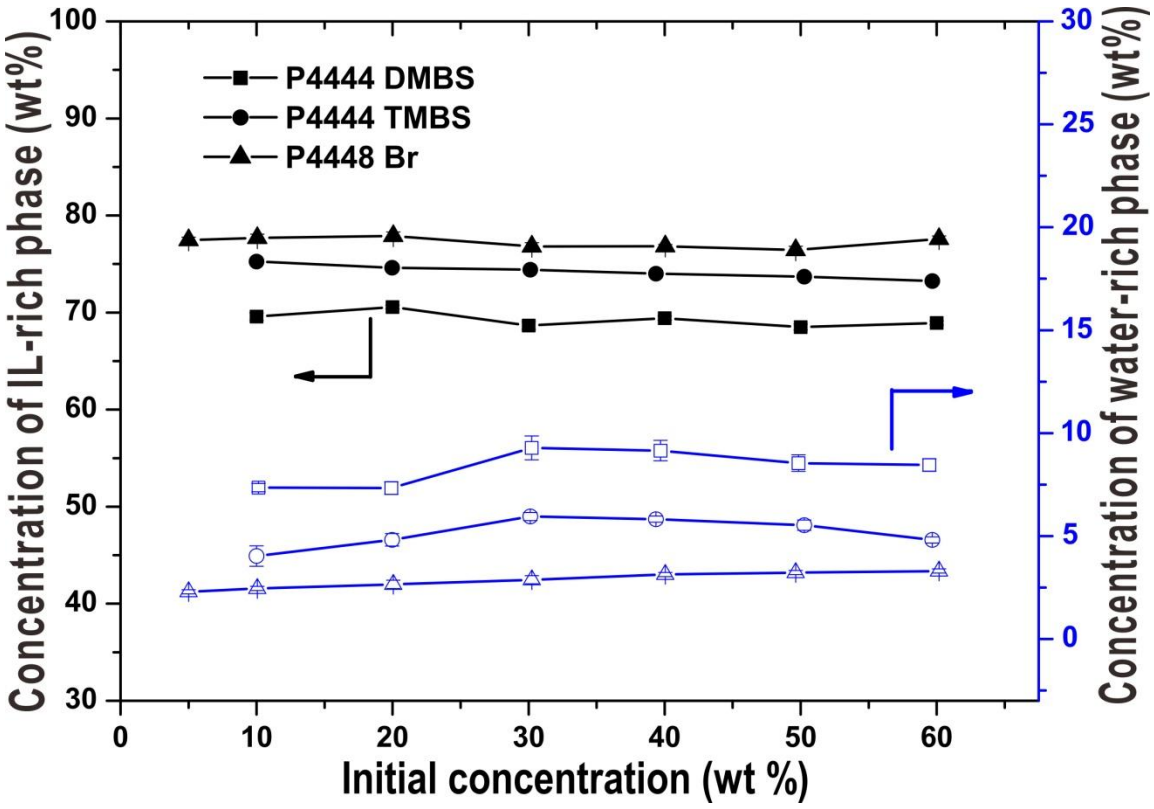

Figure 7.15 Draw agent concentrations in the water-rich supernatant phase and draw agent-rich sedimentation phase at 16℃ above the corresponding LCST of different initial draw solution concentrations.

solution concentration in regeneration process. But for these thermally responsive ionic liquids as draw agents, stable and constant concentrations in the two phases are achievable regardless of the water recovery requirement and feed solution salinity albeit the weight of each phase may vary. In fact, a stable phase separation can readily occur at a very mild temperature stimulus, e.g., at 40 and 35 ℃ for P_{4444}DMBS and P_{4444}TMBS, respectively, according to Figure 7.12. This enables the ionic liquids to be efficiently regenerated using industrial waste heat or low grade solar heat. For better clarity, a full cycle of FO process, draw agent regeneration via phase separation, and draw agent reuse

is demonstrated on a schematic phase diagram in Figure 7.16. Use the most hydrophilic P_{4444}DMBS as an example. After the FO process, the diluted draw solution at almost any concentration between 10 and 60 wt%, which is dependent on the feed solution salinity, undergoes a phase separation at 55 ℃ producing a draw agent-rich phase (70 wt%) that can be reused as the draw solution in the FO process without further treatment. Meanwhile, the draw agent concentration in water-rich supernatant phase is only 7.5 wt%. The substantially reduced osmotic pressure in supernatant enables it capable to be treated energy-efficiently by RO or NF. These characteristics are also favorable from a practical viewpoint because they enable a closed-loop process.

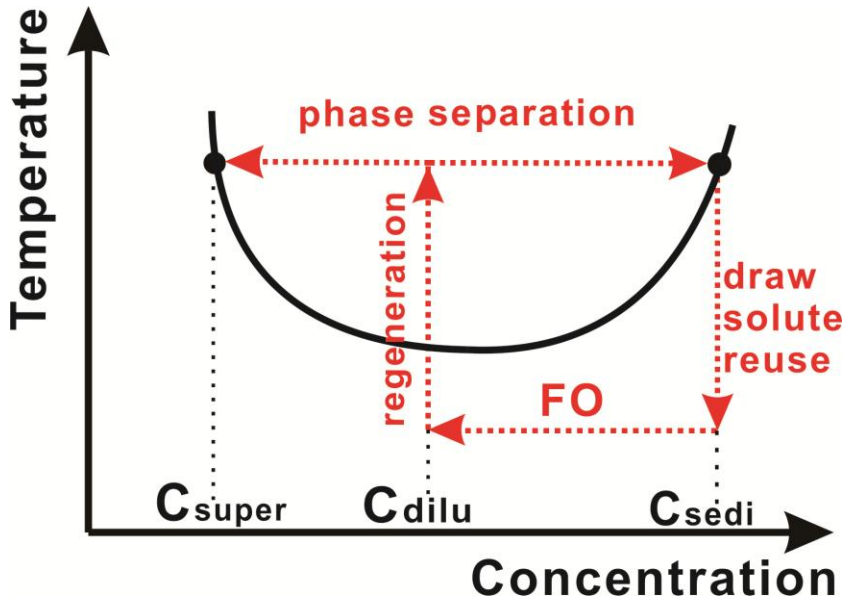

Figure 7.16 The entire FO desalination processes in phase diagram. C_{sedi}, C_{dilu} and C_{super} represent the concentration of draw agent-rich sedimentation phase, diluted draw solution after FO process and water-rich supernatant phase, respectively.

7.3.5. Energy consumption estimation

Among all the research papers published on draw agent to date, few have systematically discussed the energy issue in forward osmosis desalination.[27, 28] For the most typical CO_2-NH_3 system, thermal energy was utilized in regeneration process to raise the temperature above 60 ℃ to decompose the draw agent into CO_2 and NH_3 with significant water evaporation. A low energy consumption of 0.84 KWh/m^3 was calculated for this

draw agent,[27] albeit questioned by others.[29] Actually the theoretical minimum energy requirement for desalination is related to water activity, solution's temperature and water recovery,

$$W_{min} = -\frac{RT}{Y} \cdot \ln(\alpha_w) \cdot \ln\left(\frac{1}{1-Y}\right) \qquad \text{(Equation 7.1)}$$

where R is the gas constant, α_w is water activity, T is the temperature and Y is the water recovery. The derivation of Equation 7.1 is not conducted here and details can be found in the supporting information of Reference 2. The minimum energy requirement is derived on the assumption that the desalination occurs as reversible thermodynamic process, and is independent on the specific desalination method. The water activity is replaced by osmotic pressure via combining this equation with Equation 2.7, which is

$$\pi V_w = -RT \cdot \ln\alpha_w \qquad \text{(Equation 2.7 \& Equation 7.2)}$$

where V_w is the water molar volume, π is the osmotic pressure. Therefore, an equation of desalination's theoretical minimum energy requirement is available, which is a function of water recovery, temperature and osmotic pressure.

$$W_{min} = V_w \cdot \frac{\pi}{Y} \cdot \ln\frac{1}{1-Y} \qquad \text{(Equation 7.3)}$$

When the water recovery is approaching zero, or the osmotic pressure stays constant with water recovery, then the theoretical minimum energy requirement is

$$W_0 = V_w \cdot \pi \qquad \text{(Equation 7.4)}$$

From Equation 7.3, we can calculate that for the desalination of 3.5 wt% NaCl seawater with 50% water recovery, the minimum energy requirement is 3.74 MJ/m^3, or equivalently 1.04 kWh/m^3. Currently the state-of-the-art sweater RO energy consumption is about 2-5 kWh/m^3 with hydraulic pressure of up to 60 bar. This really sets a very high benchmark for other desalination technologies to challenge.

In fact, forward osmosis as a new technology is always focused by many researchers on the energy-input free automatic FO process, and FO desalination is always claimed to be a "low energy consumption" method. However, the energy consuming draw agent regeneration process is usually overlooked. As demonstrated in Figure 7.17, in either co-current or counter-current FO pattern, the diluted draw solution always has a higher osmotic pressure than that of the initial feed solution. Therefore, according to Equation 7.3, at the same water recovery, the regeneration process in FO theoretically consumes more energy than that of directly treating the feed solution, and possibly even higher than the ACTUAL energy consumption in RO plant. Therefore, some researchers are

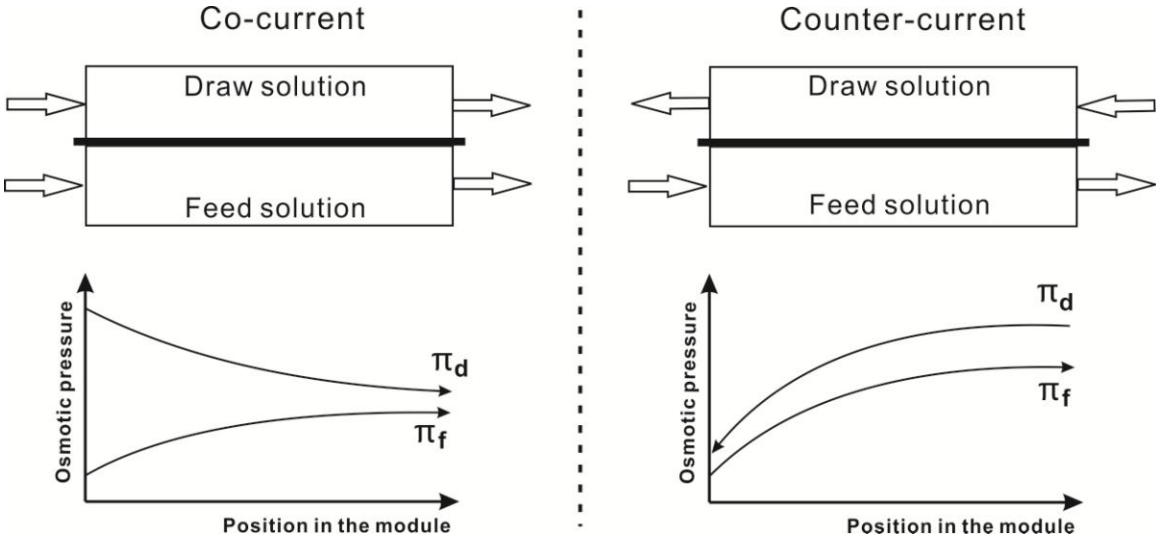

Figure 7.17 The osmotic pressure profiles of feed solution and draw solution in co-current and counter-current module. Π_d and Π_f are osmotic pressure of draw solution and feed solution, respectively.

questioning the future of using FO as an alternative method for seawater desalination energetically superior to RO.[29-32] In this section, I will calculate the theoretical energy consumption of FO seawater desalination enabled by the thermally responsive ionic liquids.

The osmotic pressures of thermally responsive draw agents were reduced below 6 bar after phase separation under heating. As shown in Figure 7.18a, a low hydraulic pressure of 7 bar is sufficient to generate a water flux of 7.6 LMH (for the water-rich phase of

P_{4444}DMBS) and 17 LMH (for the water-rich phase of P_{4444}TMBS) in the NF process using a membrane with molecular weight cutoff of 270 Da. When the hydraulic pressure is increased to 10 bar, a very high flux of 18 LMH and 31 LMH were available correspondingly, and this is comparable with, if not higher than, the water flux in the state-of-the-art seawater RO plant.[33] It is worth emphasizing that the hydraulic pressure increases in seawater RO as the feed is becoming concentrated with water recovery, and this is the reason why, as indicated in Equation 7.3, the theoretical minimum energy requirement increases with water recovery. Nevertheless, due to the unique phase separation behavior of our ionic liquid draw solutions, their osmotic pressures remain constant during the draw agent regeneration cum water recovery process via isothermal RO or NF above the LCST. As illustrated in Figure 7.18b, a similar phase separation resumes as water is recovered from the water-rich supernatant during the NF. In this case, the draw agent concentrations in the draw agent-rich phase and the water-rich phase also remain constant (e.g., at 70 and 7.5 wt% for P_{4444}DMBS). The diminishing weight ratio of water-rich phase to draw agent-rich phase is the only parameter that changes during the NF (Figure 7.18b and also inset in Figure 7.3). The retentate at the end of the NF process will be the draw agent-rich phase that can be directly reused as draw solution in FO process without further treatment.

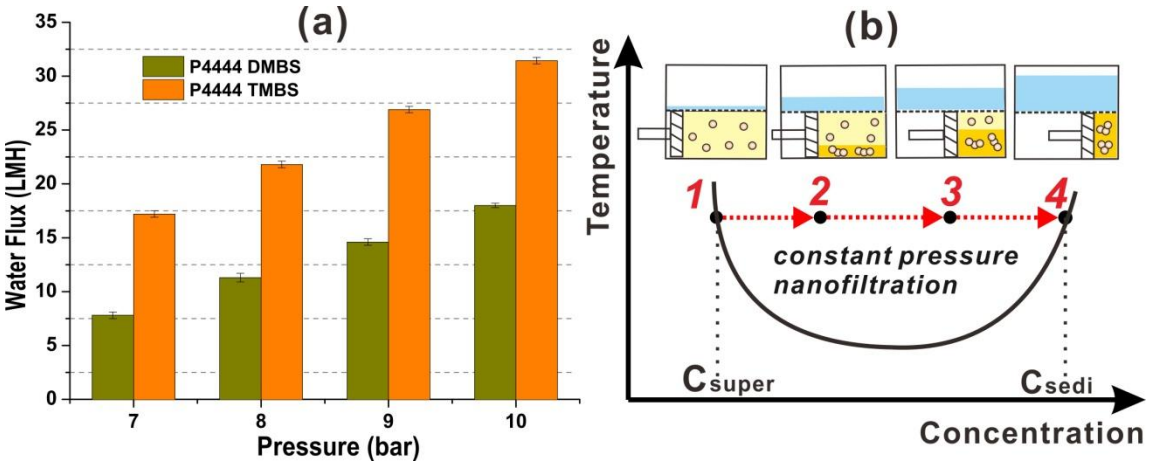

Figure 7.18 (a) Water fluxes during water recovery via low pressure nanofiltration with various hydraulic pressures. (b) Schematic depiction of further phase separation during the low and constant pressure NF process as water is recovered.

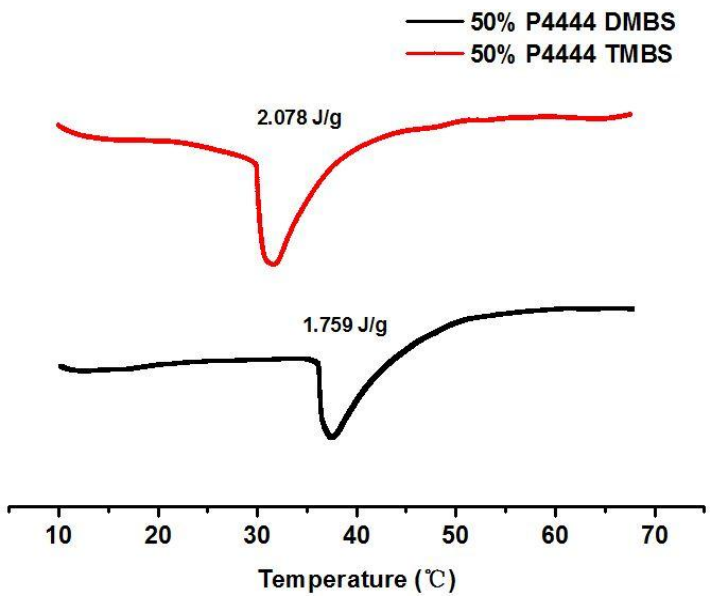

Figure 7.19 The DSC of 50 wt% draw solution phase separation.

In this FO seawater desalination enabled by thermally responsive ionic liquids, I assume that low grade thermal energy is needed for phase separations, while more expensive electrical energy is only needed in the constant-pressure NF process if pumping energy is ignored. I take the constant NF hydraulic pressure of 5 bar, which is an overestimation especially at high temperatures, as the osmotic pressure of the P_{4444}DMBS water-rich phase into Equation 7.4. Based on this estimation, the theoretical electrical energy required using P_{4444}DMBS draw agent in FO seawater desalination is 0.14 kWh/m^3, only 13% of that for seawater RO with 50% water recovery. It is anticipated that the rest of energy input comes from thermal source. For the thermal energy theoretical calculation, I assume there is no thermal energy loss during heat exchange. The only non-recoverable thermal energy comes from the latent heat during phase separation, since the separated phases never remix again at lower temperatures. Figure 7.19 shows the latent heat of draw agents phase separation. Based on these experimental data, 1 g of the diluted P_{4444}DMBS draw solution phase separates into 0.34 g of 7.5% water-rich supernatant and 0.66 g of 70% draw agent-rich sedimentation during the liquid-liquid phase separation. While the latter can be re-used directly as draw solution, the 7.5% water-rich supernatant was treated with NF which yields 0.30 g water after NF from our experiment. Therefore, the theoretical thermal energy required to produce unit weight of water would be 5.86 J/g

(1.759 J/g divided by 0.3) or 5.86 MJ/m^3, which is equivalent to 1.63 kWh/m^3. In this assumption, the thermal energy required during continuous phase separation in NF is omitted, and the two-phase system may introduce serious practical problems like fouling and severe concentration polarization.

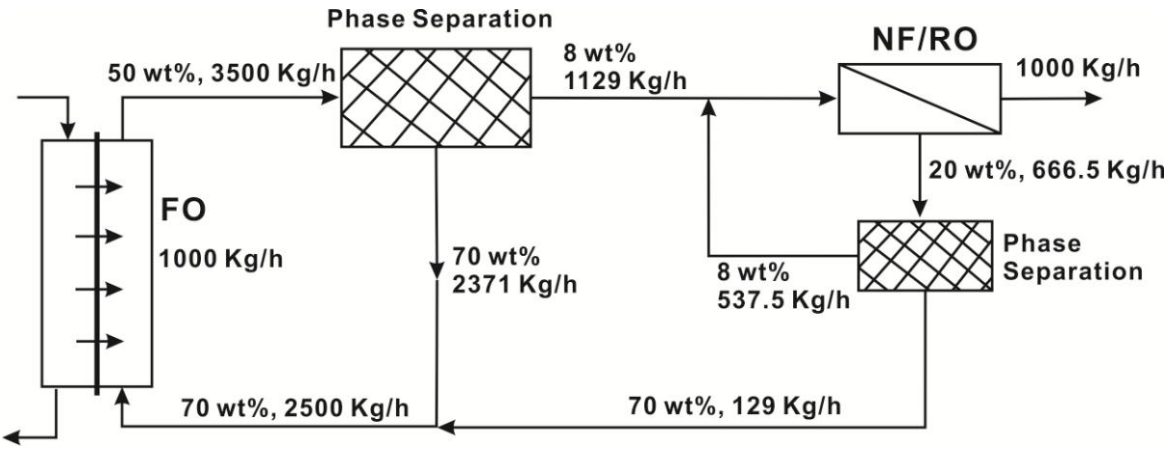

Figure 7.20 The scheme of FO-regeneration process using thermally responsive ionic liquids as draw agents. The capacity is fixed at 1000 kg per hour that is irrelevant with the capital energy calculation. The concentration and liquid flow rate at each step were marked. The water recovery of the entire seawater desalination process (counter-current pattern) is assumed to be 50% since 50 wt% draw solution can generate water flux from seawater, and 70 wt% draw solution can generate water flux from 1.2 M NaCl.

In order to calculate the theoretical energy consumption more accurately in a more practical scheme, the NF process is conducted at temperatures below LCST. As shown in Figure 7.20, no phase separation would occur in NF to avoid the fouling issue, and phase separation occurs in the ensuing step where the supernatant is pumped back for NF again, while the sedimentation was used for draw solution in FO. According to Equation 7.3, the electrical energy consumption in the NF (5 bar as the osmotic pressure of supernatant) is,

$$E_{electrical} = 18 \times 0.5 \times \frac{\mathrm{Ln}\frac{1}{0.4}}{0.6}\ \mathrm{J/mol} = 0.21\ \mathrm{kWh/m^3}.$$

This is slightly higher than the 0.14 kWh/m^3 calculated above because of the osmotic pressure increase in the NF process in this scenario. Similarly, the thermal energy consumption comes from phase-separations as shown in the two checkered boxes in

Figure 7.20. According to the DSC data that the enthalpy of 50 wt% P_{4444}DMBS is 1.759 J/g (in Figure 7.19) and 20 wt% P_{4444}DMBS is about 0.871 J/g (not shown here), we can easily calculate that the total thermal energy requirement is,

$$E_{thermal} = \frac{3500 \times 1.759\ KJ + 666.5 \times 0.871\ KJ}{1000\ L} = 6.74\ MJ/m^3 = 1.87\ kWh/m^3$$

The total theoretical energy consumption for FO desalination enabled by P_{4444}DMBS with a water recovery of 50% is 2.08 kWh/m^3. This is higher than the theoretical value for seawater RO with 50% water recovery of 1.07 kWh/m^3. However, only 0.21 kWh/m^3 electrical energy is need in FO and the rest can be complemented by much cheaper low grade thermal energy from industrial waste heat or solar source. Therefore, the energy cost of FO seawater desalination can be lower than that of seawater RO. For example, The average industrial electricity price in US in June 2014 is 7.3 US cents per kWh.[34] The thermal energy price varies with thermal source. Take the natural gas for example, the price in US on 15th, May 2015 was about $3 per million BTU (British Thermal Unit), which is equivalent to 0.28 US cents per MJ.[35] Therefore, the theoretical energy cost for RO is 7.8 cents/m^3, while for FO is only 3.4 cents/m^3. It is believed that the utilization of thermal energy from low grade industrial waste heat may even lower the theoretical energy cost for FO and reduce the carbon footprint.

Of course, energy cost is only a portion of the entire cost for desalination. If other more practical issues, such as the added-cost from draw agent loss and reduced-cost from easier fouling removal are considered, more investigations should be conducted to study the economics of using FO compared with RO to desalinate seawater. Another issue is that in this energy consumption calculation, water flux is not taken into consideration. Actually for a FO plant with fixed capacity, draw agents that can generate higher water flux require smaller membrane area thus reduce the capital cost.

7.3.6. Water quality and draw agent toxicity

If the NF membrane with a lower molecular weight cut-off (90 Da) is used in the NF process, the total organic carbon (TOC) in the permeate can be reduced to less than 20

ppm, and further reduced to as low as 3 ppm if the NF membrane is replaced by RO membrane. The phosphonium ionic liquids are not considered to be very toxic because phosphonium compounds are often present in surfactants and cleaning agents. I have initiated a cytotoxicity study of P_{4444} DMBS and P_{4444} TMBS using human fibroblast cell model, and the preliminary findings indicate that they have very low cytotoxicity. Virtually no change in cell viability was observed below the concentration of 100 μg/ml for both P_{4444}DMBS and P_{4444}TMBS. This is not surprised because the amphiphilic phosphonium ionic liquid draw agents have molecular structures analogous to phosphonium-containing lipids and polyelectrolytes. The latter have been widely used as vectors for gene delivery to living cells in biomedical research due to their low cytotoxicity.[36]

7.4. Conclusions

Thermally responsive ionic liquids have been studied as draw agents for FO desalination in this chapter. These draw agents can generate a water flux from feed solution with salinities up to 1.6 M NaCl. In the meantime, the diluted draw solutions assume LCSTs of below 50 ℃, above which there is a liquid-liquid phase separation. The ionic liquid-rich sedimentation phase can be reused as draw solution in FO without any further treatment; while the water-rich supernatant with an osmotic pressure lower than 6 bar go through a low-pressure NF to produce fresh water. The total energy consumption is doubtlessly higher than the theoretical minimum value achieved by RO. However, the electrical energy consumption of FO is much lower than that of RO, and the cheaper low grade thermal energy used in phase separation assists to reduce the energy cost of FO lower than RO. I envisage that these findings could motivate the proliferation of FO processes, and pave the way towards low cost and low carbon footprint desalination, as well as treatment of difficult industrial wastewater with high salinities.

References

1. Aldhous, P., The world's forgotten crisis. *Nature* **2003,** *422*, (6929), 251-251.

2. Elimelech, M.; Phillip, W. A., The future of seawater desalination: energy, technology, and the environment. *Science* **2011,** *333*, (6043), 712-717.

3. Klaysom, C.; Cath, T. Y.; Depuydt, T.; Vankelecom, I. F., Forward and pressure retarded osmosis: potential solutions for global challenges in energy and water supply. *Chem Soc Rev* **2013,** *42*, (16), 6959-6989.

4. Fane, A. G.; Wang, R.; Hu, M. X., Synthetic Membranes for Water Purification: Status and Future. *Angewandte Chemie International Edition* **2015**.

5. Hoover, L. A.; Phillip, W. A.; Tiraferri, A.; Yip, N. Y.; Elimelech, M., Forward with osmosis: emerging applications for greater sustainability. *Environmental science & technology* **2011,** *45*, (23), 9824-9830.

6. Duan, J.; Litwiller, E.; Choi, S.-H.; Pinnau, I., Evaluation of sodium lignin sulfonate as draw solute in forward osmosis for desert restoration. *Journal of Membrane Science* **2014,** *453*, 463-470.

7. Wang, W.; Zhang, Y.; Esparra-Alvarado, M.; Wang, X.; Yang, H.; Xie, Y., Effects of pH and temperature on forward osmosis membrane flux using rainwater as the makeup for cooling water dilution. *Desalination* **2014,** *351*, 70-76.

8. Majeed, T.; Sahebi, S.; Lotfi, F.; Kim, J. E.; Phuntsho, S.; Tijing, L. D.; Shon, H. K., Fertilizer-drawn forward osmosis for irrigation of tomatoes. *Desalination and Water Treatment* **2014,** *53*, (10), 2746-2759.

9. Achilli, A.; Cath, T. Y.; Childress, A. E., Selection of inorganic-based draw solutions for forward osmosis applications. *Journal of Membrane Science* **2010,** *364*, (1-2), 233-241.

10. Lutchmiah, K.; Lauber, L.; Roest, K.; Harmsen, D. J. H.; Post, J. W.; Rietveld, L. C.; van Lier, J. B.; Cornelissen, E. R., Zwitterions as alternative draw solutions in forward osmosis for application in wastewater reclamation. *Journal of Membrane Science* **2014,** *460*, 82-90.

11. Stone, M. L.; Wilson, A. D.; Harrup, M. K.; Stewart, F. F., An initial study of hexavalent phosphazene salts as draw solutes in forward osmosis. *Desalination* **2013,** *312*, 130-136.

12. Yen, S. K.; Mehnas Haja N, F.; Su, M.; Wang, K. Y.; Chung, T.-S., Study of draw solutes using 2-methylimidazole-based compounds in forward osmosis. *Journal of Membrane Science* **2010,** *364*, (1-2), 242-252.

13. Kravath, R. E.; Davis, J. A., Desalination of sea water by direct osmosis. *Desalination* **1975,** *16*, (2), 151-155.

14. Ge, Q.; Chung, T. S., Hydroacid complexes: a new class of draw solutes to promote forward osmosis (FO) processes. *Chem Commun (Camb)* **2013,** *49*, (76), 8471-8473.

15. Ge, Q.; Su, J.; Amy, G. L.; Chung, T. S., Exploration of polyelectrolytes as draw solutes in forward osmosis processes. *Water Res* **2012,** *46*, (4), 1318-1326.

16. Ou, R.; Wang, Y.; Wang, H.; Xu, T., Thermo-sensitive polyelectrolytes as draw solutions in forward osmosis process. *Desalination* **2013,** *318*, 48-55.

17. Mok, Y.; Nakayama, D.; Noh, M.; Jang, S.; Kim, T.; Lee, Y., Circulatory osmotic desalination driven by a mild temperature gradient based on lower critical solution temperature (LCST) phase transition materials. *Phys Chem Chem Phys* **2013,** *15*, (44), 19510-19517.

18. Nakayama, D.; Mok, Y.; Noh, M.; Park, J.; Kang, S.; Lee, Y., Lower critical solution temperature (LCST) phase separation of glycol ethers for forward osmotic control. *Phys Chem Chem Phys* **2014,** *16*, (11), 5319-5325.

19. Wei, J.; Qiu, C.; Tang, C. Y.; Wang, R.; Fane, A. G., Synthesis and characterization of flat-sheet thin film composite forward osmosis membranes. *Journal of Membrane Science* **2011,** *372*, (1), 292-302.

20. Fredlake, C. P.; Crosthwaite, J. M.; Hert, D. G.; Aki, S. N.; Brennecke, J. F., Thermophysical properties of imidazolium-based ionic liquids. *Journal of Chemical & Engineering Data* **2004,** *49*, (4), 954-964.

21. Batra, D.; Hay, D. N.; Firestone, M. A., Formation of a biomimetic, liquid-crystalline hydrogel by self-assembly and polymerization of an ionic liquid. *Chemistry of Materials* **2007,** *19*, (18), 4423-4431.

22. Stone, M. L.; Rae, C.; Stewart, F. F.; Wilson, A. D., Switchable polarity solvents as draw solutes for forward osmosis. *Desalination* **2013,** *312*, 124-129.

23. Zhang, L.; Xu, Z.; Wang, Y.; Li, H., Prediction of the solvation and structural properties of ionic liquids in water by two-dimensional correlation spectroscopy. *The Journal of Physical Chemistry B* **2008,** *112*, (20), 6411-6419.

24. Cho, E. C.; Lee, J.; Cho, K., Role of bound water and hydrophobic interaction in phase transition of poly (N-isopropylacrylamide) aqueous solution. *Macromolecules* **2003,** *36*, (26), 9929-9934.

25. Johansson, H. O.; Karlstroem, G.; Tjerneld, F., Experimental and theoretical study of phase separation in aqueous solutions of clouding polymers and carboxylic acids. *Macromolecules* **1993,** *26*, (17), 4478-4483.

26. Zheng, P.; Hu, X.; Zhao, X.; Li, L.; Tam, K. C.; Gan, L. H., Photoregulated Sol-Gel Transition of Novel Azobenzene-Functionalized Hydroxypropyl Methylcellulose and Its α-Cyclodextrin Complexes. *Macromolecular rapid communications* **2004,** *25*, (5), 678-682.

27. McGinnis, R. L.; Elimelech, M., Energy requirements of ammonia–carbon dioxide forward osmosis desalination. *Desalination* **2007,** *207*, (1), 370-382.

28. Kim, D. Y.; Gu, B.; Ha Kim, J.; Ryook Yang, D., Theoretical analysis of a seawater desalination process integrating forward osmosis, crystallization, and reverse osmosis. *Journal of Membrane Science* **2013,** *444*, 440-448.

29. Semiat, R., Energy issues in desalination processes. *Environmental science & technology* **2008,** *42*, (22), 8193-8201.

30. Semiat, R.; Sapoznik, J.; Hasson, D., Energy aspects in osmotic processes. *Desalination and Water Treatment* **2010,** *15*, (1-3), 228-235.

31. Field, R. W.; Wu, J. J., Mass transfer limitations in forward osmosis: Are some potential applications overhyped? *Desalination* **2013,** *318*, 118-124.

32. McGovern, R. K., On the potential of forward osmosis to energetically outperform reverse osmosis desalination. *Journal of Membrane Science* **2014,** *469*, 245-250.

33. Pearce, G.; Talo, S.; Chida, K.; Basha, A.; Gulamhusein, A., Pretreatment options for large scale SWRO plants: case studies of OF trials at Kindasa, Saudi Arabia, and conventional pretreatment in Spain. *Desalination* **2004,** *167*, 175-189.

34. Average Retail Price of Electricity to Ultimate Customers by End-Use Sector, June 2014. http://www.eia.gov/electricity/monthly/epm_table_grapher.cfm?t=epmt_5_6_a

35. Natural Gas Spot and Futures Prices (NYMEX). http://www.eia.gov/dnav/ng/ng_pri_fut_s1_d.htm

36. Hemp, S. T.; Allen Jr, M. H.; Green, M. D.; Long, T. E., Phosphonium-containing polyelectrolytes for nonviral gene delivery. *Biomacromolecules* **2011,** *13*, (1), 231-238.

8. A NOVEL UCST-TYPE FORWARD OSMOSIS DRAW AGENT FOR BRINE TREATMENT

In this chapter, a proprietary draw agent is introduced and studied. This thermally responsive draw agent has a UCST-type phase diagram in water. At high temperatures, *e.g.* 50℃, the draw solution is capable of concentrating a feed solution into 17 wt% NaCl brine; while at low temperatures, *e.g.* 20℃ or room temperature, the draw solution undergoes a phase separation resulting in a draw agent-rich phase that can be used as draw solution in FO process again without treatment, and a water-rich phase that can be treated in conventional seawater RO plant. This novel UCST-type draw agent may be competent energetically in brine treatment in combination with RO.

8.1. Introduction

Desalination technologies are gaining attention today owing to fresh water scarcity being widely recognized as a global crisis.[1] Among all the mature and developed desalination technologies, electro-dialysis (ED) is more suitable to treat feed streams with a concentration much lower than seawater.[2] While reverse osmosis (RO) is believed to be a mature technology for seawater desalination operating towards theoretical optimum concerning energy consumption,[3] it cannot desalinate feed streams with very high salinities, such as seawater RO brine and certain produced waste water in the oil and gas industry because of the high trans-membrane pressure (TMP) requirement.[4] Thermal distillation technologies including multi-stage flash (MSF), multi-effect distillation (MED), vapor compression (VC) or membrane distillation (MD) consume a large amount of energy albeit they can be used to desalinate brines. Therefore, it is desirable to develop alternative desalination technologies that can efficiently treat highly concentrated brines.

Forward osmosis (FO) has shown good promise.[5] The water permeation through a membrane is spontaneous process driven by an osmotic pressure difference, or equivalently a chemical potential gradient. In addition, fouling in FO is significantly alleviated and the membranes are much easier to clean since FO operates at much lower TMP than RO.[6] However, the permeate product of an FO process is a diluted draw solution, which actually has a higher osmotic pressure than the feed solution. Therefore, the success of FO as a viable desalination technology requires the discovery and development of more suitable draw agents that can be efficiently and cost effectively regenerated. Although many inorganic salts[7] and organic compounds have been studied as draw agents that display sufficiently high drawing ability against a feed with a salinity equal to or even higher than seawater, their regeneration actually consumes more electrical energy than RO.[8] Therefore, the entire process is not economically viable. In fact, all non-responsive or non-regenerable draw agents, including polyelectrolytes, zwitterionic compounds, quantum dots, organic salts and hydroacid complexes[9-13] face the same formidable problem. Therefore, exploring 'smart' and regenerable draw agents that can substantially reduce the osmotic pressure of the diluted draw agent after the FO process via a certain stimulus or reaction have recently become a focus of considerable study in connection with FO technology.

In Chapter 7, I studied the thermally responsive ionic liquids as draw agents for forward osmosis desalination. The ionic liquid draw agents can generate water flux from 1.6 M NaCl (~9 wt% NaCl), and readily undergo a liquid-liquid phase separation. The draw agent-rich phase can be reused as draw solution without any treatment, while the water-rich supernatant can be polished via a low pressure NF. The theoretical energy consumption of FO is higher than that of RO for seawater desalination with 50% recovery. However, due to the much lower consumption of electrical energy in FO, its energy cost is much less than RO. The importance of Chapter 7 is that the energetic advantages of FO over RO hinge on the involvement of cheaper and recyclable low-grade thermal energy from industry waste heat or solar source. This advantage is to be augmented if FO is used to treat the brines with salinities higher than seawater that are traditionally handled only by thermal distillation methods. The FO should assume not

only much lower energy cost, but lower energy consumption since the temperature and enthalpy in draw solution phase separation is always lower than that of water evaporation.

In search for new draw agents with improved comprehensive performances, I believe that thermally responsive ionic species are still the possible candidates. Instead of studying the LCST-type candidates whose solubilities decrease with temperature, the UCST-type ionic species whose solubilities increase with temperature are quite interesting draw agent candidates to study. For these UCST-type draw agents, their draw solutions generate water flux from feed solution at higher temperatures in FO process, while the regeneration process takes place at low temperature due to phase separation. Any further water polishing steps like NF can be used to treat the supernatant. Again, similar with the draw agent introduced in Chapter 7, isobaric process can be expected in theory since the solubility at certain temperature is constant.

Interestingly, this seemingly simple and obvious way for draw agent to reduce the osmolality in regeneration process has not been widely studied. This is possibly because for most of the ionic species the solubility dependence on temperature is insignificant. However, a successful UCST-type draw agent should have solubility difference as large as possible between high and low temperature, and this strict requirement challenges many possible candidates. Some ionic liquids including 1-butyl-3-methylimidzaolium tricyanomethanide, 1-butyl-1-methylpyrrolidinium tricyanomethanide and 1-butyl-1methylmorpholinium tricyanomethanide have been found to assume UCST in aqueous solution,[14] but the anion is toxic that excludes them from being draw agents. Some organic small molecules may also assume UCST in water,[15, 16] but they are corrosive to membrane especially at high temperatures in FO process. As for some ionic species with small molecular weights, such as itaconic acid,[17] potassium nitrate and calcium lactate,[18] they either have too high solubilities at low temperature causing difficulties in regeneration, or have too low solubilities at high temperature generating insufficient drawing ability.

In this chapter, I reveal some very promising initial findings of using a specially designed draw agent with a conspicuous solubility dependence on temperature. This draw agent

can generate a water flux in FO process at 50℃ from feed solution with salinity of 17 wt% NaCl, or around five times the salinity of seawater; when the temperature is reduced to 25 ℃, the diluted draw solution phase-separates into a sedimentation phase that can be reused again as draw solution, while the supernatant has an osmolality equivalent to that of 4.6 wt% NaCl solution. If the temperature is reduced to 20 ℃, the supernatant is further diluted and its osmolality is equivalent to that of 3.5 wt% NaCl, making it possible to be treated by any RO plant. This draw agent may enable FO desalination to be superior to thermal distillation methods in brine treatment with lower energy consumption.

8.2. Experimental section

8.2.1. Materials and apparatus

The draw agent synthesized and studied in this chapter is electrolyte in nature with a molecular weight between 100 g/mol and 700 g/mol, however the molecular structure and synthesis procedure are proprietary. Sodium chloride (>99.5%) was purchased from Merck. All other chemicals used were from Sigma Aldrich. Deionized (DI) water with electric resistance >18 MΩ was used throughout this chapter. The thin film composite FO membrane was purchased from Hydration Technology Innovations and immersed in DI water for 24 hours before use. The membrane's intrinsic parameters can be found elsewhere.[19]

8.2.2. Draw agent solubility in water

For the solubility determination, excess amount of draw agent was mixed with 10 g of DI water by magnetic stirrer in water bath at various temperatures in sealed vials. The temperature accuracy was within ±0.2℃. The upper layer solution and the bottom layer draw agent were isothermally stirred for 24 hours and stood still for 2 hours allowing for complete sedimentation. Specific volume of supernatant was taken out and weighed (m_{sol}, gram) before putting into vacuum oven at 100 ℃and 1 mbar until constant weight (m_{dry}, gram) was achieved. The draw agent solubility in molality was calculated by

$$\text{Solubility} = 1000 \cdot m_{dry}/[M \cdot (m_{sol}-m_{dry})] \qquad \text{(Equation 8.1)}$$

where M is the draw agent molecular weight. The draw agent concentration in the bottom draw-agent rich layer after regeneration was determined by Karl Fischer titration. All the experiments were conducted in triplicates.

8.2.3. Measurements of water flux, draw agent back diffusion and membrane salt rejection

The water flux was measured in a cross-flow setup by monitoring the feed solution weight decrease with time. The initial weight of feed solution and draw solution was 500 g and 200 g, respectively. The effective membrane area was 58.5 cm^2. The feed solution and draw solution flew in co-current in order to reduce the tension stress on membrane. The flow rate was 400 ml/min and plastic spacers were used in both feed and draw solution sides to introduce turbulence for concentration polarization reduction. The temperatures of draw solution and feed solution were maintained at 50±1 ℃ and 46± 2℃, respectively during FO process. The weight of feed solution and concentration of draw solution were kept virtually constant during the measurement. Both FO mode (selective layer towards feed solution) and PRO mode (selective layer towards draw solution) were tested in the water flux measurements. The water flux was calculated by

$$\text{Flux} = \Delta m/(A \cdot t) \qquad \text{(Equation 8.2)}$$

where Δm is the absolute value of feed solution weight decrease (kg), t is the corresponding measurement time (h) and A is the membrane area in square meters. Therefore, the flux is in unit of litre per square meter per hour (LMH) if the density of water is assumed to be 1 kg/l.

Draw agent back diffusion was determined by measuring the draw agent amount increase in feed solution. FO process was conducted for one hour and then feed solution was immediately diluted for ion chromatography test. A control sample was also collected from feed solution before FO test. The volume of feed solution during the FO test was

constant by adding DI water. The weight of draw agent (m_d in gram) reversely diffused into feed solution can be easily calculated by comparing the specific ion concentration in control and the sample after one hour. The draw agent reverse flux with unit in gram per square meter per hour (gMH) is determined by

$$Flux_{draw} = m_d/ (A \cdot t) \qquad \text{(Equation 8.3)}$$

where A is the effective membrane area (m^2) and t is the FO duration in hour.

The salt rejection of FO membrane in FO process was similarly determined by measuring Cl^- concentration in draw solution before and after FO process. Specifically, sample was taken from draw solution for ion chromatography after 20 gram of water permeated from feed solution to draw solution. A control sample was also collected before the FO process. The amount of Cl^- permeated can be calculated by knowing the concentrations of Cl^- and corresponding weight of draw solution before and after FO process. The weight increase in draw solution after FO should be meticulously taken into consideration when calculating the amount of Cl^- in each sample. Therefore, the NaCl concentration in the permeate can be calculated by

$$C_p = (m_{NaCl}/20) \times 100\% \qquad \text{(Equation 8.4)}$$

where m_{NaCl} is the weight of sodium chloride in gram permeating through FO membrane, and salt rejection of FO membrane can be determined by

$$\text{Salt rejection} = (1- C_p/C_f) \times 100\% \qquad \text{(Equation 8.5)}$$

where C_f is the bulk feed solution concentration.

8.3. Results and discussion

For the draw agent that shows positive correlation between solubility and temperature, it is desirable to assume a relatively high solubility at temperatures not far above room temperature to produce high osmotic pressure; while the solubility at room temperature

should be much lower to facilitate phase separation and further treatment of the saturated water-rich supernatant with low concentration. Figure 8.1 demonstrated the solubilities of the draw agent in water at various temperatures. The solubility increased rapidly from 0.83 mol/kg at 25℃ to 5.8 mol/kg at 50℃, which indicates a 6.5 times solubility increase within a short temperature range of 25 ℃ above room temperature. It is very unlikely that

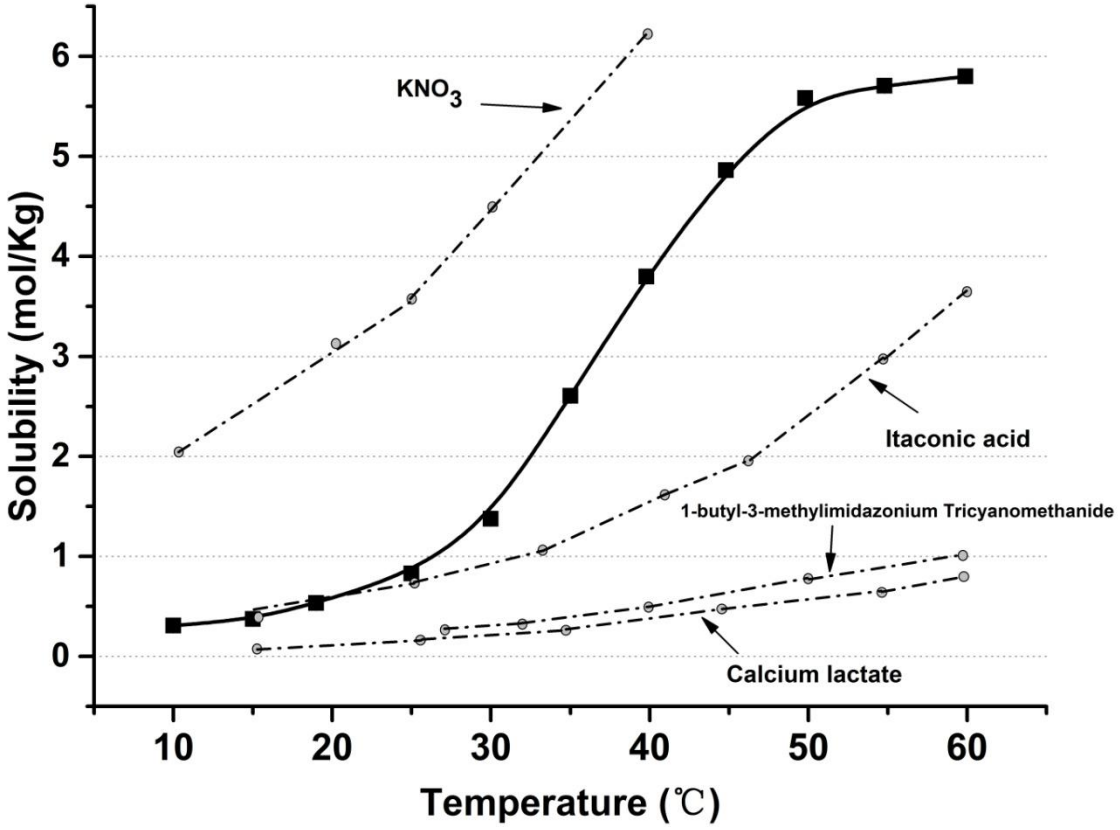

Figure 8.1 The draw agent's solubility (in solid line) as function of temperature. Four typical "smart" ionic species with solubility dependence on temperature were also shown in comparison. The solubility concentration is presented in mole of draw agent per kilogram of water.

other ionic draw agent can assume such a tremendous solubility change modulated by temperature. For example, as shown in Figure 8.1, itaconic acid, calcium lactate and the ionic liquid 1-butyl-3-methylimidazonium tricyanomethanide assume similar molalities with the draw agent at low temperatures. However, their solubilities do not increase as significantly as the draw agent studied in this chapter. Among the three, itaconic acid shows the highest molality of about 3.5 mol/kg at 60℃ albeit unfortunately it is corrosive to FO membrane. On the other hand, the solubility of KNO_3 is obviously high enough at

high temperatures, but still remains high at room temperature that complicates the regeneration onwards. Our draw agent assumes the combining advantages of generating high osmotic pressure at high temperature in FO, and generating low osmotic pressure at room temperature via phase separation in regeneration process. From Figure 8.1, it is clear that at temperatures above 50℃, the maximum molality of draw solution plateaus off. For the sake of protecting membrane in a more benign condition, FO is conducted at 50℃ but not higher temperatures. However, the maximum solubility of 5.8 mol/kg at 50 ℃ is not obtainable during cyclic FO-regeneration processes. The draw agent-rich phase after regeneration only has a molality of 4.8 mol/kg. Therefore, from stable performance point of view, the highest draw solution concentration in FO process is 4.8 mol/kg. Although the exact osmotic pressure or osmolality of draw solution cannot be obtained by freezing point depression method because of the extremely low solubility at sub-zero Celsius degrees, this draw solution is believed to be capable in brine treatment. This is because, on a conservative estimation that there is no dissociation for draw agent but complete dissociation for NaCl, we can still anticipate the draw solution to draw water flux from a feed solution with almost four times seawater salinity, since typical seawater only has a molality of 0.6 mol/kg. The real drawing ability of this draw solution should be tested in the measurement of water flux.

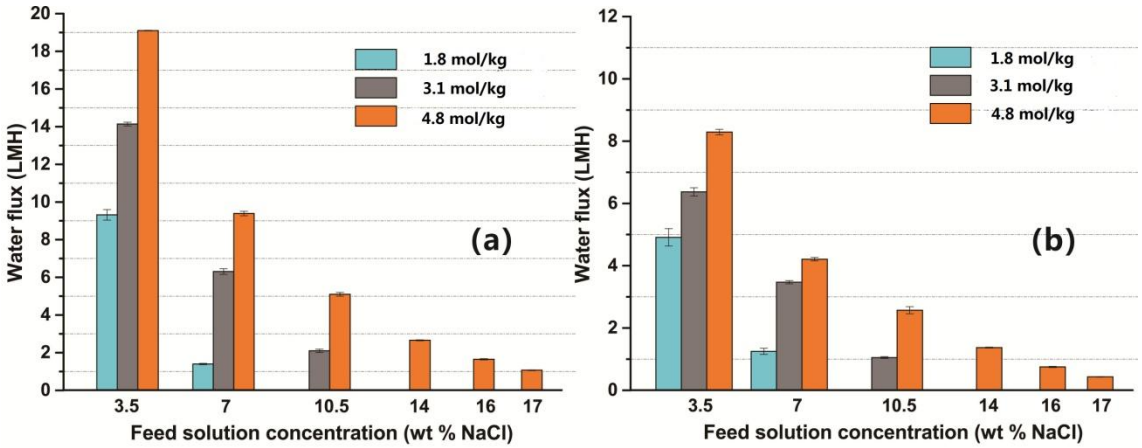

Figure 8.2 Water flux generated by draw solutions of different concentrations against feed solutions with salinities equal to or higher than seawater in (a) PRO mode and (b) FO mode. Draw solution and feed solution were maintained at 50±1 ℃ and 46±2 ℃, respectively.

Figure 8.2 shows the water flux profile generated by our draw solution against feed solution with various salinities. 4.8 mol/kg draw solution can generate a high water flux of 19 LMH and 8 LMH from artificial seawater (3.5 wt% NaCl) in PRO mode and FO mode, respectively. These water flux values are comparable to that of commercial seawater RO plant of ~15 LMH.[20] The relatively lower water flux in FO mode than PRO mode can be attributed to the severe diluted internal concentration polarization in FO mode,[5] which is a common phenomenon for any FO process that utilizes current generation asymmetric membranes. The water flux no doubt decreases with increasing feed solution salinity since the osmotic pressure gradient across membrane shrinks, and the water flux is reduced to ~1 LMH when feed solution salinity increases to 17 wt%. The water fluxes in both PRO and FO mode are expected to be higher if a better FO membrane that can produce less severe internal concentration polarization is available. However, it is still exciting to observe that 4.8 mol/kg draw solution has a higher osmotic

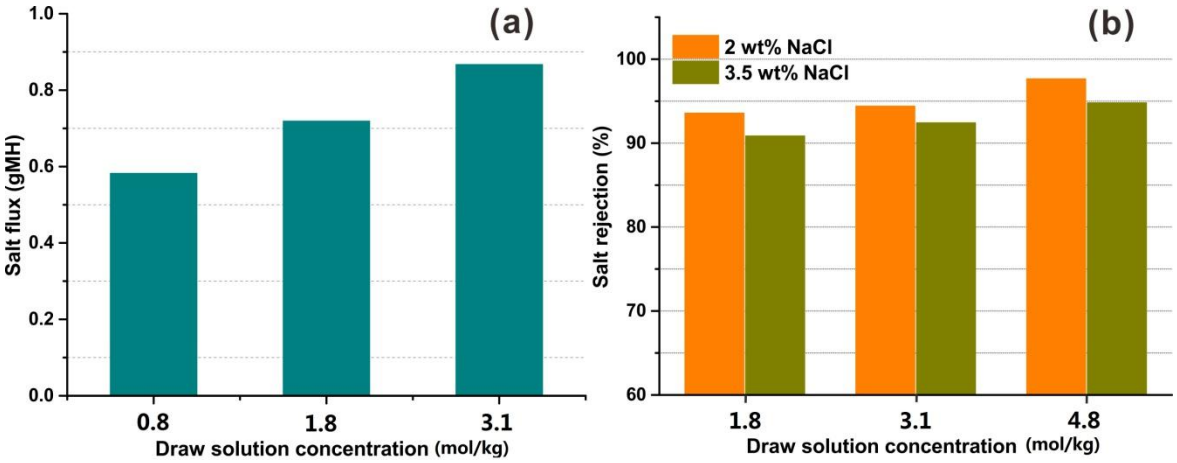

Figure 8.3 (a) back diffusion of draw agent in FO process. 2 wt% NaCl was used as the feed solution. (b) salt rejection of FO membrane in FO process with 2 wt% and 3.5 wt% NaCl as feed solutions. The draw solution and feed solution were maintained at 50±1 ℃ and 46±2 ℃, respectively. FO mode was used throughout the back diffusion and salt rejection measurements.

pressure than that of 17 wt% NaCl brine which has almost five times the salinity of seawater. This indicates that FO desalination enabled by this novel draw agent can achieve an 80% water recovery for seawater desalination in counter-current flow module,[21] which is impossible for RO to achieve. In addition, other difficult waters

beyond RO capability including RO brine and produced water from shale gas industry[4, 22] can be treated via FO since this novel draw solution can concentrate brines to the concentration that shares the osmolality of 17 wt% NaCl. The volume reduction and concentration approximate to saturation make the ensuing procedures in crystallizer more energy-effective for the purpose of zero-liquid discharge.

Besides water permeation, there is also mass transfer of draw agent and feed solute through the FO membrane driven by concentration gradient. Figure 8.3a shows that draw agent back diffusion increases with draw solution concentration. However, the general draw agent flux is lower than 1 gMH, which is superior to zwitterions,[10] and other inorganic, especially monovalent salts.[7] This low draw agent back diffusion can probably be attributed to the dissociation of draw agent. Because the FO membrane used in this article has negative zeta potentials in both supportive and selective layers,[19] the electro-static repulsion between the anion and membrane may help reduce the back diffusion. In addition, the relatively high molecular weight as well as hydration radius of draw agent may also contribute to minimize draw agent back diffusion. Figure 8.3b demonstrates the salt rejection of NaCl in FO process with different feed solution salinity. Generally, salt rejection increases with fixed feed solution salinity and increasing draw solution concentration. This is because unlike water flux that is determined by osmotic pressure gradient, salt flux is determined by concentration gradient. Increasing drawing ability results in higher water flux but imposes almost no effect on salt flux. Therefore, the salt rejection increased due to “dilution effect”. On the other hand, when the feed solution salinity increases from 2 wt% to 3.5 wt%, the salt rejection decreases correspondingly owing to “concentration effect” by enhanced salt flux but declined water flux. However, the overall salt rejection is still above 90% albeit more selective FO membrane is demanded.

Figure 8.4 schematically illustrates the phase diagram of UCST-type draw agent circulation in FO-regeneration processes at various temperatures. After the FO process, the diluted draw solution was subject to a temperature decline from 50℃ to room temperature in order to recover draw agent utilizing the reduced solubility. For the

scenario of our draw agent studied in this chapter, when the temperature is reduced to 20 ℃ in regeneration process, the diluted draw solution after FO undergoes a phase separation resulting in a 0.58 mol/kg supernatant phase and a 4.8 mol/kg sedimentation phase. The sedimentation can be pumped back directly, as the draw agents in chapter 7, to be used as draw solution in FO process. The supernatant with a relatively low concentration facilitates the water polishing step. Water flux test shows that this 0.58 mol/kg supernatant has an almost equal osmotic pressure with seawater, namely about 27 bar.

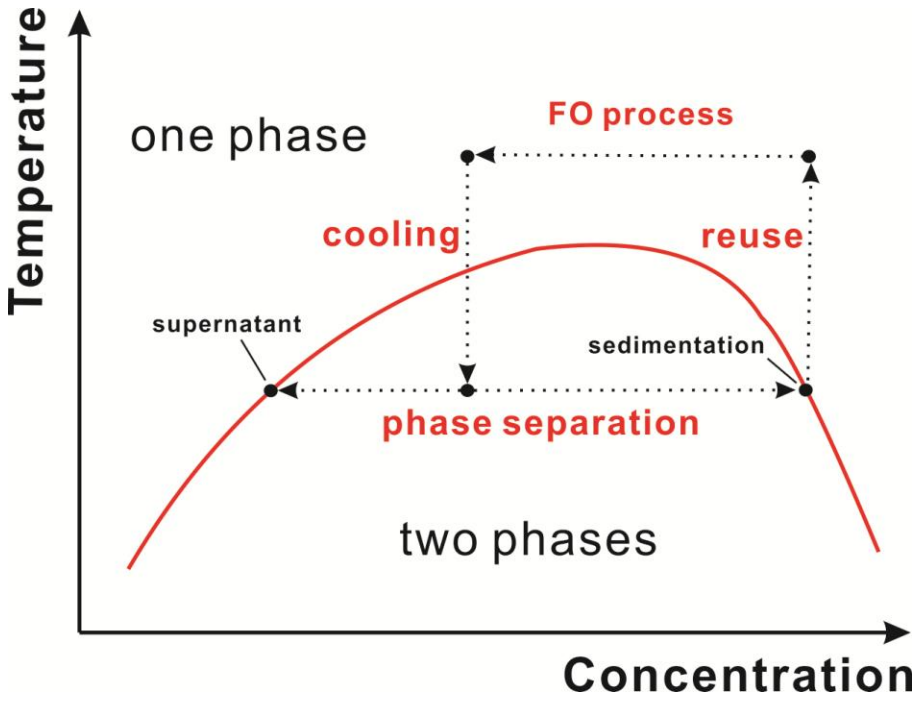

Figure 8.4 Schematic illustration of phase diagram of this UCST-type draw agent circulation in FO-regeneration processes modulated by temperature.

Therefore, one possible option to treat this supernatant is to directly apply NF or RO since any seawater RO plant (hydraulic pressure from 30 bar to 60 bar) is capable of handling such supernatant phase. It should be highlighted that, as shown in Figure 8.5, one distinct merit of the FO desalination process enabled by our draw agent is the ability to enhance the water recovery in a seawater RO plant from typically 50% to up to 80% through the combination of FO and RO processes. In addition, this new draw agent can expand the capability of an RO plant to treat other brines with even higher salinities

toward a near-zero liquid discharge process. Furthermore, another underlying advantageous feature is that only an isobaric NF or RO process is need in this case (Figure 8.5), because similarly to the draw agents in Chapter 7, as water permeates through the NF or RO membrane, the feed solution is not expected to become more concentrated due to accompanying phase separation from the supersaturated supernatant. Therefore, not only the fouling problem in RO will be ameliorated due to extra FO membrane barrier, but the theoretical electrical energy in RO would be reduced owing to the isobaric process.

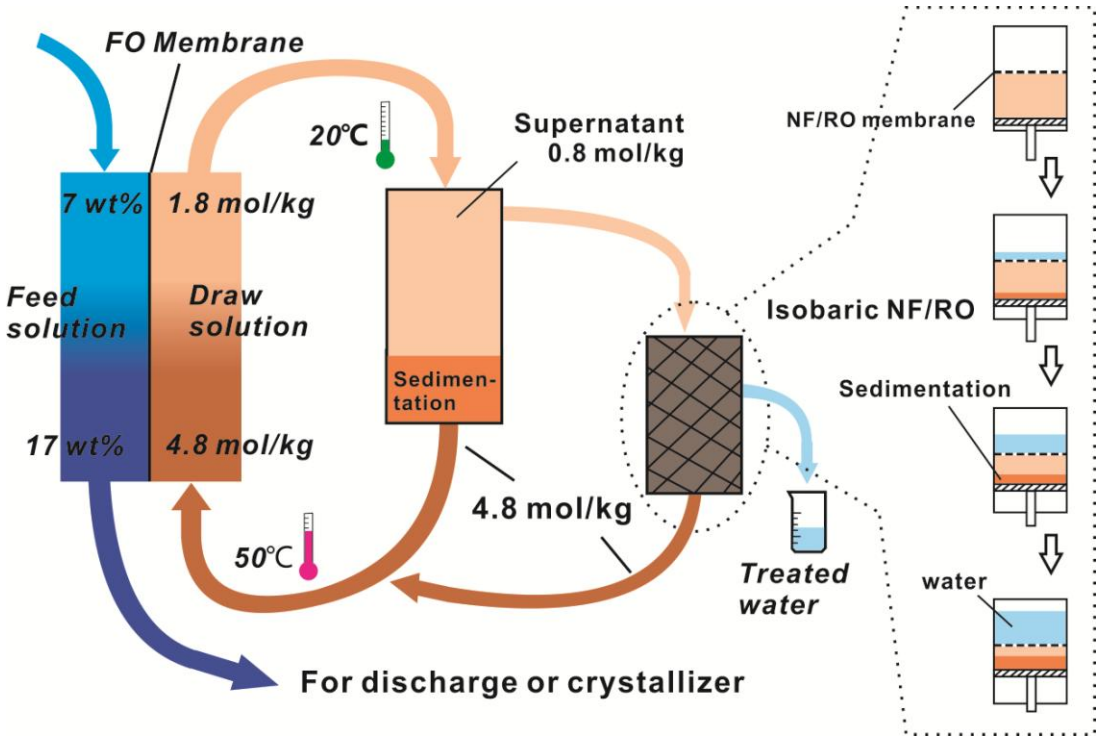

Figure 8.5 Schematic illustration of brine treatment via FO using our draw agent that concentrate the brine to 17 wt% NaCl solution that is difficult to treat directly using an RO process. Diluted draw solution after FO process is first cooled to 20℃ at which a majority of the draw agent is regenerated by phase separation. The sedimentation phase can be used directly as draw solution again, while the supernatant can be regenerated by an isobaric RO or NF process.

8.4. Conclusions

A unique UCST-type FO draw agent was tested for brine treatment in this chapter. This draw agent has such a significant solubility dependence on temperature that at 50 ℃ the 4.8 mol/l draw solution can generate water flux from a feed solution with salinity equal to 17 wt% NaCl; in regeneration process at 20 ℃, the diluted draw solution undergoes a phase separation resulting in a 4.8 mol/l sedimentation phase that can be directly used as draw solution in FO process, and a 0.58 mol/l saturated supernatant phase that shares osmotic pressure with seawater. Therefore, it can be easily treated by any seawater RO plant at constant hydraulic pressure in theory. The significance of the draw agent revealed in this chapter is that, combining with FO can improve the water recovery of seawater RO plant to 80% and possibly extend the plant's ability to treat brines. This technology is hopefully competent to challenge thermal distillation technologies in brine treatment because it only consumes the seawater RO's typical electrical energy consumption as well as low grade thermal energy.

References

1. Aldhous, P., The world's forgotten crisis. *Nature* 2003, *422*, (6929), 251-251.

2. Ghalavand, Y.; Hatamipour, M. S.; Rahimi, A., A review on energy consumption of desalination processes. *Desalination and Water Treatment* 2014, 1-16.

3. Elimelech, M.; Phillip, W. A., The future of seawater desalination: energy, technology, and the environment. *Science* 2011, *333*, (6043), 712-717.

4. Shaffer, D. L.; Arias Chavez, L. H.; Ben-Sasson, M.; Romero-Vargas Castrillón, S.; Yip, N. Y.; Elimelech, M., Desalination and reuse of high-salinity shale gas produced water: drivers, technologies, and future directions. *Environmental science & technology* 2013, *47*, (17), 9569-9583.

5. Cath, T.; Childress, A.; Elimelech, M., Forward osmosis: Principles, applications, and recent developments. *Journal of Membrane Science* 2006, *281*, (1-2), 70-87.

6. Mi, B.; Elimelech, M., Organic fouling of forward osmosis membranes: fouling reversibility and cleaning without chemical reagents. *Journal of Membrane Science* 2010, *348*, (1), 337-345.

7. Achilli, A.; Cath, T. Y.; Childress, A. E., Selection of inorganic-based draw solutions for forward osmosis applications. *Journal of Membrane Science* 2010, *364*, (1-2), 233-241.

8. McGovern, R. K., On the potential of forward osmosis to energetically outperform reverse osmosis desalination. *Journal of Membrane Science* 2014, *469*, 245-250.

9. Ge, Q.; Su, J.; Amy, G. L.; Chung, T. S., Exploration of polyelectrolytes as draw solutes in forward osmosis processes. *Water Res* 2012, *46*, (4), 1318-1326.

10. Lutchmiah, K.; Lauber, L.; Roest, K.; Harmsen, D. J. H.; Post, J. W.; Rietveld, L. C.; van Lier, J. B.; Cornelissen, E. R., Zwitterions as alternative draw solutions in forward osmosis for application in wastewater reclamation. *Journal of Membrane Science* 2014, *460*, 82-90.

11. Guo, C. X.; Zhao, D.; Zhao, Q.; Wang, P.; Lu, X., Na(+)-functionalized carbon quantum dots: a new draw solute in forward osmosis for seawater desalination. *Chem Commun (Camb)* 2014, *50*, (55), 7318-7321.

12. Stone, M. L.; Wilson, A. D.; Harrup, M. K.; Stewart, F. F., An initial study of hexavalent phosphazene salts as draw solutes in forward osmosis. *Desalination* 2013, *312*, 130-136.

13. Ge, Q.; Chung, T. S., Hydroacid complexes: a new class of draw solutes to promote forward osmosis (FO) processes. *Chem Commun (Camb)* 2013, *49*, (76), 8471-8473.

14. Królikowska, M., (Solid+liquid) and (liquid+liquid) phase equilibria of (IL+water) binary systems. The influence of the ionic liquid structure on mutual solubility. *Fluid Phase Equilibria* 2014, *361*, 273-281.

15. Łuszczyk, M., Volumetric behaviour of (3-methoxypropionitrile+ water) in the vicinity of the upper critical solution temperature. *The Journal of Chemical Thermodynamics* 1988, *20*, (1), 29-38.

16. Lee, H.-N.; Rosen, B. M.; Fenyvesi, G.; Sunkara, H. B., UCST and LCST phase behavior of poly(trimethylene ether) glycol in water. *Journal of Polymer Science Part A: Polymer Chemistry* 2012, *50*, (20), 4311-4315.

17. Apelblat, A.; Manzurola, E., Solubilities ofL-aspartic, DL-aspartic, DL-glutamic, p-hydroxybenzoic, o-anisic, p-anisic, and itaconic acids in water fromT= 278 K toT= 345 K. *The Journal of Chemical Thermodynamics* 1997, *29*, (12), 1527-1533.

18. Kubantseva, N.; Hartel, R. W., Solubility of Calcium Lactate in Aqueous Solution. *Food Reviews International* 2002, *18*, (2-3), 135-149.

19. Coday, B. D.; Heil, D. M.; Xu, P.; Cath, T. Y., Effects of transmembrane hydraulic pressure on performance of forward osmosis membranes. *Environmental science & technology* 2013, *47*, (5), 2386-2393.

20. Pearce, G.; Talo, S.; Chida, K.; Basha, A.; Gulamhusein, A., Pretreatment options for large scale SWRO plants: case studies of OF trials at Kindasa, Saudi Arabia, and conventional pretreatment in Spain. *Desalination* 2004, *167*, 175-189.

21. Shaffer, D. L.; Werber, J. R.; Jaramillo, H.; Lin, S.; Elimelech, M., Forward osmosis: Where are we now? *Desalination* 2015, *356*, 271-284.

22. Coday, B. D.; Xu, P.; Beaudry, E. G.; Herron, J.; Lampi, K.; Hancock, N. T.; Cath, T. Y., The sweet spot of forward osmosis: Treatment of produced water, drilling wastewater, and other complex and difficult liquid streams. *Desalination* 2014, *333*, (1), 23-35.

9. CONCLUSIONS AND RECOMMENDED FUTURE WORKS

In this chapter, conclusions of this thesis and suggestions on future works are provided. In a nutshell, this thesis focuses on developing responsive materials as draw agents in forward osmosis to realize an energy-efficient desalination. Forward osmosis desalination enabled by these draw agents consumes less electrical energy and the utilization of much cheaper low grade thermal energy can consequently reduce the energy cost. Some constructive suggestions on draw agent development and improvement are mentioned.

9.1. Conclusions

In comparison with other non-responsive draw agents, responsive draw agents investigated in this very thesis have demonstrated potential in enabling FO to be an energy-efficient desalination technology. Multiple choices of external stimuli, including thermal, magnetic and pH can be utilized instead of solely using electricity-intensive RO to regenerate the draw agent. The subtle balance between FO performance and regeneration performance is the key to design a suitable draw agent, and this is the foundation on which I improve our draw agent's comprehensive performances.

The first part of this thesis focused on using thermally responsive semi-IPN hydrogels as draw agents. The hydrophilic polymer or polyelectrolyte was smartly introduced into PNIPAm network in a way that water flux can be increased without jeopardizing the thermosensitivity of draw agent, which cannot be achieved by copolymerization. The importance of a balanced performance was firstly demonstrated. Poly electrolyte hydrogels can generate the highest water flux in FO but cannot release water in regeneration process; while non-electrolyte PNIPAm can release the water absorbed in FO under heating albeit the water flux in FO is low. Our semi-IPN hydrogels with improved water flux and preserved thermosensitivity can be incorporated into a

desalination module that is driven by temperature modulation. At low temperatures the hydrogels swell to absorb water from brackish water; at high temperatures the hydrogels deswell to release the water. The released water is theoretically pure exempting further polishing steps. In fact, this reveals our underlying principle for energy-efficient desalination, which is to use low grade thermal energy to replace expensive electrical energy for desalination via FO. This is different with thermal distillation methods since its enthalpy and temperature required are much lower than those for water evaporation. However, it was found that semi-IPN hydrogels can only generate a water flux of about 0.2 LMH from 2000 ppm NaCl solution.

As the ensuing endeavor, I managed to improve the water flux by combining the hydrophilicity and hydrophobicity in the monomer design rather than in hydrogel structure design as I did for semi-IPN hydrogels. The synthesized thermally responsive poly ionic liquid hydrogels showed a water production rate of 1.2 LMH after the optimizations of many parameters including monomer selection, membrane structure, hydrogel particle interstitial volume reduction, hydrogel area density on membrane and the FO-regeneration duration. I also for the first time proposed a criterion to judge hydrogel's performance as draw agent in FO desalination, which is helpful to compare each hydrogel's capability when new hydrogel candidates are studied in the future. The advent of thermally responsive poly ionic liquid hydrogels are a great forward leap towards using responsive draw agents to realize energy-efficient brackish water FO desalination.

Smart dual responsive polymers were also investigated to expand this thermal-replacing-electrical principle to seawater FO desalination. Two states were smartly designed to avoid the compromise between hydrophilicity and hydrophobicity in molecular structure. The protonated state is actually polyelectrolyte that can generate a water flux from seawater, while the deprotonated state is thermally responsive making the majority of polymer precipitate at a mild heating up to 50℃. These two states can be reversibly switched by introducing and removal of CO_2. The supernatant after precipitation is so diluted that a hydraulic pressure of only 1.5 bar can achieve a 95% water recovery in

nanofiltration water polishing step. Again, low grade thermal energy was utilized to regenerate the majority of draw agent. Apart from that, electrical energy from NF is complemented since thermal energy is unable to regenerate all the draw agents as in hydrogels. However, the electrical energy consumption should be insignificant owing to the low hydraulic pressure in NF. This dual responsive polymer is very promising draw agent, especially when the CO_2 does not need recovery. The electrical energy is assumed to increase if CO_2 has to be regenerated from the mixture with inert gas used in deprotonation, and this can be regarded as the compensation for dodging the hydrophilicity and hydrophobicity compromise in molecular design.

Thermally responsive ionic liquids were another group of responsive draw agents that successfully expanded the thermal-replacing-electrical principle to FO seawater desalination. These ionic liquids have achieved such subtle balance between hydrophilicity and hydrophobicity that slight change in adding or cutting two methyl groups would annihilate the LCSTs. At low temperatures, the thermally responsive ionic liquid draw solution can generate a water flux from 1.6 M NaCl solution that has almost three times the salinity of seawater; while at high temperatures, e.g., 50℃, the diluted draw solution undergoes a liquid-liquid phase separation. The draw agent-rich sedimentation phase can be directly reused as draw solution without treatment, while the water-rich saturated supernatant has an osmotic pressure of less than 6 bar. An isobaric low hydraulic pressure NF process is capable to polish the water. The theoretical energy consumptions for seawater desalination with 50% water recovery via RO and FO enabled by these ionic liquid draw solutions have been calculated. It was found that FO actually consumes more energy than RO in that the diluted draw solution always has a higher osmotic pressure than feed solution. However, the electrical energy consumption of FO is only about one fifth that of RO, and the rest consumption is complemented by cheap low grade thermal energy. The FO's total energy cost is found to be lower than RO. This finding really reveals the bright future of FO desalination, which is to challenge RO and thermal distillation methods in seawater and brine treatment.

This concept was further fortified by our proprietary draw agent for brine treatment. At 50℃ in FO process, the draw solution can generate water flux from 17 wt% NaCl solution, while at 20 ℃ the diluted draw solution undergoes phase separation in regeneration process. Again, the sedimentation phase can be reused as draw solution without treatment, and the supernatant has an osmotic pressure equal to seawater, making it possibly being able to be treated by any seawater RO plant. Thus, the FO-RO hybrid system enabled by responsive draw agent can help RO plant to treat brines with typical seawater RO electricity consumption, and certain amount of low-grade thermal energy. This FO-RO hybrid may be energetically superior to thermal distillation methods in brine treatment, and future work on the energy comparison is needed.

9.2. Recommendation for future work

Developing a new suitable draw agent for forward osmosis desalination is not an easy task when there are many criteria to meet. Balanced FO and regeneration performances are always the key to hold in designing draw agent for FO if fresh water is the end product. Based on the experimental results obtained, the discussion presented and the conclusions from this research, some recommendations might be interesting for future investigation.

(1) The dual responsive polymer is promising if CO_2 is provided from flue gas that is otherwise discharged. The kinetic study in the protonation and deprotonation processes would be interesting to enhance the efficiency in the switch between protonation and deprotonation. A more effective method of introducing CO_2 or inert gases other than bubbling is needed, and the influence of the interaction between carbonate and amino group in this polymer on osmotic pressure generation needs to be investigated.[1, 2] In addition, the polymer structure design, *e.g.*, star-shape polymers or dendrimers, on the FO and regeneration performance would be another interesting point, since there was report showing that polymer in star shape would generate a higher osmotic pressure and lower viscosity than linear counterpart with the same molecular weight and concentration.[3]

Another possible future work is to study the role of "deliberately" designed copolymer of electrolyte and thermally responsive monomers, *e.g.*, sodium acrylate and NIPAm, as responsive draw agent. This idea is inspired by the semi-IPN hydrogel in which localized charges would not impair the thermosensitivity. Unlike the random copolymer, block copolymer or grafted copolymer might be thermally sensitive with presence of electrolyte monomer. As shown in Figure 9.1, PNIPAm-graft-polyacrylic acid showed a constant LCST at around 32℃at pH of 7.4 even the electrolyte PAA (or rather PSA at such pH) accounted for 80% in the copolymer. Nevertheless, random copolymer of NIPAm and acrylic acid demonstrated increasing LCST and finally annihilated LCST when there was about 20% electrolyte in copolymer. This is possibly a task worth trying since thermosensitivity would not be compromised with presence and increase of electrolyte content.

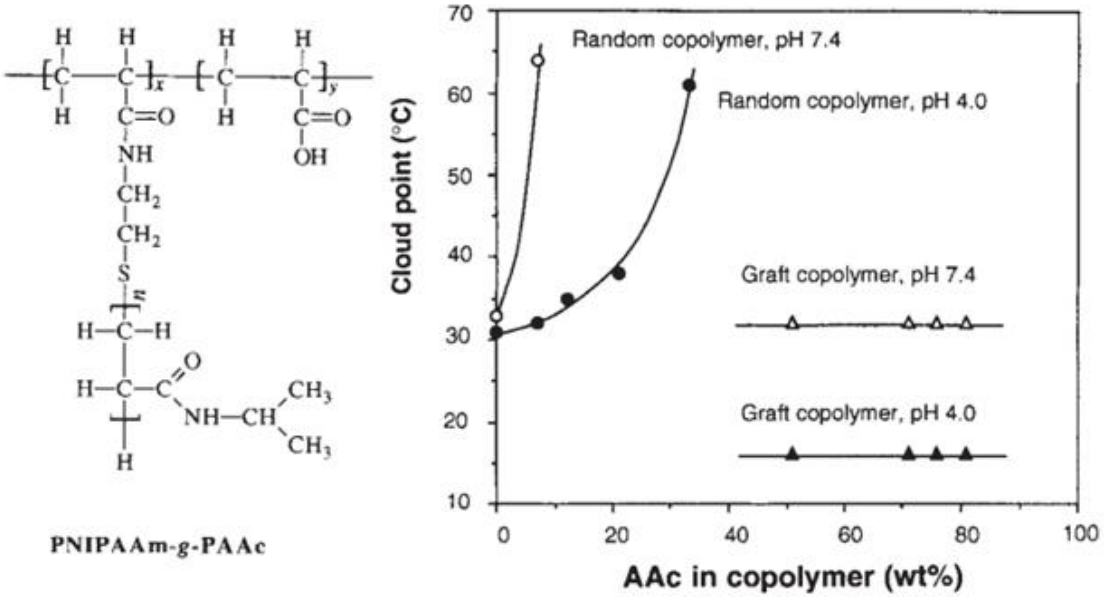

Figure 9.1 The structure of a PNIPAm-graft-Polyacrlyic acid polymer (left) and its interestingly constant LCST in solution irrespective of acrylic acid content (right). This figure is adapted from Reference 4.

(2) Thermally responsive hydrogel is quite promising due to the exemption of water polishing steps. A membrane module with hydrogel "grow on it" instead of sticking to it would be interesting to hopefully improve hydrogel-membrane contact conditions. The

water flux is anticipated to enhance since there will be no hydrogel-hydrogel boundary and the contact condition between hydrogel and membrane is improved. Currently, hydrogels have mostly been used to modify membrane surface for antifouling or block the pore to enhance salt rejection,[5-7] and the methods mentioned in these papers might be transferable to synthesize the hydrogel-membrane composite desalination device.

(3) More study on the interaction between feed solute and draw agent in FO desalination process would be conducted. The back diffusion of some inorganic ions from draw agent, such as carbonate, phosphate and sulfate may cause severe scaling on membrane and downgrade the water flux. In fact, the NH_3-CO_2 system has been found to cause scaling problem on feed solution side membrane.[8] Although the draw agents developed in this thesis are very unlikely to cause any scaling problem, yet the possible organic or bio-fouling caused by polymer or ionic liquid draw agent might need investigation.

Also, the presence of NaCl in the draw solution is another issue that has been overlooked. Current FO membrane cannot guarantee complete salt rejection and the draw solution in practice is actually a mixture with NaCl. The presence of NaCl in draw solution may cause additional issues in energy consumption and draw agent recovery, especially when the draw agent has a comparable molecular weight with NaCl so that NF (or RO) can not completely or efficiently separate draw agent from NaCl.

(4) A long term performance of FO desalination system would be necessary to investigate the actual energy consumption as well as other costs including capital investment, chemical usage, draw agent and membrane replacement costs, *etc*.

References

1. Wilson, A. D.; Stewart, F. F., Structure–function study of tertiary amines as switchable polarity solvents. *RSC Advances* **2014,** *4*, (22), 11039-11049.

2. McNally, J. S.; Noll, B. C.; Orme, C.; Wilson, A., Density Functional Theory Analysis of the Impact of Steric Interaction on the Function of Switchable Polarity Solvents. *The Journal of Physical Chemistry B* **2015**.

3. Cherayil, B. J.; Bawendi, M.; Miyake, A.; Freed, K. F., Osmotic pressure of star and ring polymers in semidilute solution. *Macromolecules* **1986,** *19*, (11), 2770-2778.

4. Chen, G.; Hoffman, A. S., Graft copolymers that exhibit temperature-induced phase transitions over a wide range of pH. *Nature* **1995,** *373*, (6509), 49-52.

5. Wang, X.; Fang, D.; Yoon, K.; Hsiao, B. S.; Chu, B., High performance ultrafiltration composite membranes based on poly (vinyl alcohol) hydrogel coating on crosslinked nanofibrous poly (vinyl alcohol) scaffold. *Journal of Membrane Science* **2006,** *278*, (1), 261-268.

6. Sagle, A. C.; Van Wagner, E. M.; Ju, H.; McCloskey, B. D.; Freeman, B. D.; Sharma, M. M., PEG-coated reverse osmosis membranes: desalination properties and fouling resistance. *Journal of Membrane Science* **2009,** *340*, (1), 92-108.

7. Sagle, A. C.; Ju, H.; Freeman, B. D.; Sharma, M. M., PEG-based hydrogel membrane coatings. *Polymer* **2009,** *50*, (3), 756-766.

8. Li, Z.; Linares, R. V.; Bucs, S.; Aubry, C.; Ghaffour, N.; Vrouwenvelder, J. S.; Amy, G., Calcium carbonate scaling in seawater desalination by ammonia–carbon dioxide forward osmosis: Mechanism and implications. *Journal of Membrane Science* **2015,** *481*, 36-43.

LIST OF PUBLICATIONS

1. **Cai, Y.**, Shen, W., Loo, S. L., Krantz, W. B., Wang, R., Fane, A. G., & Hu, X. (2013). Towards temperature driven forward osmosis desalination using Semi-IPN hydrogels as reversible draw agents. Water research, 47(11), 3773-3781.

2. **Cai, Y.**, Shen, W., Wang, R., Krantz, W. B., Fane, A. G., & Hu, X. (2013). CO 2 switchable dual responsive polymers as draw solutes for forward osmosis desalination. Chemical Communications, 49(75), 8377-8379.

3. Zhou, Y., **Cai, Y.**, Hu, X., & Long, Y. (2014). Temperature-responsive hydrogel with ultra-large solar modulation and high luminous transmission for "smart window" applications. Journal of Materials Chemistry A, 2(33), 13550-13555. **(co-first author)**

4. Zhou, Y., **Cai, Y.**, Hu, X., & Long, Y. (2015). VO 2/hydrogel hybrid nanothermochromic material with ultra-high solar modulation and luminous transmission. Journal of Materials Chemistry A, 3(3), 1121-1126.

5. **Cai, Y.**, Shen, W., Wei, J., Chong, T. H., Wang, R., Krantz, W. B., Fane, A.G., & Hu, X. (2015). Energy-efficient desalination by forward osmosis using responsive ionic liquid draw solutes. Environmental Science: Water Research & Technology, 1(3), 341-347.

6. **Cai, Y.**, Shen, W., Wei, J., Wang, R., Krantz, W. B., Fane, A.G., & Hu, X. Exploration of using thermally responsive polyionic liquid hydrogels as draw agents in forward osmosis. RSC Advances, 2015, 5, 97143-97150

7. **Cai, Y.** & Hu, X. A critical review on draw solute development for forward osmosis. Desalination, Special Issue, 2016